Archaeogenetic Perspectives on Population History and Health in Northeastern Fennoscandia

Dissertation

der Mathematisch-Naturwissenschaftlichen Fakultät

der Eberhard Karls Universität Tübingen

zur Erlangung des Grades eines

Doktors der Naturwissenschaften

(Dr. rer. nat.)

vorgelegt von

Kerttu Majander

aus Helsinki/Finnland

Tübingen

2021

Gedruckt mit Genehmigung der Mathematisch-Naturwissenschaftlichen Fakultät der Eberhard Karls Universität Tübingen.

Tag der mündlichen Qualifikation: 29.11.2021
Dekan: Prof. Dr. Thilo Stehle
1. Berichterstatter: Prof. Dr. Johannes Krause
2. Berichterstatter: Prof. Nicholas J. Conard, PhD

Acknowledgements

Table of Contents

Abbreviations

aDNA	ancient DNA
BCE	Before Common Era
bp	base pairs
BP	Before Present
CE	Common Era
CWC	Corded Ware culture
DNA	deoxyribonucleic acid
EHG	Eastern Hunter-Gatherer
kya	Thousand years ago
mtDNA	mitochondrial DNA
NGS	Next Generation Sequencing
PCR	Polymerase Chain Reaction
SNP	Single Nucleotide Polymorphism
WGS	Whole Genome Sequencing
WHG	Western Hunter-Gatherer

Summary

Many North-European populations have been studied with ancient DNA in recent years [1–10]. According to these studies the current genetic composition of northern Europeans consists of many layers of ancestries in various proportions. In the present population, ancestry components described in ancient DNA investigations of hunter-gatherer populations from Palaeolithic to early Bronze Age are commonly observed, as are those of farming populations from the Neolithic on. Additionally it has been suggested that prehistoric Siberians from the modern-day northern Russian taiga, at least as east as the Ural mountains, could have contributed genetically to northeastern European populations in specific [1,5,11–16]. The region corresponding to modern day Finland, a focus area of this thesis, was a long-time home to groups sustained by foraging, hunting and fishing, whereas agricultural communities emerged relatively late in this part of Europe and in a gradual manner, approximately only from Late Stone Age (~2000BCE) onwards [17]. The low population size throughout Finland's history is partly responsible for a reduced genetic diversity [18–21], also resulting in an original set of hereditary diseases (Finnish Disease Heritage) that has provoked wide interest in the modern medical genetics community [19,22–24]. On the other hand, the sparsity of the early settlements may have spared the nation from several larger epidemics of infectious diseases [25–27]. Increase in the population growth from the medieval to early modern period paved the way for cross-European and global trading networks and denser living arrangements. The urbanizing societies attracted a steady flow of human migrants and facilitated the spread of infectious agents from elsewhere in Europe, changing the local health conditions in the northern peripheries [28–30].

In this thesis, genetic changes in the Fennoscandian population, especially the Finns, situated at the crossroads of east and west, are inspected through ancient DNA. Firstly, a previously unrecognized Siberian ancestry source is detected in prehistoric Fennoscandia in paper I. Secondly, the genetic signals from the hunter-gatherer ancestors of Finns and Saami, and the dichotomy between southwestern and northeastern Finland [20,22,31–33] are addressed through maternal lineages from the Roman Iron Age (300-800 CE) to the early modern period (1500-1800 CE) in paper II. Finally, in paper III, the aspect of health in the historical northern communities is addressed, and one of the most

significant infectious agents of the early modern period, *Treponema pallidum*, is reconstructed genome-wide from ancient human remains found in archaeological sites from modern day Finland, Estonia and the Netherlands, in order to reveal genetic relationships between the modern treponematoses with their ancient forms, and explore the past diversity of pathogenic *Treponema pallidum* strains in early modern Europe.

Zusammenfassung

In den letzten Jahren wurde alte DNA aus vielen nordeuropäische Bevölkerungsgruppen untersucht [1–10]. Laut diesen Studien ist die derzeitige genetische Zusammensetzung der Nordeuropäer vielschichtig (komplex?) und basiert auf unterschiedlichen Abstammungen zu verschiedenen Anteilen. Vorfahrenskomponenten von Wildbeuter-Populationen des Paläolithikums bis zur frühen Bronzezeit werden üblicherweise beobachtet, ebenso wie solche von landwirtschaftlichen Populationen ab dem Neolithikum. Darüber hinaus haben prähistorische Sibirier aus der heutigen russischen Taiga spezifisch zur nordosteuropäischen Bevölkerung beigetragen [1,5,11–16]. Die heutige Region Finnland, ein Schwerpunkt dieser Arbeit, war lange Zeit die Heimat von Gruppen, die Nahrungssammeln, Jagd und Fischerei betrieben, während landwirtschaftliche Gemeinschaften erst relativ spät und schrittweise ab der Spätsteinzeit entstanden (~ 2000 v. Chr.) [17]. Die geringe Bevölkerungszahl in der Geschichte Finnlands ist teilweise für eine verringerte genetische Vielfalt verantwortlich [18–21], was auch zu einer ursprünglichen Gruppe von Erbkrankheiten (Finnish Disease Heritage) führte, die ein breites Interesse in der modernen Genetik geweckt haben [19,22–24]. Andererseits könnte die geringe Dichte der frühen Siedlungen die Nation von mehreren größeren Infektionskrankheitsepedemien verschont haben [25–27]. Das ansteigende Bevölkerungswachstum vom Mittelalter bis zur frühen Neuzeit ebnete den Weg für europaweite und globale Handelsnetzwerke und dichtere Lebensumstände. Die verstädternde Gesellschaft resultierte in einem stetigen Zustrom menschlicher Migranten und ermöglichten es Infektionserregern aus anderen Teilen Europas die nördlichen Randgebiete zu verändern [28–30].

In dieser Arbeit werden die genetischen Merkmale, die in der fennoskandischen Vergangenheit verwurzelt sind, und die entscheidende Position der finnischen Bevölkerung zwischen Ost und West mit Methoden der alten DNA-Forschung untersucht. Erstens wird in Veröffentlichung I eine zuvor unbekannte sibirische Abstammungsquelle im prähistorischen Fennoscandia entdeckt. Zweitens werden die genetischen Signale der Jäger und Sammler-Vorfahren von Finnen und Saami und die Dichotomie zwischen Südwest- und Nordostfinnland [20,22,31–33] in Veröffentlichung II durch mütterliche Abstammungslinien von der römischen Eisenzeit (300-800 n. Chr.)

bis zur frühen Neuzeit (1500-1800 n. Chr.) behandelt. Schließlich wird in Veröffentlichung III der Aspekt der Gesundheit in den historischen nördlichen Gemeinden angesprochen. Es wird einer der bedeutendsten Infektionserreger der frühen Neuzeit, *Treponema pallidum*, in antiken menschlichen Überresten aus finnischen archäologischen Stätten und zwei weiteren Fundorten in Estland und den Niederlanden nachgewiesen.

List of publications

The following manuscripts are part of this thesis and will be referred to with Roman numerals throughout the text:

I. T.C. Lamnidis*, **K. Majander***, C. Jeong, E. Salmela, A. Wessman, V. Moiseyev, V. Khartanovich, O. Balanovsky, M. Ongyerth, A. Weihmann, A. Sajantila, J. Kelso, S. Pääbo, P. Onkamo, W. Haak, J. Krause, S. Schiffels. "Ancient Fennoscandian genomes reveal origin and spread of Siberian Ancestry in Europe". Published in *Nature Communications*, 2018, 9 (1): 1-12.

II. S. Översti*, **K. Majander***, E. Salmela, K. Salo K, L. Arppe, S. Belskiy, H. Etu-Sihvola, V. Laakso, E. Mikkola, S. Pfrengle, M. Putkonen, J.-P. Taavitsainen, K. Vuoristo, A. Wessman, A. Sajantila, M. Oinonen, W. Haak, V.J. Schuenemann, J. Krause, J.U. Palo, P. Onkamo. "Human mitochondrial DNA lineages in Iron-Age Fennoscandia suggest incipient admixture and eastern introduction of farming-related maternal ancestry". Published in *Scientific reports*, 2019, 9 (1): 1-4.

III. **K. Majander***, S. Pfrengle*, A. Kocher, J. Neukamm, L. du Plessis, M. Pla-Díaz, N. Arora, G. Akgül, K. Salo, R. Schats, S. Inskip, M. Oinonen, H. Valk, M. Malve, A. Kriiska, P. Onkamo, F. González-Candelas, D. Kühnert, J. Krause, V.J. Schuenemann. "Ancient bacterial genomes reveal a high diversity of Treponema pallidum Strains in early Modern Europe". Published in *Current Biology,* 2020, 30 (19): 3788-3803.

*Denotes equal contribution

Reprints were made available with permission of the respective publishers.

Additionally, I co-authored the following articles published during my graduate studies:

Bos, K.I., Harkins, K.M., Herbig, A., Coscolla, M., Weber, N., Comas, I., Forrest, S.A., Bryant, J.M., Harris, S.R., Schuenemann, V.J., Campbell, T.J., **Majander, K**., Wilbur, A.K., Guichon, R.A., Wolfe Steadman, D.L., Collins Cook, D., Niemann, S., Behr, M.A., Zumarraga, M., Bastida, R., Huson, D., Nieselt, K., Young, D., Parkhill, J., Buikstra, J.E., Cagneux, S., Stone, A.C. and Krause, J. (2014). "Pre-Columbian mycobacterial genomes reveal seals as a source of New World human tuberculosis" *Nature*, *514*(7523), pp. 494-497.

Villa, P.M., Marttinen, P., Gillberg, J., Lokki, A.I., **Majander, K**., Ordén, M.R., Taipale, P., Pesonen, A., Räikkönen, K., Hämäläinen, E. and Kajantie, E. "Cluster analysis to estimate the risk of preeclampsia in the high-risk Prediction and Prevention of Preeclampsia and Intrauterine Growth Restriction (PREDO) study" (2017) *PloS one*, 12(3), e0174399.

Onkamo, P., **Majander, K**., Peltola, S., Salmela, E. and Nordqvist, K., "Ancient human genes of North-Eastern Europe." (2019) *Записки Института истории материальной культуры РАН* (20), pp. 25-34.

Own contributions

I. I performed all the laboratory experiments at the University of Tübingen under the supervision of Johannes Krause and Verena Schuenemann. The laboratory work included sampling, DNA extractions, library preparations and targeted DNA capture enrichment of mitochondrial genomes and nuclear DNA. I participated in the analysis of the resulting data, such as screening, exploratory methods and contamination estimation, and wrote the paper with my co-first author, Thiseas Christos Lamnidis.

II. I performed all the laboratory experiments at the University of Tübingen under the supervision of Johannes Krause and Verena Schuenemann. They included sampling, DNA extractions, library preparations and targeted capture enrichment for whole mitochondrial genomes. PhD candidate Sanni Översti and archaeologist Kati Salo took part in some of the above-mentioned procedures with either my advice or supervision. Furthermore, I participated in the analysis of the resulting data, such as screening, contamination estimation and data quality assessment, and wrote the paper with my co-first author Sanni Översti.

III. I designed and conducted the study under the supervision of Verena Schuenemann and Johannes Krause, and participated in selecting and collecting the samples. I analyzed the resulting data for the part of the screening procedures, data quality assessment and virulence analysis, and wrote the paper.

1 Introduction

1.1 Ancient DNA

1.1.1 Advancements and challenges in ancient DNA

In examining the past, ancient DNA (aDNA) has clear advantages over the statistical extrapolations based on modern genetics, as it can reveal long extinct genetic diversity of the studied species. Archaeo- and paleogenetics explore the past of various ancient organisms, from microbes to humans and spanning from individual characteristics to large-scale population structures. Techniques used in these fields are relatively recent and aim to combine classical genetics and genomics with applications specifically developed for degraded DNA present in the paleontological or archaeological findings. The first reproducible studies with molecular detection of ancient DNA were conducted in the early 1980's [34,35]. Since then, several remarkable revelations have been made on early modern humans and their paleontological sister groups [36–40], continued with the characterization of prehistoric populations and their migration patterns [3,5,13,41–48]. Among these findings are the genetic architecture of the Ice Age hunter-gatherers [3,5,11,49], the course of Neolithic revolution [43,50,51] and the European population turnover related to pastoralists from the Pontic Caspian Steppe during the Early Eastern European Bronze Age [1,41].

One of the revolutionary techniques responsible for the rapid progress in ancient DNA applications is high-throughput sequencing (Next Generation Sequencing, NGS) [52]. It enables parallel sequencing of billions of DNA fragments and has made the large-scale screening of hundreds of thousands of ancient samples affordable. In archaeogenetics, the introduction of NGS has enabled recovering nuclear genomes despite the typically scarce and highly fragmented nature of ancient DNA fragments retrieved from ancient materials, and allowed the reconstruction of ancient genomes of extinct species and early humans [39,53–55]. Another improvement achieved in the ancient DNA field is the enrichment of specific genetic regions and, on occasion, entire target organisms [56,57]. Targeted enrichment utilizes oligonucleotide baits that hybridize to individual strands of heat-denatured DNA, while the background DNA in the sample from non-target sources

is washed away [42,58,59]. The capture can be conducted on several mediums. In the microarray-based capture, hybridization happens with probes immobilised on a glass slide [58]. Another option is the "in-solution"-based approach, where DNA probes are mixed in a liquid reaction solution, and move freely, improving the likely occasions for hybridization [60–62]. Furthermore, several samples may be loaded on the same array, causing competition over the probe set, whereas the in-solution enrichment method ensures a more equal distribution since each sample is assigned its own set of probes [60,62]. A detailed comparison between these methods and a third, RNA probe-based method was recently published [63]. The study concluded that while the DNA in-solution techniques surpass the array-based method, the RNA probes show both efficiency and affordability over their DNA-based equivalents. When creating the probes, shorter genomes can be used in their entirety. This is the case for the small circular genome of the human mitochondrial organelle and some of the genomes of bacteria and viruses. For longer genomes, a selection of meaningful markers (or SNPs, i.e. Single Nucleotide Polymorphisms) carrying differences between individuals or groups are chosen. Several marker selections have been designed on the human nuclear genome to enrich for the diagnostic regions of hereditary diseases, and to ascertain modern populations from each other, based on published datasets such as Simons Genome Diversity Project [64] and the 1000 Genomes Project [65].

Recently, bioinformatic applications directed to aDNA analysis have improved reliability in detecting and authenticating ancient genetic material [66–68]. The DNA fragments retrieved from ancient samples are commonly low in quantity and quality [69,70], after having severely degraded in the soil or other natural conditions. On average, ancient DNA fragments are 40-60 bp long, and have accumulated hydrolytic damage especially at their ends. The hydrolytic reaction at the 5' -end of the DNA fragment causes cytosines to deaminate into uracils and to be subsequently read as thymines in construction of the DNA sequence in subsequent amplifications. Similarly, guanine is substituted by adenine in its reverse complement [71]. Since the amount of this damage is shown to positively correlate with the age of a specimen [70,72] it is commonly used to authenticate ancient DNA in a sample. An overall deamination pattern becomes visible, when the damage is plotted as a distribution over all sample's endogenous DNA reads [68,70,73].

1. Sample content

Human

Bacteria

2. Mapping

A B C

3. DNA damage

0,2

0,2

0

0

5' Position in read 3'

4. mtDNA contamination

reference

contaminant

consensus
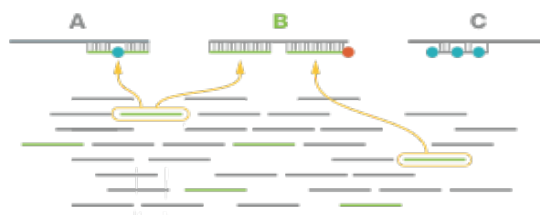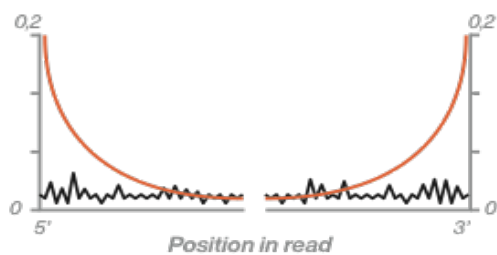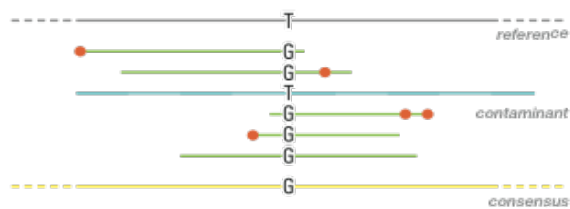
5. Nuclear DNA contamination in males

XX XY XY
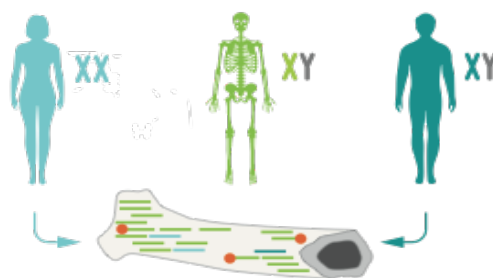
● Damage ● Mismatch

Figure 1. (Opposite page) Examples of authentication, adapted from Key et. al 2017 [67]. 1) Sample content, including target DNA (light green) and contaminating sources (blue and teal) 2) DNA reads mapping with low specificity to reference sequences A and C, and with high specificity to reference sequence B and age-related damage at the end of the reads. 3) Damage pattern typical for ancient DNA, showing base misincorporation accumulated at the last positions of the reads. 4) Mitochondrial reads from target and contaminant sources, with authentic target reads identified by ancient DNA damage and consistency of mutations, used in building a consensus sequence. 5) Several sources of X-chromosomal DNA in a male specimen, indicating contamination.

The molecular preservation of ancient remains is also significantly influenced by other factors, such as the acidity and temperature of the soil where bones have been deposited [72,74–76]. The Finnish soil, although cool in temperature, is acidic and humid, which also causes fast degradation of the bone tissue itself [77]. In cases where DNA damage patterns cannot be credibly used to confirm the age of the DNA molecules, some of the ambivalence can be amended for by bioinformatic evaluation of contaminant sources present in the sample [67,68,78,79]. For instance, contaminant bacterial background present in the soil can be separated from the target organism's DNA by mapping the sequenced reads comparatively to different species and auditing the quality of the mapping by number of mismatches and investigating individual reads for spurious substitutions that do not appear to stem from age-related damage. Human contamination can be suspected when among the DNA of one sample, authenticated as ancient by damage patterns, two different mtDNA lineages can be detected, or when a male specimen, naturally carrying only one X chromosome, yields a signal of X-chromosomal DNA from a second source. Occasionally, contamination is only discerned later in the analyses, when population-specific markers from an ancient sample show gross discrepancy with its expected origin. As these observations can also stem from accurate yet unexpected results, an exclusion of the outlier samples should only be employed when source of the contamination can be properly discerned, for example to a contamination from laboratory plastic ware or other accidental exposure to rich sources of modern human DNA. Despite the improved methodology aimed for authentication, contamination from modern DNA remains a constant risk due to its abundance in living organisms and generally better molecular preservation.

1.1.2 Approaches to ancient pathogen detection

Apart from human genetics, the advances in ancient DNA techniques also include screening and reconstructing genomes of pathogenic microbial organisms from archaeological remains [67,80–85]. Several pathogens have thus far been detected and studied in detail, such as the bacterial agents responsible for tuberculosis (*Mycobacterium tuberculosis*)[86–88], plague (*Yersinia pestis*)[89–94], lepromatous leprosy (*Mycobacterium leprae*) [95–98], paratyphoid fever (*Salmonella enterica*) [99,100], syphilis and yaws (*Treponema pallidum*) [101], and intestinal and stomach inflammation (*Helicobacter pylori*) [102,103] as well as viral agents, for example those causing viral hepatitis [104–107], influenza [108,109] smallpox [110] and "fifth disease" rash [111]. Since immortalization of DNA into libraries allows amplifying it over and over again, the same samples used for the study of the human host DNA can be used for pathogen screening and, in many cases, also for the subsequent target enrichment procedure -a beneficial feature in minimizing the material loss of precious archaeological and paleontological samples. If a focus on either population genetics or pathogenic analysis is emphasized from the start, more specific sampling strategies can be employed. Due to its exceptional density and generally good DNA preservation the petrous part of the temporal bone is preferred in human DNA sampling, when available [112,113]. Bacterial DNA is mostly abundant in parts of the bones where there was ample blood flow during the host's lifetime, and that were mechanically protected post-mortem. Commonly used parts of the skeleton are the enamel-protected dentine, cementum around the tooth's root, and especially the dental pulp cavities [114,115]. Alternatively, sampling can be done from the visible lesions denoting an active infection, or close to them, if the morphological characteristics need to be conserved. The amount of pathogen DNA is usually low compared to the endogenous DNA of the host organism, and hard to segregate from a myriad of contaminating sources of DNA, either from the original soil deposit or from the physical handling of the sample [116–118]. Some exceptions to this exist: for example *Mycobacterium leprae* bacteria, the causative agent of leprosy, possesses a protective cell wall that improves DNA preservation in human bones [95]. Many bacterial pathogens have relatives among soil-dwelling or carcass-exploiting bacteria, and the

genetic remnants from these bacteria are also commonly present in ancient samples. Since closely related environmental bacteria are often similar enough to map to the reference genome of a pathogen, they cause genetic background signals that may easily lead to false positive findings [116–118]. Additionally, the relative amount of soil-living bacteria (whether ancient or recent) can swamp the targeted sample during sequencing [119,120]. Due to these challenges, the sensitivity of the screening methods has been under improvements over the recent years. An increasing number of specialized programs and large microbial databases is available today, providing an opportunity to create a tailored selection of known pathogen DNA sequences to screen from, and to have various species individually traced down. Many of these tools, like *MetaPhlAn2* [121] and MIDAS [122] concentrate on specific marker gene queries, more reliable when using modern sequencing data. Approaches utilizing whole genomes improve the matching of the sparse ancient DNA reads: Kraken [123] employs k-mer matching among thousands of reference genomes, while MALT (Megan Alignment Tool) [99,124] is based on alignment of reads against the known reference sequences, and paired with Megan (Metagenome Analyzer program)[125] it allows interactive analysis of the taxonomic and functional content of whole genome datasets called from databases such as RefSeq [126] of NCBI (National Center for Biotechnical Information). This alignment-based tool is further extended by a recent version, MALTextract, designed to support the HOPS (Heuristic Operations for Pathogen Screening) pipeline [127], developed especially for ancient DNA analysis. Together, these tools can be used in both screening, species identification and evaluation of accuracy and authenticity of putative findings. Hybridization-based capture techniques [58] can then be applied to increase the amount of sequencing reads specific to a candidate pathogen indicated in the analysis. A successful reconstruction of an ancient pathogen genome often depends on this indispensable application. As the databases tend to also include non-pathogenic taxa, metagenomic analysis can additionally be undertaken, to investigate the sample content and to provide an overview of the proportions of different microorganisms present in the specimen. The composition of the normal flora in comparison to opportunistic or pathogenic bacteria may provide important information of the general lifetime health and conditions of the sampled individual [102,128,129]. The advantages of metagenomic studies are increasingly appreciated in assessing various conditions of bacterial

microbiomes, ranging from past to present and on a wide set of subjects, from the oceans and soil to the human gut and oral environments [128,130–135].

Downstream analyses from the screening and target enrichment include, for example, phylogenetics used to disentangle the relationships of bacterial taxa and strains, and detection of functional genes and mutations important in evolutionary adaptations of pathogens [136]. Molecular dating can assess the divergence of pathogen strains and reveal their potential involvement in the past epidemics [136–138]. Since some bacterial and viral agents typically use horizontal gene transfer to replenish their genomic diversity, evaluation of possible events of recombination can aid understanding the dynamics between and within pathogen groups [139,140].

1.2 History of Northern populations

1.2.1 Linguistic and archaeological considerations

Finland has been continuously inhabited since 11.000-9000 BP [17]. The Neolithic and Subneolithic (Fennoscandian non-farming or low-intensity farming) Comb Ceramic culture (CCC) and slightly later, although partially overlapping Corded Ware culture (CWC), are the first substantially represented archaeological entities in the region of modern Finland [141–144].
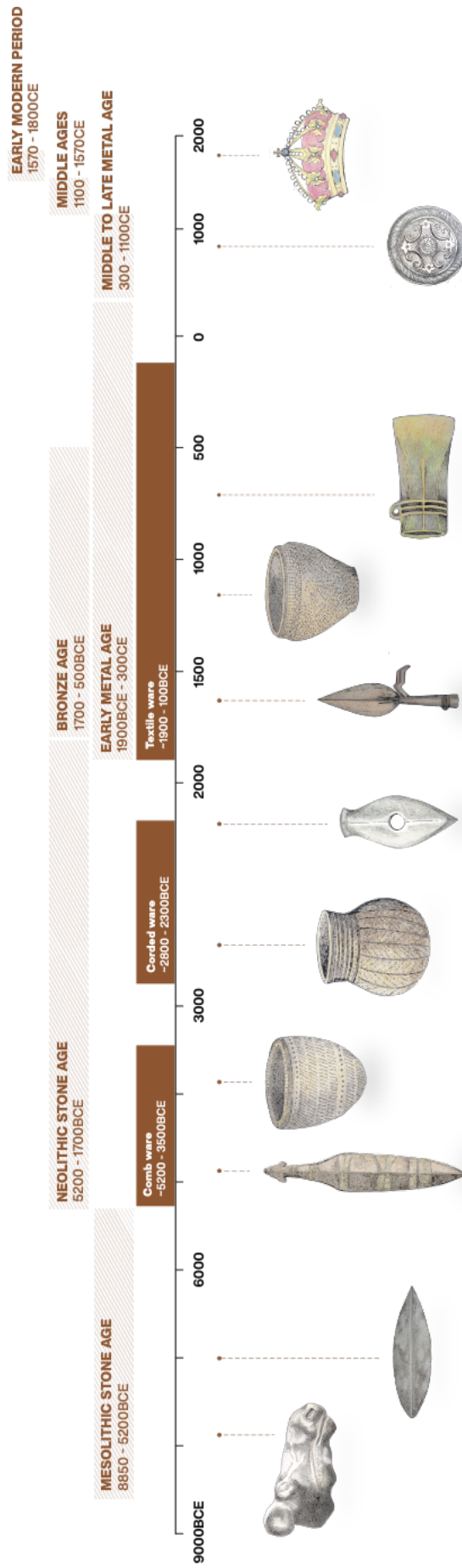
Figure 2. Schematic illustration of the cultural concepts relevant in northeastern Fennoscandian archaeology on a timeline.

The language spoken by these groups is unknown, although the Corded Ware people may have exposed them to an Indo-European language's influence on their route through central Europe from the east-Eurasian Steppes [41,145,146]. In the whole of the Baltics, including the coastal side of Finland, the later part of the Subneolithic (~5000-1500BCE) and the start of the local Bronze Age (1500-500BCE) are characterized by a decrease in archaeological finds (~1900-1200BCE), perhaps reflecting a population crisis in the Baltic Sea region, the specifics of which remain unknown [17,146]. From around 1200BCE on, this apparent void in human agency was filled on the coasts of northern Estonia and southwestern Finland by burial customs and a material culture of Scandinavian or even north-central European origin [17,146]. The Finnish inland, instead, witnessed an earlier arrival of eastern influences from ~1400-1600BCE on, such as the Textile Ceramic tradition and the influx of metal works of the Ananino culture, which had their origins in the middle-Volga region, southwest to the Urals [147–150]. The people in the Volga-Oka and Kama River regions would likely have spoken a west-Uralic language that would later radiate and create several proto-forms of Finno-Ugric descendant languages along the route to Fennoscandia [146]. Although both Finnish and Saami languages belong to the Finno-Ugric family, the two speaker groups are ethnographically and genetically distinguishable, and are assumed to have arrived in the area of modern Finland successively [149,151]. Saami languages are descendants of a northern west-Uralic proto-language and predate the Balto-Finnic languages in Finland [151,152]. They gained agency throughout Finland and Karelia around 500BCE, after having separated from the proto-Balto-Finnic group around 1000-600BCE, perhaps somewhere between Lake Ladoga and Karelia [146,153]. The Balto-Finnic languages, in contrast, appear to have originated from a southwest-Uralic root [149,152]. Following a more southern route to northern Fennoscandia, they acquired proto-Germanic and proto-Baltic substrates absent from the Saami languages. Saami languages, in contrast, carry a substrate that cannot be found in the later-arrived Finnic languages, and may stem from the early contacts of the Saami language speakers with the predecessor groups of local hunter-gatherers [146,154]. Finding remnants of genetic ancestry from the earlier hunter-gatherer inhabitants in the gene pool of ancient individuals from Finnish burials would therefore not be unexpected. The process of the Finnic colonization that caused the Saami population to retreat to the northern part of Finland started around 1000 CE

and continued well into the early modern period, leaving both groups with some gene flow from each other, when compared with the rest of European populations [20,155].

1.2.2 Genetic past of Fennoscandia

Ancient DNA studies have illuminated the European prehistory, extending the achievements of classical archaeology to a new level of precision in addressing population histories. Although locally relevant details will continue emerging, the main genetic characteristics of Europeans have been streamlined by a wave of extensive studies on large-scale ancient human genome datasets [41,43,156]. Modern-day European ancestry has been found to consist of roughly three sources of ancestry: The Upper Palaeolithic hunter-gatherers that first populated the continent, the Anatolian early farmers from the Fertile Crescent that spread throughout Europe in the Neolithic, and the Pontic Steppe pastoralists of the final Neolithic to early Bronze Age, that caused a large population replacement in Europe, especially affecting the paternal Y-chromosome lineages [3,41,43,156–158]). The early northeastern hunter-gatherers harboured genetic diversity that can be defined as a mixture of western (WHG) and eastern (EHG) hunter gatherer types, along a rough borderline running between eastern Baltics and the central part of continental Europe [159–161].

The populations at the northern edge of Europe carry varying proportions of the same deeply diverged ancestries, but they also provide a more diverse picture especially on the early trans-Eurasian contacts [4,5,15,162,163]. In northeastern Europe, several Asian-derived ancestries from northern Siberia have arrived and mixed in. These Siberian type ancestries have since derived further, and are now maximised for example in Nganasan, Ket and Selkup populations [7].

Finland's geographical position at the crossroads of east and west has affected its genetic and cultural makeup in various ways: both local population structures and subsistence strategies appear to have been in flux until as late as the Middle Ages (in Finland 13th to 16th century CE) [164]. The local northeast-southwest distinction is observed in the gene pool of the modern population, illustrating the region's past as a cultural and genetic

meeting point. Archaeologically, different cultural horizons have alternated in dominance over the region, but the involvement of human migrations has so far little tangible proof. The overlapping Subneolithic cultures (CCC and CWC) have been attributed to separate population layers [17,143], backed by genetic studies elsewhere [4,6]. The Bronze Age brought about eastern influences such as Textile Ceramics (~1900-800BCE) and the highly specialized metal works of the Seima-Turbino phenomenon that spread around 2300-1700BCE, arguably manufactured and transported by a highly mobile trader-warrior entity that actively utilized the route across northern Eurasia all the way from the Russian Altai mountains to Fennoscandia [165,166]. The southwestern coastal areas and archipelago, in contrast, were inhabited by people with Scandinavian and Baltic burial customs, in specific [146,164], but whether these practices were adopted through the influence of many or few individuals is debatable [146]. Although archaeological findings alone do not prove the presence of genetic influx, at least some of the cultural novelties likely arrived with migrant people. It is also possible that their genetic heritage remained in the local gene pool up until the late Iron Age but has since been diluted by the unifying Scandinavian and central European colonization movement and the more recent merges with the global human variation. Today, the most northern part of Finland in particular, is inhabited by the indigenous Saami people. The area they inhabit transcends the borders of modern Russia, Norway, Sweden, and Finnish nation-states latitudinally in the north. Historical sources suggest that roughly until the 1500's their settlements also included regions much more to the south [167].

1.2.3 Significance of the local uniparental lineages

Human migration events are often characterized by uneven proportions of the two biological sexes, and thus the uniparental approach occasionally reveals a separate narrative from that of the autosome-based investigations. A large body of earlier research on human population history has relied on maternal lineages represented by mitochondrial genomes [11,42,44,168–170]. For instance, the seemingly homogenous Upper Palaeolithic and Mesolithic hunter-gatherer groups could be distinguished with ancient DNA through their maternal lineages, which revealed genetic bottlenecks and replacement events in their populations during the Late Pleistocene [44]. Respectively,

Y-chromosomal haplogroups have proven informative in characterizing the genetic turnover in European paternal lineages in the wake of the massive Bronze Age migration of the Yamnaya people from the Pontic-Caspian steppe: the event resulted in the spread of the eastern type Y haplogroup R1b that had originated in the Black Sea region ~5000BP [41,171]. The genetic ancestry described in the Yamnaya and their contemporary populations on Eurasian Steppe had an indirect route to Fennoscandia, where these Y haplogroups now also reside. Other major Y haplogroups in the area point to a more northeastern origin, such as N1c1, which is most prevalent today in northern Eurasia, especially among the speakers of Uralic and Baltic languages [7,8,16,33]. This Y haplogroup is now rare elsewhere in Scandinavia and hardly existent in central Europe [7,33]. A manifestation of Scandinavian or northern central European influence from Palaeolithic to Bronze Age is also present in the Fennoscandian gene pool as a third locally well-represented Y haplogroup, I1 [146,172].

Most of the early European hunter-gatherers are characterized by the mitochondrial haplogroup U. Its sub-groups, U2, U4, U5a, U5b, and U8 have prevailed in varying proportions among the later Fennoscandian populations [4,5,7,8]. Apart from early Russian individuals, haplogroup U2 was found in the Mesolithic site of Motala, Sweden, [11,173,174]. Russian foragers and hunter-gatherers of the Eastern Baltic regions commonly possessed haplogroup U4, still present in the southeast Baltic Sea region and Scandinavia [11,174–176]. In central and southern Europe, farming-associated maternal haplogroups that originated in the Neolithic Anatolia were first described in ancient individuals found with Linear Pottery [177]. They carried haplogroups such as H, HV, V, K, J, T2, X, W and N1a, and little to none of the U lineages [146,168,178,179]. Among other lines of evidence, the maternal diversity strongly testified for the demic diffusion combined with the spread of agricultural innovations in Neolithic Europe. In Northeast Europe, the diminishing of hunter-gatherer lifestyle and the advent of agriculture happened later and in a more gradual manner since the harsh environment necessitated retaining both subsistence strategies side by side [146,180,181]. In northern Europe, the concept of animal husbandry and small-scale farming was likely introduced by the Corded Ware culture that carried with it maternal lineages I and T, along with the typically Mesolithic East-European groups U2, U4 and U5a [4,180,182].

In modern Finns, the commonly observed haplogroups are mostly similar to those in the rest of Europe, although also Asian haplogroups D and Z are represented. Sub-groups of the mitochondrial lineages differ from the European average. Altogether 23 mitochondrial sub-haplogroups can be considered Finn-typical, in that Finns constitute a large majority of their carriers on a global scale [183]. U4 haplogroup is existent only in small proportions in Finland, and very rare in all Saami [155,184]. U5b and V haplogroups are particularly typical for the modern Saami, together comprising over 90% of their maternal gene pool [184,185].

1.2 Health in Finnish history

1.2.1 Infectious diseases in pre-modern times

Genetic, cultural and geographical transitions in human history have all influenced the prevalence and spread of pathogens, as showcased by an increasing number of aDNA studies [92,94,100,102,105,186]. The success of a pathogen is usually dependent on its capacity to adapt to the host's immune responses and to other microbial agents sharing the host pool or, in the case of coinfection, the individual host. Additionally, pathogens are affected by environmental changes, such as host or vector ecology and climate [187]. The spread of infectious diseases is often heavily dependent on the size of the host populations [29,187,188]. For instance, it is estimated that typhus requires a minimum population of 200.000 human individuals to develop an endemic prevalence. For smallpox, even a slightly smaller host community is sufficient [189,190]. Most human pathogens in the past had little to gain from extreme virulence, since in the time of small hunter-gatherer populations, lethal infections could easily wipe out their entire host reservoir [189]. Leprosy, for instance, may take decades to develop and transmits mostly in persistent contacts, like families living in close quarters. Some relatively harmless or often subtly manifesting diseases, such as sexually transmitted HBV (hepatitis B virus), also flourished in the early human communities [190,191]. This situation has, however, changed drastically since the remarkable increase of sizable human settlements and domestication of several animal species that facilitate continuous zoonotic events [192]. A first global population growth surge was triggered in the wake of the invention of farming, starting from the Middle East around 10 kya [193,194]. Another growth wave of

large magnitude started around 500 years ago, when the European population reached a steady state of prosperity and began a worldwide colonization [195]. The migrations and explorations in search of new inhabitable land have created networks that benefit human societies, but also open routes for rapid pathogen transmissions and provide to more aggressive pathogens a global human host reservoir [187,192,196]. Some of the most notorious population recessions we know in human history have been caused by aggressive epidemics in the historical era, such as the Black Death that cost the lives of up to half of Europeans in the 14th century, and the extensive destruction the European expeditions caused to the indigenous American populations in form of myriad of diseases after Columbus' discovery of the New World in 1492 [29,195,197–199].

Many bacterial pathogens have an ability to change genetic material through horizontal gene transfer followed often by recombination [139,200]. Circumstances promoting such events, such as high host mobility that enables distribution overlaps and coinfections, serves to boost the spread of virulent species [140,201]. Treponemal diseases, for example, are known for their various manifestations and seem to have successfully adapted to the changes in human behaviour, perhaps utilizing the flexibility of this strategy [202–204]. The venereal syphilis epidemic in the 1500's started as a rapid and violent wave that most certainly necessitated global mobility and large, connected host populations. However, it reduced in virulence soon after, and has since established its worldwide existence, aided in part by its properties as a "stealth pathogen" that often has symptoms resembling those of other diseases [205–207]. The endemic types of treponematoses, in turn, have potentially coursed through the early human populations in a more subtle manner, ending up on most continents of the world together with the human colonisations [208,209].

The northernmost regions of Europe raise interesting considerations regarding the historical epidemics. The sparsely populated North had few large cities and international trading posts in comparison to the rest of Europe, and many diseases reached there relatively late [29,210]. It has been estimated that with an exclusively hunter-gatherer type of subsistence strategy, the current area of Finland would have been able to sustain a population of merely 10.000 inhabitants [211]. The first significant population growth dates as late as in the 16th century, when most of the farming-amenable land in Finland had finally gained permanent settlers [212,213]. Kallioinen, who has summarized

literature on infectious diseases in pre-industrialized Finland, notes that before the post-medieval population growth, many epidemic diseases would not have been able to disperse beyond individual households or villages [29]. One example is the medieval epidemic of bubonic plague that swept over most of Europe starting from 1347. Norway, Denmark and Sweden were among the last countries to be affected, whereas Iceland and Finland completely avoided the scourge at its first instance [199,214,215]. Plague continued to cause occasional outbreaks in the following centuries, and eventually caught up with the North; The first occurrences are estimated to have reached Finland at the end of 1300's and a severe local epidemic was recorded in Iceland in 1402 [199,215]. Other infectious diseases, such as leprosy and tuberculosis have likely been endemic to the north as well as the rest of Europe already for centuries [85,95,216]. Their prevalence is hard to date, since early written records are often few and far apart -in Finland, they only start at the time of Swedish reign, once the public health college was founded in 1721 to record and maintain the health of the people in Sweden and its colonies [29,217]. Smallpox, one of the major scourges Europe-wide before dr. Jenner's inoculations leading to successful vaccination routines in the 1830's, appears in the Finnish documentation only in the 1700's, although it has likely been around in the North once the population size allowed it to establish endemicity [29].

Rural areas were often spared of diseases that were common in the urban environment, except for towns that provided transit hubs for trade or other traffic [29,218]. Dense living conditions, animals kept inside human housing and generally poor hygiene in the cities contributed to the outbreaks of diseases from spoiled food and contaminated water sources, such as cholera, but also boosted epidemics of infectious diseases that transmitted in contacts between people and via animal vectors [190,218–220]. Different diseases also drew attention in the past: Typhus and smallpox, for instance, recurrently spread in children, which apparently made them less noteworthy in the times when infant mortality was generally high. Sexually transmitted diseases were granted more attention, since these were considered avoidable and depended on the morals and behaviour of the adult population, a topic already broadly discussed among the contemporary medical professionals and the upper classes. The spread of syphilis was clearly associated with urbanization [29,221], although this may have been partly due to the treponemes' adaptation, namely the replacement of the nonvenereal transmission

strategy in favour of the venereal form [209]. Sexual behaviour could be kept relatively anonymous in the cities compared to the socially restricted life in the rural communities, which provided an outlet for the venereal pathogens to flourish [29,209]. Marine ports were notoriously affected, due to the trading ships that carried goods and diseases alike [29,222]. Later the same effects were documented from the connective hubs for the growing railway networks [29,218,223]. Although city-dwellers would often have better access to doctors' services, and in time the hygiene improved as well, the available remedies were not effective and could not seriously hamper the major infectious diseases before the development and popularisation of the first antibiotic treatments in the first half of the 20th century [29,224]

1.3.2 Early modern period -new arrivals

The early modern period witnessed the emergence of many novel infectious diseases and marks the final times before the microbiological revolution that revealed the integral connection between bacterial and viral agents and infectious diseases during the 19th century. People in pre-modern communities had suffered from diseases that seemed to be slowly receding in the early modern period [29]. For example, the prevalence of leprosy had diminished already for a time, for reasons that are still debated -one of the suggested dynamics indicates a competition between leprosy and tuberculosis that would have continued in Europe throughout the 18th and 20th centuries [29,225]. Indeed, contracting tuberculosis appears to give the patient partial immunity to leprosy, whereas the contrary case does not have such an effect [190]. With the scientific worldview gaining in popularity, doctors started employing more reliable cures for the contemporary illnesses, such as chinine in the treatment of malaria. These remedies would still be used in parallel with treatments that were based on barely more than superstition [29,226]. In Finland, the first common healthcare was introduced in the 1700's by the Swedish Medical College, and parishial doctors were stated [227,228]. In time, these doctors became respected as educators and influencers that reported national health issues and developed several improvements: They worked as active correspondents between the Northern governments and their peers in the continental Europe, establishing novel treatments and advanced diagnoses [226,227].

One of the first diseases to get official attention from the Swedish Medical College as a common health issue was syphilis, known at the time just as "the venereal condition" [29,190,222]. It was at times likely mistaken for either gonorrhoea or leprosy, but according to several 18th century medical reports, the most experienced doctors could routinely tell these diseases apart [190,226,229]. People suffering from syphilis were given priority in hospitalization. In fact, many hospitals were founded with this primary function in mind [29,190]. Since the only known treatment before the invention of arsenic-based Salvarsan [230,231] were mercurial treatments, the cure was in fact more likely to poison the patient than to rid them from syphilis [222,232]. The stages of syphilis were poorly understood, and the latent periods of the disease were likely often interpreted as recovery [190,226]. Officials controlled the communities to track the contagions and hospitalized the individuals with recognized cases, targeting prostitutes and other "women of ill reputation" in particular, as well as sailors and wandering peddlers [190,222]. Although somewhat discriminatory from a modern point of view, the practice kept many of the infectants separated for a time, and probably had a constraining effect on the epidemic. Especially wars and increased mobility through construction of railroad routes caused the occurrences to escalate [190,222]. It was documented that in 1905 all 1,014 sickbeds reserved for venereal disease patients nation-wide were filled, and that one third of the psychiatric patients in Finland were committed due to the paralysis and mental impairment involved with syphilis [29]. The Finnish civil war in 1918 and the two World Wars lifted the rates of gonorrhoea to its historical peak in 1945, and the rates of syphilis infections made their respective record the next year [222]. Remarkable improvements were observed in the 1950's, after the invention of penicillin treatments. However, since the 1960's, European population has entered an era of post-war financial prosperity enabling global travel and simultaneously assumed relatively free sexual behaviour, further enhanced by easy access to hormonal birth control and better cures to life-threatening sexually transmitted diseases such as HIV/AIDS [217,233,234]. These medical advances, although generally beneficial to public and personal health, have also initiated a new, considerable rise in venereal diseases, some of which currently show the ability to generate antibiotic resistance [235,236]. The improved understanding of ancient diseases and their dynamics with newly emerging pathogens is one of the central motivations in ancient DNA studies and can prove remarkable help in establishing prevention strategies in the future.

1.3.3. Ecology and aetiology of *Treponema pallidum* bacteria

Treponemes are spirochete bacteria that can cause a variety of diseases in humans and other mammalian hosts [237–240]. Most of the human-infecting treponemes belong to the *Treponema pallidum* subspecies, such as *T.p. pallidum,* causing syphilis, as well as *T.p. pertenue* and *T.p. endemicum,* causing yaws and bejel, respectively [237–240]. The modern subspecies have mostly separate geographical distributions [240,241]. Yaws is typical for tropical and subtropical regions and bejel for hot and arid environments, whereas syphilis is globally present. Out of the three above mentioned causative agents, only the syphilis-causing *T.p.pallidum* is known to mainly transmit through sexual contact. It can inflict damage to both soft tissues and bones and, if left untreated, it may spread to the nervous system, cause mental impairment and loss of mobility and body control, and even result in death [242]. The endemic treponematoses, such as yaws and bejel, are mostly manifested in ulcerations on skin or mucous membranes but can also affect bones [240]. Endemic treponematoses are often contracted while using shared utensils, smoking equipment etc. [240], or in childhood while playing and sharing close living quarters [240]. It has been speculated that in the colder climates where children are more often clothed, this transmission route would have been disadvantageous for the pathogens, which would explain their modern-day geographical distribution [208,243,244]. Congenital transmission from mother to foetus during pregnancy or childbirth is typical for syphilis, yet rarely encountered in the cases of endemic treponematoses [208,240,245–248]. Syphilis is most recognized as a re-emerging threat to human health [244], but all of the treponemes are continuously reappearing in the modern human population, despite antibiotic treatments and eradication campaigns [234,249]. Treponemal diseases have reservoirs in non-human primates, and strains infecting monkeys often come to close contact with humans as well, further disrupting the eradication efforts [250,251]. Both bacterial adaptations and human behaviour have been shown to increase the spread of treponematoses. Recently, most of the globally dominant strains of *T.p.pallidum* have proven resistant to second-line antibiotics, while still responding to penicillin treatment [252–254]. Similar development is also observed in the endemic treponematoses [255–258]. Uninformed sexual behaviour has led to an increase of syphilis in the first world countries, while the developing countries suffer

from more rudimentary testing facilities and insufficient access to treatment, making them vulnerable to all treponemal diseases alike.

Treponemal spirochetes are notoriously hard to culture *in vitro* [242,259–261], and much of the evolution and functional mechanisms of the bacteria remain to be revealed, although some have been explored [262–266]. Recent genomic studies on modern treponemal agents have, however, increased taxonomic information on the diversity of treponemes and contributed to the theories regarding their functional genomics and cladal divergence [204,254,267–271]. Previously ambiguous categorization of Treponema pallidum into three main subspecies has found grounds in the phylogenetic analyses, and syphilis-causing strains follow a dichotomy specified between the globally dominant SS14 clade and the Nichols-type clade, mostly found in North America [254,269,272]. Findings on putatively important gene groups continue to date, improving the understanding of differences in the pathogenicity and ecology of the subspecies [202,203,267–269,273,274].

Treponemal diseases typically develop through several stages, where active infections are intercepted by long periods of latency [242,275]. Some characteristic bone changes used in osteological analyses of archaeological material, such as the "moth-eaten" appearance of the parietal bone, and the gangosa that afflict extensive destruction to the facial bone and cartilage, are usually the result of the later stages of disease [242,249]. Other bone deformations associated with treponemal infections include "sabre shins", caused by the abnormal new bone formation that results in sharp anterior bowing of the shinbone, and abnormalities in development of the permanent teeth. All these changes can be visible post-mortem, although their severity varies, and at times they can resemble marks caused by other diseases [276–278].
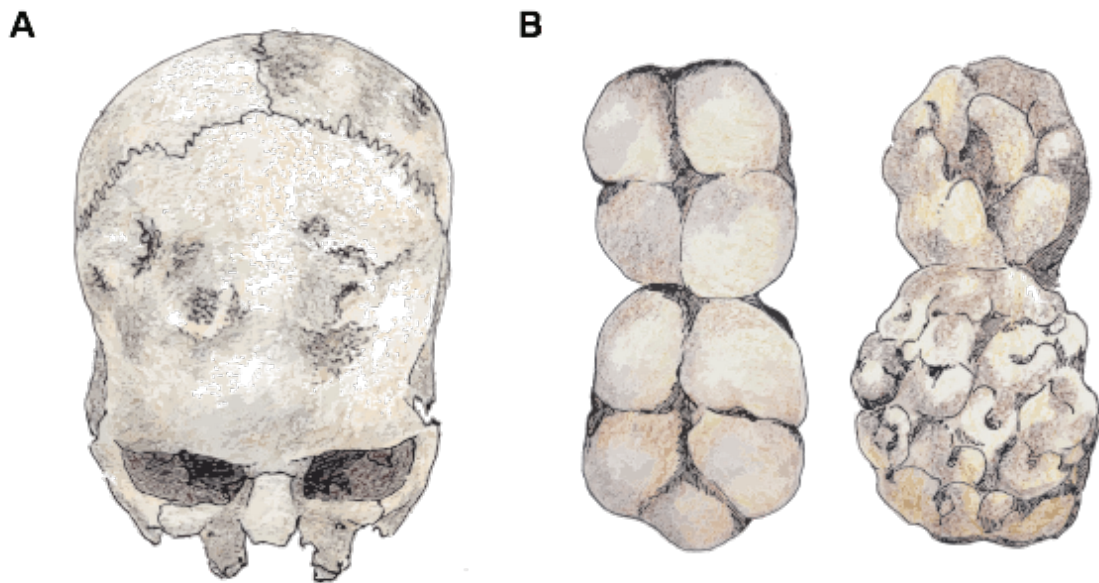
Figure 3. Characteristic bone alterations caused by treponemal infection: A) pits and "moth-eaten" patches on cranial bones, B) normally developed molars with 4-5 cusps, compared to "Mulberry molars", characterized by small, irregular cusps.

Some skeletal characteristics have been used in telling apart infections caused by the different Treponema subspecies. However, many studies have called in question their diagnostic precision and it appears the marks manifested in several treponemal diseases are often virtually indistinguishable [101,278–280].

Especially since treponematoses are hard to tell apart according to the physical pathologies, the known putative historical cases call for ancient pathogen DNA techniques to resolve the aetiology of the causative agents [237,279,280]. In the Americas, prehistoric remains are frequently found with typical treponemal lesions [281]. In Europe, the reported cases are few and far apart [282,283] and no secure dating or genetic evidence exist to confirm their presence before the turn of the 16th century [221,278]. The situation has long sustained the popular hypothesis that syphilis arrived in Europe from the Americas with Columbus and his crew [278,279]. Columbus' American expedition indeed correlates well with the first European epidemic starting in the wake of the Neapolitan war in 1495 [205,284], after which the disease rapidly spread with the mercenaries to their homelands, and was known across the continent by the end

of 17th century [221,278,285]. An alternative theory, however, suggests syphilis or similar diseases already resided in Europe. The sudden emergence of an extremely aggressive form of syphilis at the start of the 1500's could be explained with either biological adaptations of the pathogen, or simply with an assumption that the pre-16th century diagnostics had described the disease inaccurately [208,286–288]. The latter claim has provoked strong criticism, since many other Old-World diseases had been diagnosed without problems for several centuries, although medieval nomenclature was notedly inconsistent and prone to misunderstandings [221,286,289].

Apart from syphilis, some historical records also exist of the presence of endemic treponematoses in Europe: especially virulent outbreaks are documented locally from the 17th to 19th century Scotland, Ireland, Sweden and Norway [290–296]. These epidemics affected the poor people of the rural areas in particular. Contemporary physicians presumed cases of coinfections between the known treponematoses, connecting the virulent outbreaks with parallel spread of yaws and syphilis, although the two diseases had notable differences in manifestation and the latter was more commonly found in the urban environment [291,293].

The question of treponemal agency and potential origin in Europe seems an ideal case for ancient DNA research; treponemal diseases leave marks in bones, ancient skeletal material from all continents exists, and modern diversity of treponemal pathogens has been subject to several detailed whole genome sequencing (WGS) studies [204,248,254,267–273,297]. The task of retrieving ancient treponemal DNA is, however, ridden with complications that have until only lately made it infeasible [298,299]. One of the most persistent problems is that the notable bone deformations only appear at the late stages of the disease [298,300]. The inflammatory response that causes the necrotic bone lesions is commonly followed by treponemes retreating in the soft tissues, where they can remain latent for years. At the time of death, the bacterial load in bones and thus the amount of treponemal DNA might be too small to detect. Carefully conceived sampling strategies can, however, assist in dealing with these complications, as showcased in paper III of this thesis, where sampling from remains with active infections and those of a prematurely born infant yielded positive results for treponemal ancient DNA.

2 Thesis objectives

In this thesis, the northeastern European past is studied through ancient DNA analyses of skeletal material comprising archaeological remains from Finland and geographically surrounding regions. The main goal of the thesis is to provide novel information of the past genetic structure and connections of the human populations inhabiting this region through time, conditions in which they lived and challenges they experienced with their health.

Papers I and II study the change in the northeastern European human population structure through time. In paper I, an Iron Age Saami-like population with a large Siberian genetic component showcases a population from the transition gradient towards the modern northeast-European type of genetic mixture. In paper II maternal lineages point to a possibly underlying early hunter-gatherer ancestry layer, with haplogroups common in the Comb Ware Culture groups in Bronze Age Estonia and Baltic regions [4,6].

Paper III raises a subject of historical spread and diversity of *Treponema pallidum* bacteria, the causative agent of syphilis and other treponematoses. The reconstructed pathogen genomes show an overlapping distribution of ancient treponemes in the nordic countries, namely Finland and Estonia, and the Netherlands in the early modern period. The study also ties to the more general questions on the origin of the treponemal diseases by presenting the first genetically detected ancient treponemal DNA from the European continent.

Chronologically, the thesis follows genetic evidence of populations from the Bronze Age, Iron Age and Middle Ages to early modern period populations. In Finland, it addresses the Iron Age Ostrobothnian population of Levänluhta with genetic association to the modern indigenous Saami people and an early Siberian ancestry. From the Iron Age (Crusader period to Middle Ages) and early modern period individuals, mitochondrial genomes are inspected for signals of incoming gene flow from both east and west. Finally, the infectious agents of syphilis and another treponemal disease, yaws, are described from the urbanizing environments of early modern northern Europe, together with a previously unknown, extinct treponemal strain from the Netherlands.

3 Results

3.1 Ancient Fennoscandian genomes reveal origin and spread of Siberian Ancestry in Europe (paper I)

Synopsis

In this study, ancient genomic data was analysed from 11 individuals from Finland and Kola peninsula in northwestern Russia. Analyses including Admixture, f3 and f4 statistics and admixture-induced linkage disequilibrium analysis (Alder) were used to characterize a specific genetic component in northern Fennoscandia and trace it back to migrations from Siberia that began at least 3,500 years ago. The study goes on to show that this kind of Siberian ancestry was subsequently mixed into many modern populations in the region and is particularly common in populations speaking Uralic languages today. In the more local scale of past Finnish populations, it gives evidence to ancestors of modern Saami having inhabited a larger territory during the Iron Age than today. The observations support the linguistic hypothesis of Saami-speakers dominating the current region of Finland before 1000 CE.

3.2 Human mitochondrial DNA lineages in Iron-Age Fennoscandia suggest incipient admixture and eastern introduction of farming-related maternal ancestry (paper II)

Synopsis

In this study, 103 complete ancient mitochondrial genomes from human remains dated to 300–1800 CE were explored to investigate mtDNA diversity in Finland. The results suggest eastern introduction of farmer-related haplogroups into Finland: Analysis of the prehistoric samples from Iron-Age and medieval sites from western and eastern Finland revealed a high overall prevalence of haplogroup U in southwestern sites, and a high frequency of haplogroup H in the east, opposite to the contemporary genetic patterns in Finland. Moreover, the notable differentiation between the ancient sites suggests

relatively isolated or well-defined territories inhabited by contemporary groups and possibly defined by the subsistence strategies. The largely unadmixed mtDNA pools from Iron Age on point to a relatively late genetic shift from hunter-gatherer type of maternal ancestry towards farmer-associated ancestry in northeastern Europe. The data in this study represents the largest collection of individuals from Finland so far analysed for ancient human DNA.

3.3. Ancient bacterial genomes reveal a high diversity of Treponema pallidum strains in early modern Europe (paper III)

Synopsis

This study presents the first genetic data of *Treponema pallidum* from historical Europe. We could show several different strains of Treponema, related to both venereal syphilis and yaws, being present in northern Europe in the early modern period. The currently known types of treponematoses observed in this study have existed in parallel in the far northern regions of Europe, suggesting a possible Old-World origin for their ancestral forms. We also discovered a previously unknown *T. pallidum* lineage recovered as a sister group to yaws and bejel. Our findings implied a more complex pattern of geographical distribution and aetiology of early treponemal epidemics than previously understood and challenged the view of the Americas as the source of the first European epidemic of syphilis.

4 Discussion

4.1 Challenges of an archaeogenetic approach in Finland

Finnish archaeology has employed remarkably few genetic techniques until now, although elsewhere in the Nordic and Baltic countries the trending of the archaeogenetics field has resulted in high-quality publications and successful innovations in assessing the prehistoric periods of the region [2,6,10,180,182,301–303]. Reasons for the aDNA research shortage in Finland vary from few funding opportunities and lack of resources to environmental and weather conditions, discussed in the following section.

One of the most acknowledged complications for successful aDNA work in Finland is the highly acidic soil, which dissolves the structure of the bone tissue itself. In most cases, even otherwise rich burials have mostly or completely lost the skeletal material, which instead is abundant in the contemporary graves from other parts of Europe. The aDNA studies on Finnish materials are thus limited to the last two millennia. Accordingly, this thesis mainly centres around periods from the Finnish Iron Age (500BCE to 1300CE) to the early modern era (1500-1800 CE). An exemplary case is provided by the Merovingian and Viking period graves of Luistari, from where 27 individuals were originally included in the paper II of this thesis. These graves, known for their many burial goods and various preserved materials yielded only a few fragmentary pieces of crumbling bone tissue, whereas contemporary findings in Sweden, Northern Germany and Iceland [2,5,10,113,304–306] are morphologically well preserved, although contain varying amounts of ancient human DNA. The surviving samples from the Luistari site contained between 0.0001 and 0.23% of endogenous human DNA on average: remarkably little, and mostly insufficient for nuclear DNA studies. It has been stated that mitochondrial DNA is not only more abundant within ancient samples due to its many copies per cell, but also behaves differently from the nuclear DNA, with its degradation depending rather on the environmental conditions than age of the specimen *per se* [75]. These factors may in part explain why obtaining mitochondrial (MT) DNA was clearly more successful for this site. Finally, 14 out of the 27 samples were included in the ancient mitochondrial study after MT genome targeted enrichment [307].

The water burial of Levänluhta which I address in the paper I, forms an interesting exception to the previous observations. The population represented a culturally enigmatic group, for which there are no known later counterparts. The burial custom is also rare: apart from the Käldamäki burial geographically close to it, Levänluhta is the only water burial known from prehistoric Finland [308]. At the bottom of the bog, which was probably a small lake at the time of the burial, was anaerobic, dense clay that had preserved the bones to an exceptional extent [309]. Such burial practices could present better opportunities for ancient DNA sampling in Finland. Unfortunately, even if the water burials were more common than we currently know, finding similar sites is unlikely, since most natural bogs have been taken into agricultural use. Thus, much like in several cases of cremations under level ground [308,310], later practices of land usage have likely destroyed any ancient remains residing in them. Even cremation burials with preserved bone material, common up to the late Iron Age and Christian era, are problematic for genetic analysis since DNA is denatured by the heat of the burning. Although some applications have been attested to retrieve ancient DNA from burned human bone material, and specialized aDNA methodology shows promise in the use of forensic genetics [311–313], these attempts have not so far convinced the archaeogenetic field of the feasibility of such efforts. In paper III, where the pathogen DNA was concerned, the Finnish samples chosen showed excellent preservation. This is not surprising, since the archaeological sites were relatively recent. Additionally, in the case of the Turku individual found positive for yaws infection, the remains had been stored in a crypt since the excavation, in a stable environment and without much handling, and thus may have restored more integrity than samples embedded in the ground.

Another issue for the locally conducted aDNA work is a lack of facilities that would fulfil the strict criteria required for ancient DNA studies: real-time PCR commonly used in genetic laboratories produces large quantities of modern DNA molecules that persist on surfaces and equipment, causing a risk of contamination if subsequently used for aDNA research. Specialized air conditioning and direct UV-light are mandatory to minimize the contamination from modern sources and across the samples. Apart from a few specialized one-room spaces, the currently existing laboratories have been financially hindered or technically limited from establishing a fully functional ancient DNA facility that would entertain both the required capacity and expertise. Future investments may

remedy this austerity, provided that more attention is drawn to the budding ancient DNA field in Finland.

My research during this thesis was conducted as a multinational collaboration between the Universities of Helsinki and Turku in Finland, University of Tübingen and Max Planck Institute for the Science of Human History in Germany, and University of Zürich in Switzerland. This work provides a wide survey of different state-of-the-art applications, remarkably expanding the knowledge on opportunities and challenges involved in applying aDNA methodology to Finnish context and providing a functional basis for future studies on the local archaeogenetic materials.

4.2 Methodological applications (papers I, II, III)

4.2.1 Sampling strategies

Since the circumstances in the initial burial, excavation, storage, and physical studies can significantly affect the quality of the aDNA in the archaeological samples, sufficient attention should be appointed to the sampling strategies in the archaeogenetic research design. The material used in my thesis stemmed from several different types of environments. The sampling strategies varied accordingly between the three studies, yet in all cases, the selected samples underwent a process of screening for both endogenous human DNA and possible pathogen content. The studies in this thesis finally included altogether 222 samples. The archaeological collections from Turku, Porvoo, Hamina and Renko excavations represented relatively recent populations (16th to 19th centuries). As individuals from the early modern period were expected to genetically resemble the modern population to a great extent, the samples were chosen with palaeopathological research in mind. The number of individuals selected from these sites was generally lower than required for a comprehensive population genetic study. The Turku, Porvoo and Renko individuals showed physical marks of infectious diseases such as lesions, deformations, or new bone formation indicative of inflammation, whereas Hamina samples represented a mass burial with an unusually high proportion of children and young adults [27]. The Iron Age to medieval burial sites, Luistari (600-1300 CE), Tuukkala

(1200–1400CE), Hollola (1050–1400CE) and Hiitola (1200–1500CE) bore more interest for possible population level changes. The samples from these sites were generally poorly preserved, presumably due to the soil environment of the locality. This, together with the research questions regarding human population history, supported a wider sampling strategy (N=18-32 per site). Levänluhta sampling diverged from the strategies above, since the tooth samples available were from a preliminary study made in 2011. At that time, the DNA yield from the samples was insufficient for detailed downstream analysis. The aDNA techniques such as targeted enrichment of mitochondrial genomes and informative markers for nuclear DNA had, however, been optimized by the start of this thesis, enabling a successful resampling and analysis of the same material.

As no previous publications existed on ancient DNA from mainland Finland, the paper I of this thesis was pioneering in proving Finnish archaeological material as a feasible source of aDNA. The Iron Age Levänluhta remains represented exceptional DNA preservation, apparently due to their unusual deposition in the anaerobic layer of clay at the bottom of the lake used for the burial. Earlier studies had suggested that the burial might have harboured plague victims [314,315], since radiocarbon dating showed an overlap with the Justinian plague in Europe ca. 542-590 CE [316,317]. Pathogen screening was conducted on the samples, but despite the relatively abundant yield of the human DNA, no bacterial pathogens were recognized from the material. The increasingly feasible detection of viral agents [136] may yet provide another potential line of investigation for pathogen content from this site.

The sampling of the paleopathologically assessed early modern period sites included altogether five individuals with visible marks of treponemal infections, one of which I was able to genetically confirm in the paper III: a case of yaws in an adult individual from the Chapel of Holy Ghost, Turku. The preservation of the aDNA in the sample may have benefited the remains being stored in the relatively cool and dry environment of the chapel's crypt. Furthermore, congenitally contracted venereal syphilis was found in a prematurely born foetus from the Porvoo Cathedral cemetery. The foetus showed only mild inflammatory alterations on the surface of the bones and was mainly selected based on the documented tendency of syphilis to cause spontaneous abortions and premature births. The remarkable 136-fold genomic coverage of syphilis-causing bacteria,

Treponema pallidum ssp. *pallidum* in the foetus showcased how the congenital syphilis may penetrate even the most compact skeletal elements, such as the petrous bone sample we analysed for this individual. The two other treponemal cases I analysed for this study, one from Estonia and one from the Netherlands, proved for the first time the feasibility of successful sampling from the active treponemal lesions on different skeletal elements and stages of the disease. Finally, the diversity found among the genetic lineages recovered from our four positive samples demonstrates the difficulty of diagnosing the treponemal subspecies based on osteological observations alone and the benefits of the aDNA approach here applied.

4.2.2 Authenticity

Ancient DNA authentication is commonly based on the amount of hydrolytic damage in the form of a misincorporations of thymines instead of cytosines, accumulated at the ends of the DNA fragments. Once the authenticity of the aDNA is ensured in the screening round, the data quality for mapping and variant calling can be improved on a fragment level by producing new libraries with an UDG-treatment that removes the post-mortem deaminated bases entirely [318] or partially [319], using the uracil-DNA-glycosylase enzyme (UDG).

In the course of this thesis, it was noted that the bone samples from Finland showed very little of the hydrolytic deamination commonly used to authenticate ancient DNA samples. Previous studies have concluded that soil conditions the samples are subjected to, such as humidity and temperature, can cause different amounts of DNA degradation independent of their age [75,113,116]. To ensure that the low amount of damage did not in fact indicate modern contamination, all samples in papers I and II underwent additional contamination analyses via several available methods. The contamination estimates from the mitochondrial data produced by the Schmutzi program [320] and Contammix software [321] were compared with a meticulous manual investigation of individual mutations on the Geneious sequence analysis platform [322]. Schmutzi program produces two consensus sequences from sequenced reads mapped against the human mitochondrial reference: one for the likely true endogenous source and one for

the most likely contaminant. The program then gives the calculated proportion of the estimated contaminant in the authenticated sample sequences as percentage. Contammix uses a likelihood method with a Markov chain Monte Carlo (MCMC) algorithm that estimates the proportion of authentic mitochondrial sequence under a probabilistic model, where contamination is likely to rise from a dataset or 311 modern mitochondrial haplogroups. The mitochondrial consensus sequence that the programs deemed the most likely authentic one, was then run through two mitochondrial haplogroup finders, Haplofind [323] and Haplogrep2 [324] and compared between the tools to ensure an unanimous haplogroup assessment. As the conclusions within the paper heavily relied on the haplogroup assessments, the consensus sequences reconstructed for the mitochondrial genomes in each sample were manually processed in Geneious, where precarious deviations from the reference sequence were traced back and the read support was considered individually for each observed mutation. For the contamination of the nuclear data in paper I, a method testing for detectable heterozygosity on the X chromosome in males was used. Male individuals have only one copy of the X chromosome, and a signal for a second type of X chromosome is hence suggestive of contamination. The contaminating sample of either sex would be detected, as both kind of sources would contribute at least one extra X chromosome. This method was applicable for only three of the studied samples, as the rest of the individuals were female. The pathogen DNA recovered in the paper III was enriched for and showed no major contamination from external sources. Unlike some of the ancient pathogens, such as *Mycobacterium tuberculosis*, *Treponema pallidum* does not have close relatives among the soil bacteria and reads mapping to the reference genome showed high specificity to the targeted taxon.

4.2.3 Screening and enrichment in humans and pathogens

The standard post-sequencing workflow starts with a screening procedure that gives general information regarding the genetic content of the samples. The sequenced reads can be examined for human or animal DNA, or the possible pathogenic agents within the sample by mapping them to a reference genome of choice. To detect pathogen species or investigate the metagenomic content in a sample, the reads can be matched to a database

encompassing a large collection of microbial genomes. The bioinformatic programs continue to improve in sensitivity, allowing an increasing number of bacterial and viral species to be recovered from ancient samples.

In paper I, I used two capture methods to address the genetic past of the Levänluhta individuals. The mitochondrial capture was conducted first, showing haplogroups that exist in high frequency especially in the modern Saami and pointing to a common history between Levänluhta and the ancestral hunter-gatherer groups of the northern indigenous populations. Due to this finding, the geographically close Kola Peninsula groups from Bronze Age Bolshoy Oleni Ostrov and a more recent historical Saami cemetery were selected as comparisons for the whole-genome capture process that utilizes SNPs specific to select populations. This capture method enabled us to place the individuals in their unique genetic position as representatives of early Siberian ancestries, and clue us in the relations of the Bronze Age to Iron Age northern Siberian groups whose genetic inheritance has carried over 3.000 years to the modern northeastern Fennoscandia and Baltic region.

Although nuclear DNA provides a more detailed resolution and multifaceted information on the population level differentiation than the uniparental approaches, mitochondrial DNA remains the best-described and well-understood marker, and has power to reveal substantial population turnovers and gender related biases in population movements and migration patterns [44,168,169,177,325]. Mitochondria occupy each cell in multiple copies and mtDNA often preserves in larger amounts than nuclear DNA, albeit depending on factors like skeletal elements chosen for samples and environmental conditions of the burial [75,326]. In paper II, mitochondrial capture data harboured a unique picture of the Finnish past: the frequencies between farmer-associated and hunter-gatherer-related haplogroups observed showed opposite trends to that known today across the country, suggesting possible local migration patterns of women. More interdisciplinary research is, however, needed to understand the historical significance of this adversity. In addition, the U4 haplogroup found from ancient locations, now rarely met in Finnish population, points to a potential genetic vestige of the early hunter-gatherer groups that have so far been entirely unknown in their genetic attributes.

In paper III, a pipeline of screening steps was utilized to discover the samples positive for treponemal agents; the sequences were mapped against a bacterial database with a metagenomic analysis tool specifically designed for ancient DNA (MALT) [99,124] visualized in the metagenomic analysis application Megan [125]. The individual reads were investigated in respect to the reference genome within a genome browser IGV [327] and scored with the BLAST algorithm of the NCBI database [328]. The samples deemed positive in this evaluation were subsequently enriched for, using species-specific baits both in-solution and on an array [58,60]. The resulting genomic coverages varied greatly among the samples. The 136-fold genomic coverage of the most abundant treponemal sample would have allowed a positive recognition and genome reconstruction of the pathogen data directly after the initial shotgun sequencing. Conversely, the sample with the lowest coverage required three rounds and a combination of array-based in-solution hybridization enrichment to reach the final coverage of 47% 1-fold. The different volumes in the obtained DNA showcases the wide range of quality observed in ancient DNA samples and the innovative solutions frequently required in their analysis.

4.3 Ancient Fennoscandian populations (papers I and II)

In this thesis, I mainly focus on the eastern localities of Fennoscandia, namely Finland and northwestern Russia. The southern Baltics and Scandinavia, instead, are only covered in general sense, and where their influence on the target area is essential, since many previous studies have comprehensively addressed the genetic histories of these areas [3,5–7,180,182,302]. The same is exceedingly true for the early cultures of Pontic-Caspian steppe and the Black Sea region, as well as the far-eastern Eurasia [15,41,43,156,158,162,163,329–331]. All these groups have obviously provided much of the genetic influx discussed in this thesis, either as a constant, trickling gene flow or through larger migration waves to Fennoscandia. My research complements these studies by approaching the genetics of the early Finnish and eastern Fennoscandian populations and the rarely exposed cultural nexus between Scandinavia, Northeast Europe, and Russian Siberia west to the Urals.

4.3.1 Siberian ancestry in northeastern Fennoscandia

The two earliest sites addressed in the paper I, the Bronze Age Bolshoy Oleni Ostrov site in the Kola peninsula and an Iron Age water burial from Levänluhta, Finnish Ostrobothnia, showcase the layers of several eastern and southern types of ancestries in common, albeit dating almost 2,000 years apart. They both include a Siberian ancestry component that characterizes especially the individuals from the Bolshoy Oleni Ostrov but is also more dominating in the Levänluhta people's ancestry than in any of the populations we see today. The composition of the Bolshoy Oleni Ostrov genomes analysed here differs remarkably from the known ancestral groups: about half of their genomes consists of the eastern hunter-gatherer type ancestry found in several Karelian and northern Russian early individuals [11], whereas the other half comprises entirely the Siberian type ancestry, first described here for any ancient group. The people of this relatively secluded, arctic peninsula appear unintegrated by any farming and steppe pastoralist associated ancestries, already prevalent in many other contemporary individuals from more southern Russian cultures. Individuals from the Finnish Iron Age site of Levänluhta (400-800 CE) in the same study harbour a mixture of European hunter-gatherer and Anatolian Neolithic farmer-associated ancestries. Additionally, all Levänluhta individuals except for one carried the same Siberian type of ancestry that was observed in Bolshoy Oleni Ostrov. This similarity bears no proof of direct continuum between the Kola peninsula population and the inhabitants of Iron Age Finland. However, it does point to a common source contributing to the ancestry of both groups. The Siberian-originated genetic component is maximized in the modern population of Nganasan people residing at the Taimyr peninsula, at the northeastern end of the Siberian expanse. The genetic connection implies an earlier cross-Siberian width of one large genetic entity, or extremely far-ranging mobility that enabled physical contacts between the northern populations in the past. These findings provide a separate narrative from the events so far known from the Bronze Age trans-Russian cultures connecting the contemporary central European populations to the pastoralist populations of the Pontic-Caspian plains and give genetic support to the linguistic postulates of the potential Uralic speaker groups' arrival in Fennoscandia, next discussed in more detail.

From all the modern populations, the Levänluhta individuals mostly resemble the indigenous Saami. The Siberian ancestry component has been shown to exist in small amounts in most of the Northeast European populations, especially those speaking Uralic languages [7] with highest amounts of it present in the Saami people. As the more southern Russian groups from Bronze Age have not been found to be influenced by the Siberian type gene flow, it seems feasible that the Siberian ancestry has travelled roughly the same northwestern route to Fennoscandia than the proto-Saami language speakers are assumed to have followed, around the same time [146].

Although inferring the language of a past population based on material or genetic evidence is impossible, there are several points in the archaeology reported for the Bolshoy Oleni Ostrov site that would support their potential intermittent position on the transect between the Volga-Kama proto-Uralic speakers and the ancestors of Saami in the Baltic Sea region. The vessels found in the Bolshoy Oleni Ostrov burial context follow the tradition of textile or imitation textile impression ceramics, which coincides with the assumed proto-Saami speakers' move to Fennoscandia in both geography and time [146] and references therein. Furthermore, studies on physical anthropology have tied the Bolshoy Oleni Ostrov individuals to modern Ugric-speaking and Volga-Finnic populations [332,333] and an earlier ancient mitochondrial research to the western Siberian maternal lineages, as seen in their haplogroups C, D and Z [11]. The genetic links provided by our study give tangible support to both linguistic hypotheses of the movement and development of the Uralic language group, and the archaeological theories that associate population transitions with the material cultures found ranging from northwestern Russia to the Fennoscandian shores.
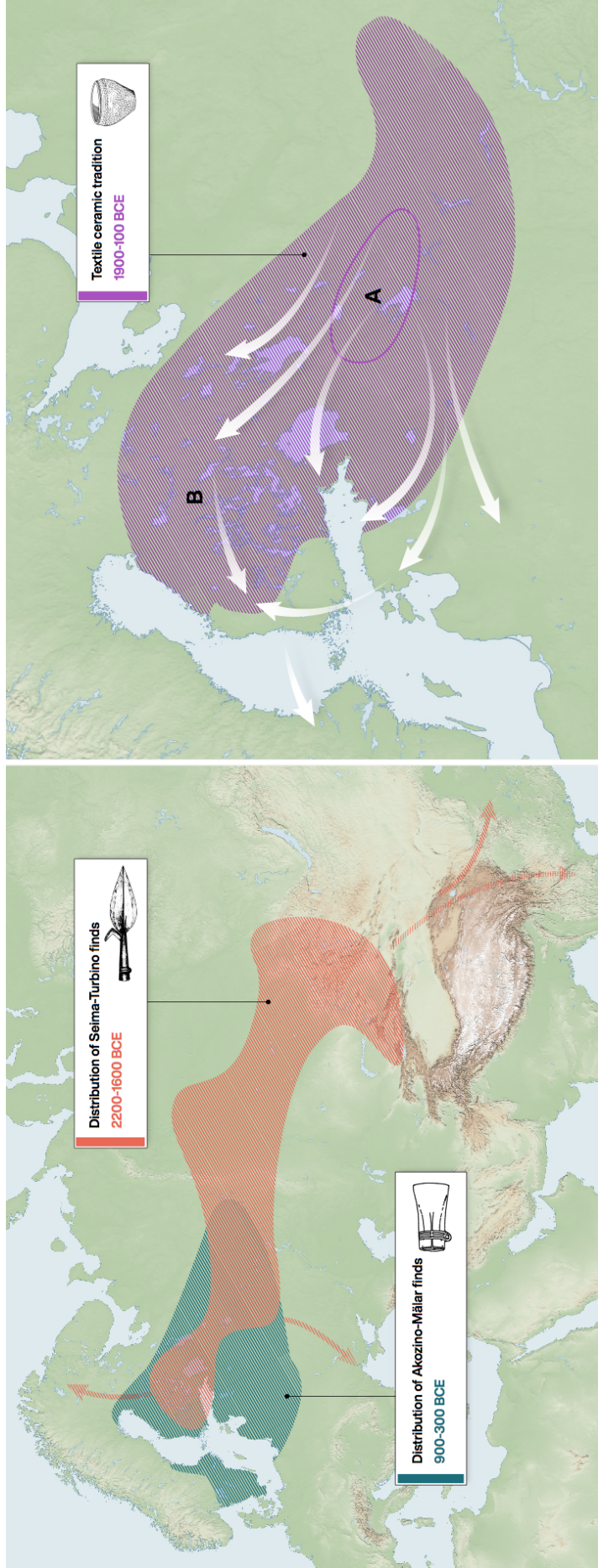
Figure 4. A map of major cultural influences originating in the Upper Volga region and represented in Finnish archaeological finds during Bronze Age and Early Metal period. Left: Seima-Turbino phenomenon (2200-1600 BCE) in orange, and Akozino-Mälar phenomenon (900-300 BCE) in green, both characterized by metalwork and style of weaponry. Right: A) Core region and B) the expanse of Textile ceramic tradition (1900-100 BCE), associated with the spread of Uralic languages. The suggested north-west and south-west routes of Uralic languages from Volga-Oka region to Fennoscandia marked in arrows. Adapted from Lang 2018 [146].

4.3.2 Finland in prehistoric time periods

The northern European denotation of "prehistory" includes all centuries predating the written documentation, which in Finland starts only as late as the final stage of the Iron Age, around the 1300's. The data presented in this thesis adds to the knowledge of the Finnish population before the formal start of the historical era, thus greatly contributing to the available means of describing the early events in the nation's past. The postulated territorial range of Saami-like inhabitants in the south of Finland receives support from the Ostrobothnian Iron Age Levänluhta individuals that share most of their ancestries with the modern Saami. Although the cultural aspects of the burial bear no similarities to Saami ethnos as such, and identities cannot be inferred from genetics, the onomastics and substrate theories discussed in the linguistic literature similarly hint to non-Finnic groups in the region until around 1000AD [152,334]. Coexistence of Finns and the indigenous Saami people has affected both groups, and these groups now resemble each other, albeit carrying some unique characteristics [20,155,335]. An exception in the genetic consistency of the Levänluhta group is a female individual that the analyses revealed as mostly resembling modern Icelandic and Norwegian populations in the nuclear DNA analysis. The same individual also carried an MT haplogroup K1a4a1b, whereas the other Levänluhta individuals represented Saami-like U5 groups. This individual demonstrates the mobility and southward connections of the Iron Age groups of Ostrobothnia, already suggested by the wide range of cross-Scandinavian and eastern European grave goods found in association with the Levänluhta burial. As a putative migrant, she may have lived her life amongst the Levänluhta population, especially since the radiocarbon dating did not deviate from the other local individuals, showing that her lifetime was contemporary to the rest of the group. Additionally, another slightly later published study including the same sample material showed Sr values which suggest a potential migratory origin for this individual.

Regarding the maternal haplogroup diversity, Levänluhta signifies its own entity, showing lineages both typical for modern Saami, such as U5b1b1a, and those absent or rare in their gene pool, such as U5a, K, T and H1. Apart from the U5 haplogroups that are especially common in Saami, we observed several cases of the haplogroup U4 in the late Iron Age sites, rarely found in modern Finns. This unexpected haplogroup was

interpreted as a plausible vestige of an older, non-Saami hunter-gatherer population layer in the southwestern Finland. The Saami-like groups have likely dominated the modern region of Finland from early Iron Age (locally starting ~500BCE) to roughly 1000CE [146,151] after which the subsequent Finnic-speaker migration started pushing them further north. The earlier populations that resided in the area are largely unknown, although linguistic studies have sometimes described them as speakers of the hypothetical Paleo-European (or West Uralic X-language), a language that has left a strong substrate to the current Saamic, in particular [152–154]. The findings pointing to their potential genetic ancestry in descendant groups are therefore an exceptional opportunity to speculate on the possible origin of these populations. The U4 haplogroup is still common in Volga-Uralic populations, and extant in eastern Baltics, for example in Latvia. This haplogroup has been connected with ancient hunter-gatherer groups in Scandinavia and Baltics and with the CCC across Europe [7,8,11,176]. Thus, theoretically, the Finnish U4 maternal lineages could span all the way from the Mesolithic to the Crusader period individuals. Since most of the clearly Baltic and Scandinavian archaeological influences are rather strictly restricted to the coastal area throughout the Bronze Age and early Iron age, the relatively inland location of the Crusader period sites with the U4 haplogroups, especially Hollola, could indeed insinuate an independent continuum from the hunter-gatherers, such as the Comb Ceramic groups, of which there are no previous genetic signals reported from Finland.

A related point of discussion is the arrival of farming and the potential demic diffusion associated with it in Finland. Whereas most regions in Europe adopted farming once the inventions of the required technologies were available, the same was not easily achieved in the Nordic climate. Indeed, in Finland the practice remained occasional and opportunistic throughout the Bronze Age and Iron Age, and many of the agricultural aspects such as metallurgy and burn-clearing appear to have followed complex routes and several directions in order to establish in the region [17,181]. Until now, the population genetic studies have been lacking means to confirm the archaeological leads from the material culture concerning these routes. Indeed, the more recent gene flow has all but certainly masked the vestiges from these early dynamics from observation. Our conclusions are based on the mitochondrial data alone, and a more detailed view for the sites will appear from the future nuclear studies. However, maternal lineages studied

here give indication that the early farming associated populations may first have arrived in Finland from the southeast rather than from the west: the ancient maternal lineages show a completely opposite trend between two major haplogroups, U and H compared to the modern-day population. Most U haplogroups, originally associated with the European palaeolithic hunter-gatherers, were found in the southwestern Iron Age to Crusade period graves. The eastern sites, conversely, possessed mostly variation of the haplogroup H, which elsewhere in Europe is associated with the early farmers, such as the people associated with Linear Pottery manufacture. The sites also showed statistically non-random separation of haplogroup frequencies from each other, pointing to locally segregated societies, which, although a presumed pattern, has previously lacked the genetic evidence. Moving from the Middle Ages towards the early modern period, the site-specific peculiarities disappear in comparison to the modern-day population. This observation illuminates the emergence of the modern population structure, which likely reflects the overarching and unifying influence of the Viking trade routes and early Christian cultures from Scandinavia and central Europe that covered the region gradually in the first millennium CE [164].

4.4 Health and infectious diseases in the northern Europe (paper III)

4.4.1 Changing societies in aid of infectious agents

In addition to the human populations in and around Finland, my thesis addresses ancient pathogen genomics from northern and central European contexts. In the course of this thesis, I screened altogether 238 samples, using a combination of techniques directed to retrieve and analyse both human and pathogen DNA. Although 123 of these samples were primarily chosen for palaeopathological indications, only two were finally deemed positive for pathogenic agents, namely treponemal bacteria, *Treponema pallidum*. Parts of the natural human flora and various opportunistic species found in oral inflammations were detected in the tooth samples and dental calculus, showing that the applied methodology was technically sound. The rarity of the positive findings is not in itself an

indication of non-existing infectious diseases in the Finnish individuals. Rather, it showcases the challenge of detecting genetic evidence of infectious agents, even when the samples demonstrate physical signs of disease and ample host DNA can be recovered.

Both population growth and urbanization increased the susceptibility for rapidly spreading infectious diseases in the late and post-medieval north. Mercenaries were commonly employed in the 17th to 19th century wars waged by the two ruling powers of the time: Sweden and Russia. The armies constantly deployed on the Finnish soil facilitated a rapid propagation of diseases like syphilis, typhus and cholera [29,222]. The overall increase in travel networks, such as Marine trade routes between the Baltic ports and railroad to St. Petersburg are well-documented causes for local epidemic events [29,222]. The paper III of this thesis illustrates the significance of these historical phenomena via the genetic evidence of syphilis gained for the first time from Estonian and Finnish cities. With the genomic variation of *Treponema pallidum* subspecies found far in northern Europe, we could clearly show that syphilis had established itself in the Baltic Sea region at latest in the early modern period, in addition to the causative agent of yaws, *Treponema pallidum* spp. *pertenue*. The wide distribution and diversity of the treponemal diseases could reflect the high speed in which the 1500's syphilis epidemic reached the European fringe zones. The simultaneously present yaws found in a contemporaneous Finnish individual suggests an underlying prevalence of endemic treponematoses in the north. An alternative explanation for the findings would be the existence of previously wide-spread ancestral forms for both yaws and syphilis in the historical communities of Europe, or at the very least, within the Old World. The next section addresses the implications of this postulate in more detail.

4.4.2 *Treponema pallidum* in Europe

Several scenarios concerning the rise of syphilis in Europe have been debated. However, the reasons behind the emergence of the disease, its violent spread of the early 16th century and the following recess to a more lenient form, are still largely unknown [205]. The initial introduction has often been attributed to an arrival event from the Americas in 1493. The rapid spread has been suggested to demonstrate a typical response of a naive population to an unprecedented pathogen. However, as long as the genetic evidence on the excessive virulence of the early syphilis bacteria compared to its later successor

type is incomplete, the novel introduction remains an uncertain cause for this phenomenon. As the radiocarbon datings remain inconclusive in all cases thus far published on archaeological samples positive for treponemal DNA, a pre-Columbian presence of treponemal diseases cannot be definitively shown, but the accumulating indirect evidence merits discussion, as outlined in this chapter.

The bacterial genomes reconstructed in this thesis reveal new aspects on the early distribution and spread of syphilis in the Old World. The molecular dating of the treponemal clades supports a radiation of all modern yaws lineages between 14th and 16th centuries, and of all venereal syphilis strains between 12th and 16th centuries. Since representatives of both clades were discovered in the northern fringe zone of Europe, it seems plausible that the modern groups had ancestral and endemic Old-World forms which had already diverged into subspecies but had not yet assumed specific strategies or geographical niches. The increasing overlap in disease distributions may have induced competition between the treponemal clades and thus enforced new adaptations, including increased virulence. The relatively late radiation of the *T.p.pallidum* and *T.p.pertenue* strains and the geographical dispersal of the subspecies correlates with such a dynamic. In the intermingling and urbanizing human societies of the early modern period, an aggressive form of treponematosis would have been favoured by the large pool of hosts. Endemic treponematoses outcompeted by the venereal syphilis in Europe could, in turn, have better thrived and transmitted in the tropics due to easier access to exposed skin and cultural behaviours such as communal use of utensils.

Some consideration should also be given to the genetic findings between the ancient lineages. Bacterial recombination, aggravated by several simultaneous infections in one host, can supply pathogenic lineages with novel properties [139,201]. Recombination events from the yaws-like *T.p.pertenue* agents to the syphilis-causing *T.p.pallidum* group were observed in the paper III of this thesis. Since all the ancient and modern genomes were implicated in these recombination events, a contribution of a novel American lineage would be hard to justify: either a yaws-like donor came overseas and affected an emerging ancestor of all syphilis-like strains extremely fast after the year 1493, giving birth to the existing diversity on the continent today, or both groups originated and recombined in the Americas. Yet, since the yaws and syphilis clades are estimated to have

diverged from each other at least 2500 years ago, this scenario would necessitate both subspecies traveling to Europe independently from the Americas and recombining while rapidly spreading all over the continent.

Recently published studies [336,337] have suggested that yaws may have been brought from Africa with the slave trade rampant at the Iberian coast already some 50 years before Columbus' expeditions to America. However, contacts between Europe and Africa have existed throughout human history, and the presence of yaws in Europe does not necessitate a pulse from elsewhere. In this thesis, I describe a high diversity of subspecies in historical Europe, including a basal group of yaws and bejel lineages found in the Netherlands. The early pool of treponemal agents represented by these lineages could well extend the strains recovered as of now. In our study, no recognized recombinant genes were found to cause functional adaptations in treponemes. Additional studies on both African continent and in Europe might assist in pinpointing the crucial historical cases of coinfections and clarify their significance in the treponemal evolution. Furthermore, the fringe zones, such as the Nordic countries and the British Isles, where abrupt and virulent local epidemics have been recorded from the start of the modern era [290–296]) provide a promising base for investigating treponemal recombination and dynamics between the historical subspecies.

4.4.3 Future aspects for ancient DNA aided *T. pallidum* research

In this section I use the information accumulated in my research to outline possible directions for upcoming ancient genomic studies on *T. pallidum.*

With the relatively few ancient genomes so far retrieved, it is difficult to assess exactly how far back does the history of the human-specific treponemal pathogens reach. The more genomic data becomes available, the more resolution can be gained in dating the relevant evolutionary events. Besides the timing, the ancient DNA could clue us in on the different manifestations of ancient treponemal diseases compared to the current forms, and on the effects of host behaviour and environment on their spread and aetiology.

In paper III of this thesis, we were able to demonstrate a historical presence of both *T.p.pallidum* and *T.p.pertenue*, and place the most recent common ancestor of all modern clades at least 2500 years in the past via molecular dating. The 1500's syphilis started out

as an aggressive disease that caused severe external symptoms, such as large and painful pustules [205,338,339]. The reported condition was so grave that it would hardly have gone unnoticed, had it been around previously in a similar form. Yet it is possible that an old disease, either previously unrecognized or newly increased in virulence may have confused the contemporary diagnostics [278,340,341]. The subsequent decades, however, witnessed a decrease in the severity of syphilis cases [205]. Applying the sexual transmission route would surely have necessitated syphilis to develop less conspicuous manifestations, lest the hosts would have been rendered unable to effectively distribute the pathogen. It appears syphilis managed this fast and remarkably well, to the point where it has earned a reputation as an extremely insidious disease, capable of imitating other medical conditions [342]. There is, however, very little indication of the genetic adaptations that may have facilitated these rapid changes. The putative virulence factors I analysed for the paper III do not seem to vary between the ancient genomes and the lineages in the respective modern clades. In-depth genetic comparisons and high-coverage ancient genomes are therefore required for a more comprehensive detection of the genes involved in adaptation. Approaches allowing for a sequence level investigation of the largely homologous Tpr-genes and the mutations associated with the macrolide resistance in the modern lineages are in demand for the future analyses on this front.

Apart from simply designating a place and time of origin, some effort should also be assigned to the past population dynamics of the treponemal subspecies. In the coming years, a combination of well-informed sample selection and bioinformatic techniques may result in more reconstructed ancient treponemal genomes, enabling the use of mathematical approaches such as Bayesian phylodynamics on bacterial evolution [343]. In these methods, statistical models can be utilized for estimating the pathogen virulence under different conditions [344]. In addition, genetic markers or entire genes can be studied for selection pressure, to detect mutations associated with adaptive strategies [345,346]. The information on host population density and behaviour may further assist in discovering the emergence of exceptionally virulent forms of treponemes. Through innovative use of statistical methodology, the future archaeogenetic studies have an unprecedented opportunity to illustrate the past epidemic events and possibly predict future ones in the process.

5 Outlook

In this thesis, I present the first ancient DNA studies conducted on Finnish archaeological material. The specifics of local preservation and variation between burial sites and circumstances is reported, facilitating the expectations for future studies from Finnish excavations. The population genetic analyses in this thesis have improved the resolution in which a large body of eastern ancestry in Fennoscandia can be interpreted. In particular, the Siberian ancestry component with genetic affinity to modern Nganasan population in the Taimyr peninsula illuminated the probable population dynamics and migration times of the modern Uralic-speakers and their ancestors across northwestern Russia. Ancestries revealed in this thesis aid in piecing together the migrations between the middle-Volga region in Russia and the surroundings of the Baltic Sea. The genetic information accumulated in the studies is crucial for tying together the archaeological evidence from the Eneolithic and Bronze Age material cultures and linguistic hypotheses on the proto-Uralic languages. Once ancient genetic data is additionally available from the boreal zone of western Russia, including locations along the presumed northern migration routes, the overarching theories of the Fennoscandian ethnogenesis will improve in precision and support further interdisciplinary interpretations.

The ancient pathogen research within this thesis reveals unprecedented diversity of historical genomes of *Treponema pallidum*, a bacterial group infamously difficult to retrieve from archaeological remains. The sample selection, ranging from adult individuals with active treponemal lesions to a foetal skeleton with only mild new bone formations, suggests that the only proper prerequisite for successful sampling is an active stage of infection. The most abundant treponemal DNA was retrieved from a petrous bone of the foetus. Hence, it is possible for a severe infection to penetrate the entire skeletal system in congenital cases of syphilis, providing a more ample range of suitable samples for future ancient treponemal DNA studies.

On the subject of treponemal phylogenetics, the first *Treponema pallidum* genomes from the European historical context were reconstructed, including a previously unknown basal lineage to the modern endemic treponematoses. The observations insinuate that several other early forms may have existed simultaneously and gone extinct, possibly

after giving rise to the modern treponemal agents or their immediate ancestors. As this diversity was shown to have existed within Europe by the early modern period, it may have emerged in the Old World before Columbus' expedition to the Americas. The archaeology of the sites in this thesis supports this view, with several samples radiocarbon-dated within a partly pre-Columbian time range. More potential early cases will have to be studied in order to verify pre-Columbian existence of treponematoses in Europe and to track back the routes of historical epidemics.

Ultimately, the archaeogenetic research on re-emerging pathogens is tied to the life histories of the host population. In the case of treponemal diseases, interdisciplinary sociohistorical investigations on the development of urban societies in Europe (and beyond) are called for. Complete with aspects of social structures, behaviour and beliefs around the infectious diseases, and the increased population density and mobility towards the modern period, such studies could provide an indispensable background against which to examine the evolution and adaptations of treponemal diseases. My research aspires in part to assist any future considerations in understanding this particular pathogen-host interaction.

6 References

1. Allentoft ME, Sikora M, Sjögren K-G, Rasmussen S, Rasmussen M, Stenderup J, et al. Population genomics of Bronze Age Eurasia. Nature. 2015;522: 167–172. doi:10.1038/nature14507

2. Krzewińska M, Bjørnstad G, Skoglund P, Olason PI, Bill J, Götherström A, et al. Mitochondrial DNA variation in the Viking age population of Norway. Philos Trans R Soc Lond B Biol Sci. 2015;370: 20130384. doi:10.1098/rstb.2013.0384

3. Fu Q, Posth C, Hajdinjak M, Petr M, Mallick S, Fernandes D, et al. The genetic history of Ice Age Europe. Nature. 2016;534: 200–205. doi:10.1038/nature17993

4. Jones ER, Zarina G, Moiseyev V, Lightfoot E, Nigst PR, Manica A, et al. The Neolithic Transition in the Baltic Was Not Driven by Admixture with Early European Farmers. Curr Biol. 2017;27: 576–582. doi:10.1016/j.cub.2016.12.060

5. Mittnik A, Wang C-C, Pfrengle S, Daubaras M, Zariņa G, Hallgren F, et al. The genetic prehistory of the Baltic Sea region. Nat Commun. 2018;9: 442. doi:10.1038/s41467-018-02825-9

6. Saag L, Varul L, Scheib CL, Stenderup J, Allentoft ME, Saag L, et al. Extensive Farming in Estonia Started through a Sex-Biased Migration from the Steppe. Curr Biol. 2017;27: 2185–2193.e6. doi:10.1016/j.cub.2017.06.022

7. Tambets K, Yunusbayev B, Hudjashov G, Ilumäe A-M, Rootsi S, Honkola T, et al. Genes reveal traces of common recent demographic history for most of the Uralic-speaking populations. Genome Biol. 2018;19: 139. doi:10.1186/s13059-018-1522-1

8. Saag L, Laneman M, Varul L, Malve M, Valk H, Razzak MA, et al. The Arrival of Siberian Ancestry Connecting the Eastern Baltic to Uralic Speakers further East. Curr Biol. 2019;29: 1701–1711.e16. doi:10.1016/j.cub.2019.04.026

9. Sjögren K-G, Olalde I, Carver S, Allentoft ME, Knowles T, Kroonen G, et al. Kinship and social organization in Copper Age Europe. A cross-disciplinary analysis of archaeology, DNA, isotopes, and anthropology from two Bell Beaker cemeteries. PLoS One. 2020;15: e0241278. doi:10.1371/journal.pone.0241278

10. Margaryan A, Lawson DJ, Sikora M, Racimo F, Rasmussen S, Moltke I, et al. Population genomics of the Viking world. Nature. 2020;585: 390–396. doi:10.1038/s41586-020-2688-8

11. Der Sarkissian C, Balanovsky O, Brandt G, Khartanovich V, Buzhilova A, Koshel S, et al. Ancient DNA reveals prehistoric gene-flow from siberia in the complex human population history of North East Europe. PLoS Genet. 2013;9: e1003296. doi:10.1371/journal.pgen.1003296

12. Sikora M, Seguin-Orlando A, Sousa VC, Albrechtsen A, Korneliussen T, Ko A, et al. Ancient genomes show social and reproductive behavior of early Upper Paleolithic foragers. Science. 2017;358: 659–662. doi:10.1126/science.aao1807

13. Mathieson I, Alpaslan-Roodenberg S, Posth C, Szécsényi-Nagy A, Rohland N, Mallick S, et al. The genomic history of southeastern Europe. Nature. 2018;555: 197–203. doi:10.1038/nature25778

14. Sikora M, Pitulko VV, Sousa VC, Allentoft ME, Vinner L, Rasmussen S, et al. The population history of northeastern Siberia since the Pleistocene. Nature. 2019;570: 182–188. doi:10.1038/s41586-019-1279-z

15. Yu H, Spyrou MA, Karapetian M, Shnaider S, Radzevičiūtė R, Nägele K, et al. Paleolithic to Bronze Age Siberians Reveal Connections with First Americans and across Eurasia. Cell. 2020;181: 1232–1245.e20. doi:10.1016/j.cell.2020.04.037

16. Wong EHM, Khrunin A, Nichols L, Pushkarev D, Khokhrin D, Verbenko D, et al. Reconstructing genetic history of Siberian and Northeastern European populations. Genome Res. 2017;27: 1–14. doi:10.1101/gr.202945.115

17. Tallavaara M, Pesonen P, Oinonen M. Prehistoric population history in eastern Fennoscandia. J Archaeol Sci. 2010;37: 251–260. doi:10.1016/j.jas.2009.09.035

18. Nevanlinna HR. The Finnish population structure. A genetic and genealogical study. Hereditas. 1972;71: 195–236. doi:10.1111/j.1601-5223.1972.tb01021.x

19. Norio R. Finnish Disease Heritage II: population prehistory and genetic roots of Finns. Human Genetics. 2003. pp. 457–469. doi:10.1007/s00439-002-0876-2

20. Palo JU, Ulmanen I, Lukka M, Ellonen P, Sajantila A. Genetic markers and population history: Finland revisited. Eur J Hum Genet. 2009;17: 1336–1346. doi:10.1038/ejhg.2009.53

21. Wang SR, Agarwala V, Flannick J, Chiang CWK, Altshuler D, GoT2D Consortium, et al. Simulation of Finnish population history, guided by empirical genetic data, to assess power of rare-variant tests in Finland. Am J Hum Genet. 2014;94: 710–720. doi:10.1016/j.ajhg.2014.03.019

22. Sajantila A, Salem AH, Savolainen P, Bauer K, Gierig C, Pääbo S. Paternal and maternal DNA lineages reveal a bottleneck in the founding of the Finnish population. Proc Natl Acad Sci U S A. 1996;93: 12035–12039. doi:10.1073/pnas.93.21.12035

23. Peltonen L. Molecular background of the Finnish disease heritage. Ann Med. 1997;29: 553–556. doi:10.3109/07853899709007481

24. Norio R. Finnish disease heritage I. Hum Genet. 2003;112: 441–456. Available: https://idp.springer.com/authorize/casa?redirect_uri=https://link.springer.com/article/10.1007/s00439-002-0875-3&casa_token=L0ztypxXMNoAAAAA:kFYiOU6nf4DC39XNFXwzEk8ZBqWTbcmKI2RLhPn7i_zgAq10BV8B0xeDRsXyF4XUTgVp5nbfNXCTGZi5cg

25. Zhang P, Atkinson PM. Modelling the effect of urbanization on the transmission of an infectious disease. Math Biosci. 2008;211: 166–185. doi:10.1016/j.mbs.2007.10.007

26. Neiderud C-J. How urbanization affects the epidemiology of emerging infectious diseases. Infect Ecol Epidemiol. 2015;5: 27060. doi:10.3402/iee.v5.27060

27. Salo KH, Others. HEALTH IN SOUTHERN FINLAND: Bioarchaeological analysis of 555 skeletons excavated from nine cemeteries (11th-19th century AD). 2016. Available: https://helda.helsinki.fi/handle/10138/163042

28. Barrett R, Kuzawa CW, McDade T. Emerging and re-emerging infectious diseases: the third epidemiologic transition. Annual review of. 1998. Available: https://www.annualreviews.org/doi/abs/10.1146/annurev.anthro.27.1.247?casa_token=2n-PoEQkUxcAAAAA:va9aJXs59NAVn3ysRZ4lnpk1kqh-HSM5Phsg9BAet21bDf3DiqY1_DyT_OFsOaWFhDFL6nhy5VE

29. Kallioinen M. Rutto ja rukous: tartuntataudit esiteollisen ajan Suomessa. Atena; 2005. Available: https://play.google.com/store/books/details?id=IjySAgAACAAJ

30. Snowden FM. Emerging and reemerging diseases: a historical perspective. Immunol Rev. 2008;225: 9–26. doi:10.1111/j.1600-065X.2008.00677.x

31. Lappalainen T, Koivumäki S, Salmela E, Huoponen K, Sistonen P, Savontaus M-L, et al. Regional differences among the Finns: a Y-chromosomal perspective. Gene. 2006;376: 207–215. doi:10.1016/j.gene.2006.03.004

32. Salmela E, Lappalainen T, Fransson I, Andersen PM, Dahlman-Wright K, Fiebig A, et al. Genome-wide analysis of single nucleotide polymorphisms uncovers population structure in Northern Europe. PLoS One. 2008;3: e3519. doi:10.1371/journal.pone.0003519

33. Neuvonen AM, Putkonen M, Översti S, Sundell T, Onkamo P, Sajantila A, et al. Vestiges of an Ancient Border in the Contemporary Genetic Diversity of North-Eastern Europe. PLoS One. 2015;10: e0130331. doi:10.1371/journal.pone.0130331

34. Higuchi R, Bowman B, Freiberger M, Ryder OA, Wilson AC. DNA sequences from the quagga, an extinct member of the horse family. Nature. 1984;312: 282–284. doi:10.1038/312282a0

35. Pääbo S. Molecular cloning of Ancient Egyptian mummy DNA. Nature. 1985;314: 644–645. doi:10.1038/314644a0

36. Green RE, Malaspinas A-S, Krause J, Briggs AW, Johnson PLF, Uhler C, et al. A complete Neandertal mitochondrial genome sequence determined by high-

throughput sequencing. Cell. 2008;134: 416–426. doi:10.1016/j.cell.2008.06.021

37. Prüfer K, Racimo F, Patterson N, Jay F, Sankararaman S, Sawyer S, et al. The complete genome sequence of a Neanderthal from the Altai Mountains. Nature. 2014;505: 43–49. doi:10.1038/nature12886

38. Noonan JP, Coop G, Kudaravalli S, Smith D, Krause J, Alessi J, et al. Sequencing and analysis of Neanderthal genomic DNA. Science. 2006;314: 1113–1118. doi:10.1126/science.1131412

39. Reich D, Green RE, Kircher M, Krause J, Patterson N, Durand EY, et al. Genetic history of an archaic hominin group from Denisova Cave in Siberia. Nature. 2010;468: 1053–1060. doi:10.1038/nature09710

40. Krause J, Fu Q, Good JM, Viola B, Shunkov MV, Derevianko AP, et al. The complete mitochondrial DNA genome of an unknown hominin from southern Siberia. Nature. 2010;464: 894–897. doi:10.1038/nature08976

41. Haak W, Lazaridis I, Patterson N, Rohland N, Mallick S, Llamas B, et al. Massive migration from the steppe was a source for Indo-European languages in Europe. Nature. 2015;522: 207–211. doi:10.1038/nature14317

42. Fu Q, Mittnik A, Johnson PLF, Bos K, Lari M, Bollongino R, et al. A revised timescale for human evolution based on ancient mitochondrial genomes. Curr Biol. 2013;23: 553–559. doi:10.1016/j.cub.2013.02.044

43. Lazaridis I, Patterson N, Mittnik A, Renaud G, Mallick S, Kirsanow K, et al. Ancient human genomes suggest three ancestral populations for present-day Europeans. Nature. 2014;513: 409–413. doi:10.1038/nature13673

44. Posth C, Renaud G, Mittnik A, Drucker DG, Rougier H, Cupillard C, et al. Pleistocene Mitochondrial Genomes Suggest a Single Major Dispersal of Non-Africans and a Late Glacial Population Turnover in Europe. Curr Biol. 2016;26: 827–833. doi:10.1016/j.cub.2016.01.037

45. Skoglund P, Posth C, Sirak K, Spriggs M, Valentin F, Bedford S, et al. Genomic insights into the peopling of the Southwest Pacific. Nature. 2016;538: 510–513. doi:10.1038/nature19844

46. Posth C, Nakatsuka N, Lazaridis I, Skoglund P, Mallick S, Lamnidis TC, et al. Reconstructing the Deep Population History of Central and South America. Cell. 2018;175: 1185–1197.e22. doi:10.1016/j.cell.2018.10.027

47. Posth C, Nägele K, Colleran H, Valentin F, Bedford S, Kami KW, et al. Language continuity despite population replacement in Remote Oceania. Nat Ecol Evol. 2018;2: 731–740. doi:10.1038/s41559-018-0498-2

48. Lazaridis I, Mittnik A, Patterson N, Mallick S, Rohland N, Pfrengle S, et al. Genetic origins of the Minoans and Mycenaeans. Nature. 2017;548: 214–218. doi:10.1038/nature23310

49. Kashuba N, Kirdök E, Damlien H, Manninen MA, Nordqvist B, Persson P, et al. Ancient DNA from chewing gums connects material culture and genetics of Mesolithic hunter-gatherers in Scandinavia. doi:10.1101/485045

50. Gamba C, Fernández E, Tirado M, Deguilloux MF, Pemonge MH, Utrilla P, et al. Ancient DNA from an Early Neolithic Iberian population supports a pioneer colonization by first farmers. Mol Ecol. 2012;21: 45–56. doi:10.1111/j.1365-294X.2011.05361.x

51. Fernández-Domínguez E, Reynolds L. The Mesolithic-Neolithic Transition in Europe: A Perspective from Ancient Human DNA. Times of Neolithic Transition along the Western Mediterranean. 2017. pp. 311–338. doi:10.1007/978-3-319-52939-4_12

52. Koboldt DC, Steinberg KM, Larson DE, Wilson RK, Mardis ER. The next-generation sequencing revolution and its impact on genomics. Cell. 2013;155: 27–38. doi:10.1016/j.cell.2013.09.006

53. Miller W, Drautz DI, Ratan A, Pusey B, Qi J, Lesk AM, et al. Sequencing the nuclear genome of the extinct woolly mammoth. Nature. 2008;456: 387–390. doi:10.1038/nature07446

54. Green RE, Krause J, Briggs AW, Maricic T, Stenzel U, Kircher M, et al. A draft sequence of the Neandertal genome. Science. 2010;328: 710–722. doi:10.1126/science.1188021

55. Rasmussen M, Li Y, Lindgreen S, Pedersen JS, Albrechtsen A, Moltke I, et al. Ancient human genome sequence of an extinct Palaeo-Eskimo. Nature. 2010;463: 757–762. doi:10.1038/nature08835

56. Gansauge M-T, Meyer M. Selective enrichment of damaged DNA molecules for ancient genome sequencing. Genome Res. 2014;24: 1543–1549. doi:10.1101/gr.174201.114

57. Gansauge M-T, Meyer M. Single-stranded DNA library preparation for the sequencing of ancient or damaged DNA. Nat Protoc. 2013;8: 737–748. doi:10.1038/nprot.2013.038

58. Hodges E, Rooks M, Xuan Z, Bhattacharjee A, Benjamin Gordon D, Brizuela L, et al. Hybrid selection of discrete genomic intervals on custom-designed microarrays for massively parallel sequencing. Nat Protoc. 2009;4: 960–974. doi:10.1038/nprot.2009.68

59. Burbano HA, Hodges E, Green RE, Briggs AW, Krause J, Meyer M, et al. Targeted investigation of the Neandertal genome by array-based sequence capture. Science. 2010;328: 723–725. doi:10.1126/science.1188046

60. Avila-Arcos MC, Cappellini E, Romero-Navarro JA, Wales N, Moreno-Mayar JV, Rasmussen M, et al. Application and comparison of large-scale solution-based DNA capture-enrichment methods on ancient DNA. Sci Rep. 2011;1: 74. doi:10.1038/srep00074

61. Gasc C, Peyretaillade E, Peyret P. Sequence capture by hybridization to explore modern and ancient genomic diversity in model and nonmodel organisms. Nucleic Acids Res. 2016;44: 4504–4518. doi:10.1093/nar/gkw309

62. Cruz-Dávalos DI, Llamas B, Gaunitz C, Fages A, Gamba C, Soubrier J, et al. Experimental conditions improving in-solution target enrichment for ancient DNA. Mol Ecol Resour. 2017;17: 508–522. doi:10.1111/1755-0998.12595

63. Furtwängler A, Neukamm J, Böhme L, Reiter E, Vollstedt M, Arora N, et al. Comparison of target enrichment strategies for ancient pathogen DNA. Biotechniques. 2020;69: 455–459. doi:10.2144/btn-2020-0100

64. Mallick S, Li H, Lipson M, Mathieson I, Gymrek M, Racimo F, et al. The Simons Genome Diversity Project: 300 genomes from 142 diverse populations. Nature. 2016;538: 201–206. doi:10.1038/nature18964

65. 1000 Genomes Project Consortium, Abecasis GR, Auton A, Brooks LD, DePristo MA, Durbin RM, et al. An integrated map of genetic variation from 1,092 human genomes. Nature. 2012;491: 56–65. doi:10.1038/nature11632

66. Peltzer A, Jäger G, Herbig A, Seitz A, Kniep C, Krause J, et al. EAGER: efficient ancient genome reconstruction. Genome Biol. 2016;17: 60. doi:10.1186/s13059-016-0918-z

67. Key FM, Posth C, Krause J, Herbig A, Bos KI. Mining Metagenomic Data Sets for Ancient DNA: Recommended Protocols for Authentication. Trends Genet. 2017;33: 508–520. doi:10.1016/j.tig.2017.05.005

68. Renaud G, Schubert M, Sawyer S, Orlando L. Authentication and Assessment of Contamination in Ancient DNA. Methods Mol Biol. 2019;1963: 163–194. doi:10.1007/978-1-4939-9176-1_17

69. Hofreiter M. DNA sequences from multiple amplifications reveal artifacts induced by cytosine deamination in ancient DNA. Nucleic Acids Research. 2001. pp. 4793–4799. doi:10.1093/nar/29.23.4793

70. Briggs AW, Stenzel U, Johnson PLF, Green RE, Kelso J, Prüfer K, et al. Patterns of damage in genomic DNA sequences from a Neandertal. Proc Natl Acad Sci U S A. 2007;104: 14616–14621. doi:10.1073/pnas.0704665104

71. Dabney J, Knapp M, Glocke I, Gansauge M-T, Weihmann A, Nickel B, et al. Complete mitochondrial genome sequence of a Middle Pleistocene cave bear reconstructed from ultrashort DNA fragments. Proc Natl Acad Sci U S A. 2013;110: 15758–15763. doi:10.1073/pnas.1314445110

72. Sawyer S, Krause J, Guschanski K, Savolainen V, Pääbo S. Temporal patterns of nucleotide misincorporations and DNA fragmentation in ancient DNA. PLoS One. 2012;7: e34131. doi:10.1371/journal.pone.0034131

73. Dabney J, Meyer M, Pääbo S. Ancient DNA damage. Cold Spring Harb Perspect Biol. 2013;5. doi:10.1101/cshperspect.a012567

74. Lindahl T. Instability and decay of the primary structure of DNA. Nature. 1993. pp. 709–715. doi:10.1038/362709a0

75. Higgins D, Rohrlach AB, Kaidonis J, Townsend G, Austin JJ. Differential nuclear and mitochondrial DNA preservation in post-mortem teeth with implications for forensic and ancient DNA studies. PLoS One. 2015;10: e0126935. doi:10.1371/journal.pone.0126935

76. Kistler L, Ware R, Smith O, Collins M, Allaby RG. A new model for ancient DNA decay based on paleogenomic meta-analysis. Nucleic Acids Res. 2017;45: 6310–6320. doi:10.1093/nar/gkx361

77. Ahola M, Salo K, Mannermaa K. Almost gone: human skeletal material from Finnish Stone Age earth graves. Fennoscandia archaeologica. 2016;33: 95–122. Available: http://www.academia.edu/download/53353398/FA2016_ahola.pdf

78. Jónsson H, Ginolhac A, Schubert M, Johnson PLF, Orlando L. mapDamage2.0: fast approximate Bayesian estimates of ancient DNA damage parameters. Bioinformatics. 2013;29: 1682–1684. doi:10.1093/bioinformatics/btt193

79. Palencia-Madrid L, de Pancorbo MM. Next generation sequencing as a suitable analysis for authentication of degraded and ancient DNA. Forensic Science International: Genetics Supplement Series. 2015. pp. e338–e340. doi:10.1016/j.fsigss.2015.09.134

80. Grody WW. Screening for Pathogenic DNA Sequences in Clinically Collected Human Tissues. In: Herrmann B, Hummel S, editors. Ancient DNA: Recovery and Analysis of Genetic Material from Paleontological, Archaeological, Museum, Medical, and Forensic Specimens. New York, NY: Springer New York; 1994. pp. 69–91. doi:10.1007/978-1-4612-4318-2_5

81. Haynes S, Searle JB, Bretman A, Dobney KM. Bone Preservation and Ancient DNA: The Application of Screening Methods for Predicting DNA Survival. Journal of Archaeological Science. 2002. pp. 585–592. doi:10.1006/jasc.2001.0731

82. Herrmann B, Hummel S. Ancient DNA: Recovery and Analysis of Genetic Material from Paleontological, Archaeological, Museum, Medical, and Forensic Specimens. Springer Science & Business Media; 2012. Available: https://play.google.com/store/books/details?id=PobTBwAAQBAJ

83. Devault AM, McLoughlin K, Jaing C, Gardner S, Porter TM, Enk JM, et al. Ancient pathogen DNA in archaeological samples detected with a Microbial Detection Array. Sci Rep. 2014;4: 4245. doi:10.1038/srep04245

84. Donoghue HD, Spigelman M, O'Grady J, Szikossy I, Pap I, -C. Lee OY, et al. Ancient DNA analysis – An established technique in charting the evolution of tuberculosis and leprosy. Tuberculosis. 2015. pp. S140–S144. doi:10.1016/j.tube.2015.02.020

85. Witas HW, Donoghue HD, Kubiak D, Lewandowska M, Gładykowska-Rzeczycka JJ. Molecular studies on ancient M. tuberculosis and M. leprae: methods of pathogen and host DNA analysis. Eur J Clin Microbiol Infect Dis. 2015;34: 1733–1749.

doi:10.1007/s10096-015-2427-5

86. Chan JZ-M, Sergeant MJ, Lee OY-C, Minnikin DE, Besra GS, Pap I, et al. Metagenomic analysis of tuberculosis in a mummy. N Engl J Med. 2013;369: 289–290. doi:10.1056/NEJMc1302295

87. Bos KI, Harkins KM, Herbig A, Coscolla M, Weber N, Comas I, et al. Pre-Columbian mycobacterial genomes reveal seals as a source of New World human tuberculosis. Nature. 2014;514: 494–497. doi:10.1038/nature13591

88. Kay GL, Sergeant MJ, Zhou Z, Chan JZ-M, Millard A, Quick J, et al. Eighteenth-century genomes show that mixed infections were common at time of peak tuberculosis in Europe. Nat Commun. 2015;6: 6717. doi:10.1038/ncomms7717

89. Bos KI, Schuenemann VJ, Golding GB, Burbano HA, Waglechner N, Coombes BK, et al. A draft genome of Yersinia pestis from victims of the Black Death. Nature. 2011;478: 506–510. doi:10.1038/nature10549

90. Rasmussen S, Allentoft ME, Nielsen K, Orlando L, Sikora M, Sjögren K-G, et al. Early divergent strains of Yersinia pestis in Eurasia 5,000 years ago. Cell. 2015;163: 571–582. doi:10.1016/j.cell.2015.10.009

91. Bos KI, Herbig A, Sahl J, Waglechner N, Fourment M, Forrest SA, et al. Eighteenth century Yersinia pestis genomes reveal the long-term persistence of an historical plague focus. Elife. 2016;5: e12994. doi:10.7554/eLife.12994

92. Spyrou MA, Tukhbatova RI, Wang C-C, Valtueña AA, Lankapalli AK, Kondrashin VV, et al. Analysis of 3800-year-old Yersinia pestis genomes suggests Bronze Age origin for bubonic plague. Nat Commun. 2018;9: 2234. doi:10.1038/s41467-018-04550-9

93. Rascovan N, Sjögren K-G, Kristiansen K, Nielsen R, Willerslev E, Desnues C, et al. Emergence and Spread of Basal Lineages of Yersinia pestis during the Neolithic Decline. Cell. 2019;176: 295–305.e10. doi:10.1016/j.cell.2018.11.005

94. Keller M, Spyrou MA, Scheib CL. Ancient Yersinia pestis genomes from across Western Europe reveal early diversification during the First Pandemic (541–750). Proceedings of the. 2019. Available: https://www.pnas.org/content/116/25/12363.short

95. Schuenemann VJ, Singh P, Mendum TA, Krause-Kyora B, Jäger G, Bos KI, et al. Genome-wide comparison of medieval and modern Mycobacterium leprae. Science. 2013;341: 179–183. doi:10.1126/science.1238286

96. Mendum TA, Schuenemann VJ, Roffey S, Taylor GM, Wu H, Singh P, et al. Mycobacterium leprae genomes from a British medieval leprosy hospital: towards understanding an ancient epidemic. BMC Genomics. 2014;15: 270. doi:10.1186/1471-2164-15-270

97. Schuenemann VJ, Avanzi C, Krause-Kyora B, Seitz A, Herbig A, Inskip S, et al. Ancient genomes reveal a high diversity of Mycobacterium leprae in medieval Europe. PLoS Pathog. 2018;14: e1006997. doi:10.1371/journal.ppat.1006997

98. Krause-Kyora B, Nutsua M, Boehme L, Pierini F, Pedersen DD, Kornell S-C, et al. Ancient DNA study reveals HLA susceptibility locus for leprosy in medieval Europeans. Nat Commun. 2018;9: 1569. doi:10.1038/s41467-018-03857-x

99. Vågene ÅJ, Herbig A, Campana MG, Robles García NM, Warinner C, Sabin S, et al. Salmonella enterica genomes from victims of a major sixteenth-century epidemic in Mexico. Nat Ecol Evol. 2018;2: 520–528. doi:10.1038/s41559-017-0446-6

100. Zhou Z, Lundstrøm I, Tran-Dien A, Duchêne S, Alikhan N-F, Sergeant MJ, et al. Pan-genome Analysis of Ancient and Modern Salmonella enterica Demonstrates Genomic Stability of the Invasive Para C Lineage for Millennia. Curr Biol. 2018;28: 2420–2428.e10. doi:10.1016/j.cub.2018.05.058

101. Schuenemann VJ, Kumar Lankapalli A, Barquera R, Nelson EA, Iraíz Hernández D, Acuña Alonzo V, et al. Historic Treponema pallidum genomes from Colonial Mexico retrieved from archaeological remains. PLoS Negl Trop Dis. 2018;12: e0006447. doi:10.1371/journal.pntd.0006447

102. Maixner F, Krause-Kyora B, Turaev D, Herbig A, Hoopmann MR, Hallows JL, et al. The 5300-year-old Helicobacter pylori genome of the Iceman. Science. 2016;351: 162–165. doi:10.1126/science.aad2545

103. Shin DH, Oh CS, Hong JH, Lee H, Lee SD, Lee E. Helicobacter pylori DNA obtained from the stomach specimens of two 17th century Korean mummies. Anthropol Anz. 2018;75: 75–87. doi:10.1127/anthranz/2018/0780

104. Kahila Bar-Gal G, Kim MJ, Klein A, Shin DH, Oh CS, Kim JW, et al. Tracing hepatitis B virus to the 16th century in a Korean mummy. Hepatology. 2012;56: 1671–1680. doi:10.1002/hep.25852

105. Mühlemann B, Jones TC, Damgaard P de B, Allentoft ME, Shevnina I, Logvin A, et al. Ancient hepatitis B viruses from the Bronze Age to the Medieval period. Nature. 2018;557: 418–423. doi:10.1038/s41586-018-0097-z

106. Krause-Kyora B, Susat J, Key FM, Kühnert D, Bosse E, Immel A, et al. Neolithic and medieval virus genomes reveal complex evolution of hepatitis B. Elife. 2018;7. doi:10.7554/eLife.36666

107. Ross ZP, Klunk J, Fornaciari G, Giuffra V, Duchêne S, Duggan AT, et al. The paradox of HBV evolution as revealed from a 16th century mummy. PLoS Pathog. 2018;14: e1006750. doi:10.1371/journal.ppat.1006750

108. Taubenberger JK, Reid AH, Lourens RM, Wang R, Jin G, Fanning TG. Characterization of the 1918 influenza virus polymerase genes. Nature. 2005;437: 889–893. doi:10.1038/nature04230

109. Tumpey TM, Basler CF, Aguilar PV, Zeng H, Solórzano A, Swayne DE, et al. Characterization of the reconstructed 1918 Spanish influenza pandemic virus. Science. 2005;310: 77–80. doi:10.1126/science.1119392

110. Duggan AT, Perdomo MF, Piombino-Mascali D, Marciniak S, Poinar D, Emery MV,

et al. 17th Century Variola Virus Reveals the Recent History of Smallpox. Curr Biol. 2016;26: 3407–3412. doi:10.1016/j.cub.2016.10.061

111.   Mühlemann B, Margaryan A, de Barros Damgaard P, Allentoft ME, Vinner L, Hansen AJ, et al. Ancient human parvovirus B19 in Eurasia reveals its long-term association with humans. Proc Natl Acad Sci U S A. 2018;115: 7557–7562. doi:10.1073/pnas.1804921115

112.   Pinhasi R, Fernandes D, Sirak K, Novak M, Connell S, Alpaslan-Roodenberg S, et al. Optimal Ancient DNA Yields from the Inner Ear Part of the Human Petrous Bone. PLoS One. 2015;10: e0129102. doi:10.1371/journal.pone.0129102

113.   Parker C, Rohrlach AB, Friederich S, Nagel S, Meyer M, Krause J, et al. A systematic investigation of human DNA preservation in medieval skeletons. Sci Rep. 2020;10: 18225. doi:10.1038/s41598-020-75163-w

114.   Margaryan A, Hansen HB, Rasmussen S, Sikora M, Moiseyev V, Khoklov A, et al. Ancient pathogen DNA in human teeth and petrous bones. Ecol Evol. 2018;8: 3534–3542. doi:10.1002/ece3.3924

115.   Mai BHA, Drancourt M, Aboudharam G. Ancient dental pulp: Masterpiece tissue for paleomicrobiology. Mol Genet Genomic Med. 2020;8: e1202. doi:10.1002/mgg3.1202

116.   Yang DY, Watt K. Contamination controls when preparing archaeological remains for ancient DNA analysis. J Archaeol Sci. 2005;32: 331–336. doi:10.1016/j.jas.2004.09.008

117.   Llamas B, Valverde G, Fehren-Schmitz L, Weyrich LS, Cooper A, Haak W. From the field to the laboratory: Controlling DNA contamination in human ancient DNA research in the high-throughput sequencing era. STAR: Science & Technology of Archaeological Research. 2017;3: 1–14. doi:10.1080/20548923.2016.1258824

118.   Peyrégne S, Prüfer K. Present-day DNA contamination in ancient DNA datasets. Bioessays. 2020;42: e2000081. doi:10.1002/bies.202000081

119.   Glassing A, Dowd SE, Galandiuk S, Davis B, Chiodini RJ. Inherent bacterial DNA contamination of extraction and sequencing reagents may affect interpretation of microbiota in low bacterial biomass samples. Gut Pathog. 2016;8: 24. doi:10.1186/s13099-016-0103-7

120.   Korlević P, Meyer M. Pretreatment: Removing DNA Contamination from Ancient Bones and Teeth Using Sodium Hypochlorite and Phosphate. Methods in Molecular Biology. 2019. pp. 15–19. doi:10.1007/978-1-4939-9176-1_2

121.   Truong DT, Franzosa EA, Tickle TL, Scholz M, Weingart G, Pasolli E, et al. MetaPhlAn2 for enhanced metagenomic taxonomic profiling. Nat Methods. 2015;12: 902–903. doi:10.1038/nmeth.3589

122.   Nayfach S, Rodriguez-Mueller B, Garud N, Pollard KS. An integrated metagenomics pipeline for strain profiling reveals novel patterns of bacterial

transmission and biogeography. Genome Research. 2016. pp. 1612–1625. doi:10.1101/gr.201863.115

123. Wood DE, Salzberg SL. Kraken: ultrafast metagenomic sequence classification using exact alignments. Genome Biol. 2014;15: R46. doi:10.1186/gb-2014-15-3-r46

124. Herbig A, Maixner F, Bos KI, Zink A, Krause J, Huson DH. MALT: Fast alignment and analysis of metagenomic DNA sequence data applied to the Tyrolean Iceman. doi:10.1101/050559

125. Huson DH, Auch AF, Qi J, Schuster SC. MEGAN analysis of metagenomic data. Genome Res. 2007;17: 377–386. doi:10.1101/gr.5969107

126. O'Leary NA, Wright MW, Brister JR, Ciufo S, Haddad D, McVeigh R, et al. Reference sequence (RefSeq) database at NCBI: current status, taxonomic expansion, and functional annotation. Nucleic Acids Res. 2016;44: D733–45. doi:10.1093/nar/gkv1189

127. Hübler R, Key FM, Warinner C, Bos KI, Krause J, Herbig A. HOPS: Automated detection and authentication of pathogen DNA in archaeological remains. doi:10.1101/534198

128. Warinner C, Rodrigues JFM, Vyas R, Trachsel C, Shved N, Grossmann J, et al. Pathogens and host immunity in the ancient human oral cavity. Nat Genet. 2014;46: 336–344. doi:10.1038/ng.2906

129. Schnorr SL, Sankaranarayanan K, Lewis CM Jr, Warinner C. Insights into human evolution from ancient and contemporary microbiome studies. Curr Opin Genet Dev. 2016;41: 14–26. doi:10.1016/j.gde.2016.07.003

130. Micah H, Claire F-L, Rob K, Others. The human microbiome project: exploring the microbial part of ourselves in a changing world. Nature. 2007;449: 804–810.

131. Dewhirst FE, Chen T, Izard J, Paster BJ, Tanner ACR, Yu W-H, et al. The human oral microbiome. J Bacteriol. 2010;192: 5002–5017. doi:10.1128/JB.00542-10

132. Karsenti E, Acinas SG, Bork P, Bowler C, De Vargas C, Raes J, et al. A Holistic Approach to Marine Eco-Systems Biology. PLoS Biology. 2011. p. e1001177. doi:10.1371/journal.pbio.1001177

133. Lagier J-C, Armougom F, Million M, Hugon P, Pagnier I, Robert C, et al. Microbial culturomics: paradigm shift in the human gut microbiome study. Clin Microbiol Infect. 2012;18: 1185–1193. doi:10.1111/1469-0691.12023

134. Gilbert JA, Jansson JK, Knight R. The Earth Microbiome project: successes and aspirations. BMC Biol. 2014;12: 69. doi:10.1186/s12915-014-0069-1

135. Neukamm J, Pfrengle S, Molak M, Seitz A, Francken M, Eppenberger P, et al. 2000-year-old pathogen genomes reconstructed from metagenomic analysis of Egyptian mummified individuals. BMC Biol. 2020;18: 108. doi:10.1186/s12915-020-00839-

8

136.   Spyrou MA, Bos KI, Herbig A, Krause J. Ancient pathogen genomics as an emerging tool for infectious disease research. Nat Rev Genet. 2019;20: 323–340. doi:10.1038/s41576-019-0119-1

137.   Comas I, Coscolla M, Luo T, Borrell S, Holt KE, Kato-Maeda M, et al. Out-of-Africa migration and Neolithic coexpansion of Mycobacterium tuberculosis with modern humans. Nat Genet. 2013;45: 1176–1182. doi:10.1038/ng.2744

138.   Stadler T, Kühnert D, Bonhoeffer S, Drummond AJ. Birth–death skyline plot reveals temporal changes of epidemic spread in HIV and hepatitis C virus (HCV). Proc Natl Acad Sci U S A. 2013;110: 228–233. doi:10.1073/pnas.1207965110

139.   Lawrence JG, Retchless AC. The interplay of homologous recombination and horizontal gene transfer in bacterial speciation. Methods Mol Biol. 2009;532: 29–53. doi:10.1007/978-1-60327-853-9_3

140.   McDonald MJ, Rice DP, Desai MM. Sex speeds adaptation by altering the dynamics of molecular evolution. Nature. 2016;531: 233–236. doi:10.1038/nature17143

141.   Núñez M. On Subneolithic pottery and its adoption in Late Mesolithic Finland. Fennoscandia archaeologica. 1990;7: 27–52. Available: http://www.sarks.fi/fa/PDF/FA7_27.pdf

142.   Pesonen P, Leskinen S, Jordan P, Zvelebil M. Pottery of the Stone Age hunter-gatherers in Finland. Ceramics before Farming: The dispersal of pottery among prehistoric Eurasian hunter-gatherers. 2009; 299–318. Available: https://books.google.com/books?hl=en&lr=&id=tbdJDAAAQBAJ&oi=fnd&pg=PA299&dq=comb+ceramic+in+Finland&ots=w89wnnku2I&sig=A4z6xnuc09_P-u_NTj0JuU54_oI

143.   Pesonen P, Oinonen M, Carpelan C, Onkamo P. Early Subneolithic Ceramic Sequences in Eastern Fennoscandia—A Bayesian Approach. Radiocarbon. 2012;54: 661–676. doi:10.1017/S0033822200047330

144.   Nordqvist K, Häkälä P. Distribution of Corded Ware in the areas North of the Gulf of Finland-an update. Estonian Journal of Archaeology. 2014;18: 3. Available: https://www.ceeol.com/search/article-detail?id=278206

145.   Carpelan C, Parpola A. On the emergence, contacts and dispersal of Proto-Indo-European, Proto-Uralic and Proto-Aryan in an archaeological perspective. Language and Prehistory of the Indo-European Peoples: A Cross-Disciplinary Perspective. Museum Tusculanums Forlag; 2017. pp. 77–87. Available: https://researchportal.helsinki.fi/en/publications/on-the-emergence-contacts-and-dispersal-of-proto-indo-european-pr

146.   Lang V. Läänemeresoome tulemised: Finnic be-comings. Tartu Ülikool Kirjastus; 2018.

147.   Patrushev VS. Textile-impressed pottery in Russia. Fennoscandia archaeologica.

1992;9: 43–56.

148. Lavento M. Textile ceramics in Finland and on the Karelian Isthmus: nine variations and fugue on a theme of CF Meinander. Finnish Antiquarian Society; 2001.

149. Parpola A. Formation of the Indo-European and Uralic (Finno-Ugric) language families in the light of archaeology: Revised and integrated "total"correlations. A linguistic map of prehistoric Northern Europe. 2012; 119–184. Available: https://www.academia.edu/download/43880501/Parpola_A_20122013_MSFOu2 66.pdf

150. Yushkova MA. Northwestern Russia at the periphery of the north European and Volga-Uralic Bronze Age. Local societies in Bronze Age Northern Europe. 2012. pp. 129–147. Available: https://books.google.com/books?hl=en&lr=&id=XPLOBAAAQBAJ&oi=fnd&pg=PA1 29&dq=Yushkova+2012+Ananino&ots=1pasjUkkmN&sig=GBe0TV1zioqc-en_fkW_Bih8aw8

151. Ánte LSS. An essay on Saami ethnolinguistic prehistory. A linguistic map of prehistoric Northern Europe. 2012; 63–117. Available: https://www.academia.edu/download/46465125/An_Essay_on_Saami_Ethnolingu istic_Prehistory.pdf

152. Kallio P. The language contact situation in prehistoric Northeastern Europe. The linguistic roots of Europe: Origin and development of European languages. 2015; 77–102. Available: https://books.google.com/books?hl=en&lr=&id=GNsyCwAAQBAJ&oi=fnd&pg=PA7 7&dq=Kallio+2015+Linguistic&ots=arWSMUkoIS&sig=3-ntgx2f72ZIgpaTHysfkaC0IT8

153. Sammallahti P. Bottlenecks and Contacts in the Linguistic Prehistory of the Saami. Damm & Saarikivi. 2012;2012: 93–104. Available: https://www.academia.edu/download/32733127/sust265_sammallahti.pdf

154. Aikio A. An essay on substrate studies and the origin of Saami.--Irma Hyvärinen, Petri Kallio & Jarmo Korhonen (toim.), Etymologie, Entlehnungen und Entwicklungen. Festschrift für Jorma Koivulehto zum 70. Geburtstag s. 5--34. Memoires de la Societe neophilologique de Helsinki. 2004;63.

155. Lahermo P, Sajantila A, Sistonen P, Lukka M, Aula P, Peltonen L, et al. The genetic relationship between the Finns and the Finnish Saami (Lapps): analysis of nuclear DNA and mtDNA. Am J Hum Genet. 1996;58: 1309–1322. Available: https://www.ncbi.nlm.nih.gov/pubmed/8651309

156. Mathieson I, Lazaridis I, Rohland N, Mallick S, Patterson N, Roodenberg SA, et al. Genome-wide patterns of selection in 230 ancient Eurasians. Nature. 2015;528: 499–503. doi:10.1038/nature16152

157. Broushaki F, Thomas MG, Link V, López S, van Dorp L, Kirsanow K, et al. Early Neolithic genomes from the eastern Fertile Crescent. Science. 2016;353: 499–503.

doi:10.1126/science.aaf7943

158. Lazaridis I, Nadel D, Rollefson G, Merrett DC, Rohland N, Mallick S, et al. Genomic insights into the origin of farming in the ancient Near East. Nature. 2016;536: 419–424. doi:10.1038/nature19310

159. Garrido-Pena R, Alt KW, Jeong C, Schiffels S. Survival of Late Pleistocene hunter-gatherer ancestry in the Iberian Peninsula. Curr Biol. 2019. Available: https://www.sciencedirect.com/science/article/pii/S0960982219301459

160. Rivollat M, Jeong C, Schiffels S, Küçükkalıpçı İ, Pemonge M-H, Rohrlach AB, et al. Ancient genome-wide DNA from France highlights the complexity of interactions between Mesolithic hunter-gatherers and Neolithic farmers. Sci Adv. 2020;6: eaaz5344. doi:10.1126/sciadv.aaz5344

161. Villalba-Mouco V, van de Loosdrecht MS, Posth C, Mora R, Martínez-Moreno J, Rojo-Guerra M, et al. Survival of Late Pleistocene Hunter-Gatherer Ancestry in the Iberian Peninsula. Curr Biol. 2019;29: 1169–1177.e7. doi:10.1016/j.cub.2019.02.006

162. Wang C-C, Reinhold S, Kalmykov A, Wissgott A, Brandt G, Jeong C, et al. Ancient human genome-wide data from a 3000-year interval in the Caucasus corresponds with eco-geographic regions. Nat Commun. 2019;10: 590. doi:10.1038/s41467-018-08220-8

163. Jeong C, Balanovsky O, Lukianova E, Kahbatkyzy N, Flegontov P, Zaporozhchenko V, et al. The genetic history of admixture across inner Eurasia. Nat Ecol Evol. 2019;3: 966–976. doi:10.1038/s41559-019-0878-2

164. Haggren G, Halinen P, Lavento M, Raninen S, Wessman A. Muinaisuutemme jäljet: Suomen esi-ja varhaishistoria kivikaudelta keskiajalle. Gaudeamus; 2015.

165. Marchenko ZV, Svyatko SV, Molodin VI, Grishin AE, Rykun MP. Radiocarbon chronology of complexes with Seima-Turbino type objects (Bronze Age) in southwestern Siberia. Radiocarbon. 2017;59: 1381–1397. doi:10.1017/rdc.2017.24

166. Molodin VI, Marchenko ZV, Kuzmin YV, Grishin AE, van Strydonck M, Orlova LA. 14C Chronology of Burial Grounds of the Andronovo Period (Middle Bronze Age) in Baraba Forest Steppe, Western Siberia. Radiocarbon. 2012. pp. 737–747. doi:10.1017/s0033822200047391

167. Cummings V, Jordan P, Zvelebil M. The Oxford Handbook of the Archaeology and Anthropology of Hunter-gatherers. Oxford University Press; 2014. Available: https://play.google.com/store/books/details?id=M4lSAwAAQBAJ

168. Bramanti B, Thomas MG, Haak W, Unterlaender M, Jores P, Tambets K, et al. Genetic discontinuity between local hunter-gatherers and central Europe's first farmers. Science. 2009;326: 137–140. doi:10.1126/science.1176869

169. Brandt G, Haak W, Adler CJ, Roth C, Szecsenyi-Nagy A, Karimnia S, et al. Ancient DNA Reveals Key Stages in the Formation of Central European Mitochondrial

Genetic Diversity. Science. 2013. pp. 257–261. doi:10.1126/science.1241844

170.   Kivisild T. Maternal ancestry and population history from whole mitochondrial genomes. Investig Genet. 2015;6: 3. doi:10.1186/s13323-015-0022-2

171.   Underhill PA, Poznik GD, Rootsi S, Järve M, Lin AA, Wang J, et al. The phylogenetic and geographic structure of Y-chromosome haplogroup R1a. Eur J Hum Genet. 2015;23: 124–131. doi:10.1038/ejhg.2014.50

172.   Rootsi S, Magri C, Kivisild T, Benuzzi G, Help H, Bermisheva M, et al. Phylogeography of Y-chromosome haplogroup I reveals distinct domains of prehistoric gene flow in europe. Am J Hum Genet. 2004;75: 128–137. doi:10.1086/422196

173.   Krause J, Briggs AW, Kircher M, Maricic T, Zwyns N, Derevianko A, et al. A complete mtDNA genome of an early modern human from Kostenki, Russia. Curr Biol. 2010;20: 231–236. doi:10.1016/j.cub.2009.11.068

174.   Mittnik A, Wang C-C, Pfrengle S, Daubaras M, Zarina G, Hallgren F, et al. The Genetic History of Northern Europe. Cold Spring Harbor Laboratory. 2017. p. 113241. doi:10.1101/113241

175.   Bermisheva MA, Tambets K, Villems R, Khusnutdinova EK. Diversity of Mitochondrial DNA Haplogroups in Ethnic Populations of the Volga–Ural Region. Mol Biol. 2002;36: 802–812. doi:10.1023/A:1021677708482

176.   Malyarchuk BA. Differentiation of the Mitochondrial Subhaplogroup U4 in the Populations of Eastern Europe, Ural, and Western Siberia: Implication to the Genetic History of the Uralic Populations. Russ J Genet. 2004;40: 1281–1287. doi:10.1023/B:RUGE.0000048671.32870.cb

177.   Haak W, Balanovsky O, Sanchez JJ, Koshel S, Zaporozhchenko V, Adler CJ, et al. Ancient DNA from European early neolithic farmers reveals their near eastern affinities. PLoS Biol. 2010;8: e1000536. doi:10.1371/journal.pbio.1000536

178.   Haak W, Forster P, Bramanti B, Matsumura S, Brandt G, Tänzer M, et al. Ancient DNA from the first European farmers in 7500-year-old Neolithic sites. Science. 2005;310: 1016–1018. doi:10.1126/science.1118725

179.   Brandt G, Szécsényi-Nagy A, Roth C, Alt KW, Haak W. Human paleogenetics of Europe--the known knowns and the known unknowns. J Hum Evol. 2015;79: 73–92. doi:10.1016/j.jhevol.2014.06.017

180.   Skoglund P, Malmström H, Raghavan M, Storå J, Hall P, Willerslev E, et al. Origins and genetic legacy of Neolithic farmers and hunter-gatherers in Europe. Science. 2012;336: 466–469. doi:10.1126/science.1216304

181.   Lahtinen M, Oinonen M, Tallavaara M, Walker JWP, Rowley-Conwy P. The advance of cultivation at its northern European limit: Process or event? Holocene. 2017;27: 427–438. doi:10.1177/0959683616660164

182. Skoglund P, Malmström H, Omrak A, Raghavan M, Valdiosera C, Günther T, et al. Genomic diversity and admixture differs for Stone-Age Scandinavian foragers and farmers. Science. 2014;344: 747–750. doi:10.1126/science.1253448

183. Översti S, Onkamo P, Stoljarova M, Budowle B, Sajantila A, Palo JU. Identification and analysis of mtDNA genomes attributed to Finns reveal long-stagnant demographic trends obscured in the total diversity. Sci Rep. 2017;7: 6193. doi:10.1038/s41598-017-05673-7

184. Tambets K, Rootsi S, Kivisild T, Help H, Serk P, Loogväli E-L, et al. The Western and Eastern Roots of the Saami—the Story of Genetic "Outliers" Told by Mitochondrial DNA and Y Chromosomes. Am J Hum Genet. 2004;74: 661–682. doi:10.1086/383203

185. Ingman M, Gyllensten U. A recent genetic link between Sami and the Volga-Ural region of Russia. Eur J Hum Genet. 2007;15: 115–120. doi:10.1038/sj.ejhg.5201712

186. Andrades Valtueña A, Mittnik A, Key FM, Haak W, Allmäe R, Belinskij A, et al. The Stone Age Plague and Its Persistence in Eurasia. Curr Biol. 2017;27: 3683–3691.e8. doi:10.1016/j.cub.2017.10.025

187. Borah W, McNeill WH. Plagues and Peoples. Hisp Am Hist Rev. 1980;60: 97. doi:10.2307/2513897

188. McEvedy C, Jones R, Others. Atlas of world population history. Penguin Books Ltd, Harmondsworth, Middlesex, England.; 1978. Available: https://www.cabdirect.org/cabdirect/abstract/19792702472

189. Stanley NF, Joske RA, Others. Changing disease patterns and human behaviour. Academic Press (London) Ltd., 24/28 Oval Road, London NW1 7DX; 1980. Available: https://www.cabdirect.org/cabdirect/abstract/19812703493

190. Vuorinen HS. Tautinen historia. Vastapaino Tampere; 2002. Available: https://core.ac.uk/download/pdf/12382410.pdf

191. Black FL. Infectious diseases in primitive societies. Science. 1975;187: 515–518. doi:10.1126/science.163483

192. Fiennes RN-W, Others. Zoonoses and the origins and ecology of human disease. Academic Press, 24/28 Oval Road, London NW1 7DX.; 1978. Available: https://www.cabdirect.org/cabdirect/abstract/19792703714

193. Zohary D, Hopf M, Others. Domestication of plants in the Old World: The origin and spread of cultivated plants in West Asia, Europe and the Nile Valley. Oxford University Press; 2000. Available: https://www.cabdirect.org/cabdirect/abstract/20013014838

194. Cohen MN. Health and the Rise of Civilization. Yale University Press; 1989.

195. Crosby AW. Ecological Imperialism: The Biological Expansion of Europe, 900-1900. Cambridge University Press; 2004. Available:

https://play.google.com/store/books/details?id=Phtqa_3tNykC

196.   Cliff AD, Haggett P, Smallman-Raynor M, Smallman-Raynor MR. Island Epidemics. Oxford University Press; 2000. Available: https://play.google.com/store/books/details?id=a9FHiwuhIuYC

197.   Crosby AW. The Columbian Exchange: Biological and Cultural Consequences of 1492. Greenwood Publishing Group; 2003. Available: https://play.google.com/store/books/details?id=n-y_bn3ZM4EC

198.   Barnes E. Diseases and Human Evolution. UNM Press; 2007. Available: https://play.google.com/store/books/details?id=caNCQQBehT8C

199.   Gottfried RS. Black Death. Simon and Schuster; 2010. Available: https://play.google.com/store/books/details?id=oK4HTBcdSJsC

200.   Hickey DA, Rose MR. 1988The role of gene transfer in the evolution of eukaryotic sex. The evolution of sex: an examination of current ideas (ed RE Michod & BR Levin). : 161–175.

201.   Cooper TF. Recombination speeds adaptation by reducing competition between beneficial mutations in populations of Escherichia coli. PLoS Biol. 2007;5: e225. doi:10.1371/journal.pbio.0050225

202.   Centurion-Lara A, Sun ES, Barrett LK, Castro C, Lukehart SA, Van Voorhis WC. Multiple Alleles of Treponema pallidumRepeat Gene D in Treponema pallidum Isolates. J Bacteriol. 2000;182: 2332–2335. doi:10.1128/JB.182.8.2332-2335.2000

203.   Gray RR, Mulligan CJ, Molini BJ, Sun ES, Giacani L, Godornes C, et al. Molecular evolution of the tprC, D, I, K, G, and J genes in the pathogenic genus Treponema. Mol Biol Evol. 2006;23: 2220–2233. Available: https://academic.oup.com/mbe/article-abstract/23/11/2220/1332718

204.   Pětrošová H, Zobaníková M, Čejková D, Mikalová L, Pospíšilová P, Strouhal M, et al. Whole genome sequence of Treponema pallidum ssp. pallidum, strain Mexico A, suggests recombination between yaws and syphilis strains. PLoS Negl Trop Dis. 2012;6: e1832. doi:10.1371/journal.pntd.0001832

205.   Knell RJ. Syphilis in renaissance Europe: rapid evolution of an introduced sexually transmitted disease? Proc Biol Sci. 2004;271 Suppl 4: S174–6. doi:10.1098/rsbl.2003.0131

206.   Mulligan CJ, Norris SJ, Lukehart SA. Molecular studies in Treponema pallidum evolution: toward clarity? PLoS neglected tropical diseases. 2008. p. e184. doi:10.1371/journal.pntd.0000184

207.   Radolf JD, Deka RK, Anand A, Šmajs D, Norgard MV, Yang XF. Treponema pallidum, the syphilis spirochete: making a living as a stealth pathogen. Nat Rev Microbiol. 2016;14: 744–759. doi:10.1038/nrmicro.2016.141

208.   Cockburn TA. The origin of the treponematoses. Bull World Health Organ.

1961;24: 221–228. Available: https://www.ncbi.nlm.nih.gov/pubmed/13694226

209.   Hudson EH. Treponematosis and Man's Social Evolution. Am Anthropol. 1965;67: 885–901. Available: http://www.jstor.org/stable/668772

210.   Benedictow OJ. The medieval demographic system of the Nordic countries. 1993. Available: https://www.oeaw.ac.at/resources/Record/990001546740504498

211.   Huurre M. Kivikauden Suomi. Kustannusosakeyhtio Otava; 1998.

212.   Orrman E. The progress of settlement in Finland during the late middle ages. Scand Econ Hist Rev. 1981;29: 129–143. doi:10.1080/03585522.1981.10407949

213.   Kaukiainen Y. Suomen asuttaminen. Suomen taloushistoria. 1980;1: 13–145.

214.   Harrison D. Plague, Settlement and Structural Change at the Dawn of the Middle Ages. Scandia: Tidskrift för historisk forskning. 1993;59. Available: https://pdfs.semanticscholar.org/416f/32892238cdfd1a2d2b9fe2db40feb3b4ecc 0.pdf

215.   Benedictow OJ, Slack P. Plague in the late medieval Nordic countries: epidemiological studies. Bulletin of the. 1993.

216.   Donoghue HD. Tuberculosis and leprosy associated with historical human population movements in Europe and beyond - an overview based on mycobacterial ancient DNA. Ann Hum Biol. 2019;46: 120–128. doi:10.1080/03014460.2019.1624822

217.   Cronberg S. The rise and fall of sexually transmitted diseases in Sweden. Genitourin Med. 1993;69: 184–186. doi:10.1136/sti.69.3.184

218.   Turpeinen O. Infectious diseases and regional differences in Finnish death rates, 1749–1773. Popul Stud . 1978;32: 523–533. doi:10.1080/00324728.1978.10412812

219.   Flinn MW. The European demographic system, 1500-1820. Johns Hopkins Univ Pr; 1981.

220.   Jutikkala E. Social differences in preindustrial demography: a case study on a middle-sized town. Finnish Yearbook of Population Research. 1987. Available: https://journal.fi/fypr/article/view/44818/48315

221.   Baker BJ, Armelagos GJ, Becker MJ, Brothwell D, Drusini A, Geise MC, et al. The Origin and Antiquity of Syphilis: Paleopathological Diagnosis and Interpretation [and Comments and Reply]. Curr Anthropol. 1988;29: 703–737. doi:10.1086/203691

222.   Vuorinen HS. Tautinen Suomi 1857-1865. Tampere University Press; 2006. Available: https://play.google.com/store/books/details?id=_v09NQAACAAJ

223.   Mielke JH, Jorde LB, Trapp PG, Anderton DL, Pitkänen K, Eriksson AW. Historical

epidemiology of smallpox in Aland, Finland: 1751-1890. Demography. 1984;21: 271–295. doi:10.2307/2061159

224.   Hakapää J. Kuolema kulkutautien aikana. Ilmestyskirjan ratsastajat: sota, nälkä, taudit ja kuolema historiassa. Vastapaino; 2000. pp. 344–366. Available: https://researchportal.helsinki.fi/en/publications/kuolema-kulkutautien-aikana

225.   Peter Richards, The medieval leper and his northern heirs, Ipswich, D. S. Brewer, 1977, 8vo, pp. xvi, 178, illus., £6.00. Med Hist. 1978;22: 451–451. doi:10.1017/S0025727300033597

226.   Kontturi S-M. Parantajat ja tieteentekijät. Piirilääkärit Ruotsin valtakunnassa 1700-luvun lopulta 1800-luvun alkuun. MSc, University of Jyväskylä. 2014.

227.   Johnsson G. Suomen piirilääkärit 1749-1927. Suomen Sukututkimusseura; 1928. Available: https://play.google.com/store/books/details?id=R6WDPQAACAAJ

228.   Peldán K. Suomen farmasian historia. Suomen Farmaseuttinen Yhdistys; 1967. Available: https://play.google.com/store/books/details?id=PT5xsWnAa-QC

229.   Lönnrot E. Suomalaisen talonpojan koti-lääkäri. Lindhardt og Ringhof; 2019. Available: https://play.google.com/store/books/details?id=9UevDwAAQBAJ

230.   Gibbard TW, Harrison LW. The Treatment Of Syphilis With Salvarsan And Neo-Salvarsan. Br Med J. 1912;2: 953–955. Available: http://www.jstor.org/stable/25298897

231.   Vernon G. Syphilis and Salvarsan. Br J Gen Pract. 2019;69: 246. doi:10.3399/bjgp19X702533

232.   Hooper R. Quincy's Lexicon-medicum: A New Medical Dictionary; Containing an Explanation of the Terms in Anatomy, Physiology, Practice of Physic, Materia Medica, Chymistry, Pharmacy, Surgery, Midwifery, and the Various Branches of Natural Philosophy Connected with Medicine. E. & R. Parker [etc.] Griggs & Company, printers; 1817. Available: https://play.google.com/store/books/details?id=6y_wpwAACAAJ

233.   Fenton KA, Breban R, Vardavas R, Okano JT, Martin T, Aral S, et al. Infectious syphilis in high-income settings in the 21st century. Lancet Infect Dis. 2008;8: 244–253. doi:10.1016/S1473-3099(08)70065-3

234.   Spiteri G, Unemo M, Mårdh O, Amato-Gauci AJ. The resurgence of syphilis in high-income countries in the 2000s: a focus on Europe. Epidemiol Infect. 2019;147: e143. doi:10.1017/S0950268819000281

235.   Forsius A. Sosiaali- ja terveydenhuollon kehitys Hollolassa ja Lahdessa vuoteen 1865. LAHDEN KAUPUNKI; 1982. Available: https://play.google.com/store/books/details?id=B5g5AAAAIAAJ

236.   Khan AU. Current Trends in Antibiotic Resistance in Infectious Diseases. I. K. International Pvt Ltd; 2009. Available:

https://play.google.com/store/books/details?id=TjSUQZoG2U0C

237.   Ho EL, Lukehart SA. Syphilis: using modern approaches to understand an old disease. J Clin Invest. 2011;121: 4584–4592. doi:10.1172/JCI57173

238.   Šmajs D, Strouhal M, Knauf S. Genetics of human and animal uncultivable treponemal pathogens. Infect Genet Evol. 2018;61: 92–107. doi:10.1016/j.meegid.2018.03.015

239.   Mitjà O, Asiedu K, Mabey D. Yaws. Lancet. 2013;381: 763–773. doi:10.1016/S0140-6736(12)62130-8

240.   Giacani L, Lukehart SA. The endemic treponematoses. Clin Microbiol Rev. 2014;27: 89–115. doi:10.1128/CMR.00070-13

241.   Radolf JD, Lukehart SA. Pathogenic Treponema: Molecular and Cellular Biology. Horizon Scientific Press; 2006. Available: https://play.google.com/store/books/details?id=bU66Huv72UcC

242.   Lafond RE, Lukehart SA. Biological basis for syphilis. Clin Microbiol Rev. 2006;19: 29–49. doi:10.1128/CMR.19.1.29-49.2006

243.   Lipozenčić J, Marinović B, Gruber F. Endemic syphilis in Europe. Clin Dermatol. 2014;32: 219–226. doi:10.1016/j.clindermatol.2013.08.006

244.   Kazadi WM, Asiedu KB, Agana N, Mitjà O. Epidemiology of yaws: an update. Clin Epidemiol. 2014;6: 119–128. doi:10.2147/CLEP.S44553

245.   Román GC, Román LN. Occurrence of congenital, cardiovascular, visceral, neurologic, and neuro-ophthalmologic complications in late yaws: a theme for future research. Rev Infect Dis. 1986;8: 760–770. Available: https://www.ncbi.nlm.nih.gov/pubmed/3538316

246.   Wicher V, Wicher K. Pathogenesis of maternal-fetal syphilis revisited. Clin Infect Dis. 2001;33: 354–363. doi:10.1086/321904

247.   Krüger C, Malleyeck I. Congenital syphilis: still a serious, under-diagnosed threat for children in resource-poor countries. World J Pediatr. 2010;6: 125–131. doi:10.1007/s12519-010-0028-z

248.   Mitjà O, Šmajs D, Bassat Q. Advances in the diagnosis of endemic treponematoses: yaws, bejel, and pinta. PLoS Negl Trop Dis. 2013;7: e2283. doi:10.1371/journal.pntd.0002283

249.   Stamm LV. Syphilis: Re-emergence of an old foe. Microb Cell Fact. 2016;3: 363–370. doi:10.15698/mic2016.09.523

250.   Knauf S, Gogarten JF, Schuenemann VJ, De Nys HM, Düx A, Strouhal M, et al. Nonhuman primates across sub-Saharan Africa are infected with the yaws bacterium Treponema pallidum subsp. pertenue. Emerg Microbes Infect. 2018;7: 157. doi:10.1038/s41426-018-0156-4

251. Mediannikov O, Fenollar F, Davoust B, Amanzougaghene N, Lepidi H, Arzouni J-P, et al. Epidemic of venereal treponematosis in wild monkeys: a paradigm for syphilis origin. New Microbes and New Infections. 2020;35: 100670. doi:10.1016/j.nmni.2020.100670

252. Stamm LV, Stapleton JT, Bassford PJ Jr. In vitro assay to demonstrate high-level erythromycin resistance of a clinical isolate of Treponema pallidum. Antimicrob Agents Chemother. 1988;32: 164–169. doi:10.1128/aac.32.2.164

253. Lukehart SA, Godornes C, Molini BJ, Sonnett P, Hopkins S, Mulcahy F, et al. Macrolide resistance in Treponema pallidum in the United States and Ireland. N Engl J Med. 2004;351: 154–158. doi:10.1056/NEJMoa040216

254. Arora N, Schuenemann VJ, Jäger G, Peltzer A, Seitz A, Herbig A, et al. Origin of modern syphilis and emergence of a pandemic Treponema pallidum cluster. Nat Microbiol. 2016;2: 16245. doi:10.1038/nmicrobiol.2016.245

255. Šmajs D, Paštěková L, Grillová L. Macrolide Resistance in the Syphilis Spirochete, Treponema pallidum ssp. pallidum: Can We Also Expect Macrolide-Resistant Yaws Strains? Am J Trop Med Hyg. 2015;93: 678–683. doi:10.4269/ajtmh.15-0316

256. Mitjà O, Godornes C, Houinei W, Kapa A, Paru R, Abel H, et al. Re-emergence of yaws after single mass azithromycin treatment followed by targeted treatment: a longitudinal study. Lancet. 2018;391: 1599–1607. doi:10.1016/S0140-6736(18)30204-6

257. Kawahata T, Kojima Y, Furubayashi K, Shinohara K, Shimizu T, Komano J, et al. Bejel, a Nonvenereal Treponematosis, among Men Who Have Sex with Men, Japan. Emerg Infect Dis. 2019;25: 1581–1583. doi:10.3201/eid2508.181690

258. Beale MA, Marks M, Sahi SK, Tantalo LC, Nori AV, French P, et al. Genomic epidemiology of syphilis reveals independent emergence of macrolide resistance across multiple circulating lineages. Nat Commun. 2019;10: 3255. doi:10.1038/s41467-019-11216-7

259. Sandok PL, Knight ST, Jenkin HM. Examination of various cell culture techniques for co-incubation of virulent Treponema pallidum (Nichols I strain) under anaerobic conditions. J Clin Microbiol. 1976;4: 360–371. Available: https://www.ncbi.nlm.nih.gov/pubmed/789395

260. Engelkens HJ, Kant M, Onvlee PC, Stolz E, van der Sluis JJ. Rapid in vitro immobilisation of purified Treponema pallidum (Nichols strain), and protection by extraction fluids from rabbit testes. Sexually Transmitted Infections. 1990. pp. 367–373. doi:10.1136/sti.66.5.367

261. Lukehart SA. New Tools for Syphilis Research. mBio. 2018. doi:10.1128/mBio.01417-18

262. Norris SJ, Cox DL, Weinstock GM. Biology of Treponema pallidum: correlation of functional activities with genome sequence data. J Mol Microbiol Biotechnol. 2001;3: 37–62. Available: https://www.ncbi.nlm.nih.gov/pubmed/11200228

263. Titz B, Rajagopala SV, Goll J, Häuser R, McKevitt MT, Palzkill T, et al. The binary protein interactome of Treponema pallidum--the syphilis spirochete. PLoS One. 2008;3: e2292. doi:10.1371/journal.pone.0002292

264. Naqvi AAT, Shahbaaz M, Ahmad F, Hassan MI. Identification of functional candidates amongst hypothetical proteins of Treponema pallidum ssp. pallidum. PLoS One. 2015;10: e0124177. doi:10.1371/journal.pone.0124177

265. Addetia A, Tantalo LC, Lin MJ, Xie H, Huang M-L, Marra CM, et al. Comparative genomics and full-length Tprk profiling of Treponema pallidum subsp. pallidum reinfection. PLoS Negl Trop Dis. 2020;14: e0007921. doi:10.1371/journal.pntd.0007921

266. Norris SJ. Polypeptides of Treponema pallidum: progress toward understanding their structural, functional, and immunologic roles. Treponema Pallidum Polypeptide Research Group. Microbiological Reviews. 1993. pp. 750–779. doi:10.1128/mmbr.57.3.750-779.1993

267. Strouhal M, Smajs D, Matejková P, Sodergren E, Amin AG, Howell JK, et al. Genome differences between Treponema pallidum subsp. pallidum strain Nichols and T. paraluiscuniculi strain Cuniculi A. Infect Immun. 2007;75: 5859–5866. doi:10.1128/IAI.00709-07

268. Čejková D, Zobaníková M, Chen L, Pospíšilová P, Strouhal M, Qin X, et al. Whole Genome Sequences of Three Treponema pallidum ssp. pertenue Strains: Yaws and Syphilis Treponemes Differ in Less than 0.2% of the Genome Sequence. PLoS Neglected Tropical Diseases. 2012. p. e1471. doi:10.1371/journal.pntd.0001471

269. Centurion-Lara A, Giacani L, Godornes C, Molini BJ, Brinck Reid T, Lukehart SA. Fine analysis of genetic diversity of the tpr gene family among treponemal species, subspecies and strains. PLoS Negl Trop Dis. 2013;7: e2222. doi:10.1371/journal.pntd.0002222

270. Zobanikova M, Strouhal M, Mikalova L, Čejková D, Ambrožová L, Pospíšilová P, et al. Whole genome sequence of the Treponema Fribourg-Blanc: unspecified simian isolate is highly similar to the yaws subspecies. PLoS Negl Trop Dis. 2013;7: e2172. Available: https://journals.plos.org/plosntds/article?id=10.1371/journal.pntd.0002172

271. Štaudová B, Strouhal M, Zobaníková M, Čejková D, Fulton LL, Chen L, et al. Whole genome sequence of the Treponema pallidum subsp. endemicum strain Bosnia A: the genome is related to yaws treponemes but contains few loci similar to syphilis treponemes. PLoS Negl Trop Dis. 2014;8: e3261. Available: https://journals.plos.org/plosntds/article?id=10.1371/journal.pntd.0003261

272. Nechvátal L, Pětrošová H, Grillová L, Pospíšilová P, Mikalová L, Strnadel R, et al. Syphilis-causing strains belong to separate SS14-like or Nichols-like groups as defined by multilocus analysis of 19 Treponema pallidum strains. Int J Med Microbiol. 2014;304: 645–653. doi:10.1016/j.ijmm.2014.04.007

273. Pinto M, Borges V, Antelo M, Pinheiro M, Nunes A, Azevedo J, et al. Genome-scale

analysis of the non-cultivable Treponema pallidum reveals extensive within-patient genetic variation. Nat Microbiol. 2016;2: 16190. doi:10.1038/nmicrobiol.2016.190

274.   Radolf JD, Kumar S. The Treponema pallidum Outer Membrane. Curr Top Microbiol Immunol. 2018;415: 1–38. doi:10.1007/82_2017_44

275.   Radolf JD. Treponema. Medical Microbiology 4th edition. University of Texas Medical Branch at Galveston; 1996. Available: https://www.ncbi.nlm.nih.gov/books/NBK7716/

276.   Hillson S, Grigson C, Bond S. Dental defects of congenital syphilis. Am J Phys Anthropol. 1998;107: 25–40. doi:10.1002/(SICI)1096-8644(199809)107:1<25::AID-AJPA3>3.0.CO;2-C

277.   de Melo FL, de Mello JCM, Fraga AM, Nunes K, Eggers S. Syphilis at the crossroad of phylogenetics and paleopathology. PLoS Negl Trop Dis. 2010;4: e575. doi:10.1371/journal.pntd.0000575

278.   Harper KN, Zuckerman MK, Harper ML, Kingston JD, Armelagos GJ. The origin and antiquity of syphilis revisited: an appraisal of Old World pre-Columbian evidence for treponemal infection. Am J Phys Anthropol. 2011;146 Suppl 53: 99–133. doi:10.1002/ajpa.21613

279.   Rothschild BM, Rothschild C. Treponemal disease revisited: skeletal discriminators for yaws, bejel, and venereal syphilis. Clin Infect Dis. 1995;20: 1402–1408. doi:10.1093/clinids/20.5.1402

280.   Hacket CJ. Diagnostic Criteria of Syphilis, Yaws and Treponarid (Treponematoses) and of Some Other Diseases in Dry Bones: For Use in Osteo-Archaeology. Springer Science & Business Media; 2013. Available: https://play.google.com/store/books/details?id=pLvEBAAAQBAJ

281.   Powell ML, Cook DC, Others. The myth of syphilis: the natural history of treponematosis in North America. University Press of Florida; 2005. Available: https://www.cabdirect.org/cabdirect/abstract/20053141733

282.   Henneberg M, Henneberg RJ. Treponematosis in an ancient Greek colony of Metaponto, southern Italy, 580--250 BCE. The Origin of Syphilis in Europe: Before or After 1493. 1994; 92–98.

283.   Blondiaux J, Bagousse AA. A treponematosis dated from the Late Roman Empire in Normandie, France. L'Origine de la syphilis en Europe: Avant ou aprés. 1994;1493: 99–100.

284.   Tampa M, Sarbu I, Matei C, Benea V, Georgescu SR. Brief history of syphilis. J Med Life. 2014;7: 4–10. Available: https://www.ncbi.nlm.nih.gov/pubmed/24653750

285.   Holcomb RC. Christopher Columbus and the American Origin of Syphilis. U.S. Government Printing Office; 1934. Available: https://play.google.com/store/books/details?id=CduKwhmapP8C

286.   Hackett CJ. ON THE ORIGIN OF THE HUMAN TREPONEMATOSES (PINTA, YAWS, ENDEMIC SYPHILIS AND VENEREAL SYPHILIS). Bull World Health Organ. 1963;29: 7–41. Available: https://www.ncbi.nlm.nih.gov/pubmed/14043755

287.   Crane-Kramer GMM. The paleoepidemiological examination of treponemal infection and leprosy in medieval populations from northern Europe. Calgary; 2000. Available: https://prism.ucalgary.ca/bitstream/handle/1880/40461/54773Crane-Kramer.pdf?sequence=1

288.   Meyer C, Jung C, Kohl T, Poenicke A, Poppe A, Alt KW. Syphilis 2001--a palaeopathological reappraisal. Homo. 2002;53: 39–58. doi:10.1078/0018-442x-00037

289.   Hudson EH. Historical Approach to the Terminology of Syphilis. Archives of Dermatology. 1961. p. 545. doi:10.1001/archderm.1961.01580160009002

290.   Böcker HH. An Account of the Radesyge of Sweden and Norway. Edinb Med Surg J. 1809;5: 420–424. Available: https://www.ncbi.nlm.nih.gov/pubmed/30329335

291.   Morton RS. Another look at the Morbus Gallicus. Postscript to the meeting of the Medical Society for the Study of Venereal Diseases, Geneva, May 26-28, 1967. Br J Vener Dis. 1968;44: 174–177. doi:10.1136/sti.44.2.174

292.   Morton RS. THE BUTTON SCURVY OF IRELAND: POSTCRIPT OF THE MSSVD MEETING IN DUBLIN, MAY 29 AND 30, 1964. Br J Vener Dis. 1964;40: 271–272. doi:10.1136/sti.40.4.271

293.   Morton RS. The sibbens of Scotland. Med Hist. 1967;11: 374–380. doi:10.1017/s0025727300012515

294.   Lie AK. Origin stories and the Norwegian Radesyge. Soc Hist Med. 2007. Available: https://academic.oup.com/shm/article-abstract/20/3/563/1650873

295.   Powell ML. Treponematosis: Past, Present, and Future. A Companion to Paleopathology. 2012; 472. Available: https://onlinelibrary.wiley.com/doi/pdf/10.1002/9781444345940#page=495

296.   Morton RS, Rashid S. "The syphilis enigma": the riddle resolved? Sex Transm Infect. 2001;77: 322–324. doi:10.1136/sti.77.5.322

297.   Fraser CM, Norris SJ, Weinstock GM, White O, Sutton GG, Dodson R, et al. Complete genome sequence of Treponema pallidum, the syphilis spirochete. Science. 1998;281: 375–388. doi:10.1126/science.281.5375.375

298.   Bouwman AS, Brown TA. The limits of biomolecular palaeopathology: ancient DNA cannot be used to study venereal syphilis. J Archaeol Sci. 2005;32: 703–713. doi:10.1016/j.jas.2004.11.014

299.   Hunnius TE von, von Hunnius TE, Yang D, Eng B, Waye JS, Saunders SR. Digging deeper into the limits of ancient DNA research on syphilis. Journal of

Archaeological Science. 2007. pp. 2091–2100. doi:10.1016/j.jas.2007.02.007

300.   Donoghue HD, Spigelman M. Pathogenic microbial ancient DNA: a problem or an opportunity? Proceedings of the Royal Society B: Biological Sciences. 2006;273: 641–642. doi:10.1098/rspb.2005.3261

301.   Kashuba N, Kırdök E, Damlien H, Manninen MA, Nordqvist B, Persson P, et al. Ancient DNA from mastics solidifies connection between material culture and genetics of mesolithic hunter–gatherers in Scandinavia. Communications Biology. 2019;2: 185. doi:10.1038/s42003-019-0399-1

302.   Saag L. The prehistory of Estonia from a genetic perspective: new insights from ancient DNA. Tartu University. 2019. Available: https://oatd.org/oatd/record?record=handle%5C%3A10062%5C%2F64633

303.   Egfjord AF-H, Margaryan A, Fischer A, Sjögren K-G, Price TD, Johannsen NN, et al. Genomic Steppe ancestry in skeletons from the Neolithic Single Grave Culture in Denmark. PLoS One. 2021;16: e0244872. doi:10.1371/journal.pone.0244872

304.   Malmström H, Gilbert MTP, Thomas MG, Brandström M, Storå J, Molnar P, et al. Ancient DNA reveals lack of continuity between neolithic hunter-gatherers and contemporary Scandinavians. Curr Biol. 2009;19: 1758–1762. doi:10.1016/j.cub.2009.09.017

305.   Lee EJ, Renneberg R, Harder M, Krause-Kyora B, Rinne C, Müller J, et al. Collective burials among agro-pastoral societies in later Neolithic Germany: perspectives from ancient DNA. J Archaeol Sci. 2014;51: 174–180. doi:10.1016/j.jas.2012.08.037

306.   Ebenesersdóttir SS, Sandoval-Velasco M, Gunnarsdóttir ED, Jagadeesan A, Guðmundsdóttir VB, Thordardóttir EL, et al. Ancient genomes from Iceland reveal the making of a human population. Science. 2018;360: 1028–1032. doi:10.1126/science.aar2625

307.   Maricic T, Whitten M, Pääbo S. Multiplexed DNA sequence capture of mitochondrial genomes using PCR products. PLoS One. 2010;5: e14004. doi:10.1371/journal.pone.0014004

308.   Wessman A. Death, Destruction and Commemoration: Tracing ritual activities in Finnish Late Iron Age cemeteries (AD 550-1150). Iskos. 2010;18. Available: https://journal.fi/iskos/article/view/100004

309.   Wessman A. Levänluhta. A place of punishment, sacrifice or just a common cemetery. Fennoscandia archaeologica. 2009;26: 81–105. Available: http://citeseerx.ist.psu.edu/viewdoc/download?doi=10.1.1.468.997&rep=rep1&type=pdf

310.   Lehtosalo-Hilander P-L. Keski-ja myöhäisrautakausi. Suomen historia. 1984;1: 250–405.

311.   Brown KA, O'Donoghue K, Brown TA. DNA in cremated bones from an early bronze age cemetery cairn. Int J Osteoarchaeol. 1995;5: 181–187.

doi:10.1002/oa.1390050212

312.   Pusch CM, Broghammer M, Scholz M. Cremation practices and the survival of ancient DNA: burnt bone analyses via RAPD-mediated PCR. Anthropol Anz. 2000;58: 237–251. Available: https://www.ncbi.nlm.nih.gov/pubmed/11082781

313.   Emery MV, Bolhofner K, Winingear S, Oldt R, Montes M, Kanthaswamy S, et al. Reconstructing full and partial STR profiles from severely burned human remains using comparative ancient and forensic DNA extraction techniques. Forensic Sci Int Genet. 2020;46: 102272. doi:10.1016/j.fsigen.2020.102272

314.   Seger T. The plague of Justinian and other scourges: an analysis of the anomalies in the development of the Iron Age population in Finland. 1982. Available: http://samla.raa.se/xmlui/bitstream/handle/raa/2453/1982_184.pdf?sequence=1

315.   Formisto T. An osteological analysis of human and animal bones from Levänluhta. Förf. 1993. Available: https://www.diva-portal.org/smash/record.jsf?pid=diva2:1356297

316.   Gräslund B, Price N. Twilight of the gods? The'dust veil event'of AD 536 in critical perspective. Antiquity. 2012;86. Available: http://search.ebscohost.com/login.aspx?direct=true&profile=ehost&scope=site&authtype=crawler&jrnl=0003598X&AN=76622922&h=LGpM4cr9yJeHaHxGy7jq%2Baa%2FNjqI3UqEvwhiQdlKyQBIuonKQwaHS69I4fRHebvvjN3o53R6mIEKbRY53OU%2Fzw%3D%3D&crl=c

317.   Oinonen M, Alenius T, Arppe L, Bocherens H, Etu-Sihvola H, Helama S, et al. Buried in water, burdened by nature—Resilience carried the Iron Age people through Fimbulvinter. PLoS One. 2020;15: e0231787. doi:10.1371/journal.pone.0231787

318.   Briggs AW, Stenzel U, Meyer M, Krause J, Kircher M, Pääbo S. Removal of deaminated cytosines and detection of in vivo methylation in ancient DNA. Nucleic Acids Res. 2010;38: e87. doi:10.1093/nar/gkp1163

319.   Rohland N, Harney E, Mallick S, Nordenfelt S, Reich D. Partial uracil–DNA–glycosylase treatment for screening of ancient DNA. Philos Trans R Soc Lond B Biol Sci. 2015;370: 20130624. doi:10.1098/rstb.2013.0624

320.   Renaud G, Slon V, Duggan AT, Kelso J. Schmutzi: estimation of contamination and endogenous mitochondrial consensus calling for ancient DNA. Genome Biol. 2015;16: 224. doi:10.1186/s13059-015-0776-0

321.   Fu Q, Li H, Moorjani P, Jay F, Slepchenko SM, Bondarev AA, et al. Genome sequence of a 45,000-year-old modern human from western Siberia. Nature. 2014;514: 445–449. doi:10.1038/nature13810

322.   Drummond AJ, Ashton B, Buxton S, Cheung M, Cooper A, Duran C, et al. Geneious v6. 1. 2011.

323.   Vianello D, Sevini F, Castellani G, Lomartire L, Capri M, Franceschi C. HAPLOFIND: A New Method for High-Throughput mt DNA Haplogroup Assignment. Hum Mutat. 2013;34: 1189–1194. Available: https://onlinelibrary.wiley.com/doi/abs/10.1002/humu.22356

324.   Weissensteiner H, Pacher D, Kloss-Brandstätter A, Forer L, Specht G, Bandelt H-J, et al. HaploGrep 2: mitochondrial haplogroup classification in the era of high-throughput sequencing. Nucleic Acids Res. 2016;44: W58–63. doi:10.1093/nar/gkw233

325.   Knipper C, Mittnik A, Massy K, Kociumaka C, Kucukkalipci I, Maus M, et al. Female exogamy and gene pool diversification at the transition from the Final Neolithic to the Early Bronze Age in central Europe. Proceedings of the National Academy of Sciences. 2017. pp. 10083–10088. doi:10.1073/pnas.1706355114

326.   Furtwängler A, Reiter E, Neumann GU, Siebke I, Steuri N, Hafner A, et al. Ratio of mitochondrial to nuclear DNA affects contamination estimates in ancient DNA analysis. Sci Rep. 2018;8: 14075. doi:10.1038/s41598-018-32083-0

327.   Robinson JT, Thorvaldsdóttir H, Winckler W, Guttman M, Lander ES, Getz G, et al. Integrative genomics viewer. Nat Biotechnol. 2011;29: 24–26. doi:10.1038/nbt.1754

328.   Johnson M, Zaretskaya I, Raytselis Y, Merezhuk Y, McGinnis S, Madden TL. NCBI BLAST: a better web interface. Nucleic Acids Res. 2008;36: W5–9. doi:10.1093/nar/gkn201

329.   Jones ER, Gonzalez-Fortes G, Connell S, Siska V, Eriksson A, Martiniano R, et al. Upper Palaeolithic genomes reveal deep roots of modern Eurasians. Nat Commun. 2015;6: 8912. doi:10.1038/ncomms9912

330.   Damgaard P de B, Marchi N, Rasmussen S, Peyrot M, Renaud G, Korneliussen T, et al. 137 ancient human genomes from across the Eurasian steppes. Nature. 2018;557: 369–374. doi:10.1038/s41586-018-0094-2

331.   de Barros Damgaard P, Martiniano R, Kamm J, Moreno-Mayar JV, Kroonen G, Peyrot M, et al. The first horse herders and the impact of early Bronze Age steppe expansions into Asia. Science. 2018;360. doi:10.1126/science.aar7711

332.   Moiseyev VG, Khartanovich VI. Early Metal Age crania from Bolshoy Oleniy Island, Barents Sea. Archaeology, Ethnology and Anthropology of Eurasia. 2012;40: 145–154. doi:10.1016/j.aeae.2012.05.018

333.   Murashkin AI, Kolpakov EM, Shumkin VY, Khartanovich VI, Moiseyev VG. Kola Oleneostrovskiy grave field: A unique burial site in the European arctic. Iskos. 2016;21. Available: https://journal.fi/iskos/article/view/99574

334.   Rahkonen P. South-Eastern Contact Area of Finnic Languages in the Light of Onomastics. Bookwell; 2013. Available: https://play.google.com/store/books/details?id=wZoXswEACAAJ

335.   Huyghe JR, Fransen E, Hannula S, Van Laer L, Van Eyken E, Mäki-Torkko E, et al. A genome-wide analysis of population structure in the Finnish Saami with implications for genetic association studies. European Journal of Human Genetics. 2011. pp. 347–352. doi:10.1038/ejhg.2010.179

336.   Giffin K, Lankapalli AK, Sabin S, Spyrou MA, Posth C, Kozakaitė J, et al. A treponemal genome from an historic plague victim supports a recent emergence of yaws and its presence in 15th century Europe. Sci Rep. 2020;10: 9499. doi:10.1038/s41598-020-66012-x

337.   Barquera R, Lamnidis TC, Lankapalli AK, Kocher A, Hernández-Zaragoza DI, Nelson EA, et al. Origin and Health Status of First-Generation Africans from Early Colonial Mexico. Curr Biol. 2020;30: 2078–2091.e11. doi:10.1016/j.cub.2020.04.002

338.   Quetel C. HISTORY OF SYPHILIS. [cited 30 Jan 2021]. Available: https://pdfs.semanticscholar.org/3293/930d968fbfb4f3d79337aca2a74313b08ffb.pdf

339.   Arrizabalaga J. Syphilis. The Cambridge World History of Human Disease. 1993. pp. 1025–1033. doi:10.1017/chol9780521332866.196

340.   Ted Steinbock R. Paleopathological Diagnosis and Interpretation: Bone Diseases in Ancient Human Populations. Thomas; 1976. Available: https://play.google.com/store/books/details?id=308eAQAAIAAJ

341.   Waldron T. Palaeopathology. Cambridge University Press; 2008. Available: https://play.google.com/store/books/details?id=vnEoUoAQe-QC

342.   Fitzgerald F. The great imitator, syphilis. West J Med. 1981;134: 424–432. Available: https://www.ncbi.nlm.nih.gov/pubmed/7257350

343.   Kuehnert D. Unifying the molecular evolution and host population dynamics of rapidly evolving pathogens. ResearchSpace@ Auckland. 2013. Available: https://researchspace.auckland.ac.nz/handle/2292/21273

344.   Baele G, Suchard MA, Rambaut A, Lemey P. Emerging Concepts of Data Integration in Pathogen Phylodynamics. Syst Biol. 2017;66: e47–e65. doi:10.1093/sysbio/syw054

345.   De Maio N, Worby CJ, Wilson DJ, Stoesser N. Bayesian reconstruction of transmission within outbreaks using genomic variants. PLoS Comput Biol. 2018;14: e1006117. doi:10.1371/journal.pcbi.1006117

346.   Möller S, du Plessis L, Stadler T. Impact of the tree prior on estimating clock rates during epidemic outbreaks. Proc Natl Acad Sci U S A. 2018;115: 4200–4205. doi:10.1073/pnas.1713314115

7 Figures

- Figure 1. Examples of authentication, adapted from Key et. al 2017. 1) Sample content, including target DNA (light green) and contaminating sources (blue and teal) 2) DNA reads mapping with low specificity to reference sequences A and C, and with high specificity to reference sequence B and age-related damage at the end of the reads. 3) Damage pattern typical for ancient DNA, showing base misincorporation accumulated at the last positions of the reads. 4) Mitochondrial reads from target and contaminant sources, with authentic target reads identified by ancient DNA damage and consistency of mutations, used in building a consensus sequence. 5) Several sources of X-chromosomal DNA in a male specimen, indicating contamination. (Appears on page 11)
- Figure 2. Schematic illustration of the cultural concepts relevant for northeastern Fennoscandian archaeology on a timeline. (Appears on page 16)
- Figure 3. Characteristic bone alterations caused by treponemal infection: A) pits and "moth-eaten" patches on cranial bones, B) normally developed molars with 4-5 cusps, compared to "Mulberry molars", characterized by small, irregular cusps. (Appears on page 28)
- Figure 4. A map of major cultural influences originating in the Upper Volga region and represented in Finnish archaeological finds during Bronze Age and Early Metal period. Left: Seima-Turbino phenomenon (2200-1600 BCE) in orange, and Akozino-Mälar phenomenon (900-300 BCE) in green, both characterized by metalwork and style of weaponry. Right: A) Core region and B) the expanse of Textile ceramic tradition (1900-100 BCE), associated with the spread of Uralic languages. The suggested north-west and south-west routes of Uralic languages from Volga-Oka region to Fennoscandia marked in arrows. Adapted from Lang 2018. (Appears on page 43).

8 Appendix

I. T.C. Lamnidis*, **K. Majander***, C. Jeong, E. Salmela, A. Wessman, V. Moiseyev, V. Khartanovich, O. Balanovsky, M. Ongyerth, A. Weihmann, A. Sajantila, J. Kelso, S. Pääbo, P. Onkamo, W. Haak, J. Krause, S. Schiffels. "Ancient Fennoscandian genomes reveal origin and spread of Siberian Ancestry in Europe". Published in *Nature Communications*, 2018, 9 (1): 1-12.

II. S. Översti*, **K. Majander***, E. Salmela, K. Salo K, L. Arppe, S. Belskiy, H. Etu-Sihvola, V. Laakso, E. Mikkola, S. Pfrengle, M. Putkonen, J.-P. Taavitsainen, K. Vuoristo, A. Wessman, A. Sajantila, M. Oinonen, W. Haak, V.J. Schuenemann, J. Krause, J.U. Palo, P. Onkamo. "Human mitochondrial DNA lineages in Iron-Age Fennoscandia suggest incipient admixture and eastern introduction of farming-related maternal ancestry". Published in *Scientific reports*, 2019, 9 (1): 1-4.

III. **K. Majander***, S. Pfrengle*, A. Kocher, J. Neukamm, L. du Plessis, M. Pla-Díaz, N. Arora, G. Akgül, K. Salo, R. Schats, S. Inskip, M. Oinonen, H. Valk, M. Malve, A. Kriiska, P. Onkamo, F. González-Candelas, D. Kühnert, J. Krause, V.J. Schuenemann. "Ancient bacterial genomes reveal a high diversity of Treponema pallidum Strains in early Modern Europe". Published in *Current Biology,* 2020, 30 (19): 3788-3803.

* Denotes equal contribution

ARTICLE

Ancient Fennoscandian genomes reveal origin and spread of Siberian ancestry in Europe

Thiseas C. Lamnidis[1], Kerttu Majander[1,2,3], Choongwon Jeong[1,4], Elina Salmela [1,3], Anna Wessman[5], Vyacheslav Moiseyev[6], Valery Khartanovich[6], Oleg Balanovsky[7,8,9], Matthias Ongyerth[10], Antje Weihmann[10], Antti Sajantila[11], Janet Kelso [10], Svante Pääbo[10], Päivi Onkamo[3,12], Wolfgang Haak[1], Johannes Krause [1] & Stephan Schiffels [1]

European population history has been shaped by migrations of people, and their subsequent admixture. Recently, ancient DNA has brought new insights into European migration events linked to the advent of agriculture, and possibly to the spread of Indo-European languages. However, little is known about the ancient population history of north-eastern Europe, in particular about populations speaking Uralic languages, such as Finns and Saami. Here we analyse ancient genomic data from 11 individuals from Finland and north-western Russia. We show that the genetic makeup of northern Europe was shaped by migrations from Siberia that began at least 3500 years ago. This Siberian ancestry was subsequently admixed into many modern populations in the region, particularly into populations speaking Uralic languages today. Additionally, we show that ancestors of modern Saami inhabited a larger territory during the Iron Age, which adds to the historical and linguistic information about the population history of Finland.

[1] Department of Archaeogenetics, Max Planck Institute for the Science of Human History, 07745 Jena, Germany. [2] Institute for Archaeological Sciences, Archaeo- and Palaeogenetics, University of Tübingen, 72070 Tübingen, Germany. [3] Department of Biosciences, University of Helsinki, PL 56 (Viikinkaari 9), 00014 Helsinki, Finland. [4] The Eurasia3angle Project, Max Planck Institute for the Science of Human History, 07745 Jena, Germany. [5] Department of Cultures, Archaeology, University of Helsinki, PL 59 (Unioninkatu 38), 00014 Helsinki, Finland. [6] Peter the Great Museum of Anthropology and Ethnography (Kunstkamera), Russian Academy of Sciences, University Embankment, 3, Saint Petersburg 199034, Russia. [7] Vavilov Institute of General Genetics, Ulitsa Gubkina, 3, Moscow 117971, Russia. [8] Research Centre for Medical Genetics, Moskvorech'ye Ulitsa, 1, Moscow 115478, Russia. [9] Biobank of North Eurasia, Kotlyakovskaya Ulitsa, 3 строение 12, Moscow 115201, Russia. [10] Max Planck Institute for Evolutionary Anthropology, Deutscher Pl. 6, 04103 Leipzig, Germany. [11] Department of Forensic Medicine, University of Helsinki, PL 40 (Kytösuontie 11), Helsinki 00014, Finland. [12] Department of Biology, University of Turku, Turku 20014, Finland. These authors contributed equally to this work: Thiseas C. Lamnidis, Kerttu Majander. These authors jointly supervised this work: Päivi Onkamo, Wolfgang Haak, Johannes Krause, Stephan Schiffels. Correspondence and requests for materials should be addressed to P.O. (email: paivi.onkamo@helsinki.fi) or to W.H. (email: haak@shh.mpg.de) or to S.S. (email: schiffels@shh.mpg.de)

The genetic structure of Europeans today is the result of several layers of migration and subsequent admixture. The incoming source populations no longer exist in unadmixed form, but have been identified using ancient DNA in several studies over the last few years[1–8]. Broadly, present-day Europeans have ancestors in three deeply diverged source populations: European hunter-gatherers who settled the continent in the Upper Paleolithic, Europe's first farmers who expanded from Anatolia across Europe in the early Neolithic starting around 8000 years ago, and groups from the Pontic Steppe that arrived in Europe during the final Neolithic and early Bronze Age ~ 4500 years ago. As a consequence, most Europeans can be modelled as a mixture of these three ancestral populations[3].

This model, however, does not fit well for present-day populations from north-eastern Europe such as Saami, Russians, Mordovians, Chuvash, Estonians, Hungarians, and Finns: they carry additional ancestry seen as increased allele sharing with modern East Asian populations[1,3,9,10]. The origin and timing of this East Asian-related contribution is unknown. Modern Finns are known to possess a distinct genetic structure among today's European populations[9,11,12], and the country's geographical location at the crossroads of eastern and western influences introduces a unique opportunity to investigate the migratory past of north-east Europe. Furthermore, the early migrations and genetic origins of the Saami people in relation to the Finnish population call for a closer investigation. Here, the early-Metal-Age, Iron-Age, and historical burials analysed provide a suitable time-transect to ascertain the timing of the arrival of the deeply rooted Siberian genetic ancestry, and a frame of reference for investigating linguistic diversity in the region today.

The population history of Finland is subject to an ongoing discussion, especially concerning the status of the Saami as the earlier inhabitants of Finland, compared to Finns. The archaeological record proves human presence in Finland since 9000 BC[13]. Over the millennia, people from Scandinavia, the north-east Baltics, and modern-day Russia have left evidence of their material cultures in Finland[14,15]. The Finno-Ugric branch of the Uralic language family, to which both Saami and Finnish languages belong, has diverged from other Uralic languages no earlier than 4000–5000 years ago, when Finland was already inhabited by speakers of a language today unknown. Linguistic evidence shows that Saami languages were spoken in Finland prior to the arrival of the early Finnish language and have dominated the whole of the Finnish region before 1000 CE[16–18]. Particularly, southern Ostrobothnia, where Levänluhta is located, has been suggested through place names to harbour a southern Saami dialect until the late first millennium[19], when early Finnish took over as the dominant language[20]. Historical sources note Lapps living in the parishes of central Finland still in the 1500s[21]. It is, however, unclear whether all of them spoke Saami, or if some of them were Finns who had changed their subsistence strategy from agriculture to hunting and fishing. There are also documents of intermarriage, although many of the indigenous people retreated to the north (see ref. [22] and references therein). Ancestors of present-day Finnish speakers possibly migrated from northern Estonia, to which Finns still remain linguistically close, and displaced but also admixed with the local population of Finland, the likely ancestors of today's Saami speakers[23].

In this study, we present new genome-wide data from Finland and the Russian Kola Peninsula, from 11 individuals who lived between 3500 and 200 years ago (and 4 more ancient genomes with very low coverage). In addition, we present a new high-coverage whole genome from a modern Saami individual for whom genotyping data was previously published[1]. Our results suggest that a new genetic component with strong Siberian affinity first arrived in Europe at least 3500 years ago, as observed in our oldest analysed individuals from northern Russia. These results describe the gene pool of modern north-eastern Europeans in general, and of the speakers of Uralic languages in particular, as the result of multiple admixture events between Eastern and Western sources since the first appearance of this ancestry component. Additionally, we gain further insights into the genetic history of the Saami in Finland, by showing that during the Iron Age, close genetic relatives of modern Saami lived in an area much further south than their current geographic range.

Results

Sample information and archaeological background. The ancient individuals analysed in this study come from three time periods (Table 1, Fig. 1, Supplementary Note 1). The six early Metal Age individuals were obtained from an archaeological site at Bolshoy Oleni Ostrov in the Murmansk Region on the Kola Peninsula (Bolshoy from here on). The site has been radiocarbon dated to 1610-1436 calBCE (see Supplementary Note 1) and the mitochondrial DNA HVR-I haplotypes from these six individuals have been previously reported[24]. Today, the region is inhabited by Saami. Seven individuals stem from excavations in Levänluhta, a lake burial in Isokyrö, Finland. Artefacts from the site have been dated to the Finnish Iron Age (300–800 CE)[25,26]. Today, the inhabitants of the area speak Finnish and Swedish. Two individuals were obtained from the 18–19th century Saami cemetery of Chalmny Varre on the Russian Kola Peninsula. The cemetery and the surrounding area were abandoned in the 1960s because of planned industrial constructions, and later became the subject of archaeological excavations. In addition, we sequenced the whole genome of a modern Saami individual to 17.5-fold coverage, for whom genotyping data has previously been published[1].

The sampling and subsequent processing of the ancient human remains was done in dedicated clean-room facilities (Methods). A SNP-capture approach targeting a set of 1,237,207 single nucleotide polymorphisms (SNPs) was used to enrich ancient-DNA libraries for human DNA[4]. The sequenced DNA fragments were mapped to the human reference genome, and pseudohaploid genotypes were called based on a random read covering each targeted SNP (see Methods). To ensure the ancient origin of our samples, and the reliability of the data produced, we implemented multiple quality controls. First, we confirmed the deamination patterns at the terminal bases of DNA reads being characteristic of ancient DNA (Supplementary Table 1). Second, we estimated potential contamination rates through heterozygosity on the single-copy X chromosome for male individuals (all below 1.6%)[27] (Table 1, see Supplementary Figure 1 for sex determination). Third, we carried out supervised genetic clustering using ADMIXTURE[28], using six divergent populations as defined clusters, to identify genetic dissimilarities and possible contamination from distantly related sources (Supplementary Figure 2, Supplementary Note 2). Fourth, we calculated mitochondrial contamination for all ancient individuals using ContamMix[29]. Finally, for individuals with sufficient SNP coverage, we carried out principal component analysis (PCA), projecting damage-filtered and non-filtered versions of each individual, to show that the different datasets cluster together regardless of the damage-filtering[30] (see Supplementary Figure 3 and Methods). Eleven ancient individuals passed those quality checks, while four individuals from Levänluhta were excluded from further analyses, due to low SNP coverage (<15,000 SNPs). We merged the data from these 15 individuals with that of 3333 published present-day individuals genotyped on the Affymetrix Human Origins platform and 538 ancient individuals sequenced using a mixture of DNA capture and shotgun sequencing (Supplementary Data 1)[1–4,8,31,32].

Table 1 Sample information

Individual ID	Site/ location	Date	Population label	Genetic Sex	# SNPs overlap with Human Origins	Avg. coverage on target (1240 K MapQ ≥ 30)	Nuclear contamination	mtDNA contamination	mtDNA, Y haplotypes
BOO001	Bolshoy Oleni Ostrov, Murmansk, Russia	3473 ± 87 calBP	Bolshoy	F	347,709	1.22	N/A	0.001 (0.000–0.007)	U4a1
BOO002			Bolshoy	M	403,994	0.81	0.004 ± 0.003	0.000 (0.000–0.002)	Z1a1a, N1c1a1a
BOO003			Bolshoy	F	300,598	1.09	N/A	0.016 (0.010–0.024)	T2d1b1
BOO004			Bolshoy	M	342,582	2.92	0.002 ± 0.001	0.003 (0.000–0.059)	C4b, N1c1a1a
BOO005			Bolshoy	F	347,042	2.88	N/A	0.005 (0.001–0.026)	U5a1d
BOO006			Bolshoy	F	390,835	1.08	N/A	0.008 (0.004–0.014)	D4e4
CHV001	Chalmny- Varre, Murmansk, Russia	18–19th cent CE	Chalmny Varre	F	426,702	1.42	N/A	0.001 (0.000–0.003)	U5b1b1a3
CHV002			Chalmny Varre	M	215,228	0.47	0.016 ± 0.011	0.000 (0.000–0.003)	V7a1, I2a1
JK1963	Levänluhta, Isokyrö, Finland	300–800 CE	N/A	f	10,492	0.02	N/A	0.004 (0.001–0.013)	N/A
JK1967			N/A	f	5267	0.01	N/A	0.000 (0.000–0.009)	N/A
JK1968			Levänluhta	F	207,076	0.47	N/A	0.004 (0.001–0.065)	U5a1a1a'b'n
JK1970			Levänluhta	F	194,764	0.44	N/A	0.023 (0.005–0.129)	U5a1a1
JK2065			Levänluhta_B	F	133,224	0.29	N/A	0.028 (0.012–0.064)	K1a4a1b
JK2066			N/A	?	4045	0.01	N/A	0.002 (0.001–0.007)	N/A
JK2067			N/A	?	2356	0.01	N/A	0.010 (0.002–0.032)	N/A
Saami001	Finland	Modern	Modern Saami	M	593,094	6.32	N/A	N/A	U5b1b1a1, I1a1b3a1

Summary information for all individuals for which we report genomic data in this study. A radiocarbon date is given for the Bolshoy samples, as described in Supplementary Text 1. Other dates are context-based, as described in Supplementary Text 1. Population labels for individuals of low coverage are shown as N/A. Genetic sex is determined as described in Methods, and lowercase letters denote probable genetic sex for low-coverage individuals. Question marks denote undefined genetic sex due to low coverage. Mitochondrial contamination estimates are given as posterior mode and 95% posterior intervals in brackets, as provided by ContamMix[70]

Eastern genetic affinities in Northern Europe. To investigate the genetic affinities of the sampled individuals, we projected them onto principal components (PC) computed from 1320 modern European and Asian individuals (Fig. 2a, Supplementary Figures 3a, b for a version focusing on West Eurasia). As expected, PC1 separates East Asian from West Eurasian populations. Within each continental group, genetic variability is spread across PC2: The East Asian genetic cline contains populations between the Siberian Nganasan (Uralic speakers) and Yukagirs at one end, and the Ami and Atayal from Taiwan at the other end. The West Eurasian cline along PC2 spans from the Bedouins on the Arabian Peninsula to north-eastern Europeans including Lithuanians, Norwegians and Finns. Between these two main Eurasian clines exist multiple clines, spanning between West and East Eurasians. These clines are likely the result of admixture events and population movements between East and West Eurasia. Most relevant to the populations analysed here is the admixture cline between north-eastern Europe and the North Siberian Nganasan, including mostly Uralic-speaking populations in our dataset (marked in light purple in Fig. 2a).

Ten of the eleven ancient individuals from this study fall on this Uralic cline, with the exception of one individual from Levänluhta (ID JK2065, here named Levänluhta_B), who instead is projected closer to modern Lithuanian, Norwegian and Icelandic populations. Specifically, two Levänluhta individuals and the two historical Saami from Russia are projected very close to the two previously published modern Saami (Saami.DG)[32] and the new Saami shotgun genome generated in this study (as well as the previously published genome of the same individual, here labelled Saami (WGA)[1]), suggesting genetic continuity in the

north from the Iron Age to modern-day Saami populations. In contrast, the six ancient individuals from Bolshoy are projected much further towards East Asian populations, and fall to an intermediate position along the Uralic cline and close to modern-day Mansi.

Unsupervised genetic clustering analysis as implemented in the ADMIXTURE[28] program suggests a similar profile to the PCA: north-eastern European populations harbour a Siberian genetic component (light purple) maximized in the Nganasan (Fig. 2b, see Supplementary Figure 4a for results over multiple K values). The hunter-gatherer genetic ancestry in Europeans (blue) is maximized in European Upper Palaeolithic and Mesolithic hunter-gatherers, including the 8000-year-old Western European hunter-gatherers from Hungary and Spain (WHG), the 8000-year-old Scandinavian hunter-gatherers from Motala (SHG) and the Narva and Kunda individuals from the Baltics. An ancestry component associated with Europe's first farmers (orange) is maximized in Early Neolithic Europeans associated with the LBK (from German: Linearbandkeramik). The steppe ancestry component within modern Europeans (green), which is associated with the Yamnaya population, is maximised in ancient Iranian populations and to a lesser extent Caucasus hunter-gatherers (CHG). This ancestry component is also present in modern Armenians from the Caucasus, Bedouins from the Arabian Peninsula and South Asian populations. Within modern Europeans, the Siberian genetic component (light purple) is maximized in the Mari and Saami, and can also be seen in similar proportions in the historical Saami from Chalmny Varre and in two of the Levänluhta individuals. The third Levänluhta individual (Levänluhta_B), however, lacks this Siberian
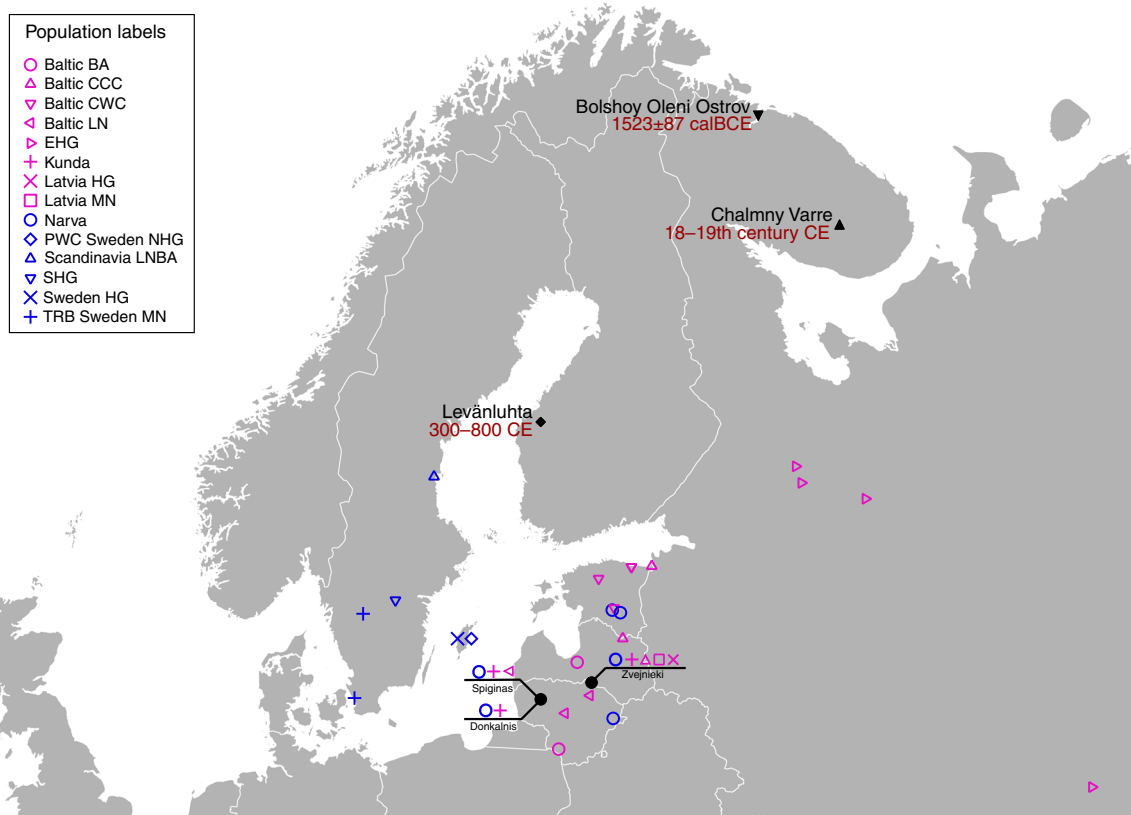
Fig. 1 Location and age of archaeological sites used in this study. The location of other sites relevant to this study is also shown. Markers used correspond to the ones used in Fig. 2. Map generated with QGIS 2.18.19 (http://www.qgis.org/) using the Natural Earth country boundary dataset (http://www. naturalearthdata.com) for the basemap. Source data are provided as a Source Data file

component. The six ancient individuals from Bolshoy show substantially higher proportions of the Siberian component: it comprises about half of their ancestry (42.3–58.2%), whereas the older Mesolithic individuals from Motala (SHG) do not possess it at all. The Native-American-related ancestry seen in the EHG and Bolshoy corresponds to a previously reported affinity towards Ancient North Eurasians (ANE)[2,33] contributing genes to both Native Americans and West Eurasians. ANE ancestry also comprises part of the ancestry of Nganasans[2].

Interestingly, results from uniparentally-inherited markers (mtDNA and Y chromosome) as well as certain phenotypic SNPs also show Siberian signals in Bolshoy: mtDNA haplogroups Z1, C4 and D4, common in modern Siberia[24,34,35] are represented by the individuals BOO002, BOO004 and BOO006, respectively (confirming previous findings[24]), whereas the Y-chromosomal haplotype N1c1a1a (N-L392) is represented by the individuals BOO002 and BOO004. Haplogroup N1c, to which this haplotype belongs, is the major Y-chromosomal lineage in modern north-east Europe and European Russia. It is especially prevalent in Uralic speakers, comprising for example as much as 54% of eastern Finnish male lineages today[36]. Notably, this is the earliest known occurrence of Y-haplogroup N1c in Fennoscandia. Additionally, within the Bolshoy population, we observe the derived allele of rs3827760 in the *EDAR* gene, which is found in near-fixation in East Asian and Native American populations today, but is extremely rare elsewhere[37], and has been linked to phenotypes related to tooth shape[38] and hair morphology[39] (Supplementary Data 2). Scandinavian hunter-gatherers from Motala in Sweden have also been found to carry haplotypes associated with this allele[4]. Finally, in the Bolshoy individuals we also see high frequencies of haplotypes associated with diets rich in poly-unsaturated fatty acids, in the *FADS* genes[4,40,41].

The arrival of Siberian ancestry in Europe. We formally tested for admixture in north-eastern Europe by calculating f_3(Test; Siberian source, European source) statistics. We used several Uralic-speaking populations—Estonians, Saami, Finnish, Mordovians and Hungarians—and Russians as Test populations. Significantly negative f_3 values correspond to the Test population being admixed between populations related to the two source populations[42]. We used multiple European and Siberian sources to capture differences in ancestral composition among proxy populations: As proxies for the Siberian source we used Bolshoy, Mansi and Nganasan, and for the European source we used modern Icelandic, Norwegian, Lithuanian and French. Our results show that all of the test populations are indeed admixed, with the most negative values arising when Nganasan are used as the Siberian source (Supplementary Data 3). Among the European sources, Lithuanians gave the most negative results for Estonians, Russians and Mordovians. For modern Hungarians, the European source giving most negative results was French, while both Bolshoy and Nganasan gave equally negative results when used as the Siberian source. With Finns as test, modern Icelanders were the European source giving most negative statistics. Finally, Icelanders and Nganasan used as the European and Siberian sources, respectively, yielded the most negative result for the present-day Saami as a Test. This result is still non-significantly negative, either due to the low number of modern Saami individuals in our dataset ($n = 3$), or due to post-admixture drift in modern Saami. A high degree of population-specific drift can affect f_3-statistics and result in less negative and even positive values[42]. Indeed, post-admixture drift would correlate well with the suggested founder effect[43] in Saami. To further test differential relatedness with Nganasan in European populations and in the ancient individuals in this study, we
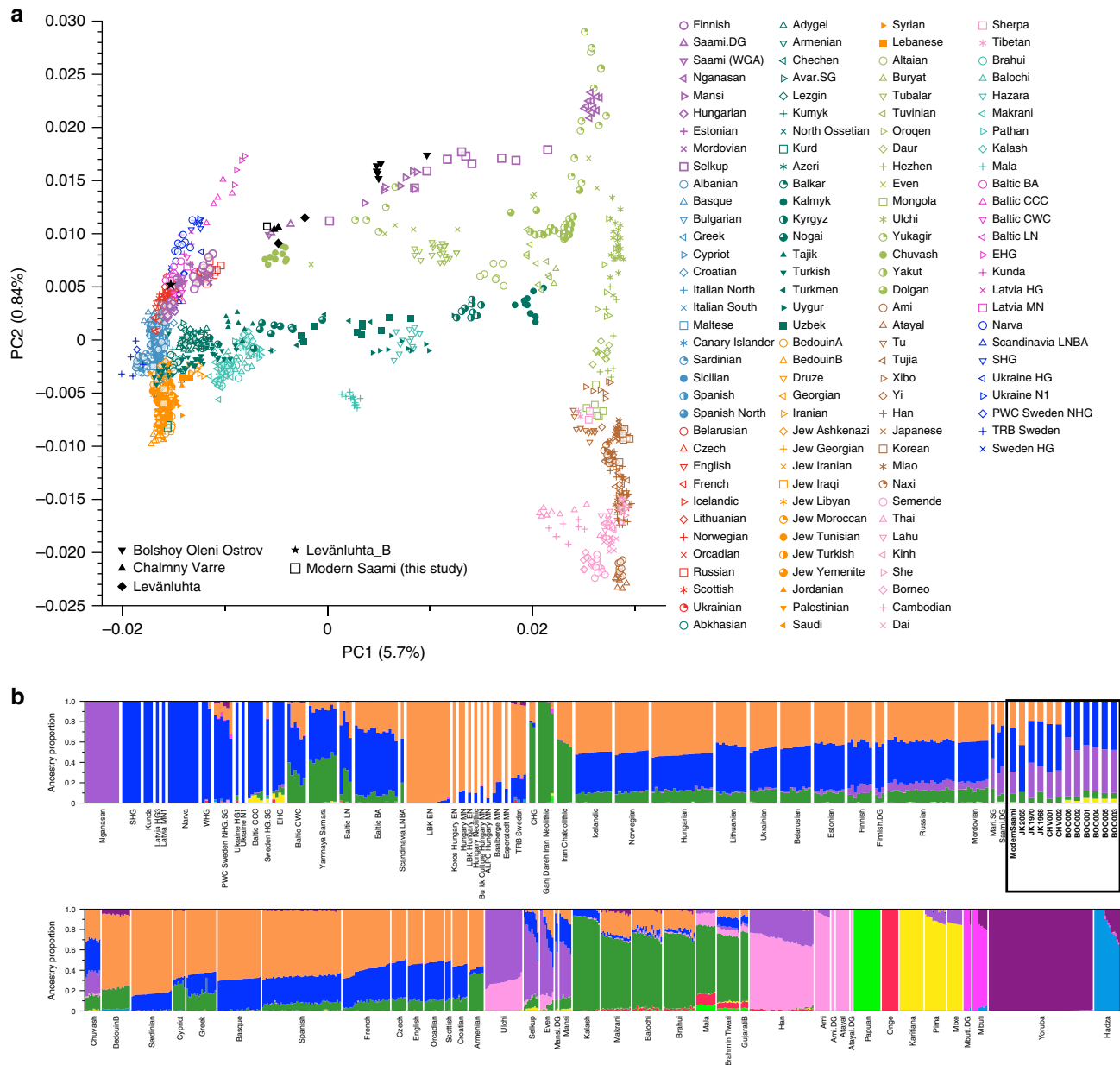
Fig. 2 PCA and ADMIXTURE analysis. **a** PCA plot of 113 Modern Eurasian populations, with individuals from this study and other relevant ancient genomes projected on the principal components, using the "shrinkmode: YES" option. Uralic-speaking populations are highlighted in dark purple. PCA of Europe can be found in Supplementary Figure 3. **b** Plot of ADMIXTURE (K = 11) results containing worldwide populations. Ancient individuals from this study (black box) are represented by thicker bars and shown in bold. For a figure of ADMIXTURE results over multiple K values see Supplementary Figure 4a. Source data are provided as a Source Data file

calculated f₄(Mbuti, Nganasan; Lithuanian, Test) (Fig. 3). Consistent with f₃-statistics above, all the ancient individuals and modern Finns, Saami, Mordovians and Russians show excess allele sharing with Nganasan when used as Test populations. Of all Uralic-speaking populations in Europe, Hungarians are the only population that shows no evidence of excess allele sharing with Nganasan compared to that of Lithuanians, consistent with their distinct population history from other Uralic populations as evidenced by historical sources (see ref. [44] and references therein).

We further estimated the genetic composition in these populations using qpAdm[3]. All ancient and modern individuals from the Baltics, Finland and Russia were successfully modelled as a mixture of five lines of ancestry, represented by eastern Mesolithic hunter-gatherers (EHG, from Karelia), Yamnaya from Samara, LBK from the early European Neolithic, western

Mesolithic hunter-gatherers (WHG, from Spain, Luxembourg and Hungary), and Nganasan, or subsets of those five (Supplementary Data 4). In contrast to previous models for European populations using three streams of ancestry[2,3], we found that some populations modelled here require two additional components: a component related to modern Nganasans, as discussed above, and additional EHG ancestry, not explained by Yamnaya (who have been shown to contain large amounts of EHG ancestry themselves[3]). Indeed, the six Bolshoy individuals have substantial amounts of EHG but no Yamnaya ancestry. We find that Nganasan-related ancestry is significantly present in all of our ancient samples except for Levänluhta_B, and in many modern, mainly Uralic-speaking populations. The 3500-year-old ancient individuals from Bolshoy represent the highest proportion of Siberian Nganasan-related ancestry seen in this
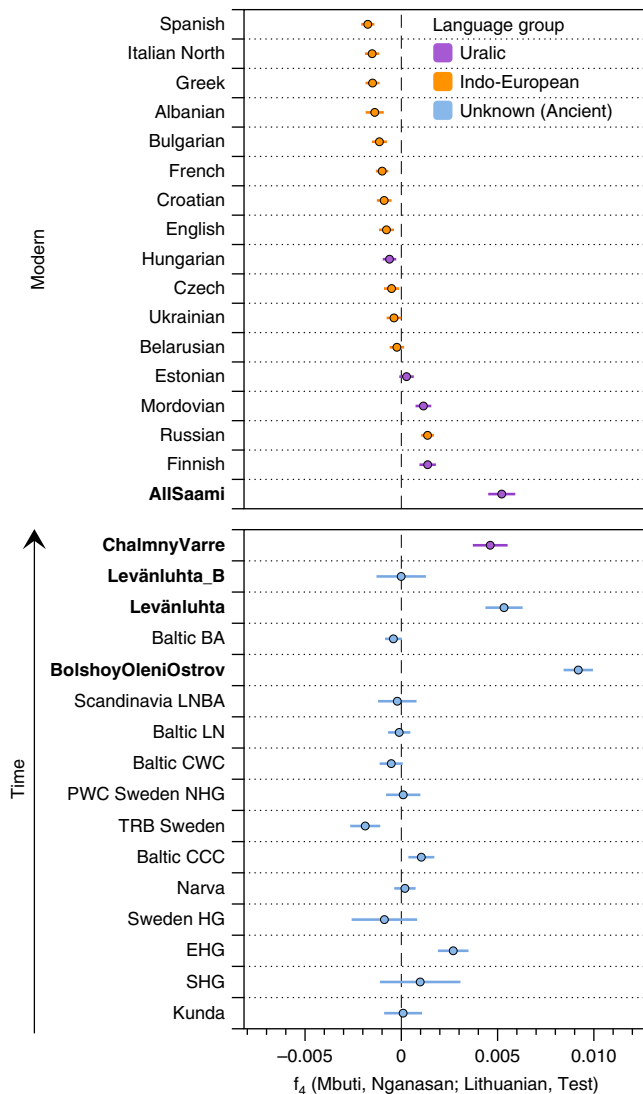
Fig. 3 Calculated f_4 (Mbuti, Nganasan; Lithuanian, Test). Modern populations are sorted by f_4 magnitude; ancient populations are sorted through time. Populations are coloured based on language family, with Ancient individuals with unknown language shown in blue. "AllSaami" refers to a grouping including the 2 individuals from the SGDP (Saami (SGDP)) and the high-coverage modern Saami shotgun genome in this study (Modern Saami). Individuals from this study are indicated by labels in bold. Error bars represent 3 standard errors, to indicate significant difference from 0. Source data are provided as a Source Data file

region so far, and possibly evidence its earliest presence in the western end of the trans-Siberian expanse (Fig. 4). The geographically proximate ancient hunter-gatherers from the Baltics (6000 and 6300 BC) and Motala (~6000 BC), who predate Bolshoy, lack this component, as do late Neolithic and Bronze Age individuals from the Baltics[7,8,45]. All later ancient individuals in this study have lower amounts of Nganasan-related ancestry than Bolshoy (Figs 3, 4), probably as a result of dilution through admixture with other populations from further south. This is also consistent with the increased proportion of early European farmer ancestry related to Neolithic Europeans (Fig. 2b) in our later samples. We note that a low but significant amount of Neolithic European ancestry is also present in the Bolshoy population. Finally, we tested whether Bolshoy, instead of Nganasan, can be used as source population. We found that

Bolshoy works as source in some ancient individuals, but not for modern Uralic speakers (see Supplementary Data 4).

As shown by these multiple lines of evidence, the pattern of genetic ancestry observed in north-eastern Europe is the result of admixture between populations from Siberia and populations from Europe. To obtain a relative date of this admixture, and as an independent line of evidence thereof, we used admixture linkage disequilibrium decay, as implemented in ALDER[46]. Our ALDER admixture estimate for Bolshoy, using Nganasan and EHG as admixture sources, dates only 17 generations ago. Based on the radiocarbon date for Bolshoy and its uncertainty, and assuming a generation time of 29 years[47], we estimate the time of introduction of the Siberian Nganasan-related ancestry in Bolshoy to be 3977 (±77) years before present (yBP) (Fig. 5b). Estimates obtained using Nganasans and Lithuanians as source populations provided a similar estimate (Supplementary Figure 5 for LD decay plots for multiple populations using Lithuanian and Nganasan as sources.). ALDER provides a relative date estimate for a single-pulse admixture event in generations. When multiple admixture events have occurred, such a single estimate should be interpreted as a (non-arithmetic) average of those events[46,48]. Therefore the admixture date estimate for Bolshoy does not preclude earlier admixture events bringing Siberian Nganasan-related ancestry into the population, in multiple waves. Indeed, for all other populations with evidence of this ancestry, we find much younger admixture dates (Fig. 5a), suggesting that the observed genetic ancestry in north-eastern Europe is inconsistent with a single-pulse admixture event.

Major genetic shift in Finland since the Iron Age. Besides the early evidence of Siberian ancestry, our ancient samples from Levänluhta and Chalmny Varre allow us to investigate the more recent population history of Finland. To test whether the ancient individuals from Levänluhta form a clade with modern-day Saami or with modern Finns, we calculated f_4(Saami(SGDP), Test; X, Mbuti) and f_4(Finnish, Test; X, Mbuti), where Test was substituted with each ancient individual from Levänluhta, the two historical Saami individuals from Chalmny Varre, as well as the Modern Saami individual, and X was substituted by worldwide modern-day populations (Supplementary Data 5 & 6, and Supplementary Figures 5 & 6). One Levänluhta (JK1968) and the two Chalmny Varre individuals consistently formed a clade with modern-day Saami, but not with modern-day Finns, with respect to all worldwide populations. One Levänluhta individual (JK1970) showed slightly lower affinity to central Europe than modern-day Saami do, while still rejecting a cladal position with modern-day Finns. This indicates that the people inhabiting Levänluhta during the Iron Age, and possibly other areas in the region as well, were more closely related to modern-day Saami than to present-day Finns; however, their difference from the modern Saami may reflect internal structure within the Saami population or additional admixture into the modern population.

One of the individuals from Levänluhta (JK2065/Levänluhta_B) rejects a cladal position with modern Saami to the exclusion of most modern Eurasian populations. This individual also rejects a cladal position with Finns. We analysed low coverage genomes from four additional individuals of the Levänluhta site using PCA (Supplementary Figure 3), confirming the exclusive position of Levänluhta_B compared to all other six individuals (including the four low-coverage individuals) from that site, as is consistent with the ADMIXTURE and qpAdm results. The outlier position of this individual cannot be explained by modern contamination, since it passed several tests for authentication (see Methods) along with all other ancient individuals. However, no direct dating was available for the Levänluhta material, and we cannot exclude the
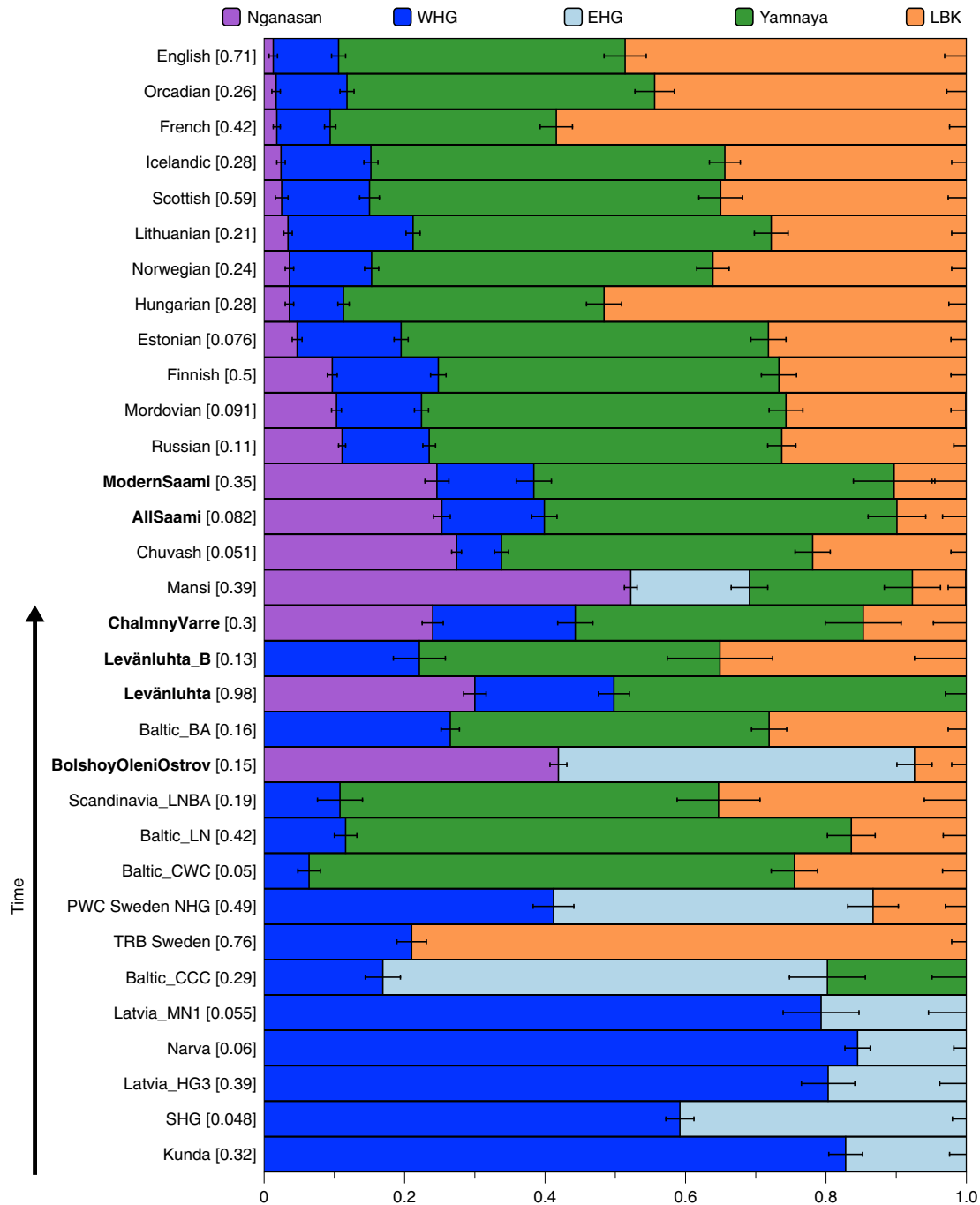
Fig. 4 Mixture proportions from five sources estimated using qpAdm. Sources used were Nganasan, WHG, EHG, Yamnaya and LBK (see Methods/ Supplementary Data 4). *P*-values (chi-square) for each model are shown in square brackets next to the test population. Results from the least complex model for each test population/individual are shown. "AllSaami" corresponds to a population consisting of the two genomes from the SGDP and the genome from this study (ModernSaami). Error bars represent one standard error and are plotted to the right of their associated mixture proportion. Populations containing individuals from this study are shown in bold. Source data are provided as a Source Data file

possibility of a temporal gap between this individual and the other individuals from that site.

Discussion

In terms of ancient human DNA, north-eastern Europe has been relatively understudied. In this study we extend the available information from this area considerably, and present the first ancient genome-wide data from Finland. While the Siberian genetic component presented here has been previously described

in modern-day populations from the region[1,3,9,10], we gain further insights into its temporal depth. Our data suggest that this fourth genetic component found in modern-day north-eastern Europeans arrived in the area before 3500 yBP. It was introduced in the population ancestral to Bolshoy Oleni Ostrov individuals 4000 years ago at latest, as illustrated by ALDER dating using the ancient genome-wide data from the Bolshoy samples. The upper bound for the introduction of this component is harder to estimate. The component is absent in the Karelian hunter-gatherers (EHG)[3] dated to 8300–7200 yBP as well as Mesolithic and
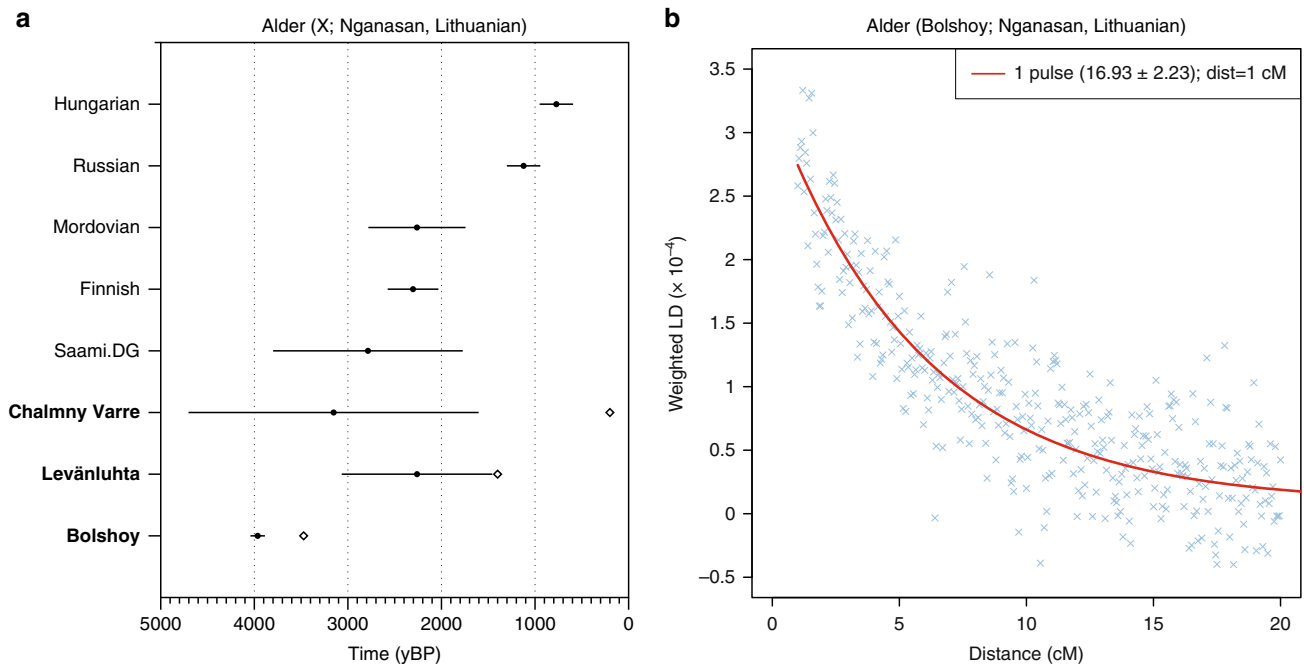
Fig. 5 Dating the introduction of Siberian ancestry using ALDER. **a** ALDER-inferred admixture dates (filled circles) for different populations, using Nganasan and Lithuanian as sources. Available dates for ancient populations are shown in white diamonds. Error bars represent one standard error provided by ALDER and include the uncertainty surrounding the dating of ancient population samples, calculated using standard propagation. Populations containing individuals from this study are shown in bold. **b** LD decay curve for Bolshoy, using Nganasan and EHG as sources. The fitted trendline considers a minimum distance of 1 cM. A full set of LD decay plots can be found in Supplementary Figure 5. Source data are provided as a Source Data file

Neolithic populations from the Baltics from 8300 yBP and 7100–5000 yBP respectively[8]. While this suggests an upper bound of 5,000 yBP for the arrival of this Siberian ancestry, we cannot exclude the possibility of its presence even earlier, yet restricted to more northern regions, as suggested by its absence in populations in the Baltics during the Bronze Age. Furthermore, our study presents the earliest occurrence of the Y-chromosomal haplogroup N1c in Fennoscandia. N1c is common among modern Uralic speakers, and has also been detected in Hungarian individuals dating to the 10th century[44], yet it is absent in all published Mesolithic genomes from Karelia and the Baltics[3,8,45,49].

The large Nganasan-related component in the Bolshoy individuals from the Kola Peninsula provides the earliest direct genetic evidence for an eastern migration into this region. Such contact is well documented in archaeology, with the introduction of asbestos-mixed Lovozero ceramics during the second millennium BC[50], and the spread of even-based arrowheads in Lapland from 1900 BCE[51,52]. Additionally, the nearest counterparts of Vardøy ceramics, appearing in the area around 1,600-1,300 BCE, can be found on the Taymyr peninsula, much further to the East[51,52]. Finally, the Imiyakhtakhskaya culture from Yakutia spread to the Kola Peninsula during the same period[24,53]. Contacts between Siberia and Europe are also recognised in linguistics. The fact that the Nganasan-related genetic component is consistently shared among Uralic-speaking populations, with the exceptions of absence in Hungarians and presence in the non-Uralic speaking Russians, makes it tempting to equate this genetic component with the spread of Uralic languages in the area. However, such a model may be overly simplistic. First, the presence of the Siberian component on the Kola Peninsula at ca. 3500 yBP predates most linguistic estimates of the spread of extant Uralic languages to the area[54]. Second, as shown in our analyses, the admixture patterns found in historic and modern Uralic speakers are complex and in fact inconsistent with a single admixture event. Therefore, even if the Siberian genetic

component partly spread alongside Uralic languages, some Siberian ancestry may have been already present in the area from earlier admixture events.

The novel genome-wide data presented here from ancient individuals from Finland opens new insights into Finnish population history. Two of the three higher-coverage genomes and all four low-coverage genomes from Levänluhta individuals showed low genetic affinity to modern-day Finnish speakers of the area. Instead, an increased affinity was observed to modern-day Saami speakers, now mostly residing in the north of the Scandinavian Peninsula. These results suggest that the geographic range of the Saami extended further south in the past, and points to a genetic shift at least in the western Finnish region since the Iron Age. The findings are in concordance with the noted linguistic shift from Saami languages to early Finnish. Further ancient DNA from Finland is needed in order to conclude, to what extent these signals of migration and admixture are representative of Finland as a whole.

Methods
Sampling. Written informed consent was obtained from the Saami individual whose genome was analysed in this study, which was approved of by The Hospital District of Helsinki and Uusimaa Ethical Committee (Decision 329/13/03/00/2013) and the ethics committee of the University of Leipzig (Approval reference number 398-13-16122013).

Sampling and extracting ancient DNA requires a strict procedure in order to avoid contamination introduced by contemporary genetic material. For the 13 Iron-Age individuals from Finland available to us, the sampling took place in a clean-room facility dedicated to ancient DNA work, at the Institute for Archaeological Sciences in Tübingen. The preliminary workflow included documenting, photographing and storing the samples in individual, ID-coded plastic tubes and plastic bags. As a result of an early pilot study, the tooth samples we used were fragmented, and some of the dentine was removed. The remaining dentine was collected by carefully separating it from the enamel with a dentist drill and cooled-down diamond drill heads, rotated at a speed below 15 rpm, to avoid possible heat-caused damaging to the ancient DNA.

For samples from the sites of Bolshoy and Chalmny Varre, we used leftover tooth powder that was originally processed at the Institute of Anthropology at the

University of Mainz for replication purposes as described in ref. [24]. In brief, the sample preparation steps included UV-irradiation for 30–45 min, followed by gentle wiping of the surface with diluted commercial bleaches. The teeth were then sand-blasted using aluminium oxide abrasive (Harnisch & Rieth) and ground to fine powder using a mixer-mill (Retsch).

Radiocarbon date calibration. We calibrated the radiocarbon date of Bolshoy, reported in refs [24,55] as 3473 ± 42 years BP, using Intcal13[56] as the calibration curve, using OxCal 4.3[57].

DNA extraction and library preparation. DNA from the six Bolshoy and the two Chalmny Varre samples was extracted in the ancient DNA facilities of the Max Planck Institute for the Science of Human History (MPI-SHH) in Jena, Germany. Extraction for the Levänluhta samples was similarly conducted in the clean-room facilities of the Institute for Archaeological Sciences in Tübingen. For each specimen, ~ 50 mg of dentine powder was used for an extraction procedure specifically designed for ancient DNA retrieval[58]. Extraction buffer containing 0.45 M EDTA, pH 8.0 (Life Technologies) and 0.25 mg/ml Proteinase K (Sigma-Aldrich) was added to bone powder and incubated at 37 °C with rotation overnight. The supernatant was separated from the pellet of bone powder by centrifugation (14,000 rpm). A binding buffer consisting of 5 M GuHCL (Sigma Aldrich) and 40% Isopropanol (Merck), together with 400 µl of 1 M sodium acetate (pH 5.5) was added to the supernatant, and the solution purified by spinning it through a purification column attached to a High Pure Extender Assembly funnel (8 min. in 1500 rpm, with slow acceleration). The column was then spun into a collection tube (1 min 14,000 rpm) 1–2 times to maximise the yield. This was followed by two subsequent washing steps of 450 µl of wash buffer (High Pure Viral Nucleic Acid Large Volume Kit) and two dry spin steps of 1 min centrifugation at 14,000 rpm. The final total volume of 100 µl eluate was reached by two separate elution rounds of 50 µl of TET (10 mM Tris-HCL, 1 mM EDTA pH 8.0, 0.1% Tween20), each spun for 1 min at 14,000 rpm into a fresh Eppendorf 1.5 ml tube. Negative controls (buffer instead of sample) were processed in parallel at a ratio of 1 control per 7 samples.

Of the 100 µl extract, 20 µl was used to immortalize the sample DNA as a double-stranded library. The procedure included a blunt-end repair, adapter ligation and adapter fill-in steps, as described by Meyer and Kircher[59]. During the blunt-end repair step, a mixture of 0.4 U/µl T4 PNK (polynucleotide kinase) and 0.024 U/µl T4 DNA polymerase, 1× NEB buffer 2 (NEB), 100 µM dNTP mix (Thermo Scientific), 1 mM ATP (NEB) and 0.8 mg/ml BSA (NEB) was added to the template DNA, followed by incubation in a thermocycler (15 min 15 °C, 15 min 25 °C) and purification with a MinElute kit (QIAGEN). The product was eluted in 18 µl TET buffer. The adapter ligation step included a mixture of 1× Quick Ligase Buffer (NEB), 250 nM Illumina Adapters (Sigma-Aldrich) and 0.125 U/µl Quick Ligase (NEB), added to the 18 µl eluate, followed by a 20 min incubation, and second purification step with MinElute columns, this time in 20 µl eluate. For the fill-in step, a mixture of 0.4 U/µl Bst-polymerase and 125 µM dNTP mix was added and the mixture then incubated in a thermocycler (30 min 37 °C, 10 min 80 °C). Libraries without Uracil-DNA-glycosylase (UDG) treatment were produced for all of the 13 extracts from Levänluhta. In addition, UDG-half treated libraries were produced for seven of the original 13 extracts from Levänluhta, and for all Bolshoy and Chalmny Varre extracts. To introduce the UDG-half treatment, an initial stage was included in the library preparation, in which 250 U USER enzyme (NEB) was added into the 20 µl of extract, followed by an incubation at 37 °C for 30 min, and then 12 °C for 1 min. This again was followed by the addition of 200 U UGI (Uracil Glycosylase inhibitor, by NEB) and another identical incubation to stop the enzymatic excision of deaminated sites, as described in[60]. For each library, a unique pair of eight-bp-long indexes was incorporated using a Pfu Turbo Cx Hotstart DNA Polymerase and a thermocycling program with the temperature profile as follows: initial denaturation (98 °C for 30 sec), cycle of denaturation/annealing/ elongation (98 °C for 10 sec/ 60 °C for 20 sec/ 72 °C for 20 sec) and final extension at 72 °C for 10 min[61]. Bone powder from a cave bear was processed in parallel serving as a positive control. Negative controls for both extraction and library preparation stages were kept alongside the samples throughout the entire workflow.

Experiment efficiency was ensured by quantifying the concentration of the libraries on qPCR (Roche) using aliquots from libraries before and after indexing. The molecular copy number in pre-indexed libraries ranged from ~ 10E8 to ~ 10E9 copies/µl, indicating a successful library preparation, whereas the indexed libraries ranged from ~ 10E10 to ~ 10E12 copies/µl, stating an admissible indexing efficiency. The negative controls showed 4–5 orders of magnitude lower concentration than the samples, indicating low contamination levels from the laboratory processing stages.

The libraries were amplified with PCR, for the amount of cycles corresponding to the concentrations of the indexed libraries, using AccuPrime Pfx polymerase (5 µl of library template, 2 U AccuPrime Pfx DNA polymerase by Invitrogen, 1 U of readymade 10× PCR mastermix, and 0.3 µM of primers IS5 and IS6, for each 100 µl reaction) with thermal profile of 2 min denaturation at 95 °C, 3–9 cycles consisting of 15 sec denaturation at 95 °C, 30 sec annealing at 60 °C, 2 min elongation at 68 °C and 5 min elongation at 68 °C. The amplified libraries were purified using MinElute spin columns with the standard protocol provided by the manufacturer (Qiagen), and quantified for sequencing using an Agilent 2100 Bioanalyzer DNA 1000 chip.

For the modern Saami individual, total DNA was phenol-chloroform extracted and physically sheared using COVARIS fragmentation. A modified Illumina library preparation was performed using blunt-end repair followed by A-tailing of the 3'-end and ligation of forked adapters. Indexing PCR was followed by excision of fragments ranging from 500 to 600 bp from a 2% agarose gel.

Capture & sequencing. We used the in-solution capture procedure from ref. [62] to enrich our libraries for DNA fragments overlapping with 1,237,207 variable positions in the human genome[4]. The sequences used as bait, attached to magnetic beads, were mixed in with the DNA sample template in solution, and left to hybridize with the target DNA during a 24-hour incubation at 60 °C in a rotation oven. 4–6 samples were pooled in equal mass ratios at a total of 2000 ng of DNA. The captured libraries were sequenced (75 bp single-end, plus additional paired-end for the three non-UDG libraries of the Levänluhta individuals) on an Illumina HiSeq 4000 platform at the Max Planck Institute for the Science of Human History in Jena. Out of the 13 originally processed Iron-Age samples from Finland, seven proved to be of an adequate quality to be used in downstream analyses. The modern Saami genome was sequenced in on a Genome Analyser II (8 lanes, 125 bp paired-end) at the Max Planck Institute for Evolutionary Anthropology in Leipzig.

Processing of sequenced reads. We used EAGER[63] (version 1.92.50) to process the sequenced reads, using default parameters (see below) for human-originated, UDG-half treated, single-end sequencing data, when processing the UDG-half libraries for all individuals. Specifically, AdapterRemoval was used to trim the sequencing adapters from our reads, with a minimum overlap of 1 bp, and using a minimum base quality of 20 and minimum sequence length of 30 bp. BWA aln (version 0.7.12-r1039, https://sourceforge.net/projects/bio-bwa/files)[64] was used to map the reads to the hs37d5 human reference sequence, with a seed length (-l) of 32, max number of differences (-n) of 0.01 while doing no quality filtering. Duplicate removal was carried out using DeDup v0.12.1. Terminal base deamination damage calculation was done using mapDamage, specifying a length (-l) of 100 bp (Supplementary Table 1).

For downstream analyses, we used bamutils (version 1.0.13, https://github.com/statgen/bamUtil.git) TrimBam to trim two bases at the start and end of all reads. This procedure eliminates the positions that are affected by deamination, thus removing genotyping errors that could arise due to ancient DNA damage.

For three Levänluhta individuals exceeding the threshold coverage of 1% in the preliminary screening, we used the non-UDG treated libraries to confirm the authenticity of the ancient data. For these untreated libraries, two rounds of sequencing were carried out, which were processed using EAGER with the above parameters, but specifying a non-UDG treatment mode and setting the correct sequencing type between the libraries. The merged reads were extracted from the resulting bam files, and merged with the bam file containing reads from the single end sequence run using samtools merge (version 1.3)[65].

The modern Saami genome was generated using Ibis for base calling and an in-house adapter trimming script. The resulting reads were then aligned to the hs37d5 human reference genome using bwa 0.5.9-r16 (parameters -e 2 -o 2 -n 0.01).

Genotyping. We used a custom program (pileupCaller) to genotype the 15 ancient individuals. A pileup file was generated using samtools mpileup with parameters -q 30 -Q 30 -B containing only sites overlapping with our capture panel. From this file, for each individual and each SNP on the 1240K panel, one read covering the SNP was drawn at random, and a pseudohaploid call was made, i.e., the ancient individual was assumed homozygous for the allele on the randomly drawn read for the SNP in question. PileupCaller is available at https://github.com/stschiff/sequenceTools.git.

For the three Levänluhta libraries that did not undergo UDG treatment, we only genotyped transversions, thus eliminating artefacts of post-mortem C- > T damage from further analyses.

The shotgun genome of the modern Saami individual was genotyped using GATK (version 1.3-25-g32cdef9) Unified Genotyper after indel realignment. The variant calls were filtered for variants with a quality score above 30, and a custom script was used to convert the variants into EigenStrat format.

The data were merged with a large dataset consisting of 3871 ancient and modern individuals genotyped on the Human Origins and/or 1240K SNP arrays, using mergeit.

Sex determination. To determine the genetic sex of each ancient individual we calculated the coverage on the autosomes as well as on each sex chromosome. We used a custom script (https://github.com/TCLamnidis/Sex.DetERRmine) for the calculation of each relative coverage as well as their associated error bars (Supplementary Figure 1, Supplementary Note 3 for more information on error calculation). Females are expected to have an x-rate of 1 and a y-rate of 0, while males are expected to have both x- and y-rate of 0.5 (ref. [49]).

Authentication. We first confirmed that the deamination pattern at the terminal bases of DNA reads were characteristic of ancient DNA (1.04–4.5% for non-UDG libraries, and 4.7–9.5% for non-UDG libraries, see Supplementary Table 1), using mapDamage (version 2.0.6)[66]. We performed a number of different tests to ensure

the authenticity of our ancient data. For male individuals, we investigated poly-morphisms on the X chromosome[27] using the ANGSD software package (version 0.910)[67]. This revealed robust contamination estimates for 2 male Bolshoy individuals, and 1 male Chalmny-Varre individual. All of these were below 1.6% contamination (Table 1). For the female individuals from these two sites, we note that they are projected close to the males in PCA space (Fig. 2a, Supplementary Figure 3), suggesting limited effects of potential contamination. In addition, we generated a PMD-filtered dataset for all individuals using pmdtools (version 0.60)[30]. PMD-filtering was done using a reference genome masked for all positions on the 1240K capture panel, to avoid systematic allelic biases on the analysed SNP positions. We set a pmd-threshold of 3, which, according to the original publication[30], effectively eliminates potential modern contaminants based on the absence of base modifications consistent with deamination.

To provide a more quantitative estimate of possible contamination in females, we used the ContamMix program (version 1.0-10)[29] for estimating mitochondrial contamination. We extracted reads mapping to the mitochondrial reference for each of the ancient individuals using samtools (version 1.3)[65]. We then generated a mitochondrial consensus sequence for each of the ancient individuals using Geneious (version 10.0.9, http://www.geneious.com,[68]), and calling N for all sites with a coverage lower than 5. Finally, all mitochondrial reads were aligned to their respective consensus sequence, using bwa aln (version 0.7.12-r1039)[64] with a maximum number of differences in the seed (-k) set to 5 and the maximum number of differences (-n) to 10, and bwa samse (version 0.7.12-r1039)[64]. A multiple alignment of the consensus sequence and a reference set of 311 mitochondrial genomes[69] was generated, using mafft (version v7.305b)[70–72] with the --auto parameter. The read alignment, as well as the multiple alignment of the consensus and the 311 reference mitochondrial genomes were then provided to ContamMix. We report here a posteriori mode of contamination, along with the upper and lower bounds of the 95% posterior interval (Table 1).

For additional authentication, we ran supervised ADMIXTURE[28] (version 1.3.0) for all samples using the six present-day populations (Atayal, French, Kalash, Karitiana, Mbuti and Papuan) as defined genetic clusters, to locate any large differences in genetic clustering among individuals from the same site (Supplementary Figure 2). We tested the power of this method to detect contamination and find that it can detect contamination that is distantly related to the ancestries present within the test individuals already at rates of 5–8%, but lacks the power to identify contamination closely related to the test individuals (see Supplementary Note 2). We did not observe significant differences (within our resolution) in the ancestry patterns between the ancient individuals from the same site, with the exception of Levänluhta, where the individual sample JK2065 seems to derive from a different ancestry. We therefore assigned it a separate population label, Levänluhta_B in this study.

Finally, using smartpca, we projected PMD-filtered and non-filtered datasets on the same set of principal components constructed on modern European populations, to ensure that the ancient individuals remain projected in the roughly equivalent positions regardless of PMD-filtering. This was possible for all samples with UDG-half treatment, except for the individuals from Levänluhta, which represented too little damage for the PMD-filtering to be applied. Regarding this site, we therefore relied on the non-UDG libraries (using transversions only) that were generated for the three individuals used in the main analysis. We found that within expected noise due to a low number of SNPs, all samples show consistency between the filtered and non-filtered datasets, suggesting a low amount of contamination in all of the samples (Supplementary Figure 3a, b). Four additional individuals from Levänluhta were excluded from the main analysis and from this authentication test because of low coverage (< 15,000 covered SNPs) and lack of non-UDG libraries.

F statistics. All programmes used for calculating F statistics in this study can be found as part of the Admixtools package (https://github.com/DReichLab/AdmixTools)[2,42].

We used qp3Pop (version 412) for all F_3 calculations.

F_4 statistics were calculated using qpDstat (version 711), and qpAdm (version 632)[2] was used to estimate mixture proportions using the following: Sources (Left Populations): Nganasan; WHG; EHG; Yamnaya_Samara; LBK_EN. Outgroups (Right Populations): OG1: Mbuti; CHG; Israel_Natufian; Onge; Villabruna; Ami; Mixe. OG2: Mbuti; CHG; Onge; Villabruna; Ami; Mixe. OG3: Mixe; CHG; Israel_Natufian; Villabruna; Onge; Ami. OG4: Mbuti; Israel_Natufian; Onge; Villabruna; Ami; Mixe. OG5: Mbuti; Samara_HG; CHG; Israel_Natufian; Villabruna; Ami.

To ensure the outgroup sets had enough power to distinguish the ancestries present in the sources, we ran qpWave (version 410) using only the sources as left populations and each outgroup set as rights. All such qpWave runs were consistent only with maximum rank, meaning all outgroup sets had enough power to distinguish between the five different sources. All qpWave and qpAdm models were run using the option allsnps: YES. When the five-way admixture models provided by qpAdm had p-values above 0.05, but included infeasible mixture proportions and one of the sources was assigned a negative mixture proportion, we ran the model again with that source was excluded. For each Test population, if outgroup set OG1 did not produce a working full model ($p < 0.05$), we tried alternative outgroup sets with one right population removed. This resulted in

outgroup sets OG2-4. In the case of Levänluhta, multiple outgroup sets produced working models, which are listed in Supplementary Data 4. The admixture model needing the minimum number of sources while still providing feasible admixture proportions is always shown. In the case of PWC from Sweden where none of the outgroup sets OG1-4 produced a working model, a revised set of right populations was used (OG5) which includes Samara_HG to provide more power to distinguish hunter-gatherer ancestries. We preferred models with OG1-4 over OG5 in general, because OG5 contains more ancient genomes with potential biases in the right populations, which more often causes failing models for modern Test populations. The excluded sources in the minimal models were specified as N/A (Supplementary Data 4). If either Yamnaya or EHG could be dropped (as is the case for Levänluhta), we show the model which is more consistent with previous publications[3,7,8,45] in Fig. 4, but show both models in Supplementary Data 4.

Principal component analysis. We used smartpca (version #16000)[73] (https://github.com/DReichLab/EIG) to carry out Principal Component Analysis (PCA), using the lsqproject: YES and shrinkmode: YES parameters.

For the Eurasian PCA (Fig. 2a), the following populations were used to construct principal components: Abkhasian, Adygei, Albanian, Altaian, Ami, Armenian, Atayal, Avar.SG, Azeri_WGA, Balkar, Balochi, Basque, BedouinA, BedouinB, Belarusian, Borneo, Brahui, Bulgarian, Buryat.SG, Cambodian, Canary_Islanders, Chechen, Chuvash, Croatian, Cypriot, Czech, Dai, Daur, Dolgan, Druze, English, Estonian, Even, Finnish, French, Georgian, Greek, Han, Hazara, Hezhen, Hungarian, Icelandic, Iranian, Italian_North, Italian_South, Japanese, Jew_Ashkenazi, Jew_Georgian, Jew_Iranian, Jew_Iraqi, Jew_Libyan, Jew_Moroccan, Jew_Tunisian, Jew_Turkish, Jew_Yemenite, Jordanian, Kalash, Kalmyk, Kinh, Korean, Kumyk, Kurd_WGA, Kyrgyz, Lahu, Lebanese, Lezgin, Lithuanian, Makrani, Mala, Maltese, Mansi, Miao, Mongola, Mordovian, Naxi, Nganasan, Nogai, North_Ossetian.DG, Norwegian, Orcadian, Oroqen, Palestinian, Pathan, Russian, Saami.DG, Saami_WGA, Sardinian, Saudi, Scottish, Selkup, Semende, She, Sherpa.DG, Sicilian, Spanish, Spanish_North, Syrian, Tajik, Thai, Tibetan.DG, Tu, Tubalar, Tujia, Turkish, Turkmen, Tuvinian, Ukrainian, Ulchi, Uygur, Uzbek, Xibo, Yakut, Yi, Yukagir.

For the West Eurasian PCA (Supplementary Figure 3a, b), the following populations were used to construct principal components: Abkhasian, Adygei, Albanian, Armenian, Balkar, Basque, BedouinA, BedouinB, Belarusian, Bulgarian, Canary_Islander, Chechen, Chuvash, Croatian, Cypriot, Czech, Druze, English, Estonian, Finnish, French, Georgian, Greek, Hungarian, Icelandic, Iranian, Italian_North, Italian_South, Jew_Ashkenazi, Jew_Georgian, Jew_Iranian, Jew_Iraqi, Jew_Libyan, Jew_Moroccan, Jew_Tunisian, Jew_Turkish, Jew_Yemenite, Jordanian, Kumyk, Lebanese, Lezgin, Lithuanian, Maltese, Mordovian, North_Ossetian, Norwegian, Orcadian, Palestinian, Polish, Russian, Sardinian, Saudi, Scottish, Sicilian, Spanish, Spanish_North, Syrian, Turkish, Ukrainian.

ADMIXTURE analysis. ADMIXTURE[28] was run with version 1.3.0, following exclusion of variants with minor allele frequency of 0.01 and after LD pruning using plink (version 1.90b3.29)[74] with a window size of 200, a step size of 5 and an R^2 threshold of 0.5 (https://www.genetics.ucla.edu/software/admixture/download.html). Five replicates were run for each K value, with K values ranging between 2 and 15. The populations used were: Ami, Ami.DG, Armenian, Atayal, Atayal.DG, Balochi, Basque, BedouinB, Belarusian, Brahmin_Tiwari, Brahui, Chuvash, Croatian, Cypriot, Czech, English, Estonian, Even, Finnish, Finnish.DG, French, Greek, GujaratiB, Hadza, Han, Hungarian, Icelandic, Kalash, Karitiana, Lithuanian, Makrani, Mala, Mansi, Mansi.DG, Mari.SG, Mbuti, Mbuti.DG, Mixe, Mordovian, Nganasan, Norwegian, Onge, Orcadian, Papuan, Pima, Russian, Saami.DG, ModernSaami, Sardinian, Scottish, Selkup, Spanish, Ukrainian, Ulchi, Yoruba, ALPC_Hungary_MN, Baalberge_MN, Baltic_BA, Baltic_CCC, Baltic_CWC, Baltic_LN, BolshoyOleniOstrov, Bu_kk_Culture_Hungary_MN, ChalmnyVarre, CHG, EHG, Esperstedt_MN, Ganj_Dareh_Iran_Neolithic, Hungary_MN, Hungary_Neolithic, Iran_Chalcolithic, JK2065, Koros_Hungary_EN, Kunda, Latvia_HG3, Latvia_MN1, LBK_EN, LBK_Hungary_EN, Levanluhta, Narva, PWC_Sweden_NHG.SG, Scandinavia_LNBA, SHG, Sweden_HG.SG, TRB, Ukraine_HG1, Ukraine_N1, WHG, Yamnaya_Samara.

We find that K = 11 results in the lowest Cross-Validation error, as shown in Supplementary Figure 4b.

Y-chromosomal haplotyping. We assigned ancient males to Y haplogroups using the yHaplo program (https://github.com/23andMe/yhaplo)[75]. In short, this program provides an automated search through the Y haplogroup tree (as provided within yHaplo, as accessed from ISOGG on 04 Jan 2016) from the root to the downstream branch based on the presence of derived alleles and assigns the most downstream haplogroup with derived alleles. For about 15,000 Y-chromosomal SNPs present both in our capture panel and in two published datasets[76,77], we randomly sampled a single base and used it as a haploid genotype. We used a custom script to convert EigenStrat genotypes to the yHaplo format. We report the haplogroup assigned furthest downstream provided by the program (Table 1). We also manually checked derived status and absence of mutations defining the designated haplogroup because missing information might lead to a premature stop in its automated search.

Mitochondrial haplotyping. We imported the trimmed mitochondrial reads for each individual with mapping quality >30 into Geneious (version 10.0.9, https://www.geneious.com)[68] and reassembled these reads to the reference genome RSRS[78], using the Geneious mapper, with medium sensitivity and 5 iterations. We used the in-built automated variant caller within Geneious to find mitochondrial polymorphisms with a minimum coverage of 3 and a minimum Variant Frequency of 0.67. The resulting variants were exported to Excel and manually compared to the SNPs reported in the online mtDNA phylogeny (mtDNA tree Build 17, 18 Feb 2016, http://www.phylotree.org/). Nucleotide positions 309.1 C(C), 315.1C, AC indels at 515-522, 16182C, 16183C, 16193.1C(C) and 16519 were masked and not included in our haplotype calls.

Phenotypic SNPs. We used samtools mpileup (version 1.3)[65], filtering for map- (-Q) and base- (-q) quality of 30, deactivating per-Base Alignment Quality (-B), on the trimmed bam files, to generate a pileup of reads mapping to a set of 43 phenotypic SNPs[4,40,41,79] that are part of our genome capture panel. A custom python script was used to parse the pileup into a table containing the number of reads supporting each allele (Supplementary Data 2).

Code availability. All software first described in this study is freely available from online repositories. Sex.DetERRmine: https://github.com/TCLamnidis/Sex.DetERRmine

ContaminateGenotypes: https://github.com/TCLamnidis/ContaminateGenotypes

Data availability

The raw sequence data of the 16 modern and ancient individuals presented in this paper are deposited at the European Nucleotide Archive (http://www.ebi.ac.uk/ena). The study accession is PRJEB29360. A reporting Summary for this Article is available as a Supplementary Information file. The source data underlying all main and Supplementary Figures are provided as a Source Data file.

References

1. Lazaridis, I. et al. Ancient human genomes suggest three ancestral populations for present-day Europeans. *Nature* **513**, 409–413 (2014).
2. Lazaridis, I. et al. Genomic insights into the origin of farming in the ancient Near East. *Nature* **536**, 419–424 (2016).
3. Haak, W. et al. Massive migration from the steppe was a source for Indo-European languages in Europe. *Nature* **522**, 207–211 (2015).
4. Mathieson, I. et al. Genome-wide patterns of selection in 230 ancient Eurasians. *Nature* **528**, 499–503 (2015).
5. Allentoft, M. E. et al. Population genomics of Bronze Age Eurasia. *Nature* **522**, 167–172 (2015).
6. Broushaki, F. et al. Early Neolithic genomes from the eastern Fertile Crescent. *Science* **353**, 499–503 (2016).
7. Jones, E. R. et al. The Neolithic transition in the Baltic was not driven by admixture with early European farmers. *Curr. Biol.* **27**, 576–582 (2017).
8. Mittnik, A. et al. The genetic prehistory of the Baltic Sea region. *Nat. Commun.* **9**, 442 (2018).
9. Salmela, E. et al. Genome-wide analysis of single nucleotide polymorphisms uncovers population structure in Northern Europe. *PLoS ONE* **3**, e3519 (2008).
10. Huyghe, J. R. et al. A genome-wide analysis of population structure in the Finnish Saami with implications for genetic association studies. *Eur. J. Hum. Genet.* **19**, 347–352 (2011).
11. Lappalainen, T. et al. Regional differences among the Finns: a Y-chromosomal perspective. *Gene* **376**, 207–215 (2006).
12. Kerminen, S. et al. Fine-Scale Genetic Structure in Finland. *G3* **7**, 3459–3468 (2017).
13. Takala, H. O. *The Ristola Site In Lahti And The Earliest Postglacial Settlement Of South Finland* (Lahti City Museum, 2004).
14. Halinen, P. *Prehistoric Hunters of Northernmost Lapland* (Tiedekirja, 2005).
15. Rankama, T. & Kankaanpää, J. in *Early Economy and Settlement in Northern Europe. Pioneering, Resource Use, Coping with Change* Vol. 3 (ed. Blankholm, H. P) 139–167 (Equinox, 2018).
16. Aikio, A. An essay on Saami ethnolinguistic prehistory. *Suom.-Ugr. Seura. Toim.=Mémoires De. la Société Finno-Ougr.* **266**, 63–117 (2012).
17. Aikio, A. *The Saami Loanwords In Finnish and Karelian* (University of Oulu, 2009).
18. Frog, M. & Saarikivi, J. De situ linguarum fennicarum aetatis ferreae, Pars I. *RMN Newsletter* **9**, 64–115 (2014).
19. Rahkonen, P. Onomasticon of Levänluhta and Käldamäki region. *Suomalais-Ugrilaisen Seuran Aikakauskirja* **96**, 287–316 (2017).
20. Häkkinen, J. Jatkuvuusperustelut ja saamelaisen kielen leviäminen (OSA 2). *Muinaistutkija* **2010**, 51–64 (2010).
21. Hausen, R. *Registrum Ecclesiae Aboensis Eller Åbo Domkyrkas Svartbok Med Tillägg Ur Skoklosters Codex Aboensis* (Kansallisarkisto, 1890).
22. Taavitsainen, J.-P. in *The Oxford Handbook of the Archaeology and Anthropology of Hunter-Gatherers* (eds Cummings, V., Jordan, P. & Zvelebil, M.) Ch. 51 (Oxford University Press, 2014).
23. Lang, V. *Läänemeresoome tulemised* Vol. 28 (University of Tartu Publisher, 2018).
24. Der Sarkissian, C. et al. Ancient DNA reveals prehistoric gene-flow from siberia in the complex human population history of North East Europe. *PLoS Genet.* **9**, e1003296 (2013).
25. Wessman, A. et al. Hidden and remote: new perspectives on the people in the Levänluhta Water Burial, Western Finland (c.ad 300–800). *Eur. J. Archaeol.* **21**, 431–454 (2018).
26. Wessman, A. L. A place of punishment, sacrifice or just a common cemetery? *Fennosc. Archaeol.* **XXVI**, 81–105 (2009).
27. Rasmussen, M. et al. An Aboriginal Australian genome reveals separate human dispersals into Asia. *Science* **334**, 94–98 (2011).
28. Alexander, D. H., Novembre, J. & Lange, K. Fast model-based estimation of ancestry in unrelated individuals. *Genome Res.* **19**, 1655–1664 (2009).
29. Fu, Q. et al. A revised timescale for human evolution based on ancient mitochondrial genomes. *Curr. Biol.* **23**, 553–559 (2013).
30. Skoglund, P. et al. Separating endogenous ancient DNA from modern day contamination in a Siberian Neandertal. *Proc. Natl Acad. Sci. USA* **111**, 2229–2234 (2014).
31. Jones, E. R. et al. Upper Palaeolithic genomes reveal deep roots of modern Eurasians. *Nat. Commun.* **6**, 8912 (2015).
32. Mallick, S. et al. The Simons Genome Diversity Project: 300 genomes from 142 diverse populations. *Nature* **538**, 201–206 (2016).
33. Raghavan, M. et al. Upper Palaeolithic Siberian genome reveals dual ancestry of Native Americans. *Nature* **505**, 87–91 (2014).
34. Derenko, M. et al. Origin and post-glacial dispersal of mitochondrial DNA haplogroups C and D in northern Asia. *PLoS One* **5**, e15214 (2010).
35. Malyarchuk, B., Derenko, M., Denisova, G. & Kravtsova, O. Mitogenomic diversity in Tatars from the Volga-Ural region of Russia. *Mol. Biol. Evol.* **27**, 2220–2226 (2010).
36. Ilumäe, A.-M. et al. Human Y chromosome haplogroup N: a non-trivial time-resolved phylogeography that cuts across language families. *Am. J. Hum. Genet.* **99**, 163–173 (2016).
37. Fondevila, M. et al. Revision of the SNPforID 34-plex forensic ancestry test: assay enhancements, standard reference sample genotypes and extended population studies. *Forensic Sci. Int. Genet* **7**, 63–74 (2013).
38. Kimura, R. et al. A common variation in EDAR is a genetic determinant of shovel-shaped incisors. *Am. J. Hum. Genet.* **85**, 528–535 (2009).
39. Tan, J. et al. The adaptive variant EDARV370A is associated with straight hair in East Asians. *Hum. Genet.* **132**, 1187–1191 (2013).
40. Fumagalli, M. et al. Greenlandic Inuit show genetic signatures of diet and climate adaptation. *Science* **349**, 1343–1347 (2015).
41. Ameur, A. et al. Genetic adaptation of fatty-acid metabolism: a human-specific haplotype increasing the biosynthesis of long-chain omega-3 and omega-6 fatty acids. *Am. J. Hum. Genet.* **90**, 809–820 (2012).
42. Patterson, N. et al. Ancient admixture in human history. *Genetics* **192**, 1065–1093 (2012).
43. Lahermo, P. et al. Y chromosomal polymorphisms reveal founding lineages in the Finns and the Saami. *Eur. J. Hum. Genet.* **7**, 447–458 (1999).
44. Csányi, B. et al. Y-chromosome analysis of ancient Hungarian and two modern Hungarian-speaking populations from the Carpathian Basin. *Ann. Hum. Genet.* **72**, 519–534 (2008).
45. Saag, L. et al. Extensive farming in Estonia started through a sex-biased migration from the Steppe. *Curr. Biol.* **27**, 2185–2193 (2017).
46. Loh, P.-R. et al. Inferring admixture histories of human populations using linkage disequilibrium. *Genetics* **193**, 1233–1254 (2013).
47. Fenner, J. N. Cross-cultural estimation of the human generation interval for use in genetics-based population divergence studies. *Am. J. Phys. Anthropol.* **128**, 415–423 (2005).
48. Lipson, M. et al. Parallel palaeogenomic transects reveal complex genetic history of early European farmers. *Nature* **551**, 368–372 (2017).
49. Fu, Q. et al. The genetic history of Ice Age Europe. *Nature* **534**, 200–205 (2016).
50. Murashkin, A. I., Kolpakov, E. M., Shumkin, V. Y., Khartanovich, V. I. & Moiseyev, V. G. Kola Oleneostrovskiy Grave Field: A Unique Burial Site In The European Arctic. In *Proc. of the Finnish-Russian Archaeological Symposium* (eds Ulino, P. & Nordqvist, K.) (Tiedekirja, 2016).
51. Carpelan, C. in *Inari–Aanaar. Inarin historia jääkaudesta nykypäivään* (ed. Veli-Pekka, L.) 28–95 (Inarin Kunta, 2003).

52. Carpelan, C. in *Early in the North. Iskos 13* Vol. 5 (ed. Lavento, M.) 30–36 (Finnish Antiquarian Society & Archaeological Society of Finland, 2004).
53. Šumkin, V. J. On the ethnogenesis of the Sami: an archaeological view. *Acta Boreal.* **7**, 3–20 (1990).
54. Honkola, T. et al. Cultural and climatic changes shape the evolutionary history of the Uralic languages. *J. Evol. Biol.* **26**, 1244–1253 (2013).
55. Moiseyev, V. G. & Khartanovich, V. I. Early Metal Age crania from Bolshoy Oleniy Island, Barents Sea. *Archaeol., Ethnol. Anthropol. Eurasia* **40**, 145–154 (2012).
56. Reimer, P. J. et al. IntCal13 and Marine13 radiocarbon age calibration curves 0–50,000 years cal BP. *Radiocarbon* **55**, 1869–1887 (2013).
57. Ramsey, C. B. Bayesian analysis of radiocarbon dates. *Radiocarbon* **51**, 337–360 (2009).
58. Dabney, J. et al. Complete mitochondrial genome sequence of a Middle Pleistocene cave bear reconstructed from ultrashort DNA fragments. *Proc. Natl Acad. Sci.* USA **110**, 15758–15763 (2013).
59. Meyer, M. & Kircher, M. Illumina sequencing library preparation for highly multiplexed target capture and sequencing. *Cold Spring Harb. Protoc.* **2010**, db.prot5448 (2010).
60. Rohland, N., Harney, E., Mallick, S., Nordenfelt, S. & Reich, D. Partial uracil-DNA-glycosylase treatment for screening of ancient DNA. *Philos. Trans. R. Soc. Lond. B Biol. Sci.* **370**, 20130624 (2015).
61. Kircher, M., Sawyer, S. & Meyer, M. Double indexing overcomes inaccuracies in multiplex sequencing on the Illumina platform. *Nucleic Acids Res.* **40**, e3 (2012).
62. Fu, Q. et al. DNA analysis of an early modern human from Tianyuan Cave, China. *Proc. Natl Acad. Sci. USA.* **110**, 2223–2227 (2013).
63. Peltzer, A. et al. EAGER: efficient ancient genome reconstruction. *Genome Biol.* **17**, 60 (2016).
64. Li, H. & Durbin, R. Fast and accurate short read alignment with Burrows-Wheeler transform. *Bioinformatics* **25**, 1754–1760 (2009).
65. Li, H. et al. The Sequence Alignment/Map format and SAMtools. *Bioinformatics* **25**, 2078–2079 (2009).
66. Jónsson, H., Ginolhac, A., Schubert, M., Johnson, P. L. F. & Orlando, L. mapDamage2.0: fast approximate Bayesian estimates of ancient DNA damage parameters. *Bioinformatics* **29**, 1682–1684 (2013).
67. Korneliussen, T. S., Albrechtsen, A. & Nielsen, R. ANGSD: analysis of next generation sequencing data. *BMC Bioinforma.* **15**, 356 (2014).
68. Kearse, M. et al. Geneious Basic: an integrated and extendable desktop software platform for the organization and analysis of sequence data. *Bioinformatics* **28**, 1647–1649 (2012).
69. Green, R. E. et al. A complete Neandertal mitochondrial genome sequence determined by high-throughput sequencing. *Cell* **134**, 416–426 (2008).
70. Katoh, K. & Toh, H. PartTree: an algorithm to build an approximate tree from a large number of unaligned sequences. *Bioinformatics* **23**, 372–374 (2007).
71. Katoh, K., Misawa, K., Kuma, K.-I & Miyata, T. MAFFT: a novel method for rapid multiple sequence alignment based on fast Fourier transform. *Nucleic Acids Res* **30**, 3059–3066 (2002).
72. Katoh, K., Kuma, K.-I., Toh, H. & Miyata, T. MAFFT version 5: improvement in accuracy of multiple sequence alignment. *Nucleic Acids Res* **33**, 511–518 (2005).
73. Patterson, N., Price, A. L. & Reich, D. Population structure and eigenanalysis. *PLoS Genet.* **2**, e190 (2006).
74. Purcell, S. et al. PLINK: a tool set for whole-genome association and population-based linkage analyses. *Am. J. Hum. Genet.* **81**, 559–575 (2007).
75. David Poznik, G. Identifying Y-chromosome haplogroups in arbitrarily large samples of sequenced or genotyped men. Preprint at https://www.biorxiv.org/content/early/2016/11/19/088716 (2016).
76. Karmin, M. et al. A recent bottleneck of Y chromosome diversity coincides with a global change in culture. *Genome Res.* **25**, 459–466 (2015).
77. 1000 Genomes Project Consortium. et al. A global reference for human genetic variation. *Nature* **526**, 68–74 (2015).
78. Behar, D. M. et al. A 'Copernican' reassessment of the human mitochondrial DNA tree from its root. *Am. J. Hum. Genet.* **90**, 675–684 (2012).
79. Walsh, S. et al. The HIrisPlex system for simultaneous prediction of hair and eye colour from DNA. *Forensic Sci. Int. Genet* **7**, 98–115 (2013).

Acknowledgements

Author contributions

S.S., J.Kr. and W.H. supervised the study. A.Wes., V.M., V.K., A.S., P.O., O.B., W.H. and J.Kr. assembled the collection of archaeological samples. A.S. and S.P. collected the modern Saami sample. K.M. performed laboratory work. K.M. and T.C.L. supervised ancient DNA sequencing and post-sequencing bioinformatics for the ancient individuals. A.Wei. performed the laboratory work of the modern Saami genome. M.O. carried out the processing of the sequenced reads and generating the genotypes of the modern Saami genome. J.Ke. and S.P. supervised sequencing of the modern Saami and post-sequencing bioinformatics. T.C.L., K.M., E.S., C.J. and S.S. analysed genetic data. T.C.L., K.M., E.S., W.H., J.Kr. and S.S. wrote the manuscript with additional input from all other co-authors.

Additional information

Supplementary Information accompanies this paper at https://doi.org/10.1038/s41467-018-07483-5.

Competing interests: The authors declare no competing interests.

Reprints and permission information is available online at http://npg.nature.com/reprintsandpermissions/

Publisher's note: Springer Nature remains neutral with regard to jurisdictional claims in published maps and institutional affiliations.

Supplementary Material for Ancient Fennoscandian genomes reveal origin and spread of Siberian ancestry in Europe

Supplementary Figures
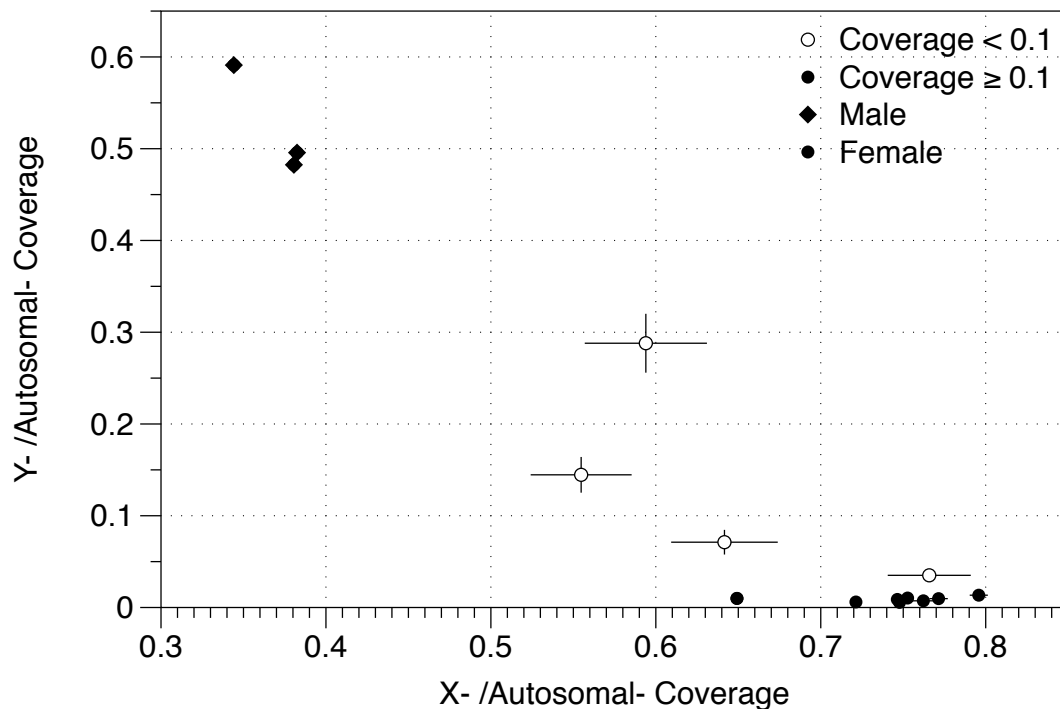
Supplementary Figure 1. Sex Determination. X-chromosomal coverage vs. Y-chromosomal coverage, normalised by autosomal coverage. Low autosomal coverage individuals (n = 4, excluded from downstream analyses) are shown as empty circles, and higher coverage individuals (n = 11) as filled circles. Error bars represent the uncertainty in the calculation of relative coverages, assuming reads map on the capture targets randomly (see Supplementary Text 2 for details). Source data are provided as a Source Data file.
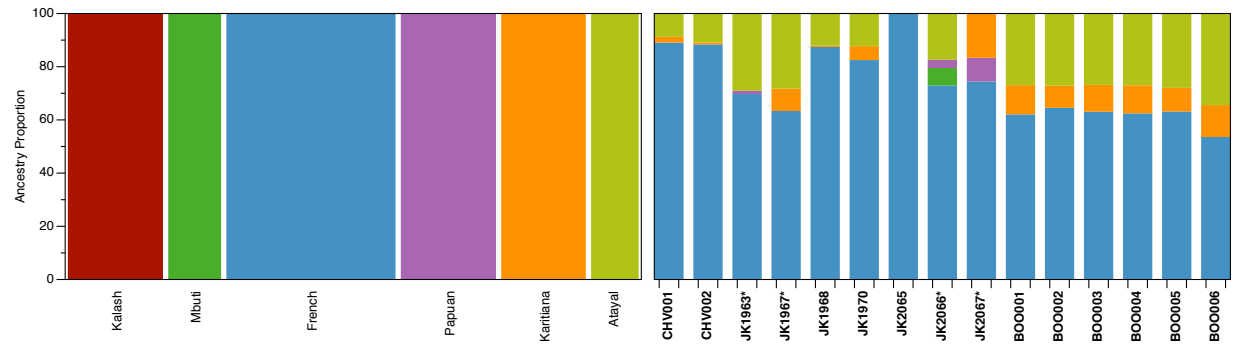
Supplementary Figure 2. Supervised ADMIXTURE. Individuals excluded from further analyses due to low coverage are signified with an asterisk. Among higher coverage genomes, the results within each population are homogeneous, with the exception of the outlier JK2065 within Levänluhta. Source data are provided as a Source Data file.
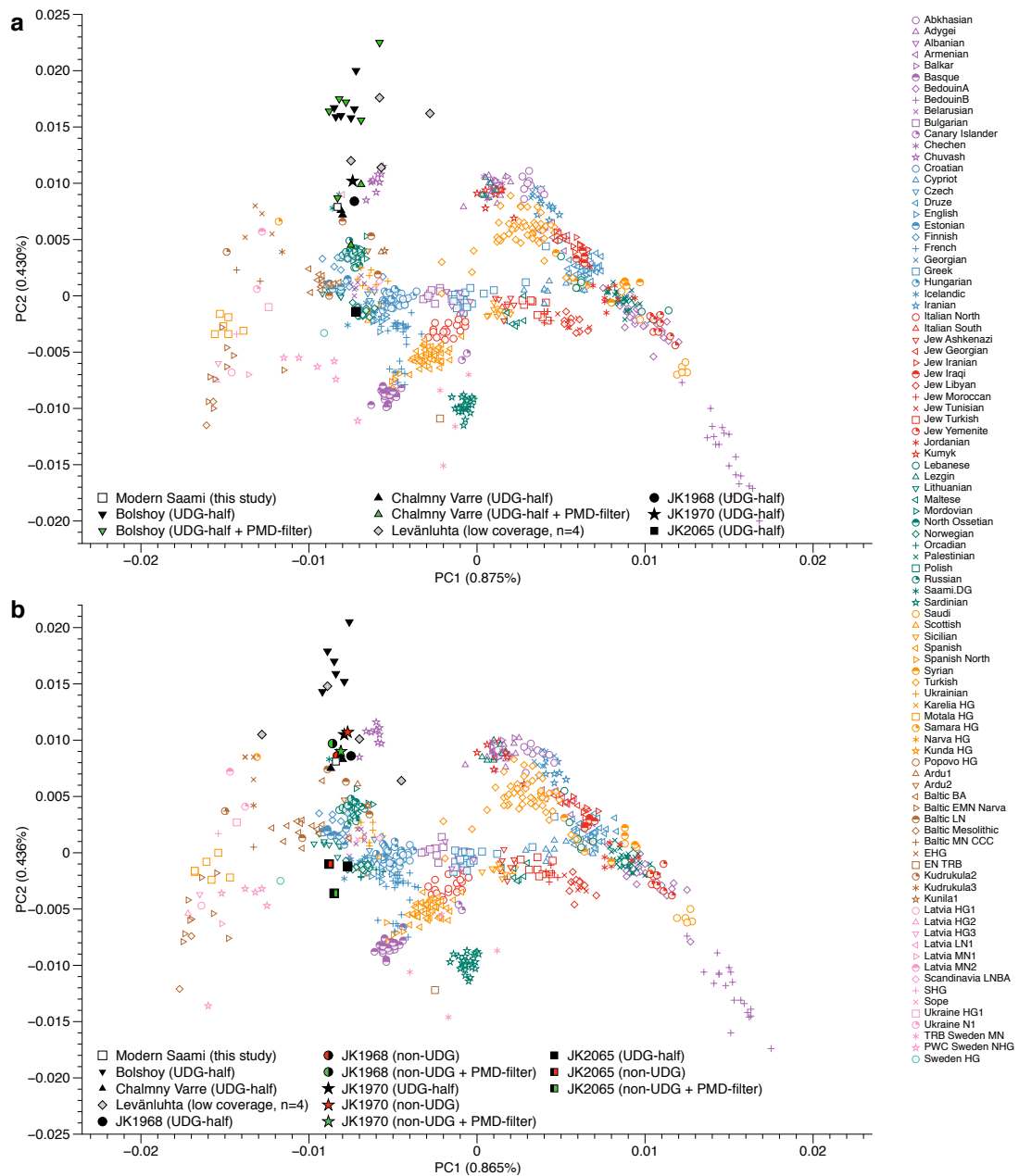
Supplementary Figure 3. Comparison of projection before and after PMD-filtering in PCA space. **a** PCA plot of Europe with individuals from this study projected on principal components constructed on the modern populations in the legend, using the option "shrinkmode: YES". For each individual from Bolshoy and Chalmny Varre, an additional projection is shown for the PMD-filtered dataset. Ancient individuals with fewer than 15,000 covered SNPs are shown in grey. **b** PCA plot of Europe with individuals from this study projected on principal components constructed using <u>only transversion</u> SNPs of the modern populations in the legend, using the option "shrinkmode: YES". For the three Levänluhta individuals with more than 15,000 covered SNPs, additional point for the PMD-filtered and the non-filtered datasets of the non-UDG treated libraries is shown. Ancient individuals with fewer than 15,000 covered SNPs are shown in grey. Source data are provided as a Source Data file.
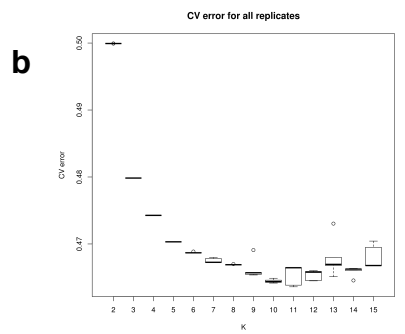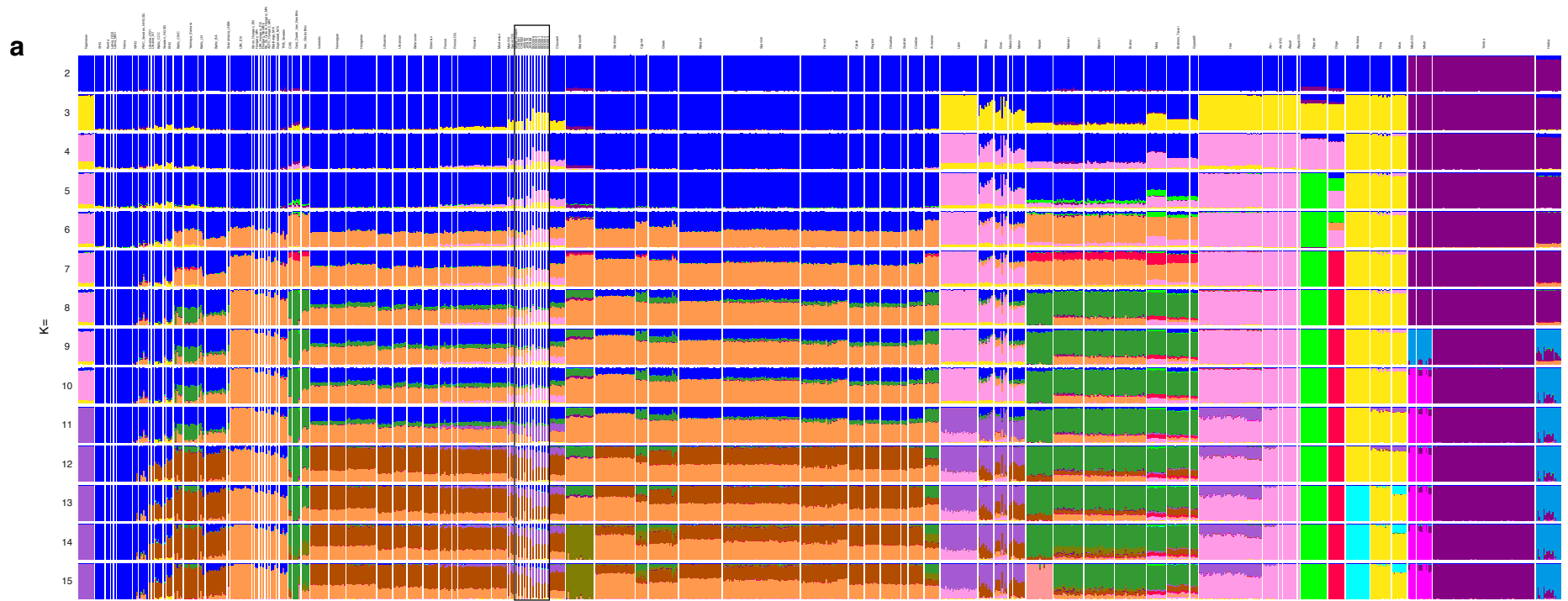
Supplementary Figure 4. ADMIXTURE analysis. **a** ADMIXTURE results. **b** CV Errors for 5 replicates per K value. Source data are provided as a Source Data file.
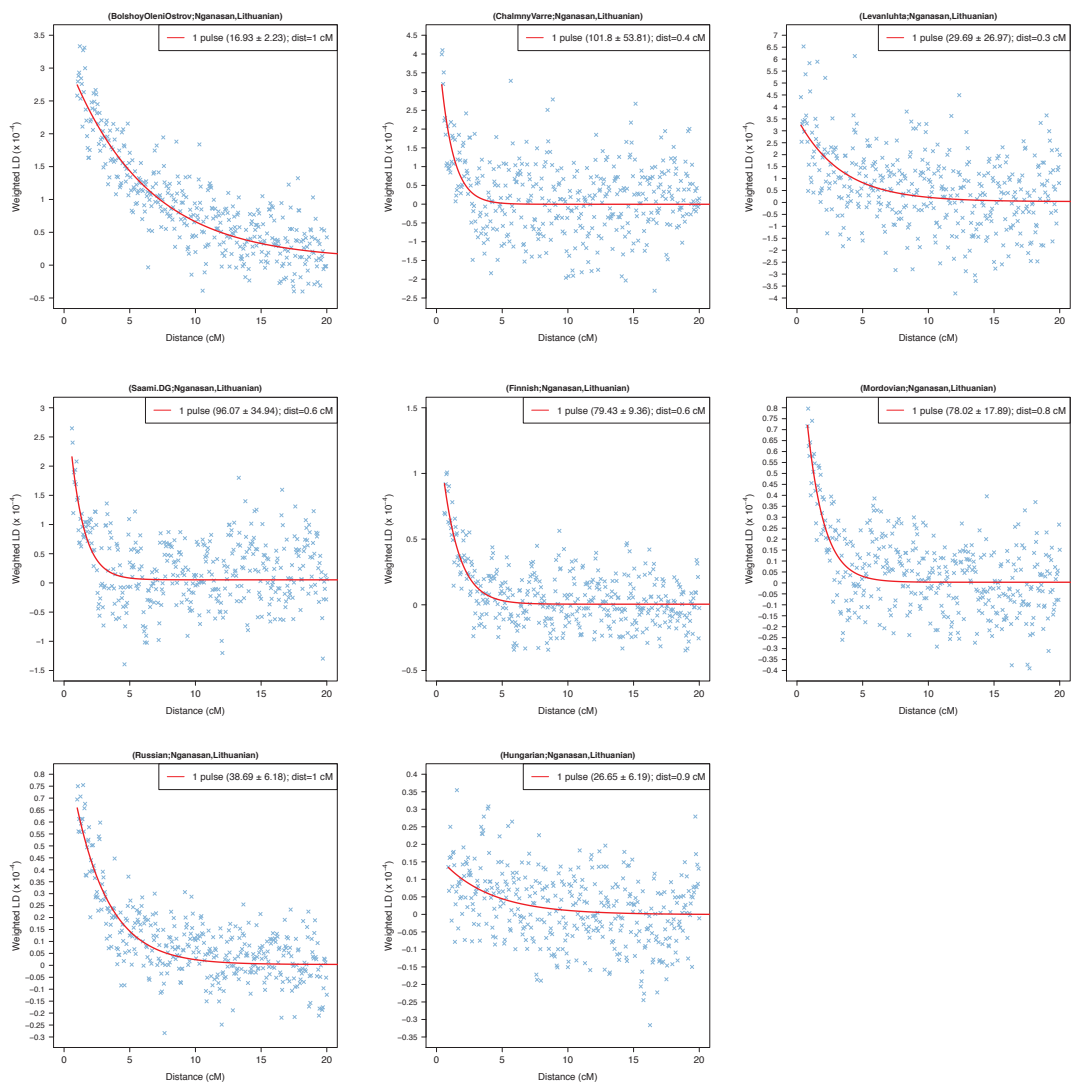
Supplementary Figure 5. Linkage Disequilibrium decay curves for ancient and modern populations. Minimum distance in cM used is the lowest distance for which ALDER provided results. Source data are provided as a Source Data file.
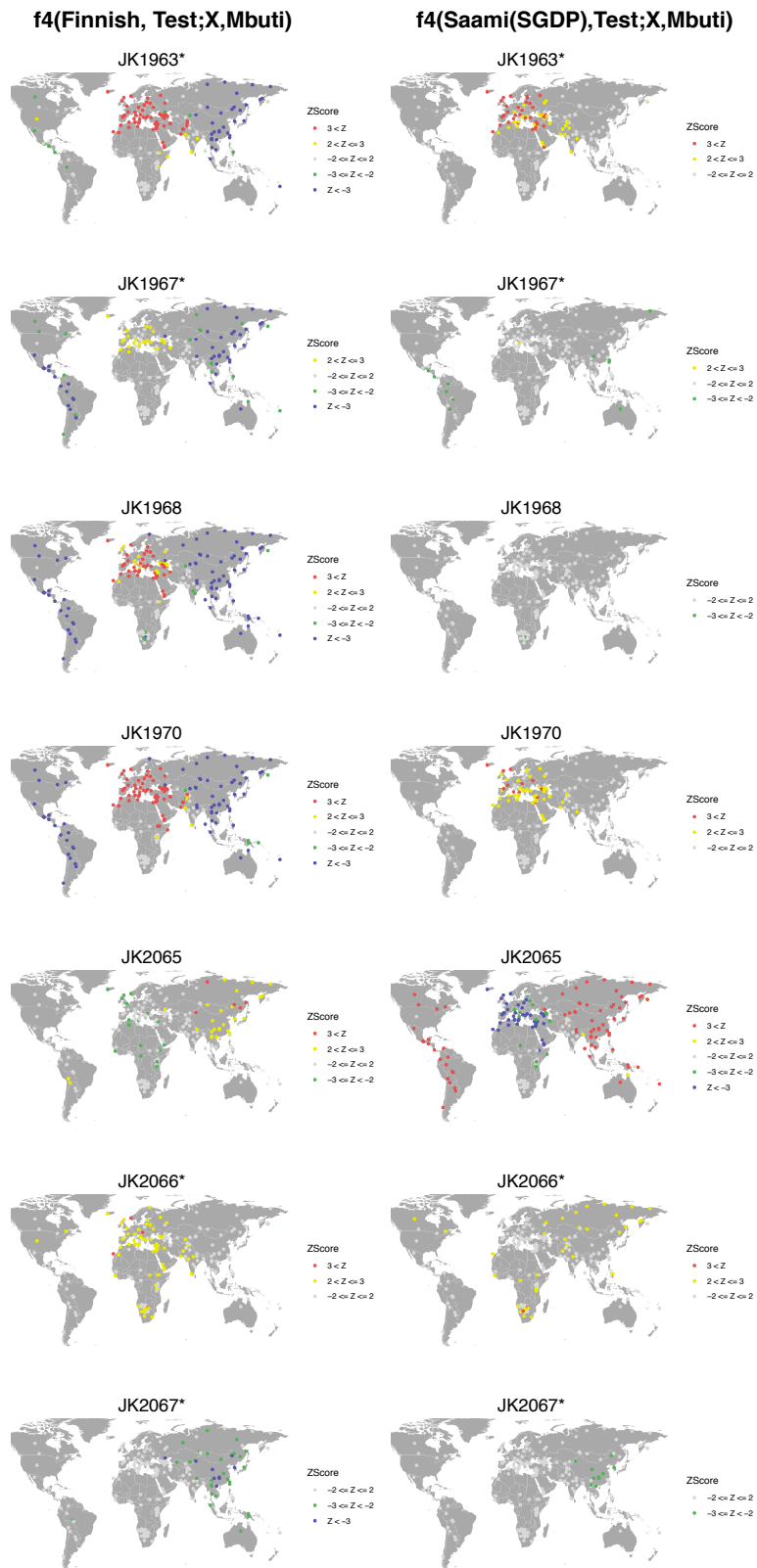
Supplementary Figure 6. Testing Levänluhta for cladality with modern Finns and/or Saami. f_4(Finnish, Test; X, Mbuti) & f_4(Saami, Test; X, Mbuti) comparison for multiple worldwide populations X, using ancient individuals from Levänluhta as *Test*. Asterisks denote individuals with low coverage (<15000 SNPs covered). Points are coloured based on bins of Z Score values, with warmer colours indicating higher affinity in Finns/Saami than in the *Test*, and vice versa for colder colours. Grey points indicate similar affinities toward population X. Map generated using ggplot2 and data from the Natural Earth project. Source data are provided as a Source Data file.
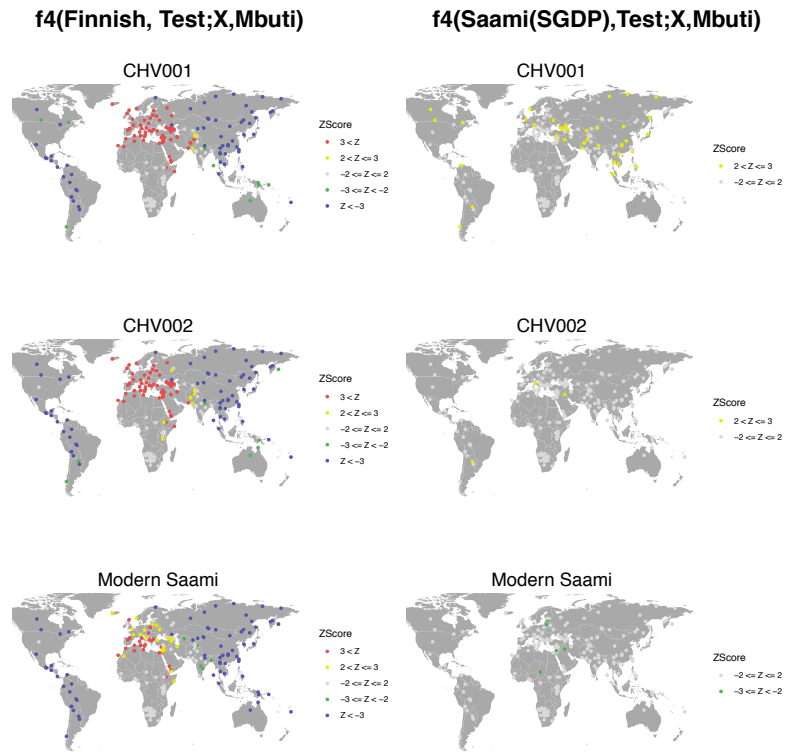
Supplementary Figure 7. Testing historical and modern Saami for cladality with modern Finns and/or Saami. f_4(Finnish, Test; X, Mbuti) & f_4(Saami, Test; X, Mbuti) comparison for multiple worldwide populations *X*, using ancient individuals from Chalmny Varre and the modern Saami genome from this study as *Test*. Points are coloured based on bins of Z Score values, with warmer colours indicating higher affinity in Finns/Saami than in the *Test*, and vice versa for colder colours. Grey points indicate similar affinities toward population *X*. Map generated using ggplot2 and data from the Natural Earth project. Source data are provided as a Source Data file.

Supplementary Tables

Supplementary Table 1. Deamination damage per library.

Library ID	UDG treatment	Damage 5' 1st base	Damage 5' 2nd base	Damage 3' 2nd base	Damage 3' 1st base
CHV001	Half	0.0287	0.0074	0.0121	0.031
CHV002	Half	0.0189	0.0062	0.0111	0.0244
JK1963	Half	0.0259	0.0071	0.0111	0.0294
JK1967	Half	0.0104	0.0048	0.009	0.0151
JK1968	Half	0.0284	0.0054	0.0088	0.0282
JK1968.nonUDG	None	0.094	0.0575	0.0521	0.0865
JK1970	Half	0.0239	0.0069	0.0109	0.029
JK1970.nonUDG	None	0.0953	0.0745	0.073	0.0937
JK2065	Half	0.0123	0.0045	0.0069	0.0155
JK2065.nonUDG	None	0.0471	0.0452	0.0448	0.0487
JK2066	Half	0.0146	0.0041	0.0059	0.0171
JK2067	Half	0.0104	0.004	0.0065	0.0129
BOO001	Half	0.0283	0.0075	0.0107	0.0302
BOO002	Half	0.0402	0.0078	0.0113	0.0333
BOO003	Half	0.0411	0.0073	0.0108	0.0398
BOO004	Half	0.0382	0.0085	0.0117	0.0344
BOO005	Half	0.045	0.0066	0.0108	0.0421
BOO006	Half	0.0381	0.0063	0.0094	0.0302

Supplementary Note 1

Extended Archaeological Information

Levänluhta

The Levänluhta site is located in the Isokyrö municipality at the southern Ostrobothnia region of Western Finland. The site represents a rarely observed case of lake burials, and is one of the most studied archaeological sites in Finland. Levänluhta context has been dated to the Iron Age in Finland (300-800 CE)[1,2] via some prestige artifacts assumed to have served as grave goods. The skeletal remains are, while numerous and well preserved, also anatomically disarticulated due to the gradual transition of the original lake environment to a marshland, and subsequent ditching and ploughing of the soil for agricultural use over the centuries. The remains of approximately 100 individuals are recognized from the cemetery to date.

The archaeological excavations were carried out by Oscar Rancken in 1886, A.M. Tallgren and Alfred Hackman from 1912 to 1913, Aarni Erä-Esko from the National Board of Antiquities from 1982 to 1984[1,2], followed by an archaeological survey of both Levänluhta and the immediate area around it in 2014. A comprehensive osteological analysis was reported by Tarja Formisto in 1993. The human remains are under the care of National Board of Antiquities, and stored currently at the National Museum of Finland. Skeletal element IDs for the analysed samples are: 2:1:a29 -L21 (JK1963), "milk tooth" -L47 (JK1967), 2:1:a16 -L20 (JK1968), 477 -L46 (JK1970), 2:1:a3 -L17 (JK2065), KM21814:735 -L22 (JK2066), 2:1:a2 -L16 (JK2067).

Chalmny Varre

The Chalmny-Varre Saami cemetery, associated with the two seasonal settlements of nomadic Kamensk Saami in the 18th century, is located on a small island in the middle flow of Ponoy River (center of Kola Peninsula). The burials have characteristics of Christian graves, combined with old traditional Saami rituals, such as birch cork pieces placed in the graves and masks (lichiny) of deceased carved on wooden crosses. Archaeological dating is confirmed by artifact findings from the graves and information on the wooden crosses which are marking the graves. The excavation, including an anthropological investigation, was organised by the Institute of Ethnography of N.N. Miklukho-Maclay Academy of Science of the USSR in the year 1976. Skeletal IDs for analysed samples are: CHV30 (CHV001), CHV38 (CHV002).

Bolshoy Oleniy Ostrov

Bolshoy Oleniy Ostrov (Great Reindeer Island), situated in the Kola Bay of the Barents Sea and separated from the mainland by Yekarerininsky Island and two straits, harbors the ancient cemetery of an unknown Early Metal Age culture. The preservation of artifacts made from bone and antler, wooden structures, as well as human remains is remarkable for the location and age this site represents. Altogether 19 skeletons of adults and children have been recognized from both single and collective burials of the site, together with more than 250 artifacts. Archaeological

surveys and excavations at the location were performed by G.D. Richter and S.F. Yegorov in 1925, by A.V. Schmidt on the USSR Academy of Science Kola Expedition in 1928, by N.N. Gurina in 1947–1948, as a part of Kola Expedition from the Leningrad Department of the Institute of Archaeology of the Academy of Sciences, and by V.Y. Shumkin from the same institute, later named as the Institute for the History of Material Culture Russian Academy of Sciences (RAS), starting from 1998-1999 and continuing in 2001-1004. Apart from these excavations, approximately 25 burials were revealed in 1934 during the construction of fortifications. Four finds are known to have been stored by the USSR Academy of Sciences at the time, but the location of all other remains from this instance is unknown. Part of the cemetery was never excavated and has possibly been destroyed by erosion. Morphological analyses, largely concentrated on cranial characteristics, have been performed by S.D. Sinitsyn in 1930, and V.P. Yakmov in 1953 and V.G. Moiseyev and V.I. Khartanovich in 2012[3]. A radiocarbon date for the site is provided by Moiseyev and Khartanovich as 3473±42 BP [3], which we calibrated as described in Methods. We note that radiocarbon dating on individuals with marine-based diets can be affected by the marine reservoir effect, which may result in overestimates of the true date[4]. Other dates provided by Murashkin et al (2016)[5] also date the site to the middle to late 2nd millennium BC. The human remains are stored at Peter the Great Museum of Anthropology and Ethnography (Kunstkamera) RAS in St. Petersburg, with the exception of burial 13, the remains of which are admitted to the Historical Museum in Polarnyi, Murmansk Oblast.[3] Skeleteal IDs for analysed samples are: BOO57.1 (BOO001), BOO72.1 (BOO002), BOO72.4 (BOO003), BOO72.7 (BOO004), BOO72.10 (BOO005), BOO72.15 (BOO006).

Supplementary Note 2

Assessment of power to detect contamination using continental supervised ADMIXTURE analysis.

To test the power of our approach to identify contamination using supervised ADMIXTURE using a set of continental populations as defined clusters, we devised a way to contaminate our data in silico. We assume that the rate of nuclear contamination in a library will be directly related to the proportion of reads mapping to the nuclear chromosomes that are of contaminant origin. Therefore, when a random draw genotyping approach is used, that contamination rate should also be directly proportional to the rate of genotypes called from the reads of the contaminant source. This assumption is violated if the distribution of contaminant and ancient DNA fragments across the nuclear genome is not uniform.

As a means to contaminate genotypes in silico, we provide ContaminateGenotypes.py (https://github.com/TCLamnidis/ContaminateGenotypes), a python script that contaminates the genotypes of a set of Sample individuals with genotypes from a provided contaminant individual, at multiple specified rates. We used this script to create a set of dummy individuals contaminated by one of seven contaminant individuals at nine different contamination rates.

As contamination sources we provided one individual from each population used as a pre-defined continental cluster during the supervised ADMIXTURE analysis (Atayal: NA13597, French: HGDP00511, Kalash: HGDP00267, Karitiana: HGDP00995, Mbuti: HGDP00449, Papuan: HGDP00540). We additionally used one Han Chinese individual (HGDP00774) as a contaminant to assess the power of this analysis to identify contamination that is not within the pre-defined continental clusters.

We generated dummy individuals at contamination rates of 0.01, 0.02, 0.03, 0.04, 0.05, 0.08, 0.10, 0.25, 0.50 for each of the contaminant sources. The dummy individuals were then separated by contaminant source and contamination rate, before running supervised admixture on each subset separately, to avoid artefacts in ADMIXTURE from essentially clonal individuals.

Our results show that contaminants that are distantly related to the ancestries within the ancient individuals (e.g. Mbuti and Papuan in our case), are detected from contamination rates of 0.05 and above, while more closely related ancestries, though ones not present in the dataset (e.g. Kalash) can be detected less consistently at that threshold, but quite consistently at contamination rates of 0.08 and above (Supplementary Figure 8).

Finally, contamination from sources whose continental ancestry was already detected in the uncontaminated data (e.g. Atayal, French, Karitiana) cannot be reliably detected as such (Supplementary Figure 9). We conclude that such an approach only has power to detect contamination from distantly related populations.
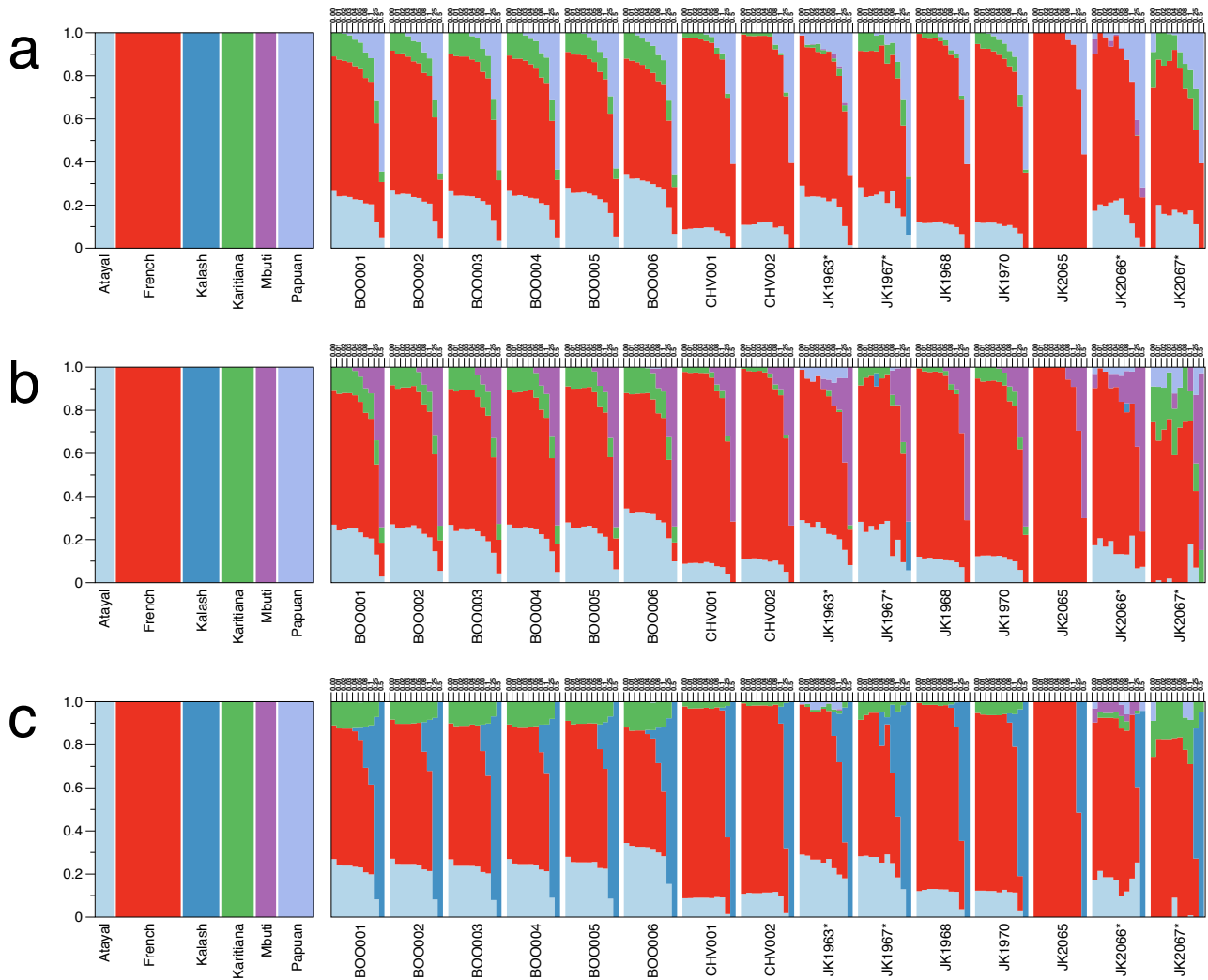
Supplementary Figure 8. Compiled supervised ADMIXTURE runs. Each individual from this study was contaminated at different rate by a distantly related contaminant individual. Low coverage (>15,000 SNPs) individuals marked with an asterisk. **a** Contaminant was Papuan. **b** Contaminant was Mbuti. **c** Contaminant was Kalash. Source data are provided as a Source Data file.
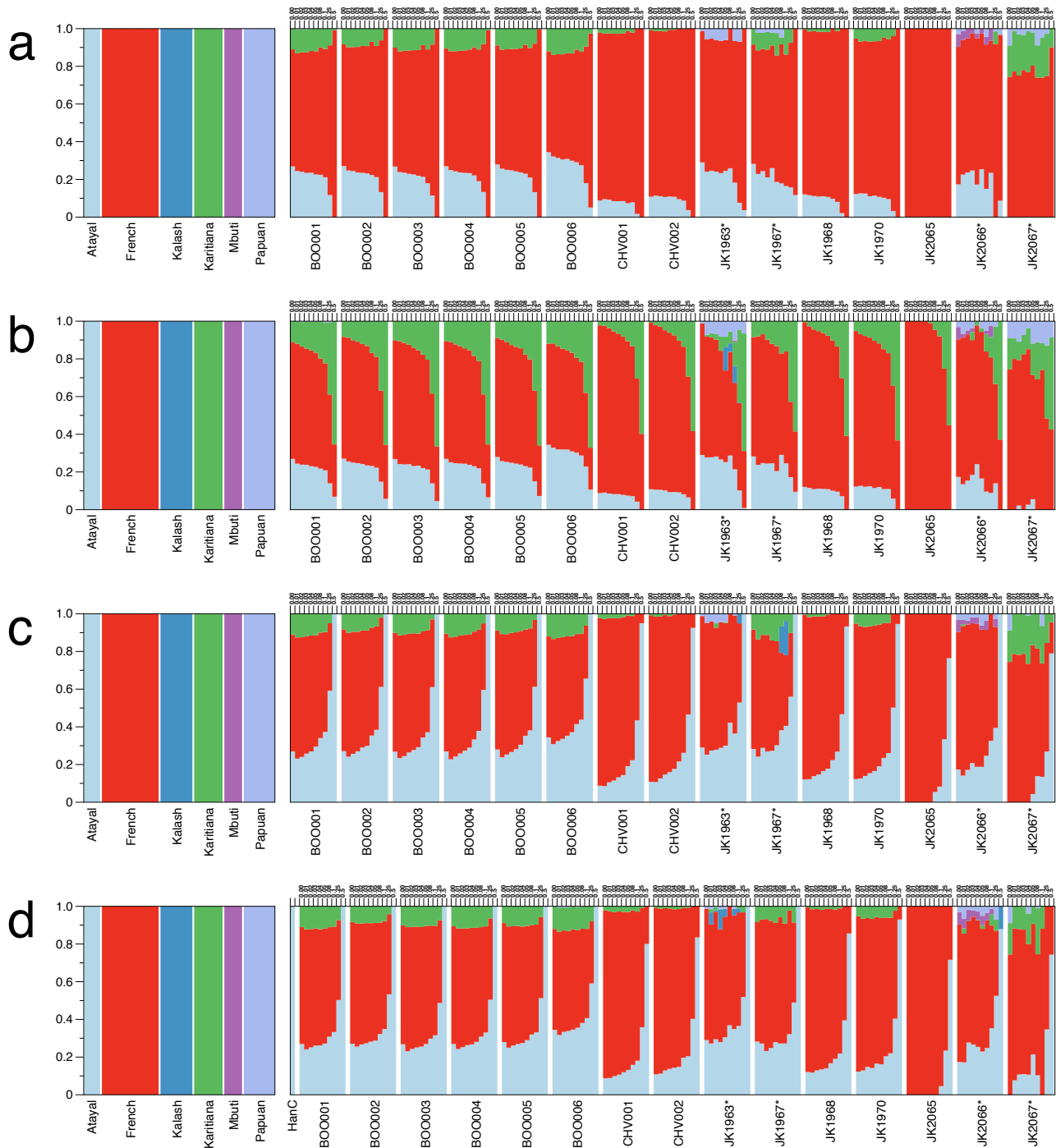
Supplementary Figure 9. Compiled supervised ADMIXTURE runs. Each individual from this study was contaminated at different rate by a contaminant individual from a genetic cluster that was already present in the uncontaminated data. Low coverage (>15,000 SNPs) individuals marked with an asterisk. **a** Contaminant was French. **b** Contaminant was Karitiana. **c** Contaminant was Atayal. **d** Contaminant was Han Chinese. Contaminant individual is labelled "HanC". Source data are provided as a Source Data file.

Supplementary Note 3

Sex determination with error bar calculation

We provide a python script (https://github.com/TCLamnidis/Sex.DetERRmine.git) that calculates the relative coverage of X and Y chromosomes, and their associated error bars, from the depth of coverage at specified SNPs. The error calculation relies on the assumption that reads are randomly and independently distributed across a list of specified SNPs. This is justified if SNPs are further apart from each other than typical sequencing length, which is largely the case for the SNP panel considered here (1240K). The script takes as input the output of the samtools depth command, which reports the depth at each of the specified SNPs. The depths are partitioned into three bins: Autosomal, X- and Y-chromosome, so that:

$$N = \sum_i N_i$$

Where N_i is the number of sequenced reads overlapping the SNPs within each bin i, and N is the total number of reads overlapping with SNPs within our capture panel. We can then calculate the proportion of all sequenced reads that cover SNPs in bin i (p_i). Its associated error is then calculated as the error of the binomial distribution of N_i.

$$p_i = \frac{N_i}{N}$$
$$\mathrm{Err}(N_i) = \sqrt{Np_i(1 - p_i)}$$

The average SNP depth within bin i (d_i) can be calculated as the ratio of N_i to the number of SNPs within bin i (S_i). The error of the average SNP depth is proportional to the error associated with N_i.

$$d_i = \frac{N_i}{S_i}$$
$$\mathrm{Err}(d_i) = \frac{\mathrm{Err}(N_i)}{S_i}$$

The relative coverage on the X and Y chromosomes can then be calculated as the ratio of the average SNP depth on the X/Y chromosome over the average SNP depth on the autosomes. The error of this measurement can then be calculated using standard error propagation.

$$\mathrm{rate}_{X/Y} = \frac{d_{X/Y}}{d_{aut}}$$
$$\mathrm{Err}(\mathrm{rate}_{X/Y}) = \sqrt{\left(\mathrm{Err}(d_{X/Y}) \times \frac{1}{d_{aut}}\right)^2 + \left(\mathrm{Err}(d_{aut}) \times \frac{d_{X/Y}}{d_{aut}^2}\right)^2}$$

Supplementary References

1. Wessman, A. Levänluhta. A place of punishment, sacrifice or just a common cemetery? *Fennoscandia archaeologica* **XXVI,** 81–105 (2009).

2. Wessman, A. *et al.* Hidden and Remote: New Perspectives on the People in the Levänluhta Water Burial, Western Finland (c.ad 300–800). *European Journal of Archaeology* **21,** 431–454 (2018).

3. Moiseyev, V. G. & Khartanovich, V. I. Early Metal Age crania from Bolshoy Oleniy Island, Barents Sea. *Archaeology, Ethnology and Anthropology of Eurasia* **40,** 145–154 (2012).

4. Ascough, P., Cook, G. & Dugmore, A. Methodological approaches to determining the marine radiocarbon reservoir effect. *Progress in Physical Geography: Earth and Environment* **29,** 532–547 (2005).

5. Murashkin, A. I., Kolpakov, E. M., Shumkin, V. Y., Khartanovich, V. I. & Moiseyev, V. G. Kola Oleneostrovskiy grave field: a unique burial site in the European Arctic. *New Sites, New Methods; Iskos 21* (2016).

SCIENTIFIC REPORTS

natureresearch

OPEN

Human mitochondrial DNA lineages in Iron-Age Fennoscandia suggest incipient admixture and eastern introduction of farming-related maternal ancestry

Sanni Översti[1], Kerttu Majander[1,2,3], Elina Salmela [1,2], Kati Salo[4], Laura Arppe[5], Stanislav Belskiy[6], Heli Etu-Sihvola [5], Ville Laakso[7], Esa Mikkola[8], Saskia Pfrengle[3], Mikko Putkonen[9], Jussi-Pekka Taavitsainen[7], Katja Vuoristo[8], Anna Wessman [4,7], Antti Sajantila[9], Markku Oinonen [5], Wolfgang Haak [2], Verena J. Schuenemann[3,10], Johannes Krause [2], Jukka U. Palo[9,11] & Päivi Onkamo[1,12]

Human ancient DNA studies have revealed high mobility in Europe's past, and have helped to decode the human history on the Eurasian continent. Northeastern Europe, especially north of the Baltic Sea, however, remains less well understood largely due to the lack of preserved human remains. Finland, with a divergent population history from most of Europe, offers a unique perspective to hunter-gatherer way of life, but thus far genetic information on prehistoric human groups in Finland is nearly absent. Here we report 103 complete ancient mitochondrial genomes from human remains dated to AD 300–1800, and explore mtDNA diversity associated with hunter-gatherers and Neolithic farmers. The results indicate largely unadmixed mtDNA pools of differing ancestries from Iron-Age on, suggesting a rather late genetic shift from hunter-gatherers towards farmers in North-East Europe. Furthermore, the data suggest eastern introduction of farmer-related haplogroups into Finland, contradicting contemporary genetic patterns in Finns.

Genetic studies on anthropological remains have exceedingly helped to shed light on various human populations as well as past events and processes. These include for instance the initial colonization of Europe by modern humans c. 40 kya[1,2], the Holocene hunter-gatherer communities[1,3], the major population turnover associated with the Neolithic spread of agriculture from Anatolia[3–5], and the massive Bronze-Age influx of genes, culture and customs of the Yamnaya-related people into Europe from the Pontic-Caspian steppe[6,7].

In terms of mitochondrial DNA (mtDNA), these cultural turnovers and population migrations in Europe involved also changes in the haplogroup composition. In hunter-gatherer populations the dominating mitochondrial lineage has been U, especially its subgroups U4, U5a and U5b[3]. In the advent of the Neolithic revolution, these U subgroups were largely supplanted by farmer-associated haplogroups H, HV, J, K, N1a, T2 and W[4,5]. The

[1]Department of Biosciences, University of Helsinki, Helsinki, Finland. [2]Department of Archaeogenetics, Max Planck Institute for the Science of Human History, Jena, Germany. [3]Institute for Archaeological Sciences, Archaeo- and Palaeogenetics, University of Tübingen, Tübingen, Germany. [4]Department of Cultures, University of Helsinki, Helsinki, Finland. [5]Laboratory of Chronology, Finnish Museum of Natural History, University of Helsinki, Helsinki, Finland. [6]Peter the Great Museum of World Anthropology and Ethnography (Kunstkamera), Russian Academy of Science, St. Petersburg, Russia. [7]Department of Archaeology, University of Turku, Turku, Finland. [8]Finnish Heritage Agency, Helsinki, Finland. [9]Department of Forensic Medicine, University of Helsinki, Helsinki, Finland. [10]Institute of Evolutionary Medicine, University of Zürich, Zürich, Switzerland. [11]Forensic Genetics Unit, National Institute for Health and Welfare, Helsinki, Finland. [12]Department of Biology, University of Turku, Turku, Finland. Sanni Översti and Kerttu Majander contributed equally. Johannes Krause, Jukka U. Palo and Päivi Onkamo jointly supervised this work. Correspondence and requests for materials should be addressed to S.Ö. (email: sanni.oversti@helsinki.fi)

subsequent spread of Yamnaya-related people and Corded Ware Culture in the late Neolithic and Bronze Age were accompanied with the increase of haplogroups I, U2 and T1 in Europe (See[8] and references therein).

Whereas the ancient DNA (aDNA) composition and its changes in mainland Europe are increasingly well understood, northeastern Europe has been far less studied. The oldest human DNA analyzed in this region derive from the Mesolithic burial sites in Huseby Klev, western Sweden (9800 calBP[9]), Hummervikholmen in Norway (9300 calBP[10]) and Yuznuy Olennij Ostrov on Lake Onega, Russia (~8400 calBP[7,11]). In addition, Mesolithic to Bronze-Age DNA data from several sites in the Baltic countries have been published[6,12–14].

Despite the relatively close geographical proximity, little is known about the ancient DNA diversity in regions immediately north of the Baltics. This is largely due to the scarcity of preserved anthropological remains. In the hemiboreal forest zone the soil pH, together with annual freeze-thaw cycles has highly detrimental effects on bone material to the extent to which no unburnt remains older than ~2000 years exist[15]. However, archaeological evidence strongly suggests that the most notable colonization events in the region have taken place much earlier[16,17]. Consequently, the lack of archaeological bone material gravely limits the capability of aDNA studies in resolving the human population history of the Taiga belt and the processes that have shaped present-day diversity. Despite these shortcomings, aDNA has recently been recovered from c. 1500 year-old bones from Levänluhta in western central Finland[18,19]. Genomic data from these samples show a Siberian ancestry component still prominently present today, particularly in the indigenous Saami people, and to a lesser extent in modern Finns. Although these data suggest a widespread presence of genetically Saami-like people around eastern Fennoscandia during the Iron Age, more wide-spread sampling in space and time is necessary for understanding the past population dynamics, and emerging of the contemporary genetic diversity in Finland.

In terms of both genetics and culture, modern Finns show a unique combination of eastern and western European elements, which most likely reflects the settlement history. The first archaeological evidence of human presence in Finland dates relatively late to c. 11000–9000 years ago, soon after the continental ice sheet retreated. According to the archaeological record, the region has since supported a continuous human occupation until today[17]. Several influential waves of material culture have been shown to extend into Finland: the first one brought the Sperrings or Säräisniemi pottery to the area c. 7500 years ago[20], the second presented the typical Comb-Ceramic at 6000 years ago[16,17], one of the most influential prehistoric cultures in the wider region. Finally, around 4700 years ago, the Corded-Ware culture reached Finland[16,17,21]. The most significant cultural changes, possibly driven by expansions, proceeded from east/south-east and extended into most of today's territory of Finland, while the Corded-Ware culture influence spread from south occupying only the southwestern part of Finland. Later, Bronze Age brought an increase of human activity[17] and coinciding advance of cereal cultivation[22]. Finland also saw a pronounced Scandinavian impact along the western coast, while the inland was dominated by eastern influences, seen e.g. in the arrival of ferrous metallurgy c. 500 BC and stylistic features of Bronze-Age and Iron-Age items[21]. Iron Age in Finland starts around 500 BC and continues until the end of Crusade period (c. 1200 AD in west and 1300 AD in east). Unlike most of the Europe, the Middle Ages starts as late as 1200 AD in western parts of country and 1300 AD in east and shifts into Early modern period in the beginning of 16th century (for a review of archaeological and historical periods in Finland see[21]).

Linguistically, contemporary Finns and Saami differ from most other Europeans in speaking a Uralic language, unrelated to the majority of European languages, which belong to the Indo-European language family. Finns are also genetically distinct from their neighboring populations and form outliers in the genetic variation within Europe[23]. This genetic uniqueness derives from both reduced genetic diversity[24,25] and an Asian influence to the gene pool[24]. Within Finland, an unusually strong genetic border bisects the population along a northwest to southeast axis[24,26,27], and is interpreted to reflect an ancient boundary between hunter-gatherer and farmer populations[28]. The expanse of agriculture north-east of this border was probably limited by environmental factors, especially the length of the growing season. Later, this border has most likely acted in demarcating the spread of western and eastern political and cultural impacts influencing the placement of first political border between Sweden and Novgorod through the middle of Finland (Treaty of Noteborg 1323 AD).

In order to gain better insight into the genetic history of Finns, we here describe 103 complete mitochondrial genomes reconstructed from bone samples from ten burial sites in southern Finland and the Republic of Karelia, Russia (former Finnish territory; Fig. 1). The main focus is on the 70 complete mitochondrial genomes from five archaeological burial sites in Finland spanning spatially from western coast to Lake Ladoga, and Late Roman Iron Age (300 AD) to the Middle Ages (1500 AD) (Tables 1, S1 and Supplementary Material S1). In addition, we include 33 mitochondrial genomes from later, mainly historical burials (1400–1800 AD) from five sites across southern Finland. While mtDNA genomes of Iron-Age and Early-Medieval Finland cannot be used to directly target questions about the colonization of Finland, they provide a spatio-temporal transect to the maternal ancestry of the early inhabitants in this region, and help to understand patterns observed in Finland's modern mtDNA diversity.

Results

Authenticity of ancient-DNA results. Based on the shotgun sequencing, out of the total of 141 individuals sampled, 134 were included in mitochondrial capture. Mitochondrial genomes for 103 individuals passed the quality control thresholds, while 31 samples were excluded from further analyses due to insufficient data (less than fivefold mitochondrial coverage) or high contamination levels (Supplementary Table S1). Ancient-DNA yield for all 103 samples was studied with several criteria of authentication. All samples showed fragment sizes ranging between 40–250 bp, as expected for ancient DNA[29]. Fragments under 30 bp were filtered out as a mapping quality control. All samples had an average fragment length of 47 to 95 bp. The authentic ancient DNA is often fragmented compared to the modern DNA, and fragments as short as 50–65 bp are common. The samples included in the downstream analyses yielded between 1426 and 395345 unique human mitochondrial fragments with an average coverage ranging from 5-fold to 1683-fold. The first-base damage on the fragments
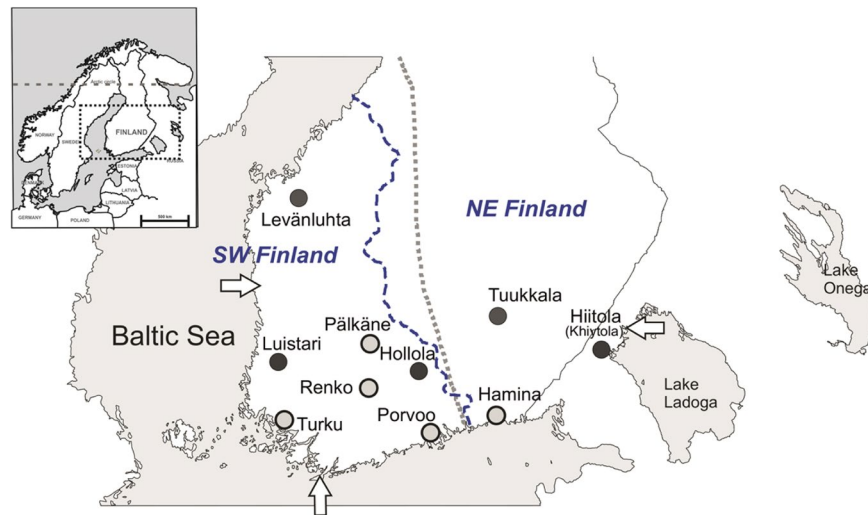
Figure 1. Map of Finland and the burial sites presented in this study. Iron-Age and medieval sites (Levänluhta, Luistari, Hollola, Hiitola and Tuukkala) are marked with dark grey circles. Early-modern and modern sites (Pälkäne, Porvoo, Renko, Turku and Hamina) are marked with light grey circles. Arrows indicate three reference points (Hanko, Uusikaupunki and Lahdenpohja) used in the multinomial logistic regression analysis (see Section 2.7). Small map of northern Europe is modified from Neuvonen *et al.*[28]. Blue dashed line represents the border of southwestern (SW) and northeastern (NE) subpopulations of contemporary Finns (Neuvonen *et al.*[28] was used as a reference for this border). Grey dotted line represents the boundary of Finnish folk culture between western and northeastern Finland described in Talve 2000[74].

Site	Archaeological dating (AD)*	Period based on archaeological dating	Number of individuals with ^{14}C date	[14]C (calAD)**	Number of individuals sampled	Number of individuals in mtDNA capture	Number of complete mtDNA sequences obtained	Number of complete mtDNA sequences used in statistical analyses
Levänluhta	300–800	Roman Iron-Age, Merovingian	4	370–720	13	13	12	12
Luistari	600–1300	Merovingian, Viking, Crusade	10	760–1295	25	21	10	10
Hollola	1050–1400	Crusade	11	955–1390	20	18	16	14
Hiitola	1200–1500	Crusade, medieval	10	1170–1470	16	16	14	13
Tuukkala	1200–1400	Crusade, medieval	4	1225–1525	30	30	18	17
Pälkäne	1200–1700	Crusade, medieval, post-medieval	4	1280–1640	4	4	4	4
Porvoo	1300–1900	medieval, post-medieval	5	1610–1825	9	9	7	7
Renko	1500–1800	medieval, post-medieval	3	NA	8	8	8	8
Turku	1550–1650	post-medieval	NA	NA	5	5	5	4
Hamina	1700–1800	post-medieval	NA	NA	9	9	9	9
TOTAL			47		141	134	103	98

Table 1. Sites presented in this study. *Dating based on the burial contexts. **Defined based on individual's ^{14}C dates with Oxcal commands 'Phase/Boundary'. Phase boundaries provide estimate for starts and ends of the site usages. Phase boundaries are here defined for sites with four or more individuals with ^{14}C dates. The mean values are given. Radiocarbon dates include datings presented in this study and datings published elsewhere. See Section 2.2, Supplementary Material S2 and Supplementary Table S2 for more detailed information.

varied between 5–36% on the 3′-end and 4–34% on the 5′-end. Previous studies have proven that cytosine deamination is influenced by the age of the sample[30,31] and the mean temperature of the site[31]. Considering the climatic conditions in Finland, e.g., low mean temperature, and the relatively young age especially for the post-medieval samples, 3′ and 5′ damage values below 5% are plausible. No samples were therefore omitted from the study based on these criteria.

The contamination rates of the 103 samples were further evaluated by Schmutzi[32]. 36 samples had Schmutzi contamination estimates exceeding 5% and were excluded (Supplementary Table S1). The remaining samples were then analyzed with ContamMix[33]: the resulting crude contamination estimates as well as the *a posteriori* estimates of contamination along with their 95% confidence intervals (CI) from the MCMC are reported in Supplementary Table S1. The CIs ranged from 0% to 17.2%; in ten cases they exceeded 10%, even though estimates by Schmutzi had remained below 5%. These cases were visually inspected with Geneious 11.0.3 (www.geneious.com). For each of them, the majority call supported the previously assigned haplogroup.
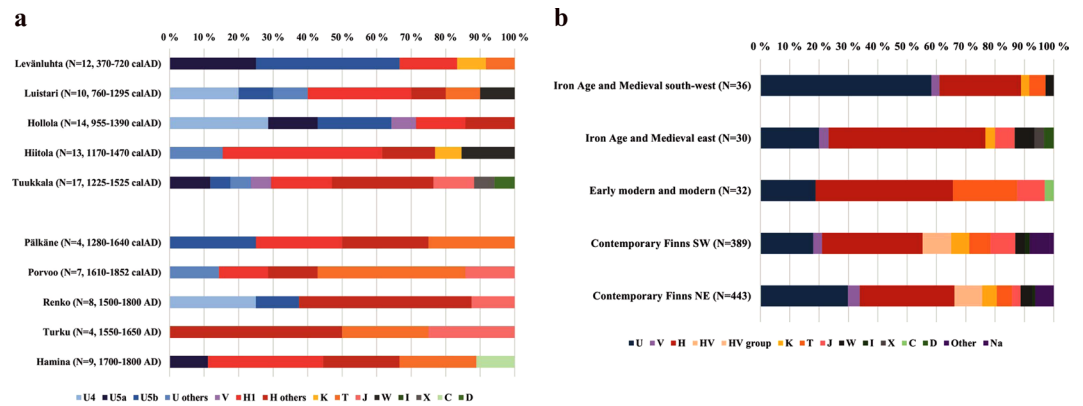
Figure 2. (**a**) MtDNA haplogroup distribution at each site. Only unique haplotypes per site are included. Ages of the sites are presented based on the interval for mean values of phase boundaries for start and end distribution when available (i.e. for Levänluhta, Luistari, Hollola, Hiitola, Tuukkala, Pälkäne, and Porvoo, see Section 2.2.) and based on archaeological context for other sites. (**b**) MtDNA haplogroup frequencies when pooled according to chronological and geographical criteria. Only unique haplotypes within site are included. Iron-Age and medieval south-west includes Levänluhta, Hollola and Luistari; Iron-Age and medieval east includes Hiitola and Tuukkala; Early modern and modern includes Pälkäne, Porvoo, Renko; Frequencies for contemporary Finns from[28].

Radiocarbon datings. For this study, we report new ^{14}C dates for 42 individuals (Supplementary Table S1). Radiocarbon dates for nine individuals were determined previously (see Supplementary Table S1). Based on radiocarbon dates and/or dating of the context, the studied burial sites cover the timespan from the Roman Iron Age (300 AD) to historical times (19th century). For sites Levänluhta, Luistari, Hollola, Hiitola, Tuukkala, Pälkäne and Porvoo the highest posterior densities (HPD) for site's start and end boundaries were determined. The mean values for obtained phase boundaries are presented in Table 1, and 68% and 95% HPD regions are presented in Supplementary Table S2 and in Supplementary Fig. S1. Intervals for mean values of boundaries obtained based on radiocarbon dates were in accordance with dates determined based on the archaeological context (Table 1).

MtDNA data and haplotypic variation. A total of 95 unique complete-mitogenome haplotypes were observed among the 103 complete sequences retrieved: three haplotypes were shared between sampling sites and five within a site. In the latter cases, the placement of the skeletal samples suggests that the shared haplotypes have been carried by different individuals, who may have been maternally related: identical haplotypes (haplogroup U5a2a1e) were obtained from remains of a c. 5-year-old child (grave 18, TU666) and an older woman (grave 7, TU655) from Hollola. Identical haplotypes (haplogroup H85) were also observed in a middle-aged adult (grave 6, TU661) and a c. 18-month-old child (grave 15, TU668) from Hollola. At the Hiitola site, identical haplotypes (haplogroup W6) were shared between two individuals from distinct graves (individual TU566 from grave 80 and individual TU675 from grave 30). At the Tuukkala site, two individuals showed identical haplotypes (haplogroup H10e, individuals TU631 and TU645). At Turku, two adults shared the same haplotype belonging to the basal haplogroup H (samples TU582 and TU588). Haplotypes for 103 individuals are presented in Supplementary Table S3.

As the subsequent statistical methods assume that samples derive from unrelated individuals, five samples - one of each identical haplotype pairs within sites (TU666, TU668, TU675, TU645 and TU588) - were removed from the subsequent analyses due to their possible maternal relatedness.

The mean number of pairwise differences, calculated from complete mitochondrial genomes, was highest within Porvoo (MNPD = 33.7 ± 16.8) and lowest within Renko (MNPD = 21.8 ± 10.8) (Supplementary Table S4). Due to the small number of individuals per site and utilization of unique complete mtDNA sequences, haplotype diversities (H) were relatively high (with mean 1.0 and standard deviation ranking from 0.0202 to 0.1768).

MtDNA haplogroup composition at the ancient sites. Burial site-specific haplogroup frequencies of the 98 complete mitochondrial sequences showed considerable between-site variation (Fig. 2 and Supplementary Table S5). The observed frequencies of the main haplogroups in the whole dataset resembled the prevalence among contemporary Finns. As today, haplogroups U and H were the most common, yet with slightly higher overall frequencies than today (U 33.7% vs. 24.1%, and H 41.8% vs. 33.2%). However, when grouped temporally into Iron-Age and medieval sites (IAM) and early-modern and modern sites (EMM), differences were observed: the IAM sites (i.e., Levänluhta, Luistari, Hollola, Hiitola and Tuukkala) demonstrated significantly higher overall prevalence of haplogroup U (40.9%) than the EMM sites (i.e., Pälkäne, Porvoo, Renko, Turku and Hamina, 18.8%) but also high inter-site variability. Among the EMM samples haplogroup H dominated (U 18.8%, H 46.9%).

This inter-site variability of the haplogroup U/H ratio had a clear spatial pattern also among the IAM samples. The western cluster (IAM south-west: Levänluhta, Luistari and Hollola) had average U and H frequencies of 58.3% and 27.8%, respectively, whereas the corresponding values in the eastern cluster (IAM east: Hiitola,

Tuukkala) were 20.0% and 53.3%. In IAM east the highest frequency for an individual subhaplogroup was 30.0% obtained for H1. Strikingly, this U/H ratio is the opposite compared to contemporary eastern and western Finns.

Differences in haplogroup composition between the sites. Among the 12 Levänluhta samples, five individuals carried haplogroup (hg) U5b, four of which belonged to the sub-hg U5b1b1a. Additionally, the Levänluhta site included three individuals with hg U5a, resulting in a total frequency of 66.7% for hg U5. In contrast, with only two haplotypes of sub-hg H1, the frequency of hg H was well below values observed in modern European populations. The high U5b1b1a frequency resembles that observed today in Saami populations of northern Europe. This actually corresponds well to a related recent study that is showing the close genetic affinity between Levänluhta individuals and modern Saami[18]. However, the Levänluhta individuals also carried mtDNA haplogroups that are absent or rare among the Saami population today, U5a, H1 (0.0–4.0%[34]) and haplogroups K and T. The Levänluhta site clearly showed a unique composition, which resulted in significant genetic distances to all other ancient sites at sequence level, with Φ_{ST} values of >10% (see below).

Individuals from the Hollola site, ^{14}C dated to 955–1390 calAD (Table 1), also showed a high overall frequency of hg U (64.3%), similar to Levänluhta. However, differences in subhaplogroup distribution between Hollola and Levänluhta suggest a possible non-modern-Saami-like hunter-gatherer ancestry in this region. Interestingly, sub-haplogroup U5b1b1a, typical among contemporary Saami, was not observed in Hollola. In contrast, most of the Hollola U haplotypes belong to haplogroups U4 and U5a (frequencies in Hollola 28.6% and 14.3%, respectively), which are rare or absent in Saami today[34]. Moreover, U4 is also rare in modern Finns while the frequency for U5a is around 6%[28,35]. Haplotypes belonging to different subhaplogroups of hg H were more common in Hollola than in Levänluhta, occurring in altogether five samples. Haplogroups K and T were absent in the Hollola sample.

A rather different picture emerged from the Luistari samples, showing a substantial genetic distance to Levänluhta ($\Phi_{ST} = 0.134$, p < 0.01). Haplogroup U5b1 was entirely absent, and the U haplotypes observed belong to subhaplogroup U4, U5b2 and U2. Lineage U2 is prevalent in some Uralic speaking groups today[36]. The overall haplogroup distribution in Luistari was more similar to the modern European populations dominated by agriculture-associated Neolithic haplogroups H and occurrences of T2 and W1 (see Introduction), than in Levänluhta and Hollola sites.

The two easternmost sites, Hiitola and Tuukkala, proved genetically distant from the western Levänluhta and Hollola sites, despite being approximately contemporaneous with the Hollola individuals. The Neolithic signal in the mtDNA gene pool of ancient Finns in general was much stronger in the east. Both Hiitola and Tuukkala samples showed high frequencies of hg H (61.5% and 47.1%, respectively), together with other Neolithic haplogroups J, K, W and X. Notably, these eastern sites shared three haplogroups: H1a7, H1a8a and H10g. According to GenBank searches these three haplogroups are rare in modern populations: for H1a7 four modern sequences were found, two in Finnish (KY620272 and MF686118), one in Swedish (KJ487971) and one in British (GU797829) populations. For haplogroup H1a8a only two matches were found, one among Finnish (JX153203) and one of an unknown origin (JQ701944), whereas three modern sequences were found for haplogroup H10g: two Finnish (KR732275 and MF497508) and one from Russia (GU122976). Notably, H1* are known to be common in modern Karelia[37]. The eastern sites also comprise rare subhaplogroups U1 (hg U1b2 in Hiitola) and U8 (hg U8b1a2b in Tuukkala), which are atypical for contemporary Finns.

Early modern and modern sites represents similar frequencies of U and H as the combined Iron Age and Medieval East (18.8% and 46.9%, respectively). Contrasting IAM sites and contemporary Finns, EMM sites harbors high prevalence of haplogroup T; frequency in EMM is as high as 21.9%, while in other Finnish populations the frequency is less than 8% (Supplementary Tables S5 and S8). Individual JK1954 from Hamina belonged to haplogroup C, which is lacking from contemporary Finns[28] (Supplementary Table S5) and suggests possible eastern origin. Nevertheless, additional autosomal data is needed to confirm the genetic background of the individual JK1954.

When contrasted with haplogroup frequencies observed in contemporary Finns, our simulations (Supplementary Fig. S2) showed that the ancient sites are significantly different, and that these differences cannot be explained by sampling effects. This applied especially to haplogroup U5 in total and to subhaplogroup U5b in Levänluhta, hg U4 in both Luistari and Hollola as well as hg H1 in the Hiitola dataset.

Genetic distances among sites and to contemporary Finns. When we calculated genetic distances between sites, we observed that Levänluhta differed significantly from all the other sites, except Hollola ($\Phi_{ST} = 0.05042$, p = 0.02441) and Tuukkala ($\Phi_{ST} = 0.04387$, p = 0.06055) (Fig. 3a and Supplementary Table S6). The largest distance from Levänluhta was to the eastern Hiitola site ($\Phi_{ST} = 0.15468$). The distance between Levänluhta and contemporary Finns was smaller but still significant, with a distance to contemporary north-east (NE) $\Phi_{ST} = 0.04077$ and to contemporary south-west (SW) slightly higher $\Phi_{ST} = 0.06473$. While Luistari differed only from Levänluhta, the Hollola site differed both from Hiitola and the EMM ($\Phi_{ST} = 0.05205$ and $\Phi_{ST} = 0.05135$, respectively, p < 0.05 for both), but not from Levänluhta ($\Phi_{ST} = 0.06445$, p > 0.05) (Fig. 3a and Supplementary Table S6). Hiitola differed, in addition to Levänluhta and Hollola, from EMM and from both groups of contemporary Finns ($\Phi_{ST} = 0.04111$ for NE and $\Phi_{ST} = 0.03437$ for SW). When considering the genetic distances between individual sites, it has to be noted that the relatively low sample sizes might affect the Φ_{ST} values and the results should be interpreted with caution. However, for pooled IAM and EMM sites (see Fig. 2b), for which the sample sizes are ≥30, the genetic distance calculations should not be that sensitive for bias caused by small sample sizes.

Clustering the IAM sites further roughly according to their geographical location to IAM south-west (hg U more prevalent) and IAM east (hg H more prevalent) further demonstrated the pattern opposite to modern mtDNA diversity distribution (Fig. 3b). IAM south-west differed statistically significantly from contemporary SW ($\Phi_{ST} = 0.01670$, p = 0.00488) and EMM ($\Phi_{ST} = 0.05350$, p = 0.00098) but not from contemporary NE ($\Phi_{ST} = 0.00036$, p = 0.41895). In addition, EMM and contemporary SW differed from each other ($\Phi_{ST} = 0.01140$,
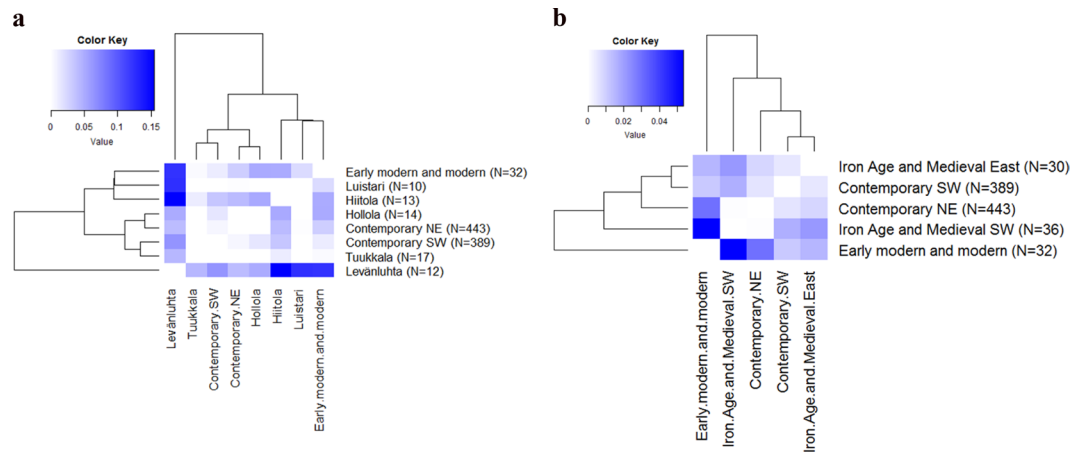
Figure 3. (**a**) Pairwise Φ_{ST} distances for ancient and contemporary Finns. Early modern and modern Finns consists of individuals from Pälkäne, Porvoo, Renko, Julin and Hamina sites. Contemporary Finns are divided into south-west (SW) and north-east (NE) subpopulations according to[28]. Φ_{ST} values are presented on a scale starting from zero (Φ_{ST} values and p-values are presented in Supplementary Table S6). (**b**) Pairwise Φ_{ST} distances for ancient and contemporary Finns. Iron-Age and medieval (IAM) sites are grouped into subpopulations: IAM south-west consists of Levänluhta, Luistari and Hollola; IAM east consists of Hiitola and Tuukkala. Early modern and modern Finns contain individuals from Pälkäne, Porvoo, Renko, Julin and Hamina sites. Contemporary Finns are divided into south-west (SW) and north-east (NE) subpopulations according to Palo *et al.*[27] and Neuvonen *et al.*[28].

p = 0.04102). Conversely, IAM east differed from the contemporary NE (Φ_{ST} = 0.00849) more than from contemporary SW (Φ_{ST} = 0.00514).

Haplotype level median-joining network (Supplementary Fig. S3) demonstrates that ancient and contemporary Finns exhibit in principle same main haplogroups, whereas the most notable differences are within the haplogroup frequencies between the ancient populations. Individuals from IAM eastern sites are more prevalent in the haplogroup H cluster, while individuals from IAM southwestern sites are more concentrated on the haplogroup U cluster. Contemporary Finns are in both clusters, indicating possible mixture of IAM southwestern and IAM eastern populations.

Main haplogroup frequencies in space and time. To evaluate the possible impact of spatial and temporal factors on the distributions of haplogroup U, largely associated with European hunter-gatherers, and farmer-associated haplogroup H within the IAM sites, we performed multinomial logistic regression analyses. In a stepwise forward analysis, the only statistically significant independent variable explaining the differences in the haplogroup composition was the distance from eastern reference point Lahdenpohja (compared to 'H' and 'Others' significance for Lahdenpohja was 0.013 and 0.103, respectively) (Supplementary Table S7). Neither the ages of the samples nor distance from the southern and western reference points were requisite for the best-fit model. However, the addition of the eastern reference point significantly improved the fit between model and data (p = 0.027). Based on the odds ratios, it is less likely that an individual from southwest belongs to haplogroups 'H' or 'Others' than an individual from an eastern archaeological site. Similar results were obtained when using hunter-gatherer associated haplogroups (U and V), farmer associated haplogroups (H, J, K and T) and 'Others' as categorically distributed dependent variables. We chose to include the haplogroup V as 'hunter-gatherer' while there is no direct evidence for association of hg V with the hunter-gatherers. This is assumed here because of V's northern distribution and its high prevalence (up to 58%[34]) among the Saami, the archetypal nomadic population lacking many farmer-associated haplogroups[34,38]. Distance from the eastern reference point was the only predictor included in the model (with significance of 0.031 for farmer associated haplogroups and 0.082 for other haplogroups). Assuming that haplogroups U and H can be associated to hunter-gatherers and farmers, respectively, the results suggest a spread of the more central European like, farmer-related haplogroups spreading from the east. However, as mentioned above, association of hg V is unclear. Omitting V from the hunter-gatherer group does not change results noteworthily (Supplementary Table S7).

Genetic affinities of ancient Finns to other ancient and contemporary populations. To further explore the affinity of ancient Finns to other ancient and contemporary populations, we carried out principal component analysis (PCA) based on haplogroup frequencies. We plotted the first two components of the PCA plot for ancient Finns, 31 other ancient populations, contemporary Finns and Saami, which account for 55% of the total variance (Figs 4, S4). Interestingly, southwestern Iron-Age sites Levänluhta and Hollola fall close to hunter-gatherer populations from Baltic, Central and Southern Europe. In addition Levänluhta is located in proximity to modern day Saami. This suggests the hunter-gatherer type of maternal ancestry in these two sites. In contrast, eastern IAM sites Hiitola and Tuukkala, EMM sites and contemporary SW Finns clustered with European Neolithic, Bronze-Age and Iron-Age populations. The southwestern site Luistari, as well as the contemporary NE Finns, were located roughly between these two clusters, indicating a possible mix of maternal ancestry
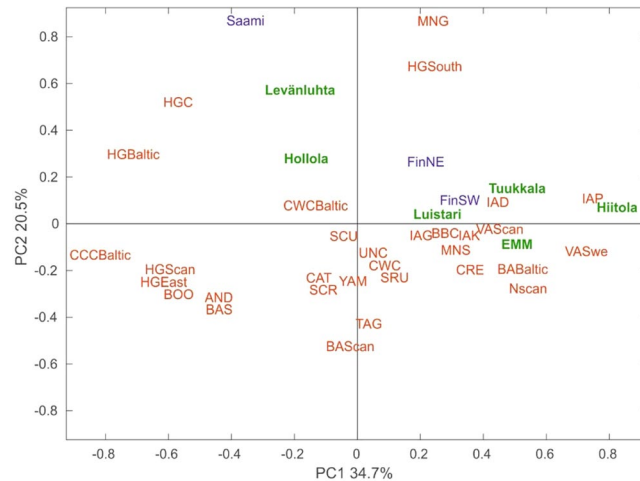
Figure 4. PCA biplot based on mitochondrial haplogroup frequencies. Ancient populations presented in this study (marked with green): Levänluhta, Luistari, Hollola, Hiitola, Tuukkala and Early modern and modern Finns (EMM). Contemporary populations (marked with blue): north-east Finland (FinNE), south-west Finland (FinSW), Saami (SAA). Ancient populations (marked with red): Andronovo culture (AND), Baltic Bronze-Age (BAB), Siberian Bronze-Age (BASi), Scandinavian Bronze-Age (BASc), Bell Beaker culture (BBC), Siberian Early Metal Period (BOO), Catacomb culture (CAT), Comb ceramic culture Baltic (CCCB), Crete Minoans (CRE), Corded Ware culture (CWC), Baltic Corded Ware Culture (CWCB), Baltic hunter-gatherers (HGB), central European hunter-gatherers (HGC), eastern hunter-gatherers (HGE), Scandinavian hunter-gatherers (HGSc), south European hunter-gatherers (HGSo), Denmark Iron-Age (IAD), Germany Iron-Age (IAG), Kazakhstan Iron-Age (IAK), Poland Iron-Age (IAP), Germany Middle-Neolithic (MNG), southern Europe Middle-Neolithic (MNS), Scandinavian Neolithic (NSc), Scythians from Russia (SCR), Scythians from Moldova and Ukraine (SCU), Srubnaya culture (SRU), Tagar culture (TAG), Unetice culture (UNC), Scandinavian Viking-Age (VASc), Sweden Viking-Age (VASw),Yamnaya culture (YAM). The contribution of main mitochondrial haplogroups are represented by loading vectors in Supplementary Fig. S4.

from hunter-gatherers and Neolithic farmers. However, as with the genetic distances presented in Section 2.6., the small sample sizes of ancient populations might distort the haplogroup frequencies to deviate from the original source population, subsequently affecting PCA. To evaluate the possible bias, we performed random subsampling of contemporary SW and NE Finns (fifty iterations, for each N = 15) and carried out PCA with the same reference populations as for Fig. 4. Supplementary Fig. S5 demonstrates the amount of variation induced.

Discussion

Here we report 103 human mitochondrial DNA genomes from approx. 300 AD to 1800 AD, a transect both in time and space, which represents thus far the largest collection of individuals with ancient human DNA analyzed from Finland. Analysis of the prehistoric samples from Iron-Age and medieval sites from western and eastern Finland revealed a high overall prevalence of haplogroup U in southwestern sites, in stark contrast with a high frequency of haplogroup H in the east, which is opposite to what is observed in modern day Finland. Moreover, there is relatively high differentiation between the ancient sites.

Genetic layers of mitochondrial variation among the Iron Age and Medieval Finns. Unexpectedly high variation in maternal lineages could be observed between the southwestern Levänluhta, Luistari and Hollola Iron-Age sites. Especially the distribution of U subhaplogroups differed clearly between sites: The oldest site, Levänluhta, represented a high frequency of U5a and the modern Saami-related haplogroup U5b1b1a, which is present in contemporary Finns only in moderate frequency of around 3.0%[35]. Indeed, recent studies considering Levänluhta, in which nuclear genomes have been retrieved, confirm the genetic continuation with the modern Saami population[18,19]. The strong drift experienced by the Saami groups of present day, shown by their high levels of LD throughout genome and low diversity in uniparental markers (See[38] and references therein) could explain why some mtDNA lineages, such as U5a, would have vanished from present day Saami.

Both Luistari and Hollola lacked the U5b1b1a, but instead Hollola displayed a wider variety of other U5 subhaplogroups, such as U5a1, U5a2 and U5b2. In addition, Luistari and Hollola sites showed relatively high frequencies of different subhaplogroups of U4 (i.e., U4a, U4b and U4d), which are rare in contemporary Finns and absent from modern Saami. Instead, in contemporary populations, U4 exists in high frequencies in Volga-Ural region (up to 24% in Komi-Zyrians)[36] and with lower frequencies around the Baltic Sea, such as in Latvians and Tver Karelians (both around 8%)[37]. Taking into account that U4 have been prevalent in neighboring areas among Scandinavian[10,39–43] and Baltic hunter-gatherers[12,13,44], Baltic Comb Ceramics Culture[12–14] and in Siberia during the Early metal period[11], we might be observing ancestries belonging to an earlier layer of ancient inhabitants of the region.

Taking these different distributions of mtDNA haplogroups from the Iron-Age and medieval sites into consideration, our results suggest three different streams of mitochondrial ancestry: Saami-like haplogroups (U5b1b1a, possible also U5a), non-Saami-like hunter-gatherer related haplogroups (especially U4) and haplogroups associated with Neolithic farmers (H, J, K and T). In this context we use 'Saami-like' as a term that shows genetic continuity with modern-day Saami groups. Different proportions of these ancestries could be observed both in later EMM sites and also modern-day southwestern and northeastern Finns. This suggests a fluctuation of each of these mitochondrial ancestry proportions over space and time.

The ancient distribution of mtDNA lineages contradicts the contemporary east-west divergence.
The Finnish population has been a subject of multitude medical genetic studies for many decades. Assessments of genetic diversity have revealed a number of idiosyncrasies in the modern Finnish gene pool. These include, for instance, the enrichment of c. 40 rare genetic diseases and the absence of some major ones in the rest of European metapopulation, as a clear distinction from the largely clinal differences observed in most of Europe[45]. Furthermore, these studies have demonstrated the existence of notable genetic differentiation between southwestern and northeastern parts of Finland[24,26,27]. This differentiation is especially pronounced in Y-chromosomes, showing opposite frequency trends of haplogroups N1c (25% SW, 75%NE) and I (56% SW, 24% NE)[26].

The modern mitochondrial DNA diversity in Finland resembles that observed in the Central Europe, but holds a relatively high overall frequency of haplogroup U, and also a notable proportion of subhaplogroups which have frequency peaks in or are exclusive to Finland[35]. The genetic substructure within Finland is minimal when at the level of mtDNA haplotypes are considered, but pronounced in the frequencies of haplogroups assumed Paleolithic (here U and V) or Neolithic (H, J, K, T) in Europe: the palaeolithic haplogroups are more common in the north-east ("Contemporary NE" subpopulation), and Neolithic haplogroups in the south-west ("Contemporary SW"). This, together with the Y-chromosomal subdivision, has been interpreted to reflect an ancient border between populations relying on farming (south-west Finland) and foraging (north-east). The observed genetic border running diagonally from north-west to south-east coincides with differences in a number of linguistic and cultural differences all the way to folk traditions. It also coincides with the first medieval political border, the Treaty of Nöteborg, between the Swedish and Novgorodian spheres of influence agreed in 1323 AD (see[28]).

The ancient mitochondrial genomes analyzed here show a notable pattern opposite to the modern variation: mtDNA types usually associated with the hunter-gatherer communities were significantly more common in the ancient western cluster (Levänluhta, Luistari and Hollola) than in the east (Hiitola, Tuukkala), with the haplogroup U frequency as high as 58.3%. In contrast, the farming-related lineages were observed in particular in the ancient eastern cluster. This pattern of division between the ancient sites, and the contradictions with their respective local modern population frequencies emerged also in formal testing of pairwise Φ_{ST} values: the western cluster was closer to the modern NE subpopulation than to the modern SW subpopulation whereas the eastern cluster showed closer affinity with the modern mtDNA variation in southwestern Finland.

Bidirectional expansion of agriculturally oriented populations into Finland?.
Assuming that the haplogroup composition has correlated with the mode of subsistence, the observed pattern of east to west transect suggests a bidirectional spreading of agricultural human groups into Finland. Although there is evidence of sporadic small-scale cultivation in southeastern Finland already during the Neolithic Stone Age (c. 5300–4000 BC)[46,47], the start of agriculture in Finland has been traditionally associated with the Corded-Ware Culture (CWC) arriving across the Baltic Sea approximately 4700 years ago. Indeed, there are scattered findings of animal husbandry from southwestern parts of country starting from c. 2500 calBC[48], but in general archaeological evidence supporting transition to agriculture as a consequence of introduction of Corded-Ware culture, are sparse (for discussion see[49]). Some independent observations of animal domestication[50] and cultivation (see[22] and references there in) are identifiable during the Bronze Age, but documentation remains still very limited. This suggests that cultivation has probably been relatively uncommon and local for centuries, as little direct evidence for cereal cultivation in Finland prior Iron Age exists[22,49]. Pollen records show notable increase of cereals starting only at 100 AD and reaching maximum as late as 1300 AD[22] overlapping the time span of Iron Age and Medieval sites presented in this study.

As a support for the late introduction of farming populations in to Finland we do not see strong affinities of western IAM to for example the CWC maternal gene pools from Estonia and Lithuania[6,12–14], suggesting either that the mtDNA gene flow between these two regions has been low or that shared mtDNA variation had dissolved before the Iron-Age in Finland. Alternatively, the CWC expansion may have been largely male-driven as suggested by[51]. However, we observe a strong Neolithic signal in the Iron-Age mtDNA pool in Eastern Finland, thus rather suggesting a southeastern/eastern arrival route of an agro-pastoralist population into the country. Interestingly, their maternal genetic legacy also corresponded to the contemporary modern Finland, especially in SW. We therefore propose that either there has been east-to-west directed gene flow during the Middle Ages, after the introduction of agricultural haplogroups into the east, or that the late change in SW maternal gene pool may reflect recent immigration from more western/southern sources, such as the migration from Sweden during the Swedish reign in Finland (from 1200s–1809). Iron-Age has evidenced high mobility around the Baltic Sea, as evidenced by the genetic and isotope analyses of human remains from 10th to 12th century in Sigtuna, eastern Sweden[52].

The multinomial logistic regression analysis lent support to the eastern introduction of agriculturally related maternal ancestry. The likely migration routes for the observed ancestral elements were investigated through different combinations of factor dependencies as the multinomial logistic regression. The test revealed the distance from Lahdenpohja on the eastern border of Finland as the only statistically significant variable explaining the differences in the haplogroup composition. Neither time scale, nor distance from the southwestern locations

(i.e. Hanko and Uusikaupunki) were supported by the best-fit model. It thus seems likely that the major spread of haplogroup H can be explained by presuming its introduction via the eastern landroute. In accordance with the inference here, population genetic studies of many organisms in Finland as well as in all Fennoscandia have suggested bidirectional colonization of the current habitats. The reasons behind this are largely geographical: the Baltic Sea acts, for most species, as a migration barrier.

The Neolithic farmer-related signal in the mtDNA diversity in the Iron-Age samples is mainly found in the southeast, whereas in contemporary population it predominates in the southwest. The reasons for this discrepancy are likely diverse, and could be affected by such recent events as the evacuation of nearly 0.5 M inhabitants of Karelia during the World War II and their resettling into the area of current Finland. However, these evacuees were resettled rather evenly across southern Finland and should not create the observed pattern. It rather suggests that the division between SW and NE Finland had still been more substantial in the early 1900s. Another, more fundamental explanation for the genetic subdivision comes from the environmental demands of sedentary farming. In southwestern Finland the soil is more amenable to field-farming and due to the warming Atlantic effect that gradually shades into more arid continental climate, the growing season in Finland is the longest in the southwestern coast. These environmental differences follow the NW-SW border similarly to the genetic distances. As the country has been sparsely inhabited until modern times, it is plausible that farming oriented populations, in search of more favorable conditions, have over the centuries concentrated into the SW parts of the country.

The mitochondrial DNA genomes from Iron-Age Finland show variation that can be linked to either hunter-gatherer or agricultural human groups. These elements are still present in the mitochondrial gene pool of contemporary Finns but relatively evenly distributed throughout the country. In contrast, the Iron-Age mtDNA variation show significant differences between sampling sites, with hunter-gatherer and farmer-associated elements dominating in different regions than today. Rather surprisingly, the agricultural population signal has been stronger in eastern Finland in the past, which might reflect a bidirectional arrival of farming-associated populations into Finland.

Materials and Methods

Sample selection.
The human skeletal remains used in this study were collected from five archaeological sites and five historical cemeteries (for more detailed information of the sites and references for original publications in Supplementary Material S1). Archaeological sites include Levänluhta, used as a burial place from Roman Iron Age until the end of Merovingian Period (archaeological dating 300–800 AD), Luistari, consisting of graves from Merovingian to Crusade Period (archaeological dating 600–1200 AD) and Hollola, Hiitola and Tuukkala, largely Christian-style cemeteries spanning from Crusade Period to Early Middle Ages (archaeological datings 1050–1400 AD, 1200–1500 AD and 1200–1400 AD, respectively) (Fig. 1, Table 1 and Supplementary Material S1). The five historical sites include the cemetery of the Church of St. Michael in Pälkäne, the cemetery of the Church of St. Jacob in Renko, the Cathedral site in Porvoo, the Julin's site in Turku, and the Ryazan regimental church cemetery in Hamina. Samples were obtained from the archaeological collections of the Finnish Heritage Agency, Department of Archaeology in the University of Turku, Department of Anatomy in the University of Helsinki, and the Peter the Great Museum of Anthropology and Ethnography (Kunstkamera), Russian Academy of Sciences.

Contextual archaeological evidence, such as grave goods and burial customs, together with radiocarbon analyses were used to confirm the dating of each site and/or individual. Details of dating, sample sizes and number of genomes obtained are presented in Table 1. Detailed information on individual burial sites and samples are given in Supplementary Material S1 and Supplementary Table S1.

Reference populations used in comparative analyses.
To evaluate possible changes in the Finnish mitochondrial gene pool during the past thousand years, samples were compared to HVR1 + HVR2 (16024–16385, 72–340) data from 832 modern Finns[27] for which the county-level geographical origin is known. In order to compare the mitochondrial profile of ancient Finns to other ancient nearby populations, haplogroup frequencies were collected from 31 ancient populations (Supplementary Table S8).

Sampling.
All samples were processed in dedicated aDNA facilities with regularly UV:d and bleach-treated laminar hoods, inside a clean room space. For Levänluhta, Porvoo, Renko, Pälkäne and Hamina sites, sampling was conducted at the University of Tübingen, Germany from the start. For the Luistari, Hiitola, Hollola and Tuukkala sites, the bone powder was produced in a clean-room space for small-scale ancient DNA work at the Helsinki University Department of Forensic Medicine, and then transferred to Tübingen University facilities, stored in plastic tubes. All subsequent laboratory work with the bone powder was conducted at the facilities in Tübingen. A protective overall, facemask, hair net and two layers of disposable gloves were used at all times when handling the samples. Decontamination was carried out by ultraviolet light exposure of the plastic ware, reagents and samples, and by removal of the immediate surface at the point of sampling before drilling into the bone. Teeth were sawed in two, with the exception of the Levänluhta samples, where dentine was already exposed due to heavy fragmentation. Dental pulp and the surrounding dentine were used for DNA sampling, drilling into the crown or the root. For the petrous part of the temporal bone, a wedge was cut off to reveal the inner ear channels and sample was taken from the inside of the channel, as previously described[53]. A dentist's drill together with cooled-down drill heads for minimal heat exposure were used at the University of Tübingen facility and a "field kit" with Dremel or dentist's drill were used at the Helsinki University Department of Forensic Medicine.

Extraction of ancient DNA.
The extraction was performed according to a modified version of the original protocol[29]. For each sample, ~50 mg of bone powder was used for the extraction by eluting it in 100 μl of TET

(10 mM Tris-HCL, 1 mM EDTA pH 8.0, 0.1% Tween20). The extracts were used to prepare DNA libraries of 20 µl, without additional treatments. To enable multiplex sequencing, the double-stranded library preparation and the subsequent indexing procedure were performed according to standard recommended protocols for ancient DNA[54,55]. The original molecular copy number in the DNA library, as well as the subsequent indexing efficiency, were measured by qPCR, using AccuPrime Pfx polymerase. The molecular copy numbers in pre-indexed libraries varied, ranging from ~1–100 × 108 copies/µl, and the indexed libraries from ~1–100 × 1011 copies/µl, indicating a successful library composition and admissible indexing efficiency. The indexed libraries were amplified using PCR, with heating cycles chosen individually per library according to the copy number after indexing. Amplified libraries were purified using MinElute spin columns with the standard protocol provided by the manufacturer (Qiagen). A qPCR together with Agilent Bioanalyzer 2100 device, and a DNA1000LabChip were subsequently used on the amplified libraries to measure the concentration of DNA, as well as fragment size distribution. A positive control extracted from a cave bear bone, to confirm the success of extraction and library preparation, as well as two negative laboratory controls to measure the levels of contamination were carried along for every batch of 10–16 samples.

Mitochondrial capture and sequencing. Mitochondrial genomes were achieved using a mitochondrial in-solution capture as described in Maricic *et al.*[56]. Complete human mitochondrial DNA sequence was used to produce in-house made baits, which were ligated to adapters. The bait DNA was then purified and denatured to the single stranded form, and attached to streptavidin-coated magnetic beads. Pools of 4–6 samples, combined in equal mass ratios for altogether 2 µg of DNA, were captured with the above mentioned beads, and sequenced on the Illumina platforms: for samples from sites Turku, Hiitola, Tuukkala and Hollola, along with four samples from the Luistari site (TU619, TU621, TU622, TU623), single-end sequencing data was produced on HiSeq4000 run for 75 + 8 + 8 cycles, whereas samples from all the other sites, including the rest of the samples from Luistari, paired-end data was produced with NextSeq500 for 2 × 150 + 8 + 8 cycles, at the Max Planck Institute for the Science of Human History, Jena.

Processing of the sequence data. Raw-read sequencing data were processed using the EAGER-pipeline for aDNA sequencing data[57]. Reads were demultiplexed using both indices, and the adapters were clipped off with the AdapterRemoval program integrated in EAGER, with minimum overlap set to 1 bp. Short reads reaching a minimum of 10 bp overlap were merged, validated by the paired-end fragment compatibility. For the single-end-sequenced samples this step was omitted. Minimum read length of 30 bp and base quality of 20 was required for all final reads. The reads were aligned to the complete human reference genome Hg19 with the BWA mapping algorithm for the shotgun sequence data, whereas CircularMapper, a custom-made tool for circular genomes included in EAGER, was used to map the enriched mitochondrial reads to the human mitochondrial reference genome (revised Cambridge reference sequence, rCRS[58]).

Authentication of ancient DNA and haplogroup assignments. In order to evaluate the authenticity of the reconstructed mitochondrial genome sequences, contamination rates, read-length distributions and deamination patterns at the 5′ and 3′ ends of DNA fragments were inspected for each sample with the program MapDamage[59] integrated in EAGER. Further contamination estimation was carried out with Schmutzi[32] and ContamMix[33] programs.

The mitochondrial consensus-calling in Schmutzi was used to produce the consensus sequences of both the endogenous source and the most likely single contaminating source. Complete consensus sequences were called against the rCRS with a filter value of q20. For the Schmutzi-based consensus sequences a manual correction was performed for position 3107 to correspond to the "N" embedded in rCRS. The mtDNA haplogroups were determined using HaploGrep2[60] with respect to PhyloTree version 17[61].

For contamination estimation in ContamMix, consensus sequences created by Schmutzi were combined with a reference dataset of 311 mitochondrial genomes from worldwide populations (provided by ContamMix) and aligned with mafft version 7.305[62,63]. The untrimmed mitochondrial reads from the Eager pipeline were then extracted from BAM files into fastQ files and mapped back to the assembly. ContamMix then evaluates whether the reads assign more probably to their respective consensus or one of the worldwide mitochondrial genomes, i.e possible contaminant source. The ContamMix was run with trimming of seven bases of each side of the read to remove the accumulated damage typical for ancient DNA.

The mitochondrial genome sequences with highest ContamMix estimates were further visually inspected in Geneious 11.0.3 (www.geneious.com). In this inspection, the majority call support for relevant diagnostic mutations against the rCRS reference genome was compared to the PhyloTree version 17. We applied the automated variant caller in Geneious to the alignments with minimum support of 3x coverage and variant frequency of 66.6% for diagnostic SNPs to confirm the authenticity of the haplogroup assignments.

Radiocarbon dating. Radiocarbon dates were produced by the Laboratory of Chronology, Finnish Museum of Natural History Luomus in Helsinki, Finland (Hela) and Klaus-Tschira C14-laboratory in Mannheim, Germany (MAMS). Bone collagen was extracted with the modified Longin method[64,65], the collagen samples combusted, graphitized and measured by using Accelerator Mass Spectrometry (AMS). The results are provided as conventional radiocarbon dates without potential reservoir effect corrections. The radiocarbon dates were calibrated using the OxCal program version 4.3[66], IntCal 13 as the calibration curve[67]. For sites with four or more individuals with ^{14}C dates also the boundaries for phase's start and end were determined with OxCal 4.3. Example of the OxCal code is given in Supplementary Material S2. Timescale discussed throughout the text is defined as calendar years.

Analysis	Data type	Populations used	Results presented in
Basic diversity indices	Complete sequences	Ancient Finns	Supplementary Table S4
Φ_{ST}	HVR1 + HVR2	Ancient and contemporary Finns	Fig. 3 and Supplementary Table S6
Multinomial logistic regression	Presence/absence of haplogroup	Ancient Finns	Supplementary Table S7
Principal component analysis (PCA)	Haplogroup frequencies	Ancient Finns, other ancient and contemporary populations (Supplementary Table S8)	Figs 4 and S4
Evaluation of the possible sampling bias in the observed haplogroup frequencies	Haplogroup frequencies	Ancient and contemporary Finns	Supplementary Fig. S2
Network analysis	HVR1 + HVR2 sequence data	Ancient and contemporary Finns	Supplementary Fig. S3
Evaluation the impact of small sample size on PCA	Haplogroup frequencies	Contemporary Finns, ancient Finns and other ancient populations (reference populations presented in Supplementary Table S8)	Supplementary Fig. S5

Table 2. Overview of statistical analyses and datasets used in this study.

Statistical analyses. A summary of statistical analyses performed in this study for different sets of populations and dataset (i.e., complete sequence, HVR1 + HVR2, haplogroup frequencies) is presented in Table 2.

For the statistical analysis, sequences were aligned with Muscle v3.8.31[68]. To explore the genetic diversity within ancient populations, basic diversity indices such as haplotype diversity, mean pairwise distance and nucleotide diversity were calculated for the complete mitochondrial genomes with Arlequin 3.5.2.2[69]. To determine genetic distances between ancient and modern Finns, pairwise Φ_{ST} values based on the sequence data were calculated with Arlequin 3.5.2.2. Genetic distances, were calculated by utilizing HVR1 + HVR2, as the contemporary reference data with detailed geographical origin were restricted to HVR regions only[27,28]. To estimate the significance for the Φ_{ST} values, permutation tests with 10000 permutations were used. The visualization of the Φ_{ST} values was done by R heatmap.2 function with hierarchical clustering based on the Euclidean distance. The best-fit models for different datasets were estimated with jModelTest[70]. The substitution model used was Tamura & Nei[71] with gamma correction (shape parameter $\alpha = 0.67$) and Tamura & Nei with gamma correction ($\alpha = 0.44$) for the complete sequence data and HVR1 + HVR2 data, respectively. Poly-C region (positions 309–315), AC indels (positions 515–522) and mutational hotspot at position 16519 were masked for the population level analysis. Further to evaluate the relation of ancient individuals to contemporary Finns on a haplotype level, median-joining network analysis[72] was performed with PopArt[73]. Positions bearing more than 5% of missing data were masked for the network analysis.

To statistically test the impact of possible factors affecting the spatial and temporal distribution of haplogroups U and H in our ancient samples, we conducted a multinomial logistic regression analysis. Each individual was considered as separate occurrence and haplogroups 'U', 'H' and 'Others' were set as categorical dependent variables. Because the main interest was to estimate the impact of time and geography on the occurrence of the haplogroups, the following independent variables were chosen: (1) Median age of sample (or the mean age of the site if radiocarbon dates were not available) (2) site's distance (in km) from southern reference point Hanko, (3) site's distance (in km) from western reference point Uusikaupunki and (4) site's distance (in km) from eastern reference point Lahdenpohja (see Fig. 1). These geographical points were chosen to represent the most plausible entry points of different migration routes to the study area, south (Hanko on the southern coast), west (Uusikaupunki on the western coast) and east/south-east (Lahdenpohja). The last mentioned represents the eastern migration route both along the Karelian Isthmus and north of Lake Ladoga, strongly supported by archaeological evidence[21]. For multinomial logistic regression a stepwise forward method was used with entry probability 0.05, and probability was tested with likelihood ratios. To evaluate the impact of grouping the haplogroups into hunter-gatherer and farmer related hgs' also categories 'U + V', 'H + J + K + T' and 'Others' were tested. In addition, categories 'U', 'H + J + K + T' and 'Others' were tested, due to controversial definition of haplogroup V (See Section 2.7). Analyses were performed with IBM SPSS version 25 (IBM Corp. Released 2017, IBM SPSS Statistics for Windows, Version 25.0 Armonk, NY: IBM Corp.).

To trace genetic affinities between ancient Finns and other ancient populations, we visualized haplogroup composition of each site (based on haplogroup frequencies) using principal component analysis (PCA). PCA was computed using MATLAB and Statistical Toolbox Release 2015b (The MathWorks, Inc., Natick, Massachusetts, United States). Populations and haplogroup frequencies used are presented in Supplementary Table S8.

Data Availability

Complete mitochondrial sequences will be deposited in GenBank under accession numbers MN540463-MN540565.

References

1. Posth, C. *et al.* Pleistocene mitochondrial genomes suggest a single major dispersal of non-Africans and a Late Glacial population turnover in Europe. *Current Biology* **26**, 827–833 (2016).
2. Fu, Q. *et al.* An early modern human from Romania with a recent Neanderthal ancestor. *Nature* **524**, 216 (2015).
3. Bramanti, B. *et al.* Genetic discontinuity between local hunter-gatherers and central Europe's first farmers. *Science* **326**, 137–140 (2009).

4. Haak, W. *et al*. Ancient DNA from the first European farmers in 7500-year-old Neolithic sites. *Science* **310**, 1016–1018 (2005).
5. Haak, W. *et al*. Ancient DNA from European early neolithic farmers reveals their near eastern affinities. *PLoS Biology* **8**, e1000536 (2010).
6. Allentoft, M. E. *et al*. Population genomics of Bronze Age Eurasia. *Nature* **522**, 167–172 (2015).
7. Haak, W. *et al*. Massive migration from the steppe was a source for Indo-European languages in Europe. *Nature* **522**, 207–211 (2015).
8. Stolarek, I. *et al*. A mosaic genetic structure of the human population living in the South Baltic region during the Iron Age. *Scientific Reports* **8**, 2455 (2018).
9. Kashuba, N. *et al*. Ancient DNA from mastics solidifies connection between material culture and genetics of mesolithic hunter–gatherers in Scandinavia. *Communications Biology* **2**, 185 (2019).
10. Günther, T. *et al*. Population genomics of Mesolithic Scandinavia: Investigating early postglacial migration routes and high-latitude adaptation. *PLoS Biology* **16**, e2003703 (2018).
11. Der Sarkissian, C. *et al*. Ancient DNA reveals prehistoric gene-flow from Siberia in the complex human population history of North East Europe. *PLoS Genetics* **9**, e1003296 (2013).
12. Jones, E. R. *et al*. The Neolithic transition in the Baltic was not driven by admixture with early European farmers. *Current Biology* **27**, 576–582 (2017).
13. Saag, L. *et al*. Extensive farming in Estonia started through a sex-biased migration from the Steppe. *Current Biology* **27**, 2185–2193. e6 (2017).
14. Mittnik, A. *et al*. The genetic prehistory of the Baltic Sea region. *Nature communications* **9**, 442 (2018).
15. Ahola, M., Salo, K. & Mannermaa, K. Almost Gone: Human Skeletal Material from Finnish Stone Age Earth Graves. *Fennoscandia Archaeologica* **33**, 95–122 (2016).
16. Carpelan, C. Käännekohtia Suomen esihistoriassa aikavälillä 5100–1000 eKr. *Pohjan poluilla.Suomalaisten juuret nykytutkimuksen mukaan.Bidrag till kännedom av Finlands natur och folk* **153**, 249–280 (1999).
17. Tallavaara, M., Pesonen, P. & Oinonen, M. Prehistoric population history in eastern Fennoscandia. *Journal of Archaeological Science* **37**, 251–260 (2010).
18. Lamnidis, T. C. *et al*. Ancient Fennoscandian genomes reveal origin and spread of Siberian ancestry in Europe. *Nature Communications* **9**, 5018 (2018).
19. Sikora, M. *et al*. The population history of northeastern Siberia since the Pleistocene. *Nature* **570**, 182–188 (2018).
20. Pesonen, P., Oinonen, M., Carpelan, C. & Onkamo, P. Early Subneolithic ceramic sequences in eastern Fennoscandia—a Bayesian approach. *Radiocarbon* **54**, 661–676 (2012).
21. Haggren, G., Halinen, P., Lavento, M., Raninen, S. & Wessman, A. In Muinaisuutemme jäljet: Suomen esi-ja varhaishistoria kivikaudelta keskiajalle (Gaudeamus, 2015).
22. Lahtinen, M., Oinonen, M., Tallavaara, M., Walker, J. W. & Rowley-Conwy, P. The advance of cultivation at its northern European limit: Process or event? *The Holocene* **27**, 427–438 (2017).
23. Lao, O. *et al*. Correlation between genetic and geographic structure in Europe. *Current Biology* **18**, 1241–1248 (2008).
24. Salmela, E. *et al*. Genome-wide analysis of single nucleotide polymorphisms uncovers population structure in Northern Europe. *PloS One* **3**, e3519 (2008).
25. Sajantila, A. *et al*. Paternal and maternal DNA lineages reveal a bottleneck in the founding of the Finnish population. *Proc. Natl. Acad. Sci. USA* **93**, 12035–12039 (1996).
26. Lappalainen, T. *et al*. Regional differences among the finns: A Y-chromosomal perspective. *Gene* **376**, 207–215 (2006).
27. Palo, J. U., Ulmanen, I., Lukka, M., Ellonen, P. & Sajantila, A. Genetic markers and population history: Finland revisited. *Eur. J. Hum. Genet.* **17**, 1336–1346 (2009).
28. Neuvonen, A. M. *et al*. Vestiges of an Ancient Border in the Contemporary Genetic Diversity of North-Eastern Europe. *PLoS One* **10**, 1–19 (2015).
29. Dabney, J. *et al*. Complete mitochondrial genome sequence of a Middle Pleistocene cave bear reconstructed from ultrashort DNA fragments. *Proc. Natl. Acad. Sci. USA* **110**, 15758–15763 (2013).
30. Sawyer, S., Krause, J., Guschanski, K., Savolainen, V. & Pääbo, S. Temporal patterns of nucleotide misincorporations and DNA fragmentation in ancient DNA. *PloS One* **7**, e34131 (2012).
31. Kistler, L., Ware, R., Smith, O., Collins, M. & Allaby, R. G. A new model for ancient DNA decay based on paleogenomic meta-analysis. *Nucleic Acids Res.* **45**, 6310–6320 (2017).
32. Renaud, G., Slon, V., Duggan, A. T. & Kelso, J. Schmutzi: estimation of contamination and endogenous mitochondrial consensus calling for ancient DNA. *Genome Biol.* **16**, 224 (2015).
33. Fu, Q. *et al*. A revised timescale for human evolution based on ancient mitochondrial genomes. *Current Biology* **23**(7), 553–559 (2013).
34. Tambets, K. *et al*. The western and eastern roots of the Saami—the story of genetic "outliers" told by mitochondrial DNA and Y chromosomes. *The American Journal of Human Genetics* **74**, 661–682 (2004).
35. Översti, S. *et al*. Identification and analysis of mtDNA genomes attributed to Finns reveal long-stagnant demographic trends obscured in the total diversity. *Scientific Reports* **7**, 6193 (2017).
36. Bermisheva, M., Tambets, K., Villems, R. & Khusnutdinova, E. Diversity of mitochondrial DNA haplotypes in ethnic populations of the Volga-Ural region of Russia. *Molecular Biology (Mosk)* **36**, 990–1001 (2002).
37. Lappalainen, T. *et al*. Migration waves to the Baltic Sea region. *Ann. Hum. Genet.* **72**, 337–348 (2008).
38. Ingman, M. & Gyllensten, U. A recent genetic link between Sami and the Volga-Ural region of Russia. *European Journal of Human Genetics* **15**, 115–120 (2007).
39. Malmström, H. *et al*. Ancient DNA reveals lack of continuity between neolithic hunter-gatherers and contemporary Scandinavians. *Current Biology* **19**, 1758–1762 (2009).
40. Skoglund, P. *et al*. Origins and genetic legacy of Neolithic farmers and hunter-gatherers in Europe. *Science* **336**, 466–469 (2012).
41. Lazaridis, I. *et al*. Ancient human genomes suggest three ancestral populations for present-day Europeans. *Nature* **513**, 409–413 (2014).
42. Malmstrom, H. *et al*. Ancient mitochondrial DNA from the northern fringe of the Neolithic farming expansion in Europe sheds light on the dispersion process. *Philos. Trans. R. Soc. Lond. B. Biol. Sci.* **370**, 20130373 (2015).
43. Skoglund, P. *et al*. Genomic diversity and admixture differs for Stone-Age Scandinavian foragers and farmers. *Science* **344**, 747–750 (2014).
44. Mathieson, I. *et al*. The genomic history of southeastern Europe. *Nature* **555**, 197 (2018).
45. Norio, R. Finnish disease heritage I. *Hum. Genet.* **112**, 441–456 (2003).
46. Alenius, T., Mökkönen, T. & Lahelma, A. Early Farming in the Northern Boreal Zone: Reassessing the History of Land Use in Southeastern Finland through High-Resolution Pollen Analysis. *Geoarchaeology* **28**, 1–24 (2013).
47. Herva, V., Mökkönen, T. & Nordqvist, K. A northern Neolithic? Clay work, cultivation and cultural transformations in the boreal zone of north-eastern Europe, c. 5300–3000 bc. *Oxford Journal of Archaeology* **36**, 25–41 (2017).
48. Cramp, L. J. *et al*. Neolithic dairy farming at the extreme of agriculture in northern Europe. *Proceedings of the Royal Society B: Biological Sciences* **281**, 20140819 (2014).
49. Lahtinen, M. & Rowley-Conwy, P. Early farming in Finland: was there cultivation before the Iron Age (500 BC)? *European Journal of Archaeology* **16**, 660–684 (2013).

50. Bläuer, A. & Kantanen, J. Transition from hunting to animal husbandry in Southern, Western and Eastern Finland: new dated osteological evidence. *Journal of Archaeological Science* **40**, 1646–1666 (2013).
51. Goldberg, A., Günther, T., Rosenberg, N. A. & Jakobsson, M. Ancient X chromosomes reveal contrasting sex bias in Neolithic and Bronze Age Eurasian migrations. *Proceedings of the National Academy of Sciences*, 201616392 (2017).
52. Krzewińska, M. *et al.* Genomic and Strontium Isotope Variation Reveal Immigration Patterns in a Viking Age Town. *Current Biology* **28**, 2730–2738. e10 (2018).
53. Pinhasi, R. *et al.* Optimal ancient DNA yields from the inner ear part of the human petrous bone. *PloS One* **10**, e0129102 (2015).
54. Meyer, M. & Kircher, M. Illumina sequencing library preparation for highly multiplexed target capture and sequencing. *Cold Spring Harb Protoc.* **2010**, pdb.prot5448 (2010).
55. Kircher, M. In Ancient DNA 197–228 (Springer, 2012).
56. Maricic, T., Whitten, M. & Pääbo, S. Multiplexed DNA sequence capture of mitochondrial genomes using PCR products. *PloS One* **5**, e14004 (2010).
57. Peltzer, A. *et al.* EAGER: efficient ancient genome reconstruction. *Genome Biology* **17**, 60 (2016).
58. Andrews, R. M. *et al.* Reanalysis and revision of the Cambridge reference sequence for human mitochondrial DNA. *Nature Genetics* **23**, 147–147 (1999).
59. Ginolhac, A., Rasmussen, M., Gilbert, M. T. P., Willerslev, E. & Orlando, L. mapDamage: testing for damage patterns in ancient DNA sequences. *Bioinformatics* **27**, 2153–2155 (2011).
60. Weissensteiner, H. *et al.* HaploGrep 2: mitochondrial haplogroup classification in the era of high-throughput sequencing. *Nucleic Acids Res.* (2016).
61. Van Oven, M. & Kayser, M. Updated comprehensive phylogenetic tree of global human mitochondrial DNA variation. *Human Mutation* **30**, E386–E394 (2009).
62. Katoh, K. & Standley, D. M. MAFFT multiple sequence alignment software version 7: improvements in performance and usability. *Molecular Biology and Evolution* **30**, 772–780 (2013).
63. Katoh, K. *et al.* MAFFT: a novel method for rapid multiple sequence alignment based on fast Fourier transform. *Nucleic Acids Research* **30**, 3059–3066 (2002).
64. Longin, R. New method of collagen extraction for radiocarbon dating. *Nature* **230**, 241 (1971).
65. Bocherens, H. *et al.* Paleobiological implications of the isotopic sig*Nature*s (13 C, 15 N) of fossil mammal collagen in Scladina Cave (Sclayn, Belgium). *Quatern. Res.* **48**, 370–380 (1997).
66. Ramsey, C. B. Bayesian analysis of radiocarbon dates. *Radiocarbon* **51**, 337–360 (2009).
67. Reimer, P. J. *et al.* Selection and treatment of data for radiocarbon calibration: an update to the International Calibration (IntCal) criteria. *Radiocarbon* **55**, 1923–1945 (2013).
68. Edgar, R. C. MUSCLE: multiple sequence alignment with high accuracy and high throughput. *Nucleic Acids Research* **32**, 1792–1797 (2004).
69. Excoffier, L. & Lischer, H. E. Arlequin suite ver 3.5: a new series of programs to perform population genetics analyses under Linux and Windows. *Molecular ecology resources* **10**, 564–567 (2010).
70. Darriba, D., Taboada, G. L., Doallo, R. & Posada, D. jModelTest 2: more models, new heuristics and parallel computing. *Nature methods* **9**, 772 (2012).
71. Tamura, K. & Nei, M. Estimation of the number of nucleotide substitutions in the control region of mitochondrial DNA in humans and chimpanzees. *Molecular Biology Evolution* **10**, 512–526 (1993).
72. Bandelt, H., Forster, P. & Röhl, A. Median-joining networks for inferring intraspecific phylogenies. *Molecular Biology Evolution* **16**(1), 37–48 (1999).
73. Leigh, J. W. & Bryant, D. PopART: Full-feature software for haplotype network construction. *Methods Ecological Evolution* **6**(9), 1110–1116 (2015).
74. Talve, I. *Finnish Folk Culture. Finnish Literature Society*; English edition. pp. 349 (2000)

Acknowledgements

Author Contributions

K.S., L.A., S.B., H.E.-S., V.L., E.M., J.-P.T., K.V., A.W. provided archaeological material and related information. K.M., K.S., S.Ö., M.P. performed the sampling. K.M., S.Ö., S.P. performed the laboratory work. K.M., S.Ö. processed the sequence reads and generated the mtDNA genotypes. S.Ö., J.U.P., E.S. performed the statistical analyses. M.O., L.A., H.E.-S. performed the radiocarbon dating analysis. S.Ö., M.O. post-processed the ^{14}C datings (i.e. phase start and end boundaries). S.Ö., J.U.P., K.M., P.O., E.S., K.S. wrote the manuscript with input from all co-authors. P.O., J.K., J.U.P., V.J.S., W.H., A.S. supervised the study.

Additional Information

Supplementary information accompanies this paper at https://doi.org/10.1038/s41598-019-51045-8.

Competing Interests: The authors declare no competing interests.

Publisher's note Springer Nature remains neutral with regard to jurisdictional claims in published maps and institutional affiliations.

Human mitochondrial DNA lineages in Iron-Age Fennoscandia suggest incipient admixture and eastern introduction of farming-related maternal ancestry

Supplementary Materials and Figures

Sanni Översti[1,†,*], Kerttu Majander[1,2,3,†], Elina Salmela[1,2], Kati Salo[4], Laura Arppe[5], Stanislav Belskiy[6], Heli Etu-Sihvola[5], Ville Laakso[7], Esa Mikkola[8], Saskia Pfrengle[3], Mikko Putkonen[9], Jussi-Pekka Taavitsainen[7], Katja Vuoristo[8], Anna Wessman[4,7], Antti Sajantila[9], Markku Oinonen[5], Wolfgang Haak[2], Verena J. Schuenemann[3,10], Johannes Krause[2,‡], Jukka U. Palo[9,11,‡], Päivi Onkamo[1,12,‡]

Material S1. Detailed information about archaeological sites and samples.

Material S2. Example of the OxCal code used to determine the start and end distribution.

Figure S1. Phase boundary outputs for each site containing four or more ^{14}C dates.

Figure S2. Evaluation of the possible sampling bias in the observed haplogroup frequencies.

Figure S3. Median-joining Network for ancient and contemporary Finns.

Figure S4. PCA with main loading vectors.

Figure S5. The impact of small sample size on PCA.

(**Supplementary Tables S1-S8** are presented in separate Excel file)

Material S1. Detailed information about archaeological sites and samples.

Two of the archaeological sites, Levänluhta and Luistari, represent the oldest burial sites with preserved unburnt human skeletal remains in Finland. Both sites have been the target of extensive archaeological studies. Levänluhta, a lake burial in Isokyrö, southern Ostrobothnia, has yielded 98 macroscopically well-preserved skeletons in several excavations conducted over the last 200 years. The grave goods from Levänluhta have stylistic features from around the Baltic Sea region but the burial cannot be linked to any known settlement or more distinct archaeological findings. A total of 13 tooth samples from Levänluhta individuals were included in this study (**Table 1**).

The Luistari site in Eura is a large burial ground consisting of 400 excavated graves from the Merovingian, Viking and Crusade Periods in Finland. A total of 25 individuals were included from Luistari, of which five were assigned to the Merovingian Period, 14 to the Viking Period, and the remaining six roughly to the Crusade Period, based on artefact datings. The data was further complemented by another Crusade Period burial ground of Kirkkailanmäki in Hollola, contributing 20 individuals. Two more eastern burial grounds, Kylälahti Kalmistonmäki in Hiitola (today Khiytola in Russian Karelia) and Tuukkala in Mikkeli, dating from the Crusade to medieval Periods, provided 18 and 30 individuals, respectively.

The remains from the Early-Modern period individuals originate from five Christian churchyards: four individuals from Pälkäne (cemetery of the Church of St. Michael), where the earliest burials date to the 13th century and the latest ones to the 19th century; eight individuals from Renko (Church of St. Jacob) and nine from Porvoo (Cathedral site) dated based on the archaeological context to14[th] - 18th century; five from Turku (Julin's site) dated to 16th - 17th century; nine from Hamina (Ryazan regimental church cemetery) dated to 18th century.

Levänluhta

Levänluhta cemetery in Isokyrö, historical province of Osthrobotnia is an exceptional middle Iron-Age (4th to 7th century AD) burial site, because here the burials have been done in water. The prevailing form of burial in Finland during this time, until the beginning of the Crusade Period (mid-11th century) was cremation. Levänluhta was probably a pond or a lake during its time of usage. It seems that these individuals were brought to a remote area, outside the local Iron-Age settlement, to be buried in a very different way than was the norm [1-3].

Luistari

Luistari site in Eura in south-west Finland includes a Bronze-Age settlement site, Iron-Age cremation burial cairns and a medieval inhumation cemetery. Inhumating began during the Merovingian Period (7th century AD) and continued at least until the 14th century AD [4, 5]. The site has been extensively studied, yielding c. 400 graves dating to Merovingian and Viking Periods and over 800 later, but very few of these have human skeletal remains [5-7].

Hollola, Kirkkailanmäki

Kirkkailanmäki cemetery in Hollola, historical province of Häme, is dated from 11th to 14th centuries [8-10]. The cemetery has furnished and unfurnished inhumations as well as cremations [8, 11]. The grave finds are from Crusade Period and early medieval times and they show influences from several different origins: Eastern influences in the site are shown by Karelian type of brooches [8, 9] and a Russian type of pendant [8, 9, 12]. Southern influences in the site are shown by an Estonian type of pendant [8, 13] and brooches originating from the southern side of the Baltic Sea [8, 10, 14]. A bird pendant found from one grave is of western Finnish type, but it originates from Livonia in the modern Latvia [8, 14].

Hiitola, Kylälahti Kalmistonmäki

Kylälahti Kalmistomäki cemetery in Hiitola in the north-western bank of Ladoga Lake shore is in modern day Russia and dates to Crusade Period and medieval times [15]. Field investigations were carried out in 2006–2009 on the Kalmistomäki Hill by an archaeological expedition of the Museum of Anthropology and Ethnography (Kunstkamera) Russian Academy of Sciences (Saint-Petersburg) in cooperation with the University of Turku (Finland). The total excavated area amounted to 426 m2. The number of undisturbed burials uncovered was 93, of which 91 are inhumations and two cremations. The number of excavated burials containing grave goods (n=51) is the largest among all the known cemeteries, including the burial grounds in present-day eastern Finland and Karelia (see [15]).

Tuukkala

Tuukkala cemetery in Mikkeli is dated from 13th to 15th centuries and it contains both inhumations and cremation burials. With over 80 inhumation burials, this eastern Finnish burial site is the largest and richest inhumation cemetery excavated in the area of the historical Savo province [16, 17]. Tuukkala cemetery was found and mainly excavated in 1886, and several excavations have been conducted since then (see [17]). Despite the extensive excavations, no signs of a church have been found and there are arguments for and against the cemetery being Christian [16, 18]. Osteological research has showed signs of severe trauma and exceptionally tall men [11, 17, 18]. On the basis of the grave goods taller men could have a western origin and the shorter men an eastern origin [18].

Pälkäne, Church of St. Michael

The medieval stone Church of St. Michael in Pälkäne has been built around the year 1500, but based on the radiocarbon datings the burial ground has been used already from 13th century [19, 20]. During the year 2003 over fifty burials were excavated [19]. Most of these burials were unfurnished, and based on the archaeological context they are dated to 17th and 18th centuries [19]. Osteological analysis revealed that the skeletons show shorter stature than other post-medieval sites in Finland [11].

Porvoo, Cathedral site

The first wooden church at the Porvoo Cathedral site was built in the middle of 13th century, followed by a stone church built in the beginning of the 15th century [21]. The cathedral's burial ground dates from 14th to 18th centuries although the individuals used in this study date most likely to 17th and 18th centuries based on the burial customs (see [11, 22]). Porvoo is situated along the southern coast of Finland and there have been trade connections and even migration to Porvoo from all over the Baltic Sea, especially from Tallinn and Stockholm [11, 23, 24].

Renko, the Church of St. Jacob

The stone church of St. Jacob in Renko has been built in the beginning of 16th century, although based on the coins found in the excavations, it has been proposed that site had a wooden church already in the beginning of the 15th century [25]. In the middle of 17th century the stone church was abandoned, but it was renovated and reintroduced at the end of 18th century [21]. In the excavations during 1984 around 70 burials were identified [25]. The most famous historical road, Hämeen Härkätie from Turku to Hämeenlinna passes by Renko and historical records demonstrates some migration events at the end of 18th century [26]. The origin of the immigrants in the parish is not known, but most likely most came from neighboring provinces.

Turku, Julin's site

Julin's site consisted in addition to the Church of the Holy Spirit and its cemetery also a hospital and/or a house of the poor people. Based on its location, it has been assessed that the cemetery, dated to 16th and 17th centuries [27], was a cemetery for the lower social class. Several excavations have been conducted and several hundreds of individual burials have been identified (See [11]). Julin's site lies in Turku, which is the first town in Finland (established at the turn of 13th and 14th centuries). The population density in Turku has been higher than any other sites in this research even in the following century and the city has also had most vivid trade and other contacts across the Baltic Sea.

Hamina, Ryazan Regimental Church

Ryazan Regimental church in Hamina, on the southeastern coast of Finland, was presumably built by the Russian army ca. 1744 [28]. Excavations conducted in this Orthodox cemetery in 2011 found traces of 35 individual burials [28]. The cemetery has an exceptional demographic profile with 4 young adult males, likely soldiers, and rest of the deceased were children less than 7 years old [11, 28]. Based on this bias it has been proposed that the most probable cause of death for individuals buried in the Ryazan Regimental Church's burial ground was infectious disease(s) [28].

Material S2. Example of the OxCal code used to determine the start and end distribution.

Example is presented for Luistari site, for which all ten individuals included in this study were radiocarbon dated.

```
Sequence("Luistari")
{
Boundary("Start of Luistari");
Phase("Luistari")
 {
R_Date("Luistari TU620  Hela-3962", 1210, 39);
R_Date("Luistari TU622  Hela-3961", 1199, 39);
R_Date("Luistari TU464  Hela-3968", 915, 34);
R_Date("Luistari TU465  Hela-3954", 1186, 34);
R_Date("Luistari TU471  Hela-3959", 873, 34);
R_Date("Luistari TU472  Hela-3963", 780, 39);
R_Date("Luistari TU473  Hela-3964", 1075, 36);
R_Date("Luistari TU478  Hela-3969", 1015, 36);
R_Date("Luistari TU480  Hela-3967", 839, 28);
R_Date("Luistari TU481  Hela-3973", 804, 34);
Span("Span of Luistari");
Interval("Duration");
};
Boundary("End of Luistari");
 };
```

Supplementary Figures S1a-S1g. Phase boundary outputs for each site containing four or more ¹⁴C dates.

Phase boundaries were determined with Oxcal version 4.3 and IntCal 13 as the calibration curve for sites Levänluhta, Luistari, Hollola, Hiitola, Tuukkala, Pälkäne and Porvoo. Exact values are presented in Supplementary Table S2.
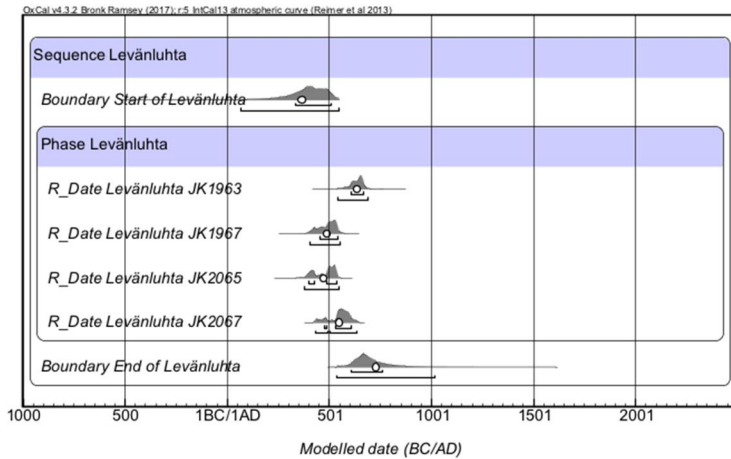
Supplementary Figure S1a. Phase's start and end boundaries determined for Levänluhta based on four ¹⁴C datings. The mean value is presented with the circle. Under each individual probability distribution 68.2% and 95.4% rages are shown.
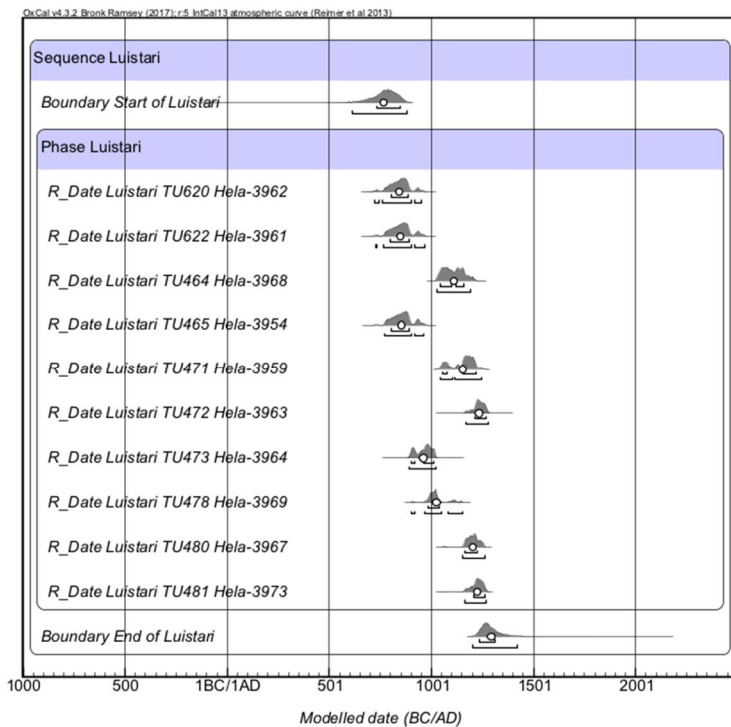
Supplementary Figure S1b. Phase's start and end boundaries determined for Luistari based on ten ¹⁴C datings. The mean value is presented with the circle. Under each individual probability distribution 68.2% and 95.4% rages are shown.
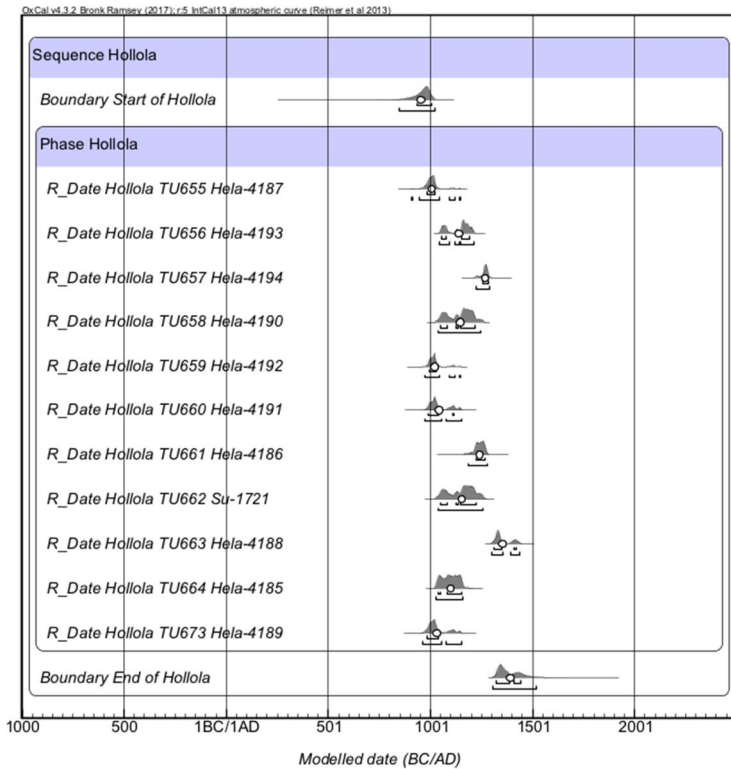
Supplementary Figure S1c. Phase's start and end boundaries determined for Hollola based on eleven ^{14}C datings. The mean value is presented with the circle. Under each individual probability distribution 68.2% and 95.4% rages are shown.
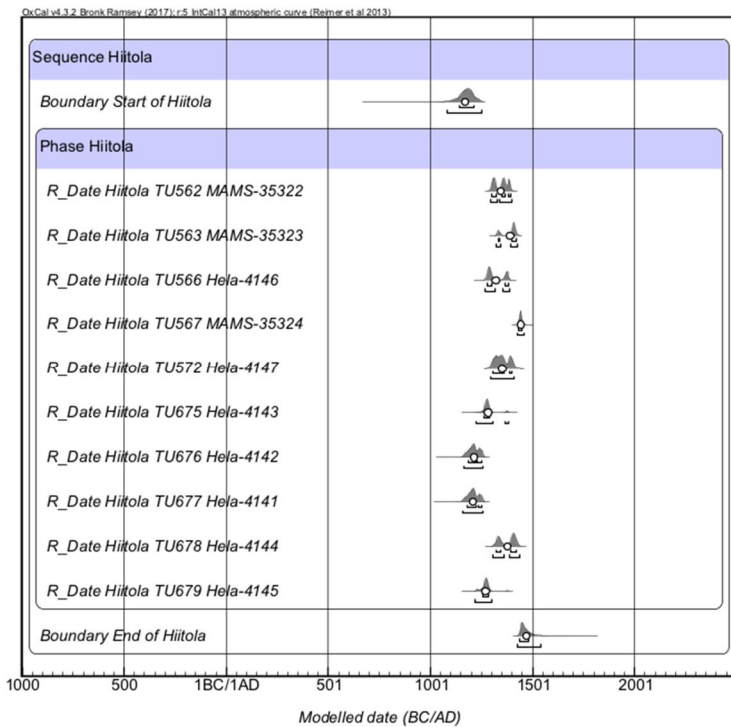
Supplementary Figure S1d. Phase's start and end boundaries determined for Hiitola based on ten ^{14}C datings. The mean value is presented with the circle. Under each individual probability distribution 68.2% and 95.4% rages are shown.
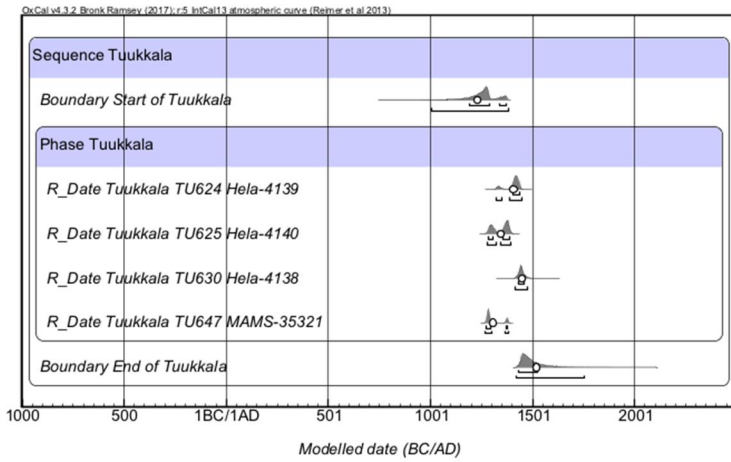
Supplementary Figure S1e. Phase's start and end boundaries determined for Tuukkala based on four ^{14}C datings. The mean value is presented with the circle. Under each individual probability distribution 68.2% and 95.4% rages are shown.
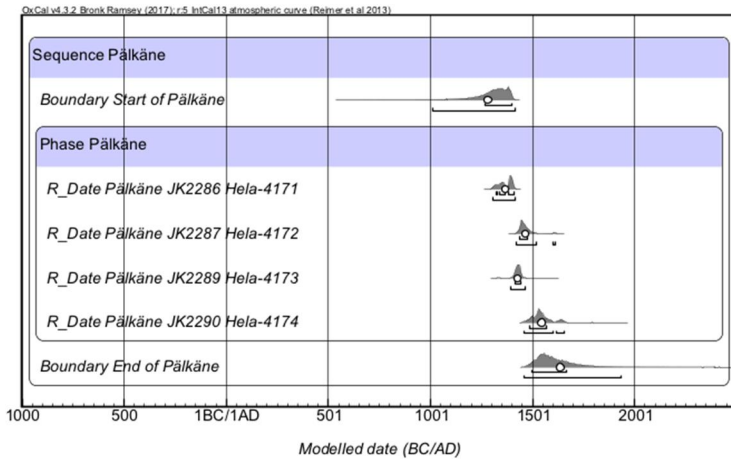
Supplementary Figure S1f. Phase's start and end boundaries determined for Pälkäne based on four ^{14}C datings. The mean value is presented with the circle. Under each individual probability distribution 68.2% and 95.4% rages are shown.
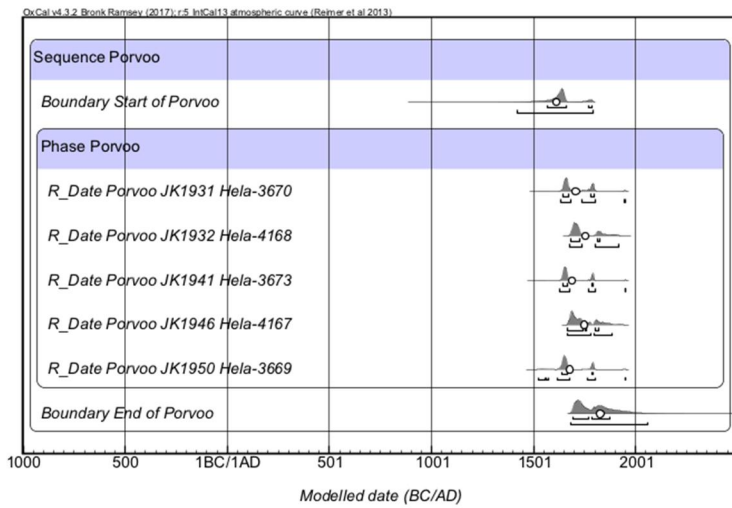
Supplementary Figure S1g. Phase's start and end boundaries determined for Porvoo based on five ^{14}C datings. The mean value is presented with the circle. Under each individual probability distribution 68.2% and 95.4% rages are shown.

Supplementary Figures S2a-S2e. Evaluation of the possible sampling bias in the observed haplogroup frequencies.

To evaluate whether sampling error (i.e., low sample sizes) alone could explain the observed differences in haplogroup frequencies in Iron-Age and medieval sites, simulation studies were performed by using the haplogroup frequencies observed in contemporary Finns as a reference (frequencies based on Neuvonen *et al.* 2015 [30]). Reference population was sampled N times according to the sample size of the ancient population of interest with 10000 permutations. Obtained distributions were compared with the observed haplogroup frequencies. For those haplogroups for which the observed frequency was less than 2.5 % or more than 97.5 % compared to the simulated frequency distribution, the observed frequency couldn't be explained by the sampling error alone (these haplogroups marked with red colour).
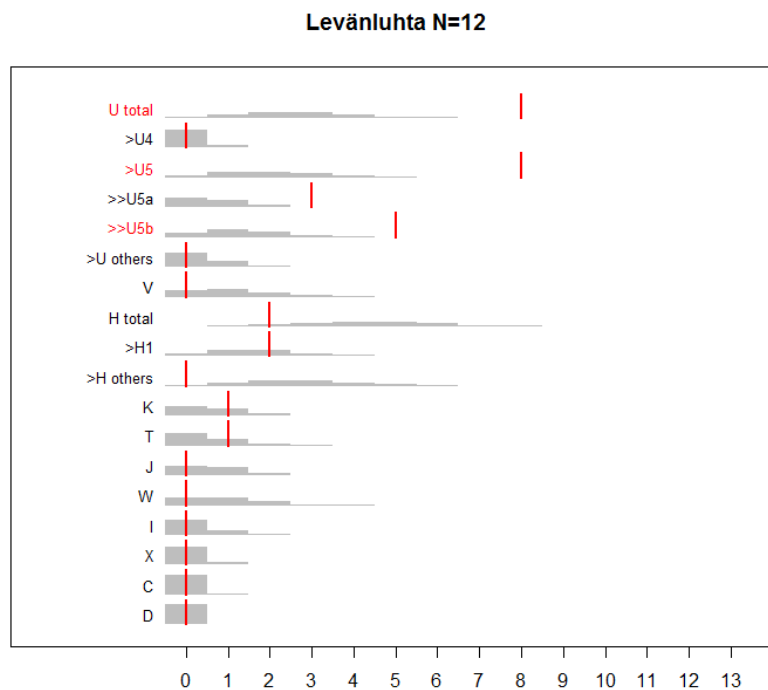
Supplementary Figure S2a. For Levänluhta frequencies for subhaplogroups U5a and U5b cannot be explained only by the sampling error.
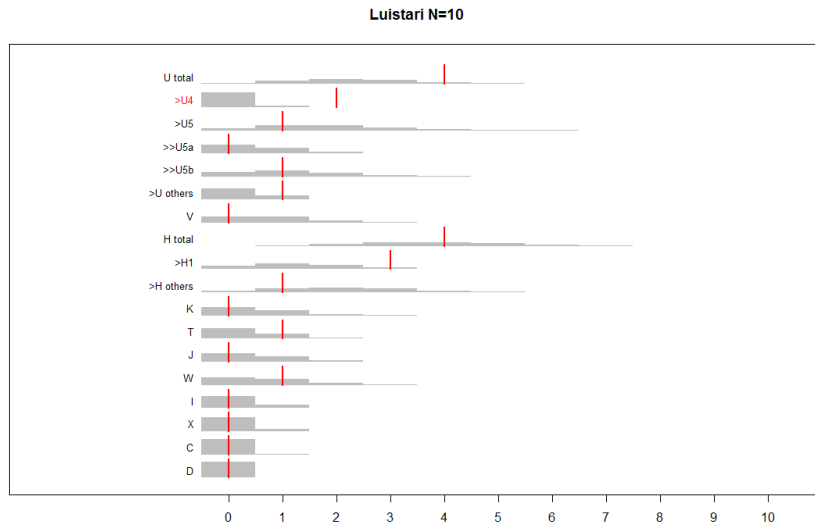
Luistari N=10

Supplementary Figure S2b. For Luistari frequency for subhaplogroup U4 cannot be explained only by the sampling error.

Hollola N=14
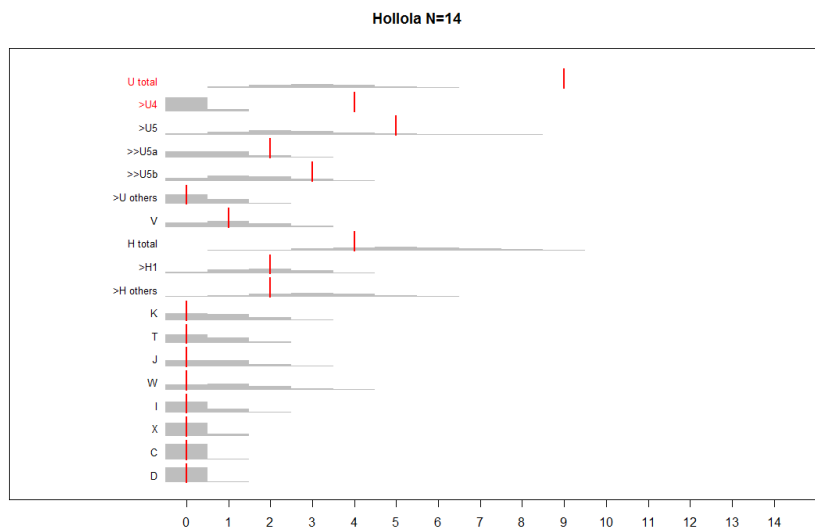
Supplementary Figure S2c. For Hollola frequency for subhaplogroup U4 cannot be explained only by the sampling error.

Hiitola N=13
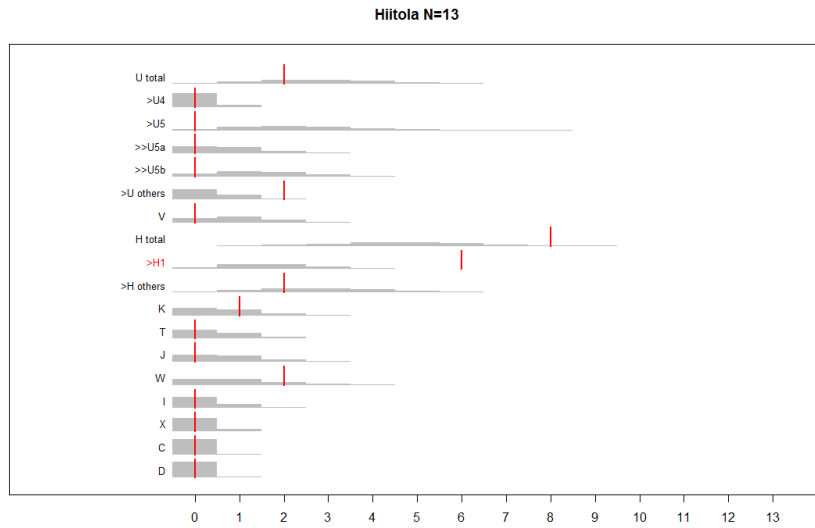
Supplementary Figure S2d. For Hiitola frequency for subhaplogroup H1 cannot be explained only by the sampling error.
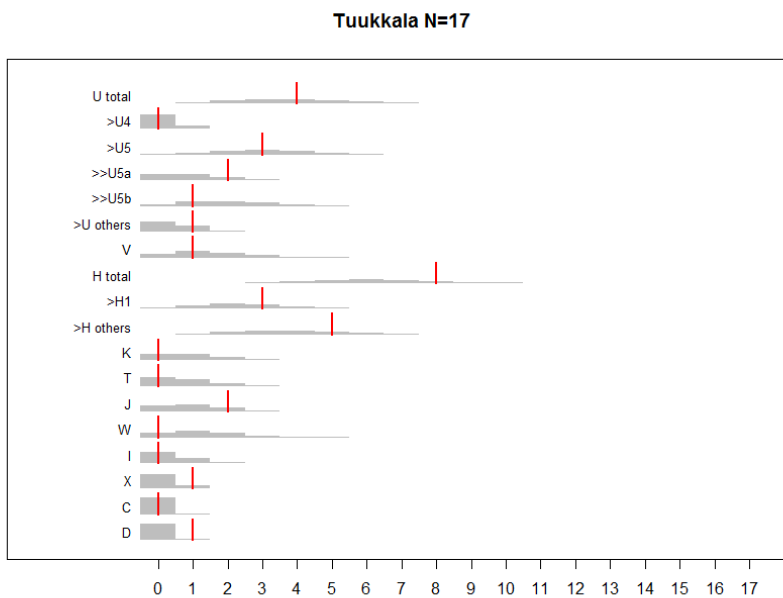
Tuukkala N=17

Supplementary Figure S2e. For Tuukkala observed haplogroup frequencies could be explained by the sampling error.
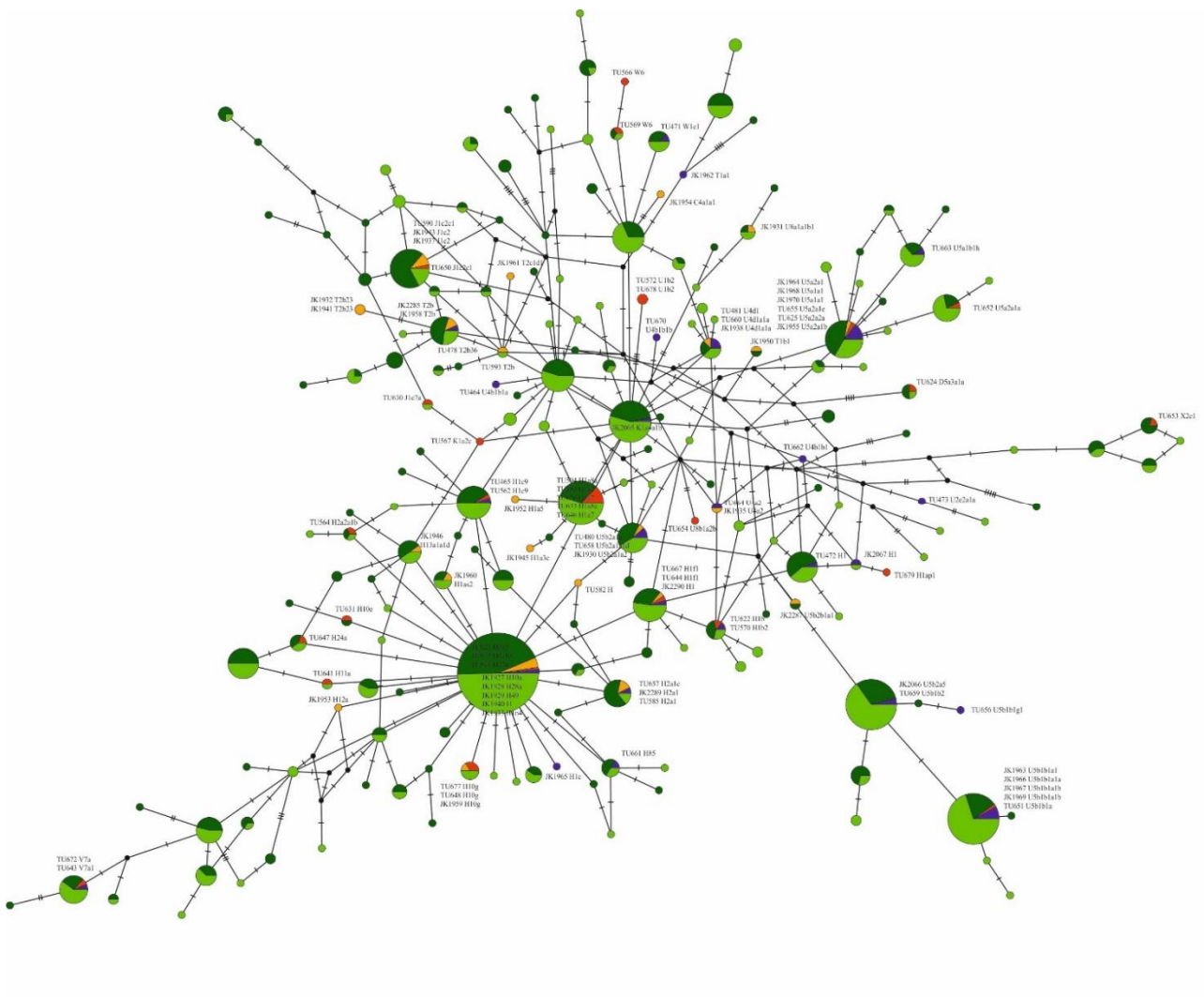
Supplementary Figure S3. Median-joining Network for ancient and contemporary Finns. Haplotype based median-joining network for ancient and contemporary Finns constructed based on HVR1+HVR2 data. Contemporary Finns obtained from Palo *et al.* 2009 [29] and Neuvonen *et al.* 2015 [30]. Iron Age and Medieval south-west = blue, Iron Age and Medieval East = red, Early modern and modern = yellow, contemporary south-west = dark green and contemporary north-east = light green.
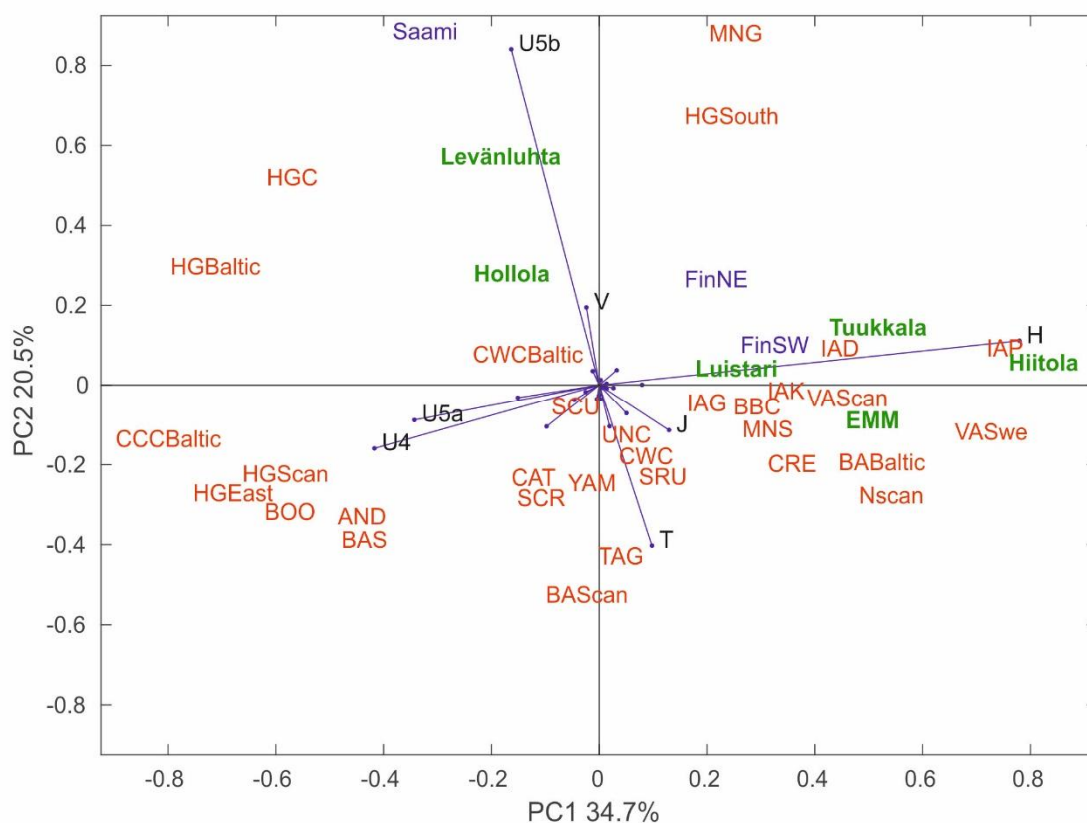
Supplementary figure S4. PCA biplot based on mitochondrial haplogroup frequencies with main loading vectors. Ancient populations presented in this study (green): Levänluhta, Luistari, Hollola, Hiitola, Tuukkala and Early modern and modern Finns (EMM). Contemporary populations (blue): north-east Finland (FinNE), south-west Finland (FinSW), Saami (SAA). Ancient populations (red): Andronovo culture (AND), Baltic Bronze-Age (BAB), Siberian Bronze-Age (BASi), Scandinavian Bronze-Age (BASc), Bell Beaker culture (BBC), Siberian Early Metal Period (BOO), Catacomb culture (CAT), Comb ceramic culture Baltic (CCCB), Crete Minoans (CRE), Corded Ware culture (CWC), Baltic Corded Ware Culture (CWCB), Baltic hunter-gatherers (HGB), central European hunter-gatherers (HGC), eastern hunter-gatherers (HGE), Scandinavian hunter-gatherers (HGSc), south European hunter-gatherers (HGSo), Denmark Iron-Age (IAD), Germany Iron-Age (IAG), Kazakhstan Iron-Age (IAK), Poland Iron-Age (IAP), Germany Middle-Neolithic (MNG), southern Europe Middle-Neolithic (MNS), Scandinavian Neolithic (NSc), Scythians from Russia (SCR), Scythians from Moldova and Ukraine (SCU), Srubnaya culture (SRU), Tagar culture (TAG), Unetice culture (UNC), Scandinavian Viking-Age (VASc), Sweden Viking-Age (VASw) ,Yamnaya culture (YAM).

Supplementary Figure S5. The impact of small sample sizes on PCA. PCA was run with the observed ancient and modern data (as in Fig. 4 in the main article) as well as with fifty random samples (N=15 in each) drawn from contemporary a) northeastern (N = 443), b) southeastern (N = 389) Finns. Black dots denote the locations of these random samples. The scattering of these dots reveal substantial effect of limited sample sizes on the PCA. Blue asterisks: contemporary northeastern Finns (FinNE), southwestern Finns (FinSW) and Saami, green dots: ancient populations presented in this study (Levänluhta, Luistari, Hollola, Hiitola, Tuukkala and Early modern and modern Finns (EMM)); red dots: other ancient populations.

References

1. T. Formisto, An Osteological Analysis of Human and Animal Bones from Levänluhta (Vammalan Kirjapaino, 1993)

2. A. Wessman, Levänluhta. A place of punishment, sacrifice or just a common cemetery. Fennoscandia Archaeologica 26, 81–105 (2009)

3. A. Wessman, T. Alenius, E. Holmqvist, K. Mannermaa, W. Perttola, T. Sundell, S. Vanhanen, Hidden and Remote: New perspectives on the people in the Levänluhta water burial, Western Finland (c. AD 300-800). European Journal of Archaeology 21, 431–454 (2018)

4. P-L. Lehtosalo-Hilander, Luistari in Eura. From pagan burial-ground to Christian cemetery. Abhandlungen der Geistes-und Sozialwissenschaftlichen Klasse-Akademie der Wissenschaften und der Literatur 3, 389–403 (1997)

5. K. Uotila, Eura, Kauttua. Luistarintien kaivaukset 29.7.–7.10.2013. Muuritutkimus ky. (Excavation report in Finnish) https://www.kyppi.fi/palveluikkuna/raportti/read/asp/hae_liite.aspx?id=122587&ttyyppi=pdf&kansio_id=50 (2014)

6. P-L. Lehtosalo-Hilander, Luistari I (The Graves), II (The Artefacts) & III (An Inhumanition Burial-ground Reflecting the Finnish Viking Age Society) (Suomen Muinaismuistoyhdistyksen Aikakausikirja 82, Vammalan Kirjapaino, Vammala, 1982)

7. P-L. Lehtosalo-Hilander, Luistari: A History of Weapons and Ornaments (Suomen Muinaismuistoyhdistyksen Aikakausikirja 107, Vammalan Kirjapaino, Vammala, 2000)

8. A-L. Hirviluoto, in Hollolan Kirkko- Asutuksen, Kirkon ja Seurakunnan Historiaa (Hollolan seurakunta, Hollola, 1985), pp.8–36

9. J-P. Taavitsainen, Ancient Hillforts of Finland: Problems of Analysis, Chronology, and Interpretation with Special Reference to the Hillfort of Kuhmoinen (Suomen Muinaismuistoyhdistyksen Aikakausikirja 94, Ekenäs Tryckeri ab, Ekenäs, 1990)

10. P. Sarvas, Ristiretkiajan Ajoituskysymyksiä (Suomen Museo, 1971)

11. K. Salo, PhD Thesis, University of Helsinki (2016) Thesis available online https://helda.helsinki.fi/handle/10138/163042

12. J. Ailio, Karjalaiset Soikeat Kupurasoljet: Katkelmia Karjalan Koristetyylin Kehityshistoriasta (Suomen Muinaismuistoyhdistyksen Aikakausikirja 32, Suomen Muinaismuistoyhdistys, Helsinki, 1922)

13. E. Tõnisson, in Eesti Esiajalugu, (Eesti Raamat, Tallinn, 1982), pp. 355

14. E. Kivikoski, Die Eisenzeit Finnlands: Bildwerk und Text (Suomen Muinaismuistoyhdistys, Helsinki, 1973)

15. S. Bel'skiy, V. Laakso, in Rome, Constantinople and Newly-Converted Europe: Archaeological and Historical Evidence, M. Salamon, M. Wołoszyn, A. Musin, P. Špehar, M. Hardt, M.P. Kruk, A. Sulikowska-Gąska, Eds. (U źródeł Eu ropy Środkowo-ws chodniej/Frühzeit Ostmitteleuropas, 2012), pp. 767–775

16. P. Purhonen, Maiseman Muisti: Valtakunnallisesti Merkittävät Muinaisjäännökset (Museovirasto, 2001)

17. E. Mikkola, The Mikkeli Tuukkala cemetery - the 2009 excavation and new interpretations. Fennoscandia Archaeologica 26, 177–185

18. P-L. Lehtosalo-Hilander, in Savon Historia I: Esihistorian Vuosituhannet Savon Alueella ja Savon Keskiaika, P-L. Lehtosalo-Hilander, K. Pirinen, Eds. (Kustannuskiila, Kuopio, 1988), pp. 217–218

19. E. Mikkola, K. Vuoristo, Pälkäneen Rauniokirkko, Myöhäiskeskiaikaisen kivikirkon kaivaus 4.6–4.7.2003 ja 8.9–19.9.2003, Museovirasto (Excavation report in Finnish) https://www.kyppi.fi/palveluikkuna/raportti/read/asp/hae_liite.aspx?id=118133&ttyyppi=pdf&kansio_id=635 (2004)

20. K. Vuoristo, Pälkäne Rauniokirkko, Myöhäiskeskiaikaisen kivikirkon asehuoneen kaivaus 31.5–18.6.2010 ja 21–22.7.2010, Museovirasto (Excavation report in Finnish) https://www.kyppi.fi/palveluikkuna/mjhanke/read/asp/hae_liite.aspx?id=113663&ttyyppi=pdf&kansio_id=635 (2011)

21. M. Hiekkanen, Suomen Keskiajan Kivikirkot (Suomalaisen Kirjallisuuden Seura, Helsinki, 2014)

22. J. Lagerstedt, Porvoon tuomiokirkon kirkkomaa, arkeologinen kaivaus, Museovirasto/RHO (Excavation report in Finnish) https://www.kyppi.fi/palveluikkuna/raportti/read/asp/hae_liite.aspx?id=118055&ttyyppi=pdf&kansio_id=638 (2008)

23. C.J. Gardberg, in Porvoon Kaupungin Historia I: Porvoon Seudun Esihistoria, Keskiaika ja 1500-luku, T. Edgren, C.J. Gardberg, Eds. (WSOY, 1996), pp. 200–205

24. I. Mäntylä, Porvoon Kaupungin Historia II: 1602–1809 (WSOY, 1994)

25. M. Hiekkanen, in Rengon Historia, M. Hiekkanen, J. Härme, Eds. (Gummerus, Jyväskylä, 1993), pp. 52–252

26. J. Härme, in Rengon Historia, M. Hiekkanen, J. Härme, Eds. (Gummerus, Jyväskylä, 1993), pp. 479–489

27. S. Pihlman, in Finskt Museum, M. Schauman-Lönnqvist, Eds. (Finska Fornminnesföreningen, Vammala, 1994)

28. K. Vuoristo, Hamina rykmentinkenttä, historiallisen ajan arkeologinen kaupunkikaivaus 5.5–12.8.2011, Museovirasto (Excavation report in Finnish) https://www.kyppi.fi/palveluikkuna/mjhanke/read/asp/hae_liite.aspx?id=114380&ttyyppi=pdf&kansio_id=75 (2012)

29. J.U. Palo *et al.* Genetic markers and population history: Finland revisited. *Eur. J. Hum. Genet.* 17, 1336–1346 (2009).

30. A. Neuvonen *et al.* Vestiges of an Ancient Border in the Contemporary Genetic Diversity of North-Eastern Europe. *PLoS ONE* 10, 1-19 (2015).

Ancient Bacterial Genomes Reveal a High Diversity of *Treponema pallidum* Strains in Early Modern Europe

Graphical Abstract
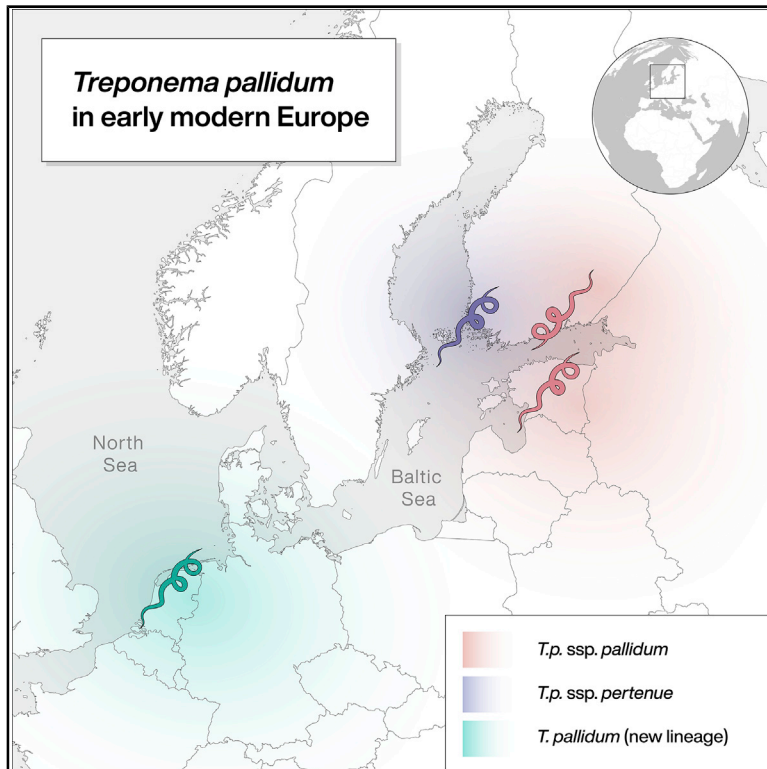
Authors

Kerttu Majander, Saskia Pfrengle, Arthur Kocher, ..., Denise Kühnert, Johannes Krause, Verena J. Schuenemann

Correspondence

kerttu.majander@uzh.ch (K.M.), krause@shh.mpg.de (J.K.), verena.schuenemann@iem.uzh.ch (V.J.S.)

In Brief

Majander et al. find a high diversity among the first ancient European treponemal genomes, including a newly discovered lineage. Dated around Columbus' contact with the Americas, these lineages and their overlapping spatial distributions suggest a possible Old-World origin of syphilis and the existence of endemic treponematoses in Europe.

Highlights

- Four ancient *Treponema pallidum* genomes from early modern Europe were reconstructed

- The genomes are highly diverse and include syphilis, yaws, and an unknown lineage

- The new ancient *T. pallidum* lineage is a basal sister group to yaws and bejel

- Molecular clock dating would allow a pre-Columbian origin of *T. pallidum* in Europe

CellPress

Article

Ancient Bacterial Genomes Reveal a High Diversity of *Treponema pallidum* Strains in Early Modern Europe

Kerttu Majander,[1,2,3,4,18,*] Saskia Pfrengle,[1,2,18] Arthur Kocher,[5] Judith Neukamm,[1,2,6] Louis du Plessis,[7]
Marta Pla-Díaz,[8,16] Natasha Arora,[9] Gülfirde Akgül,[1] Kati Salo,[4,10] Rachel Schats,[11] Sarah Inskip,[12] Markku Oinonen,[13]
Heiki Valk,[14] Martin Malve,[14] Aivar Kriiska,[14] Päivi Onkamo,[4,15] Fernando González-Candelas,[8,16] Denise Kühnert,[5]
Johannes Krause,[2,3,17,*] and Verena J. Schuenemann[1,2,17,19,*]

[1]Institute of Evolutionary Medicine, University of Zurich, Winterthurerstrasse 190, 8057 Zurich, Switzerland
[2]Institute for Archaeological Sciences, University of Tübingen, Rümelinstrasse 19-23, 72070 Tübingen, Germany
[3]Department of Archaeogenetics, Max Planck Institute for the Science of Human History, Kahlaische Strasse 10, 07745 Jena, Germany
[4]Department of Biosciences, University of Helsinki, Viikinkaari 9, 00014 Helsinki, Finland
[5]Transmission, Infection, Diversification and Evolution Group, Max Planck Institute for the Science of Human History, Kahlaische Strasse 10, 07745 Jena, Germany
[6]Institute for Bioinformatics and Medical Informatics, University of Tübingen, Sand 14, 72076 Tübingen, Germany
[7]Department of Zoology, University of Oxford, Oxford OX1 3SZ, UK
[8]Joint Research Unit "Infection and Public Health" FISABIO-University of Valencia, Institute for Integrative Systems Biology (I2SysBio), Valencia, Spain
[9]Zurich Institute of Forensic Medicine, University of Zurich, Winterthurerstrasse 190/52, 8057 Zurich, Switzerland
[10]Archaeology, Faculty of Arts, University of Helsinki, Unioninkatu 38F, 00014 Helsinki, Finland
[11]Laboratory for Human Osteoarchaeology, Faculty of Archaeology, Leiden University, Einsteinweg 2, 2333CC Leiden, the Netherlands
[12]McDonald Institute for Archaeological Research, University of Cambridge, Downing Street, Cambridge CB2 3ER, UK
[13]Laboratory of Chronology, Finnish Museum of Natural History, University of Helsinki, Gustaf Hällströmin katu 2, 00560 Helsinki, Finland
[14]Institute of History and Archaeology, University of Tartu, Jakobi 2, 51005 Tartu, Tartumaa, Estonia
[15]Department of Biology, University of Turku, Vesilinnantie 5, 20500 Turku, Finland
[16]CIBER de Epidemiología y Salud Pública (CIBERESP), Madrid, Spain
[17]Senckenberg Centre for Human Evolution and Palaeoenvironment (S-HEP), University of Tübingen, Tübingen, Germany
[18]These authors contributed equally
[19]Lead Contact
*Correspondence: kerttu.majander@uzh.ch (K.M.), krause@shh.mpg.de (J.K.), verena.schuenemann@iem.uzh.ch (V.J.S.)
https://doi.org/10.1016/j.cub.2020.07.058

SUMMARY

Syphilis is a globally re-emerging disease, which has marked European history with a devastating epidemic at the end of the 15th century. Together with non-venereal treponemal diseases, like bejel and yaws, which are found today in subtropical and tropical regions, it currently poses a substantial health threat worldwide. The origins and spread of treponemal diseases remain unresolved, including syphilis' potential introduction into Europe from the Americas. Here, we present the first genetic data from archaeological human remains reflecting a high diversity of *Treponema pallidum* in early modern Europe. Our study demonstrates that a variety of strains related to both venereal syphilis and yaws-causing *T. pallidum* subspecies were already present in Northern Europe in the early modern period. We also discovered a previously unknown *T. pallidum* lineage recovered as a sister group to yaws- and bejel-causing lineages. These findings imply a more complex pattern of geographical distribution and etiology of early treponemal epidemics than previously understood.

INTRODUCTION

Treponemal infections, namely yaws, bejel, and, most notoriously, syphilis, represent a reoccurring, global threat to human health. Venereal syphilis, caused by infections with *Treponema pallidum pallidum* (TPA) results in millions of new cases every year [1]. The two endemic treponemal subspecies closely related to *T. p. pallidum* are *T. pallidum pertenue* (TPE) and *T. pallidum endemicum* (TEN). TPE is common in the tropical regions of

the world, where it causes yaws and a non-human primates' treponematosis [2–4]. TEN is the causative agent of bejel, which is mostly found in hot and arid environments [2, 3]. All three *T. pallidum* subspecies are re-emerging across numerous countries, prompting renewed international eradication campaigns [5, 6]. Furthermore, resistance against second-line antibiotics has recently been observed for each of them [7–9], although penicillin treatment still remains effective [8, 10–12]. Yaws, bejel, and syphilis are all transmitted through direct contact with skin

lesions or mucous membranes [2, 3]. Syphilis is generally transmitted sexually or congenitally, although incidental transmission through other routes, such as blood transfusions, is occasionally observed [2, 3]. Contrarily, the endemic treponematoses (yaws and bejel) are most commonly transmitted through skin lesions, primarily in childhood or preadolescence [3, 13]. All three diseases overlap in clinical manifestations, with progression through multiple stages and damage to the skin and other tissues [14, 15]. The syphilis-causing bacterium (TPA) is considered highly invasive, disseminating through the body and into the central nervous system; if untreated, it can result in severe damage to organs and tissues, including the skeletal system [3, 14–16].

The re-emergence of treponemal diseases after the devastating outbreaks documented in historical times showcases a spread facilitated by pathogen evolution in combination with social factors [8, 12, 17–19]. Early medical reports from the late 15th century portray the most well-known epidemic, a rapid and Europe-wide spread of venereal syphilis in the wake of the 1495 Italian war [17, 20], whereas reports from later periods appear to indicate a gradual shift to a milder, more chronic disease in the subsequent decades, similar in manifestation to modern-day syphilis [17, 21, 22]. The European outbreak coincides with the first American expeditions and has ignited a persisting theory suggesting that syphilis was introduced to Europe by Columbus and his crew upon their return from the New World in 1493 [23, 24]. The alternative multiregional hypothesis contradicts this scenario and presumes the pre-Columbian presence of syphilis on the European continent, potentially as a result of prehistoric spread of the disease through African and Asian routes [25–27]. Medieval literature mentions cases of syphilis, but it is often diagnostically confounded by similarities with other diseases and spuriously called "venereal" or "hereditary" leprosy [22, 28]. Pre-Columbian human remains with characteristic marks of treponematoses have been reported [29, 30] yet are thus far unconfirmed with genetic evidence [23, 28]. Distinguishing the *T. pallidum* infections from other diseases is often challenging [31], and although serological tests allow diagnosing them, more precise distinction among treponemal subspecies requires molecular typing [15, 32, 33]. Before modern genetic classifications were introduced, supporters of the "unitarian hypothesis" claimed all treponematoses to be one and the same disease [34, 35]. Improved understanding of phylogenetic cladality among the treponemal subspecies [36, 37], further refined by genomic studies, has since disputed the unitarian view [3, 38, 39]. Questioning the geographical distribution and clinical symptoms as the main means of categorization can, nevertheless, be justified, as the geographical origin and time of emergence of TPA and TPE remain ambiguous [17, 40, 41]. A recent genomic study on modern lineages of *T. pallidum* supported a common ancestor of all current TPA strains in the 1700s [41], whereas the more general diversification of *T. pallidum* into subspecies is assumed to have happened in prehistoric times [24, 42]. However, mutation rate estimates drawn from modern genome isolates may be biased, because natural selection has not affected the most recent mutations yet [43] and large parts of the past species diversity may have been lost in time [44]. Reconstructed ancient pathogen genomes thus show an unprecedented potential to illuminate their species' unresolved divergence times,

origin, and evolution [45–47]. Ancient DNA studies on treponematoses have so far remained scarce for both biological and methodological reasons. The treponemal spirochetes survive poorly outside their host organism and are present in extremely low quantities during late-stage infections, often evading detection even in living patients [48]. The final, tertiary-stage treponematoses produce the most frequently detected skeletal alterations, but in these cases, the disease has often already reached the latent stage, thwarting attempts to retrieve its DNA [49, 50]. Most notably, the bones most likely containing large amounts of treponemal agents belong to congenitally infected neonates. Such finds, however, are very rare in the archaeological record [51, 52]. Currently, technical advancements, together with careful selection of samples exhibiting signs of treponemal pathogenesis, are enabling genomic studies on this elusive pathogen for the first time [53]. The means to recover *T. pallidum* from historic human remains were recently established in a study on perinatal and infant individuals from colonial Mexico, in which two ancient *T. p. pallidum* genomes and one ancient *T. p. pertenue* genome were described [52]. Attempts to retrieve authentic *T. pallidum* DNA from ancient adult individuals have so far been unsuccessful.

Here, we analyze ancient bacterial genomes from four ancient *T. pallidum* strains retrieved with target enrichment from subadult and adult human remains originating from central and northern Europe. The newly reconstructed ancient genomes represent a variety of *T. pallidum* subspecies, including a formerly unknown form of treponematosis phylogenetically basal to both bejel- and yaws-causing lineages. For the first time, treponemal genomes dated temporally close to New World contact have been retrieved from European samples, including strains closely related to *T. pallidum* subspecies that are today mostly restricted to the tropics and subtropics.

RESULTS

Geographical Origins and Osteological Analyses of Samples

For this study, remains from nine individuals were included: five from the Holy Ghost Chapel in Turku, Finland; one from the Dome churchyard in Porvoo, Finland; one each from St. Jacob's cemetery and from St. George's cemetery in Tartu, Estonia; and, finally, one from Gertrude's Infirmary in Kampen, the Netherlands (STAR Methods). Four samples from these individuals tested positive for treponemal infection in the DNA screening with high-throughput sequencing (Figure 1A). The sampled premolar CHS119 (Figure 1A1) is from an adult individual from Turku with several treponemal changes on the skull and both tibias [54]. The petrous bone sample PD28 from Porvoo (Figure 1A2) showed no syphilis-associated lesions [55]; an infection was implicated primarily by the individual's perinatal death. The skeleton of a young adult from Tartu (Figure 1A3) yielding the sample SJ219 displayed putative albeit inconclusive indicators of syphilis. From the adolescent individual from Kampen, only a disarticulated tibia was available [24] with an active lesion on the cortical surface, which was used to obtain sample KM14-7 (Figure 1A4).

All four positive samples in this study were radiocarbon dated (STAR Methods). The putatively pre-Columbian samples
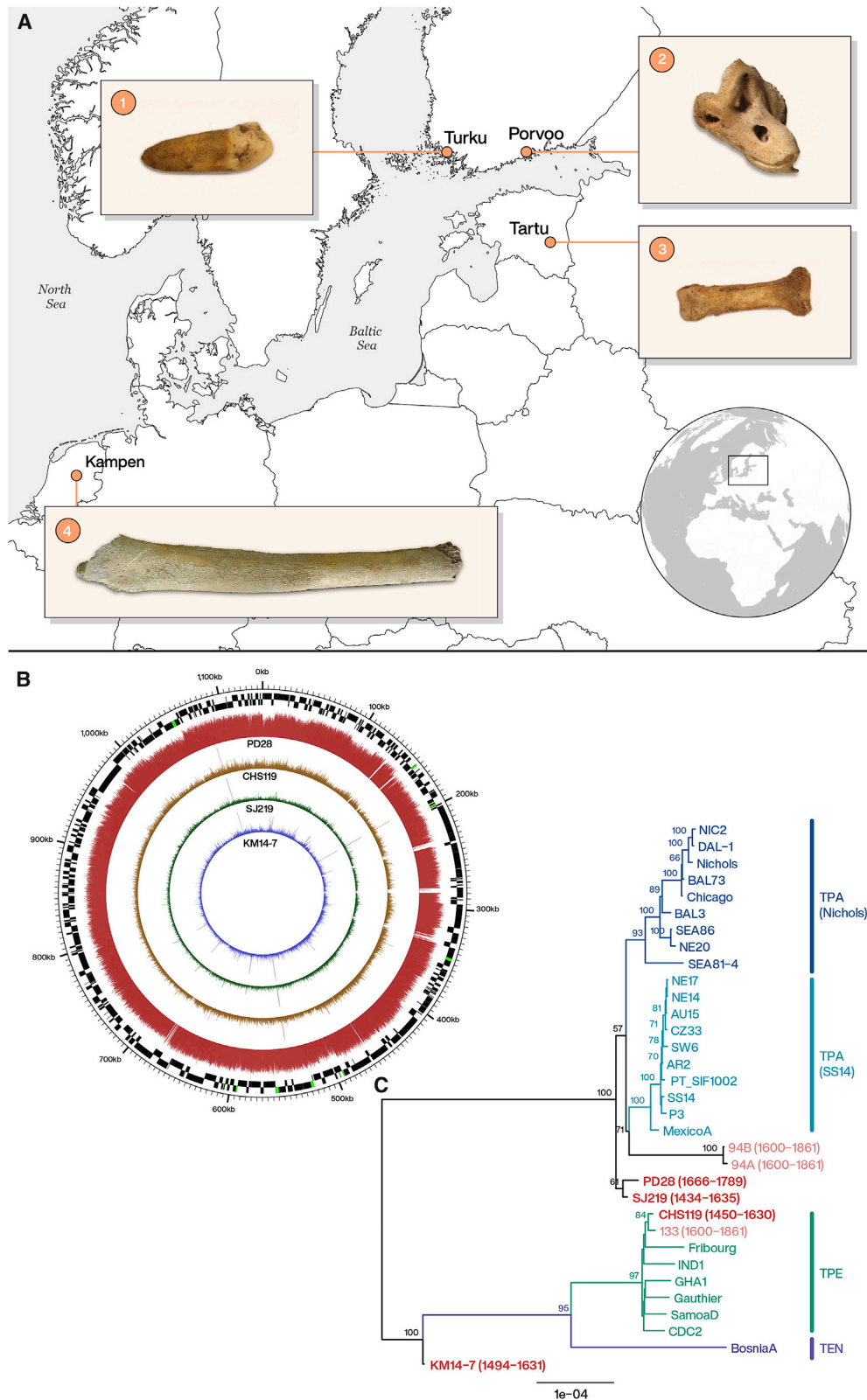
Figure 1. Geographical Origin and Phylogenetic Placement of *T. pallidum*-Positive Samples

(A) Locations of archeological sites from which the samples used in this study originate: (1) a premolar from an adult individual 119, crypt of the Holy Ghost Chapel, Turku, Finland; (2) petrous portion of temporal bone of a perinatal individual from the grave 28 at the Porvoo Dome cemetery, Porvoo, Finland; (3) a proximal

CHS119 and SJ219 went through additional attestation of the dating procedures: a fragment of the wooden platform from the grave was dated in addition to the individual SJ219, and reservoir effect corrections were calculated for the sample CHS119 dating results [57, 58]. These additional estimates, however, resulted in upper limit date ranges within the 17th century CE for both individuals (STAR Methods).

Authenticity Estimation of Ancient DNA and Genome Reconstruction

All samples included in this study (Table 1; STAR Methods) were subjected to a screening procedure using direct shotgun sequencing and genome-wide enrichment [41, 59]. In this screening, samples yielding a minimum 1,000 post-duplicate-removal reads mapping to a *T. pallidum* reference (SJ219: 1,205 reads; CHS119: 1,496 reads; KM14-7: 1,496 reads; PD28: 1,637 reads) were deemed positive for this pathogen (for damage profiles, see Figure S2). The percentage of deaminated bases at the ends of reads, signaling authenticity of ancient DNA [60, 61], ranged from 4% to 18% (*T. pallidum* DNA; screening capture) and 10% to 18% (mitochondrial DNA [mtDNA]; mitochondrial capture), and the average fragment length of the four samples varied between 49 and 69 bases (Table 1). An array capture enrichment for *T. pallidum* DNA [41, 59] using uracil-DNA glycosylase (UDG)-treated libraries [62] was then conducted on all four positive samples, and additionally, human mtDNA was enriched for samples CHS119, SJ219, and KM14-7 [59, 63] (STAR Methods). The mtDNA ranged from 3,414 to 29,031 mapped reads, with an average coverage of 11–119× on the mitochondrial genome (Table 1). Haplogroups identified were J1c2c1 for CHS119, HV16 for SJ219, and U2e1f1 for KM14-7 (Table 1), all representative of the early modern variation present within northern and central European populations, further supporting the geographical origin of the samples [64, 65].

After high-throughput sequencing of the enriched DNA on Illumina platforms, the resulting 98–256 million raw reads were merged sample-wise and duplicate reads were removed. Genomes for each sample were reconstructed by mapping to the *T. p. pallidum* reference genome Nichols (CP004010.2), using the EAGER pipeline [69] (STAR Methods). The samples yielded between 18,034 and 1,430,292 endogenous unique reads mapping to the reference, covering 47%–98% of the reference genome at least once, respectively (Table 1; Figures 1B and S3). We filtered positions based on read coverage and excluded recombining and other potentially mapping-obstructing genes (*FadL* homologs, *tpr* genes, and *arp* gene), as well as the genomic positions for which >25% of the genomes had missing data, gaining complete genome alignments containing a total of 1,631 variable positions. We refer to these positions as single nucleotide polymorphisms (SNPs) throughout the manuscript.

Phylogenetic Analysis and Genetic Recombination

Midpoint-rooted maximum-likelihood (ML) trees of our ancient European genomes, previously published colonial Mexican genomes [52], and 26 modern treponemal genomes [41, 70–78] were reconstructed from the alignments. The four ancient European genomes are placed at three distinct positions in the phylogenetic tree (Figures 1C and 2). The PD28 and SJ219 genomes most closely resemble syphilis-causing strains and form a sister group to all other TPA strains, although this position is not highly supported and seems highly sensitive to the set of genes excluded from the alignment (Figure S4). The CHS119 genome, conversely, is consistently placed in the TPE clade of the treponemal family tree and forms a cherry with the ancient TPE genome 133 from colonial Mexico. The affinity of these two ancient genomes may in part result from similarly missing data with respect to the complete genomes of modern strains in the clade. The KM14-7 genome, remarkably, falls basal to all TPE lineages known today, as well as to the TEN genome Bosnia A [76]. This unexpected position was further corroborated by investigating genomic loci for which the ancestral variants of the TPE/TEN and TPA clades were likely different. Among 30 of these positions for which the variant was resolved in KM14-17, 60% were TPE/TEN-like and 40% were TPA-like, which supports the branching of this genome on the evolutionary path between TPA and TPE/TEN clades. In comparison, all other genomes had 100% variant characteristics of one or the other clade at these positions, except for 94A, 94B, and SEA81-4, which had 16%, 14.3%, and 10.7% of TPE/TEN-like variants, respectively (Tables S1 and S2). The basal position of KM14-7 retained strong support also when using an alignment including only nucleotide positions resolved in this genome (Figure S4F) or using an alternative alignment based on mapping to the TPE CDC2 reference genome (Figures 2B and 2C), thus disputing the possibility that its phylogenetic placement would be an artifact of missing data or dependent on a specific reference genome.

A recombination analysis was conducted as described in Arora and colleagues [41], including 26 modern genomes [41, 70–78] and six ancient ones: the colonial Mexican genomes 94A, 94B, and 133 from an earlier study [52] and three of our ancient European genomes, namely PD28, CHS119, and SJ219 (Table 2). Sample KM14-7 was excluded from the analysis, due to its sporadic placement in the ML tree topologies,

---

manual phalanx of a young adult individual from St. Jacob's cemetery, Tartu, Estonia; and (4) a tibia from a subadult individual from Gertrude's Infirmary, Kampen, the Netherlands.

(B) Circleator [56] plot representing the entire data from the respective BAM files after duplicate removal and mapped with a quality threshold 37, showing the coverage of the four ancient strains. The genome coverage of the ancient strains is shown from lowest to highest: KM14-7; SJ219; CHS119; and PD28, with colors from inside to outside in violet, green, brown, and red. As setting the quality threshold above zero allows no reads mapping to identical sequences, gaps in coverage occur in each of the genomes on the identical regions. The black outer rim visualizes the protein-coding regions in forward and the black inner rim in the reverse direction, according to the annotation of the Nichols reference genome (CP004010.2).

(C) Midpoint-rooted maximum-likelihood phylogenetic tree of *Treponema pallidum* strains. The analysis is based on an alignment of 1,631 SNPs after exclusion of recombining and hypervariable genes as well as genomic positions with >25% missing data. Branch lengths represent numbers of substitutions per site. Bootstrap support values are written above nodes when >50. Ancient genomes from this study are marked in red and the previously published ones in pink. See also Figures S3 and S4.

Table 1. Mapping Statistics

Data Type	Ind. ID	Arch. ID	Mol. Sex (from Shotgun Data)	Raw Reads	Mapped Reads (Post-duplicate Removal)	AVG Cov.	% Gen. Cov. 1x	% Gen. Cov. 2x	% Gen. Cov. 3x	% Gen. Cov. 5x	DNA Dmg 1st Base 5' (Non-UDG)	AVG Frag. Length	Cont. Est.	Haplogroup
TP	PD28	grave 28	XY	98,204,923	1,430,292	136.23	98.09	98.07	98.06	98.04	0.04	59.91	N/A	N/A
MT					N/A	N/A	N/A	N/A	N/A	N/A	N/A	N/A	N/A	N/A
TP	SJ219	individual 219	XX	193,609,543	29,198	1.41	64.31	34.00	15.69	2.58	0.10	49.12	N/A	N/A
MT					29,031	118.91	100	100	100	100	0.13	67.74	0.02	HV16
TP	CHS119	individual 119	XX	255,889,929	52,054	2.82	83.32	62.31	42.04	15.13	0.18	54.16	N/A	N/A
MT					4,490	16.25	100	100	99.99	99.79	0.14	59.85	0.02	J1c2c1
TP	KM14-7	individual 14, bone fragment 7	XY	152,268,578	18,034	0.91	46.89	19.35	7.93	1.61	0.18	51.69	N/A	N/A
MT					3,414	11.02	99.98	99.77	99.37	96.08	0.16	53.35	0.01	U2e1f1

Statistics from the EAGER pipeline against the Nichols reference genome for the four ancient samples screened as positive for treponemal infection. The individual (Ind) and original archaeological (Arch.) identifiers are reported for each sample. The table includes final number of raw reads; mapped reads after duplicate removal; average coverage (AVG cov.); percent of the genome covered at 1-fold, 2-fold, 3-fold, and 5-fold coverage; percent of reads with DNA damage (DNA dmg) for the 1st base at the 5' end (non-UDG treated); and average fragment length (AVG frag. length) in base pairs for the treponemal and T. pallidum (TP) capture data. Same statistics are given for the human mitochondrial capture data (MT) where applicable, with the addition of an estimated amount of contamination (Cont. est.) from Schmutzi program [66] and haplogroup assignments from HaploGrep2 [64] program. Molecular sexing (Mol. sex) of individuals is based on the human endogenous reads from shotgun data [67, 68].
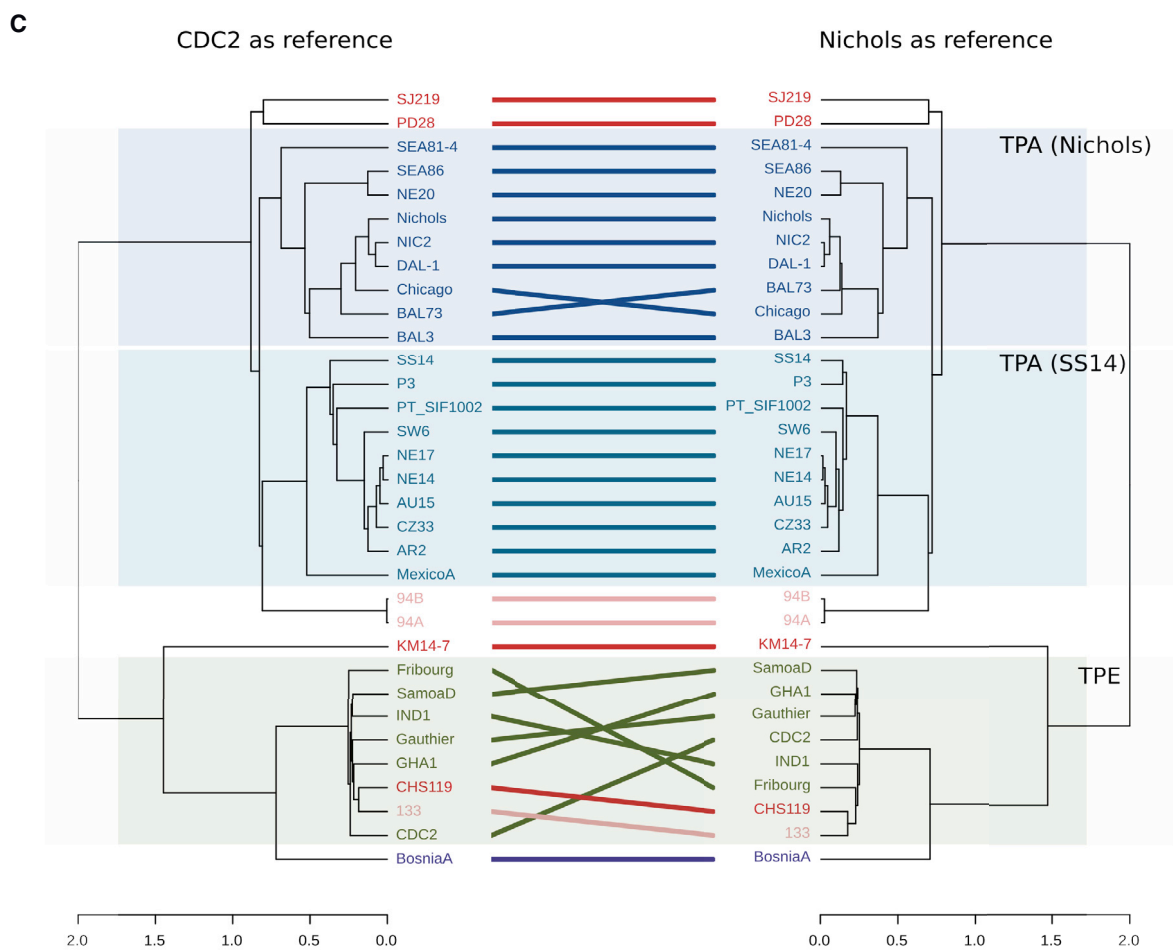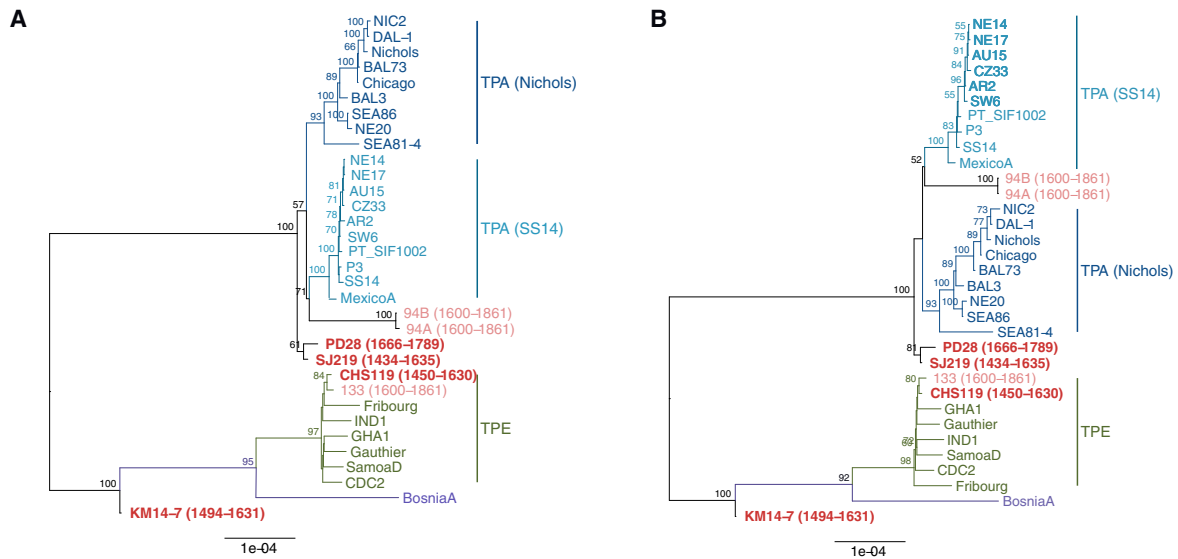
which were derived for entire genomes and for each gene individually. Congruence between the complete genome alignments and gene trees was tested after evaluating the corresponding phylogenetic signal for each gene. The phylogenetic signal and incongruence proved significant for 40 loci, twelve of which were further verified by the presence of at least three consecutive SNPs supporting a recombination event. A total of 316 SNPs was identified in 16 recombinant regions in 12 different genes. Two of the recombining gene candidates identified by Arora and colleagues [41] were also confirmed in association with the ancient European genomes. Among our ancient genomes, PD28 (along with the Nichols clade) was possibly involved in one recombinant event of the TP0136 gene as a putative recipient, with the TPE/TEN clade, CHS119, and colonial Mexican 133 genomes as putative donors. Similar possibility was observed in the recombination event detected in the TP0179 gene, although only with TPE/TEN clade and 133 as presumptive donors. One putative recombination event concerning the TP0865 gene was identified between the CHS119 and 133 genomes (along with the TPE/TEN clade) and the SEA86, NE20, and SEA81-4 lineages. Finally, another recombination event concerned the TP0558 gene, with the TPE/TEN clade and CHS119 genome as potential donors and the SS14 clade, MexicoA, 94A, and 94B from colonial Mexico and PD28 genomes as recipients. The events observed between the modern strains and including the previously published colonial Mexican genomes are listed in Table 2.

Molecular Clock Dating

Molecular clock dating analyses were performed on a dataset of 28 genomes [41, 70–78] (STAR Methods). Linear regression of root-to-tip genetic distance against sampling date indicated that the T. pallidum strains possess a good temporal signal (r = 0.66; p < 0.001; Figures S5A–S5C; STAR Methods).

The date randomization test (DRT) [81] showed that neither the mean nor median estimate of the clock rate estimated under the true sampling dates was contained within the highest posterior density (HPD) intervals of estimates from any of the replicates with permuted sampling dates (Figure S5D). Furthermore, the HPD intervals of only 1 out of 50 replicates intersect with the HPD interval estimated under the true sampling dates. We interpret these results as evidence of a substantially stronger molecular clock signal in the dataset than is expected by chance. Finally, robustness analyses with different combinations of demographic and clock models showed that the demographic model has little effect on the estimated divergence times and sampling dates and that a relaxed clock model receives strong support (Figure S6).

Posterior distributions of divergence dates of T. pallidum clades and sampling dates of ancient genomes are shown in Figure 3A. Figure 3B shows the maximum clade credibility (MCC) tree estimated in BEAST2 v.2.6 [82]. Sampling date estimates under different models are given in Figures S6I–S6L and Table 3. The time to the most recent common ancestor (T_{MRCA}) calculated for the whole T. pallidum family is placed far in the prehistoric era, at least 2000 BCE. However, time dependency of molecular rates (TDMR) may lead to underestimating deep divergence times when mutation rates are inferred from genomes collected within a relatively restricted time period [83, 84]. Applying a model accounting for TDMR may be possible in the

Table 2. Recombination Events

Gene ID	Event	Start	End	Minimal Size	Strains Involved
TPANIC_0136	3	158,271	158,336	65	yaws → Nichols clade
	4	158,346	158,364	18	yaws/Bosnia A → Nichols clade
	5	158,915	158,976	61	yaws/Bosnia A/133/CHS119? → PD28, Nichols clade[a]
	6	159,312	159,323	11	yaws/Bosnia A/133 → Nichols clade
TPANIC_0164	1	187,064	187,177	113	yaws/Bosnia A → Sea86, NE20, 94A, 94B
TPANIC_0179	1	198,040	198,428	388	yaws/Bosnia A/133 → PD28, Nichols clade[a]
TPANIC_0326	1	345,859	347,956	2,097	Bosnia A → SS14 clade
TPANIC_0462	1	492,772	493,605	833	yaws/Bosnia A → Sea86, NE20
TPANIC_0488	1	522,981	523,620	639	Bosnia A → Mexico A
TPANIC_0515	1	555,872	557,768	1,896	yaws/Bosnia A/133 → 94A, 94B, Nichols clade
TPANIC_0548	1	593,563	594,215	652	yaws/Bosnia A → Nichols clade
TPANIC_0558	1	606,171	606,591	420	yaws/Bosnia A/CHS119?/133? → PD28, 94B, 94A? SS14 clade, Mexico A[a]
TPANIC_0865	1	945,224	945,542	318	yaws/Bosnia A/CHS119?/133? → Sea86, NE20, Sea81-4[a]
	2	945,830	946,298	468	Bosnia A → Sea86, NE20, Sea81-4
TPANIC_0967	1	1,051,257	1,052,366	1,109	yaws/Bosnia A → Sea81-4
TPANIC_0968	1	1,052,414	1,053,617	1,203	Bosnia A → Sea81-4

All detected recombination events across the complete dataset of 26 modern *Treponema pallidum* [41, 70–78] and six ancient genomes (94A, 94B, and 133 from [52] and genomes PD28, CHS119, and SJ219 from this study). For each recombination event are reported the start and end position of the event referred to as TPA Nichols strain, accession CP004010.2. Slashes are used to separate the different potential gene donor strains. The affected recipient strains are separated by commas. Arrows point to the likely direction of recombination between the donor and recipient strains. An interrogation mark indicates an uncertain yet likely involvement in the event.
[a]Events involving ancient genomes from this study

future, if genomes covering wider and more distinct time periods become available [85, 86]. The latest common ancestor of the venereal syphilis strains was placed between the 12th and 16th centuries CE. The divergence of TPE and TEN was dated to between the 4th century BCE and the 12th century CE, although the most recent common ancestor of TPE was placed between the 14th and 16th centuries CE. The best supported tree topology places the ancient European genomes basal to all TPA strains, with the T_{MRCA} of the modern Nichols clade between the 15th and 18th centuries CE and that of the SS14 clade slightly later, between the 18th and 20th centuries CE. Due to the inclusion of four ancient European genomes, the above divergence times are substantially older than the times reported by Arora and colleagues [41]. Similarly, the estimated mean molecular clock rate (1.069×10^{-7} s/s/y; 95% HPD $7.277 \times 10^{-8} - 1.516 \times 10^{-7}$ s/s/y) is slower than those reported in recent studies [8, 41] for either *T. pallidum* as a whole or for TPA strains exclusively. Nonetheless, the 95% HPD of the mean clock rate overlaps with previous estimates [8] (Figure S6A).

Molecular clock dating allows us to refine the sampling date estimates for three of the four ancient genomes (Figure 3A). The posterior distribution of the sampling date of CHS119 places most of the weight on a more recent date, although those of PD28 and 133 favor older sampling dates. This is especially

pronounced for CHS119 and 133 with the 95% HPD interval not including any dates older than 1546 CE for CHS119 or younger than 1782 CE for 133. On the other hand, for SJ219, the 95% HPD of the sampling date spans nearly the entire range defined by radiocarbon dating, making it impossible to exclude a pre-Columbian sampling date (posterior probability 0.28; Table 3).

Virulence Factor Analysis
A set of 60 TPA candidate genes associated with virulence and outlined in previous studies [52, 87, 88] were queried in the ancient European samples to determine their presence or absence and thus to broadly assess the extent of functional changes between ancient and modern treponemal lineages. A color-coded heatmap was produced to visualize the percentage of coverage on these 60 candidate genes for each genome (Figure 4). These selected genes included the family of *tpr* genes, which mostly encode putative outer membrane proteins. The *tpr* genes are grouped into three subfamilies of paralogous genes and pose challenges to their distinction with short read data due to high sequence homology. Given that mapping and filtering parameters with a MAPQ score threshold above 0 results in the exclusion of reads mapping to more than one location, and therefore in lower genetic coverage, MAPQ score thresholds of

Figure 2. Phylogenies Comparing the Effect of Mapping to TPA (Nichols) and TPE (CDC2) Reference Genome
(A and B) A comparison of the phylogenetic ML trees based on SNP alignments after evaluation of precarious SNPs and removal of hypervariable and recombinant genes, when mapped against (A) *Treponema pallidum pallidum* reference genome Nichols (CP004010.2) and (B) *Treponema pallidum pertenue* reference genome CDC2 (CP002365.1). Scale bar represents substitutions per nucleotide site.
(C) Tanglegram visualization of the observed topological differences between the two mappings, produced using R packages ape [79] and dendextend [80]. Horizontal scales measure statistical similarity of the two trees in comparison to each other.
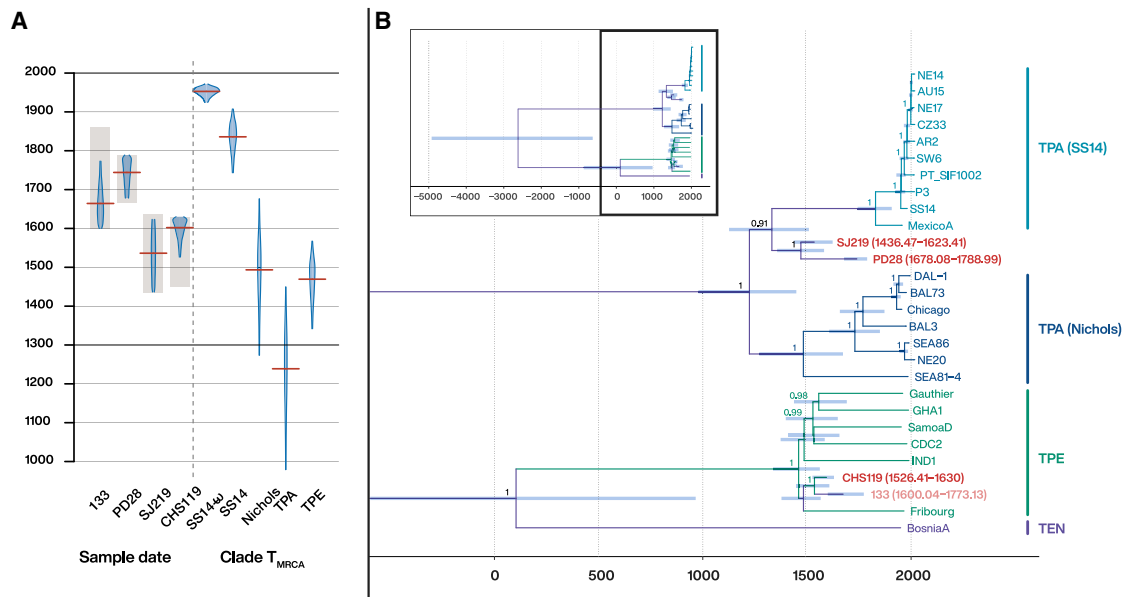
Figure 3. Molecular Clock Dating

(A) Posterior distributions for the sampling dates of ancient genomes (left) and the divergence dates of more recent clades in the tree (right). The distributions are truncated at the upper and lower limits of the 95% highest posterior density (HPD) intervals, and the red lines indicate the median estimates. The shading indicates the prior distributions used for the sampling dates of ancient samples (informed by radiocarbon date ranges). Vertical scale denotes time in years CE.

(B) Maximum clade credibility (MCC) tree of the dataset consisting of 24 modern and four ancient genomes estimated in BEAST2 v2.6 [82] under a relaxed clock model and a Bayesian skyline plot demographic model. Node bars indicate the 95% HPD interval of internal nodes and sampling dates of the ancient genomes (HPD intervals of the sampling dates in parentheses). The genomes from this study are marked in red and previously published ancient genome 133 in pink. Horizontal scale denotes time in years BCE/CE.

See also Figures S5 and S6.

0 and 37 were compared, allowing duplicated regions to be covered or omitted, respectively. The annotated Nichols genome (GenBank: CP004010.2) [75] was used as reference. The observed coverage per gene of six modern TPA lineages (SS14, Mexico A, SW6, NIC2, Sea81-4, and Chicago) [41, 70, 77] was compared with the four ancient treponemal genomes from Europe (this study) and three previously published treponemal genomes from colonial Mexico [52]. Despite the reduced coverage for highly similar sequences, such as *tprC* and *tprD* genes, with mapping threshold greater than zero, a strong indication for the presence of all virulence factors in the ancient European genomes was observed. Indeed, at least a small amount of reads could be mapped specifically for all putative virulence genes, except for the *tprF* on two genomes (SJ219 and KM14-7). This absence is likely due to the low coverage of these genomes, as well as the high similarity of *tprF* gene with its paralogs (Table S3). Conversely, in the high-coverage PD28 genome, all investigated virulence factors were detected, including the *tpr* genes (Table S3). Notably, the ancient European genomes all contain the FadL family homolog TPANIC_0856, which is missing in the colonial Mexican TPA genomes 94A and 94B [52].

DISCUSSION

Early Emergence of Syphilis in Europe

In this study, four ancient *Treponema* genomes were retrieved from human skeletal remains dating to early modern Europe,

providing unprecedented insights into the first reported epidemics of syphilis at the end of the 15th century. Two genomes, PD28 and SJ219, were identified as strains of syphilis-causing TPA, representing the first molecularly identified specimen of this *T. pallidum* subspecies from early modern Europe. In most of the tested settings, these genomes fall within the modern variety of the TPA strains, albeit with bootstrap values ~60–85. They form a sister clade to the modern TPA branch, basal to all its lineages with good support, when hypervariable and recombining regions are excluded. The molecular clock dating analysis of the genomes also lends support to the basal placement of these two ancient genomes with respect to the modern TPA diversity. The PD28 sample was dated to the early modern period by combined analyses of archaeological context and 14C dating. Two independent radiocarbon analyses were performed on the sample SJ219 from Estonia, placing it in the early to mid-15th century, distinctly before Columbus' expeditions. This dating would place the first TPA contagions in Europe prior to the New World contact, suggesting that the original causative agent of the continent-wide epidemic at the end of the 15th century may have resided within the Old World. A reservoir effect could have influenced the radiocarbon analysis results of the individual SJ219 through the diet, and the dating could not be confirmed with certainty (STAR Methods; Figure S1). However, such direct evidence of TPA from an early European context gives unprecedented support for the existence of venereal syphilis around and potentially prior to the contact Columbus initiated in the Americas.

Table 3. Posterior Estimates of the Sampling Dates of Ancient Genomes and the Divergence Dates of Clades Inferred by Molecular Clock Dating

Sample/Clade	Radiocarbon Date Range	Posterior Date Estimate		Posterior Probability	
		Median	95% HPD Interval	Pre-Columbian	Monophyletic
133 (TPE)	1600–1861	1663.72	1600–1780.22	0	–
PD28 (TPA)	1666–1789	1713.01	1666.07–1777.66	0	–
SJ219 (TPA)	1434–1635	1535.41	1440.72–1632.46	0.278	–
CHS119 (TPE)	1450–1630	1609.09	1547.07–1629.99	0.005	–
SS14-w	–	1954.58	1927.80–1973.75	–	0.9779
SS14	–	1834.92	1729.45–1912.34	–	0.981
Nichols	–	1625.48	1485.25-1757.74	–	0.971
TPA	–	1339.12	1117.16–1515.99	–	0.977
TPE	–	1488.78	1376.73–1570.28	–	0.969
TPE/TEN	–	472.19246	−371.68–1110.10	–	0.963

Date ranges defined by radiocarbon dating were used as prior distributions for ancient sequences in the molecular clock dating analyses. The posterior probability that a sample is pre-Columbian is calculated as the proportion of posterior samples with a date <1493, and the posterior probability that a clade is monophyletic is calculated as the proportion of posterior trees where the clade is monophyletic.

Yaws-like Strains in Europe

Out of our four ancient genomes, two fell outside the variation of TPA. One of them, CHS119 from Finland, clusters with the TPE subspecies, the causative agent of yaws: an endemic treponematosis mostly restricted to tropical regions today. A direct radiocarbon dating places the sample in the 15th to 16th century, yet full confidence of the date cannot be gained due to the potential marine reservoir effect [57, 58]. Some cases of endemic treponematoses are assigned to Europe prior to the apparent eradication of the disease in the 20th century [89–91], and although the early infections' likeness to the modern clinical condition is not assured, this sample provides the first direct evidence of a TPE infection in historical Northern Europe, far from its typical present-day distribution. Strikingly, the contemporaneous genome KM14-7 from the Netherlands falls basal to both the bejel- and yaws-causing lineages, unveiling a previously unidentified lineage of *T. pallidum*.

The low sequencing coverage obtained for the KM14-7 genome prevented its inclusion in the recombination and time-calibrated phylogenetic analysis. However, the ML tree topology with KM14-7 in the basal position to TPE and TEN clades was further confirmed through closer inspection at the nucleotide level. The lineage shows genetic similarities to both current TPA (12 characteristic SNPs) and TPE/TEN (18 characteristic SNPs) strains but represents a distinct form from both and has apparently diverged from their common ancestor before TPE and TEN divergence, which we dated to at least 1,000 years BP. Altogether, our ancient treponemal genomes from northern and central Europe point to an early-existing diversity of *T. pallidum* in the Old World. Their existence does not refute the potential introduction of new strains of treponemes from the New World in the wake of the European expeditions yet lends credibility to a potentially endemic origin of the 15th century epidemics.

Whereas recombination events between the three modern-day treponemal subspecies are deemed rare [92], such events were observed across the subspecies in our study. These recombination events presumably happened in the past, before

TPA, TPE, and TEN acquired their currently separated geographical niches [41, 52]. Contemporaneous historical cases of syphilis and yaws in a geographically overlapping region provide a plausible opportunity for recombination [73, 76]. The potential recombination events observed in this study involved lineages from the modern-day diversity, the ancient genomes PD28 and CHS119 from Europe, and 94A and 94B genomes from Mexico [52].

Overall, our observations point to recombination events that are directed toward the syphilis-causing clades from the yaws- and bejel-causing ancestors. The recombinations between the clades further support a geographically close common history of the TPA and TPE lineages, which cannot be concluded from the geographical distribution of extant lineages.

Old Hypotheses Revisited

Assuming the ancient infectious agents had similar clinical manifestations to modern-day *T. pallidum* subspecies, the reconstructed TPA and TPE genomes from ancient Finnish and Estonian human remains are showing an early spread of both venereal syphilis and yaws at the northern end of Europe. Although the 14C analyses and the archaeological context of the individuals CHS119 and SJ219 support pre-Columbian dating, these claims are thwarted by methodological uncertainties (STAR Methods; Figure S1). In addition to the direct dating of the individual samples, we used our novel ancient genomes for molecular dating of the phylogenetic clades of *T. pallidum* (Figure 3). This dating analysis sets the T_{MRCA} for the entire *T. pallidum* family to at least 1000 BCE. The available calibration points, however, provide only the lower bound for the subspecies' divergence, permitting a possibility of a deep prehistoric background of treponemes in association with their human hosts [25, 26]. The T_{MRCA} for all TPA strains between the 10th and 15th centuries CE supports a radiation of these strains within Europe instead of having a single ancestral source from the New World. The separation of TPE and TEN clades between 9th century BCE and 10th century CE clearly predates contact period and, together with the genome KM14-7 and its
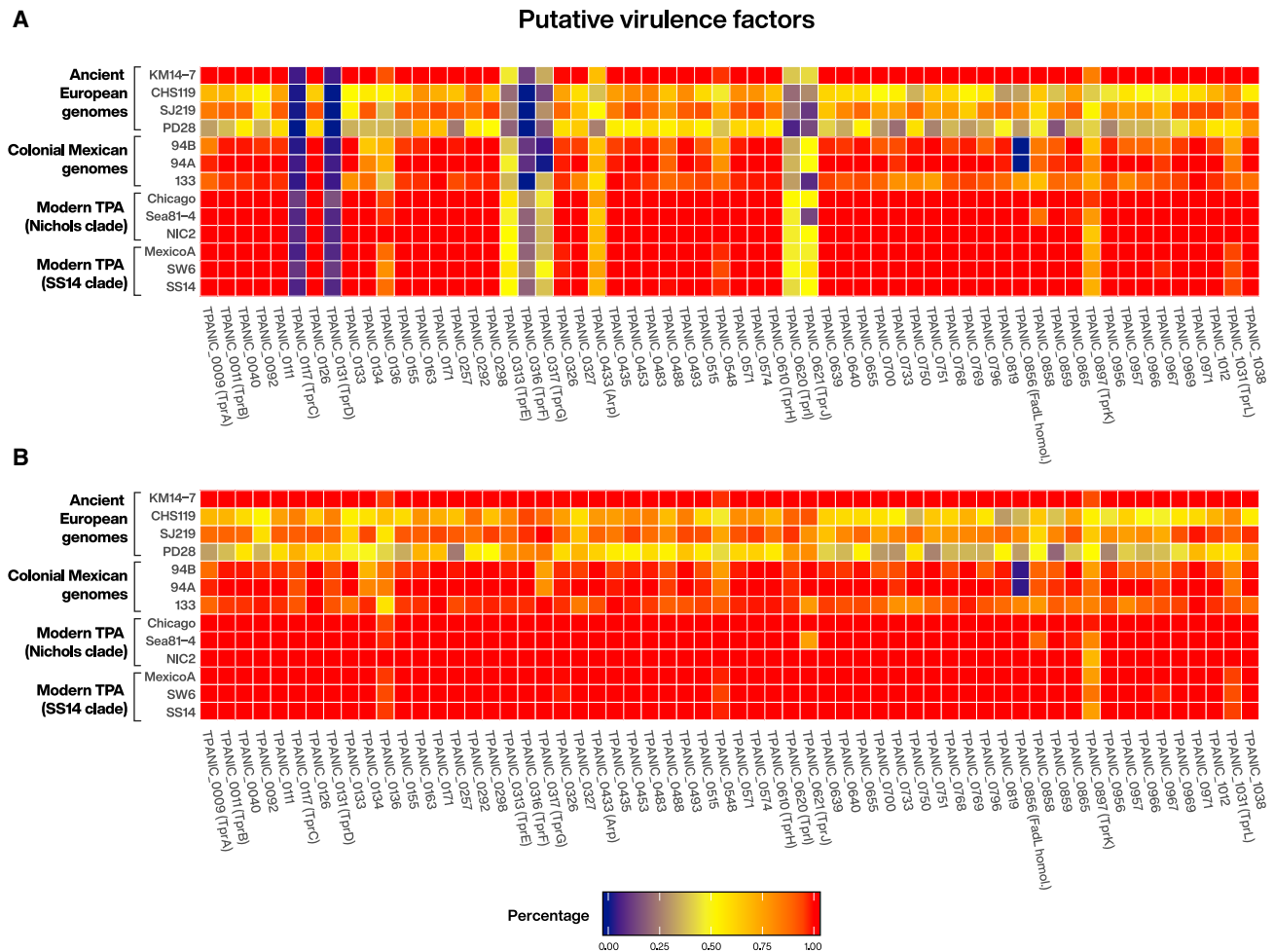
A Putative virulence factors

B

Figure 4. Virulence Analysis

A heatmap visualization of 60 putative virulence genes analyzed on the four ancient genomes from early modern Europe (Ancient European genomes) based on Nichols reference genome (CP004010.2) annotation, in comparison with a selection of six modern TPA strains, three from Nichols and SS14 clades each, and the previously published colonial Mexican genomes [52], using (A) a quality filtering threshold of 37, excluding any mapping of reads, should the exact region appear more than once along the genome and (B) a quality filtering threshold of 0, i.e., allowing a mapping of reads on identical regions. See also Table S3.

ancestral characteristics, suggests a common history of these diseases in the Old World. All currently known lineages of yaws have a common ancestor as late as 14th to 16th century CE, which could point to a novel radiation simultaneously with the rise of the early venereal syphilis, possibly enabled by the same evolutionary opportunities around the contact period or due to competition between concurrent subspecies.

The KM14-7 genome represents a possibly unprecedented type of treponemal infectious agent that possessed genetic similarities to both currently existing syphilis and yaws yet appears to have been distinct from both. In its pathogenesis, this agent may have resembled endemic treponematoses, because the majority of its recovered SNPs are shared with the yaws and bejel lineages. It has been suggested that yaws or its ancestors represent the original form of treponematosis that appeared and spread around the world thousands of years ago, was then re-introduced to the Iberian Peninsula via the Central and Western African slave trade some 50 years before Columbus'

travels, and eventually gave rise to the venereal syphilis [42, 93]. It is indeed possible that the venereal form in the Old World developed from an endemic type of disease, enhanced by genetic recombination events or in response to a competition between existing pathogens [34, 38]. Likewise, recombination events may have occurred between the endemic European strains and novel lineages introduced in the wake of the New World contact, precipitating the epidemic events at that time. Although cladality between the different subspecies clearly exists in both the past and present, it now seems likely that recombination has interconnected these clades in the past and that the genetic differences do not necessarily define the treponemal pathogenesis observed in the archaeological remains. Furthermore, recent studies of apparently endemic cases of sexually transmitted bejel from Japan and Cuba possess potential to challenge the modern-day views on geographical and etiological particularity and transmission routes of the different subspecies [9, 94]. Recombination occurring between TPA and TEN clades

has been proposed as a plausible course of evolution, leading to these still poorly known local strains, the Bosnia A bejel-causing strain, and an isolate 11q/j found from a syphilis-like lesion in a bejel patient [76, 95]. These recombination events may stem from a historical time that provided more geographical overlap and thus allowed encounters between *T. pallidum* subspecies.

Our data show that all genes associated with virulence in modern *T. pallidum* strains were likely already present in ancient European strains. In particular, the *FadL* homolog gene, possibly representing a deletion specific to the colonial Mexican strains, was recovered in all the ancient European genomes reported here. Thus, any excess of virulence potentially developed by *T. pallidum* during the second half of the 20th century was likely not through novel gene acquisition. To ascertain the alleged gradual reduction of virulence in syphilis after the initial European outbreak and highlight possible changes in protein functions coded by individual genes, more detailed sequence comparisons between ancient and modern genomes would be required, likely accompanied by *de novo* approaches with functional predictions that are beyond assessing with our current low-coverage data. Apart from the etiology and sequence diversity of these newly discovered ancient genomes, many past *T. pallidum* lineages can be presumed to remain entirely unknown today. Once revealed, they may prove pivotal in uncovering the relationship between treponemal strains and dating their emergence.

Outlook and Implications on Sampling Strategies

Retrieving treponemal DNA from skeletal material is highly challenging, and the feasibility of the effort was widely questioned before the recently published colonial Mexican genomes [49, 50, 52]. Furthermore, diagnostic signs between endemic and venereal syphilis are difficult to distinguish, especially in skeletal remains, and several forms of treponematoses appear to have existed concurrently in early modern Europe. Although the previously published Mexican genomes were obtained only from neonates and infants [52], our four positive cases represent both non-adult (KM14-7, SJ219, and PD28) and adult (CHS119) individuals, including one only tentatively diagnosed case of treponematosis (SJ219). Successful retrieval of treponemal DNA was likely facilitated by sampling hard tissue directly involved with an ongoing inflammatory response, such as an active lesion (KM14-7), or one possessing ample blood flow, such as dental cavity (CHS119). With the perinatal sample (PD28), we witnessed the first retrieval of pathogen DNA from a petrous bone, yielding an ancient TPA genome with up to 136-fold coverage. Presumably, an extremely high bacterial load that contributed to this exceptionally successful case was a consequence of an early, systemic congenital infection [96]. Retrieving ancient treponemal DNA from such a large variety of skeletal materials raises hopes of achieving future progress with the paleopathological cases of advanced and latent infections. Altogether, we were able to reconstruct four ancient treponemal genomes, from two of the known subspecies and one formerly unknown strain. These cases support the notion that different treponemal agents cause essentially similar skeletal alterations and are highly adaptable to environmental circumstances [40, 97]. We therefore propose that the geographical separation criteria between treponemal diseases should be used with caution, especially when related to earlier forms of treponematoses and their diagnostic manifestations within the archaeological record. Improving methodologies specifically targeted for samples with low bacterial load or sparse genomic coverage may soon aid in recovering positive ancient DNA results from putative cases of treponematoses from early- to prehistoric contexts, thereby illuminating the most persistent quandaries of the field, including the ultimate origin of venereal syphilis.

STAR★METHODS

Detailed methods are provided in the online version of this paper and include the following:

- KEY RESOURCES TABLE
- RESOURCE AVAILABILITY
  - Lead Contact
  - Materials Availability
  - Data and Code Availability
- EXPERIMENTAL MODEL AND SUBJECT DETAILS
  - Ethical approvals
  - Description of archaeological contexts and sample selection
- METHOD DETAILS
  - Sample processing
  - Reservoir effect correction of the CHS119 sample
  - Sampling and DNA extraction
  - Library preparation
  - Double-stranded DNA library preparation
  - Uracil-DNA Glycosylase (UDG) treated double-stranded DNA library preparation
  - Single-stranded DNA library preparation
  - Capture techniques
  - Sequencing
  - Read processing, mapping and variant calling
  - Genomic dataset and multisequence alignment
  - SNP quality assessment
  - Phylogenetic and recombination analysis
  - KM14-7 SNP analysis
  - Molecular clock dating
  - Robustness of molecular clock dating
  - Virulence analysis
- QUANTIFICATION AND STATISTICAL ANALYSIS
  - *In silico* screening
  - Phylogenetic analysis
  - Molecular clock test
  - Dating analysis

AUTHOR CONTRIBUTIONS

DECLARATION OF INTERESTS

The authors declare no competing interests.

REFERENCES

1. Kent, M.E., and Romanelli, F. (2008). Reexamining syphilis: an update on epidemiology, clinical manifestations, and management. Ann. Pharmacother. 42, 226–236.

2. Mitjà, O., Šmajs, D., and Bassat, Q. (2013). Advances in the diagnosis of endemic treponematoses: yaws, bejel, and pinta. PLoS Negl. Trop. Dis. 7, e2283.

3. Giacani, L., and Lukehart, S.A. (2014). The endemic treponematoses. Clin. Microbiol. Rev. 27, 89–115.

4. Šmajs, D., Strouhal, M., and Knauf, S. (2018). Genetics of human and animal uncultivable treponemal pathogens. Infect. Genet. Evol. 61, 92–107.

5. Kazadi, W.M., Asiedu, K.B., Agana, N., and Mitjà, O. (2014). Epidemiology of yaws: an update. Clin. Epidemiol. 6, 119–128.

6. Spiteri, G., Unemo, M., Mårdh, O., and Amato-Gauci, A.J. (2019). The resurgence of syphilis in high-income countries in the 2000s: a focus on Europe. Epidemiol. Infect. 147, e143.

7. Mitjà, O., Godornes, C., Houinei, W., Kapa, A., Paru, R., Abel, H., González-Beiras, C., Bieb, S.V., Wangi, J., Barry, A.E., et al. (2018). Re-emergence of yaws after single mass azithromycin treatment followed by targeted treatment: a longitudinal study. Lancet 391, 1599–1607.

8. Beale, M.A., Marks, M., Sahi, S.K., Tantalo, L.C., Nori, A.V., French, P., Lukehart, S.A., Marra, C.M., and Thomson, N.R. (2019). Genomic epidemiology of syphilis reveals independent emergence of macrolide resistance across multiple circulating lineages. Nat. Commun. 10, 3255.

9. Kawahata, T., Kojima, Y., Furubayashi, K., Shinohara, K., Shimizu, T., Komano, J., Mori, H., and Motomura, K. (2019). Bejel, a nonvenereal treponematosis, among men who have sex with men, Japan. Emerg. Infect. Dis. 25, 1581–1583.

10. Stamm, L.V., Stapleton, J.T., and Bassford, P.J., Jr. (1988). In vitro assay to demonstrate high-level erythromycin resistance of a clinical isolate of Treponema pallidum. Antimicrob. Agents Chemother. 32, 164–169.

11. Šmajs, D., Paštěková, L., and Grillová, L. (2015). Macrolide resistance in the syphilis spirochete, Treponema pallidum ssp. pallidum: can we also expect macrolide-resistant yaws strains? Am. J. Trop. Med. Hyg. 93, 678–683.

12. Stamm, L.V. (2016). Syphilis: re-emergence of an old foe. Microb. Cell 3, 363–370.

13. Mitjà, O., Asiedu, K., and Mabey, D. (2013). Yaws. Lancet 381, 763–773.

14. Radolf, J.D. (1996). Treponema. In Medical Microbiology, Fourth Edition, , S. Baron, ed. (University of Texas Medical Branch at Galveston).

15. Lafond, R.E., and Lukehart, S.A. (2006). Biological basis for syphilis. Clin. Microbiol. Rev. 19, 29–49.

16. Norris, S.J., Cox, D.L., and Weinstock, G.M. (2001). Biology of Treponema pallidum: correlation of functional activities with genome sequence data. J. Mol. Microbiol. Biotechnol. 3, 37–62.

17. Knell, R.J. (2004). Syphilis in renaissance Europe: rapid evolution of an introduced sexually transmitted disease? Proc. Biol. Sci. 271 (Suppl 4), S174–S176.

18. Fenton, K.A., Breban, R., Vardavas, R., Okano, J.T., Martin, T., Aral, S., and Blower, S. (2008). Infectious syphilis in high-income settings in the 21st century. Lancet Infect. Dis. 8, 244–253.

19. Giacani, L., Molini, B.J., Kim, E.Y., Godornes, B.C., Leader, B.T., Tantalo, L.C., Centurion-Lara, A., and Lukehart, S.A. (2010). Antigenic variation in Treponema pallidum: TprK sequence diversity accumulates in response to immune pressure during experimental syphilis. J. Immunol. 184, 3822–3829.

20. Tampa, M., Sarbu, I., Matei, C., Benea, V., and Georgescu, S.R. (2014). Brief history of syphilis. J. Med. Life 7, 4–10.

21. Tognotti, E. (2009). The rise and fall of syphilis in Renaissance Europe. J. Med. Humanit. 30, 99–113.

22. Arrizabalaga, J. (1993). Syphilis. In The Cambridge World History of Human Disease, K.F. Kiple, ed. (Cambridge University), pp. 1025–1033.

23. Harper, K.N., Zuckerman, M.K., Harper, M.L., Kingston, J.D., and Armelagos, G.J. (2011). The origin and antiquity of syphilis revisited: an appraisal of Old World pre-Columbian evidence for treponemal infection. Am. J. Phys. Anthropol. 146 (Suppl 53), 99–133.

24. Rothschild, B.M. (2005). History of syphilis. Clin. Infect. Dis. 40, 1454–1463.

25. Hackett, C.J. (1963). On the origin of the human treponematoses (pinta, yaws, endemic syphilis and venereal syphilis). Bull. World Health Organ. 29, 7–41.

26. Cockburn, T.A. (1961). The origin of the treponematoses. Bull. World Health Organ. 24, 221–228.

27. Meyer, C., Jung, C., Kohl, T., Poenicke, A., Poppe, A., and Alt, K.W. (2002). Syphilis 2001—a palaeopathological reappraisal. Homo 53, 39–58.

28. Crane-Kramer, G.M. (2000). The paleoepidemiological examination of treponemal infection and leprosy in medieval populations from northern Europe. PhD thesis (University of Calgary).

29. Henneberg, M., and Henneberg, R.J. (1994). Treponematosis in an ancient Greek colony of Metaponto, southern Italy, 580–250 BCE. The Origin of Syphilis in Europe: Before or After 1493, 92–98.

30. Blondiaux, J., and Bagousse, A.A. (1994). A treponematosis dated from the Late Roman Empire in Normandie, France. L'Origine de la Syphilis en Europe: Avant ou Aprés 1493, 99–100.

31. Fonseca, E., García-Silva, J., del Pozo, J., Yebra, M.T., Cuevas, J., and Contreras, F. (1999). Syphilis in an HIV infected patient misdiagnosed as leprosy. J. Cutan. Pathol. 26, 51–54.

32. Bruisten, S.M. (2012). Protocols for detection and typing of Treponema pallidum using PCR methods. Methods Mol. Biol. 903, 141–167.

33. Grillová, L., Bawa, T., Mikalová, L., Gayet-Ageron, A., Nieselt, K., Strouhal, M., Sednaoui, P., Ferry, T., Cavassini, M., Lautenschlager, S., et al. (2018). Molecular characterization of Treponema pallidum subsp. pallidum in Switzerland and France with a new multilocus sequence typing scheme. PLoS ONE 13, e0200773.

34. Hudson, E.H. (1965). Treponematosis and man's social evolution. Am. Anthropol. 67, 885–901.

35. Powell, M.L., and Cook, D.C. (2005). The Myth of Syphilis: The Natural History of Treponematosis in North America (University Press of Florida).

36. Centurion-Lara, A., Molini, B.J., Godornes, C., Sun, E., Hevner, K., Van Voorhis, W.C., and Lukehart, S.A. (2006). Molecular differentiation of Treponema pallidum subspecies. J. Clin. Microbiol. 44, 3377–3380.

37. Mikalová, L., Strouhal, M., Čejková, D., Zobaníková, M., Pospíšilová, P., Norris, S.J., Sodergren, E., Weinstock, G.M., and Šmajs, D. (2010). Genome analysis of Treponema pallidum subsp. pallidum and subsp. pertenue strains: most of the genetic differences are localized in six regions. PLoS ONE 5, e15713.

38. Gray, R.R., Mulligan, C.J., Molini, B.J., Sun, E.S., Giacani, L., Godornes, C., Kitchen, A., Lukehart, S.A., and Centurion-Lara, A. (2006). Molecular evolution of the tprC, D, I, K, G, and J genes in the pathogenic genus Treponema. Mol. Biol. Evol. 23, 2220–2233.

39. Ho, E.L., and Lukehart, S.A. (2011). Syphilis: using modern approaches to understand an old disease. J. Clin. Invest. 121, 4584–4592.

40. Mulligan, C.J., Norris, S.J., and Lukehart, S.A. (2008). Molecular studies in Treponema pallidum evolution: toward clarity? PLoS Negl. Trop. Dis. 2, e184.

41. Arora, N., Schuenemann, V.J., Jäger, G., Peltzer, A., Seitz, A., Herbig, A., Strouhal, M., Grillová, L., Sánchez-Busó, L., Kühnert, D., et al. (2016). Origin of modern syphilis and emergence of a pandemic Treponema pallidum cluster. Nat. Microbiol. 2, 16245.

42. de Melo, F.L., de Mello, J.C.M., Fraga, A.M., Nunes, K., and Eggers, S. (2010). Syphilis at the crossroad of phylogenetics and paleopathology. PLoS Negl. Trop. Dis. 4, e575.

43. Cui, Y., Yu, C., Yan, Y., Li, D., Li, Y., Jombart, T., Weinert, L.A., Wang, Z., Guo, Z., Xu, L., et al. (2013). Historical variations in mutation rate in an epidemic pathogen, Yersinia pestis. Proc. Natl. Acad. Sci. USA 110, 577–582.

44. Spyrou, M.A., Bos, K.I., Herbig, A., and Krause, J. (2019). Ancient pathogen genomics as an emerging tool for infectious disease research. Nat. Rev. Genet. 20, 323–340.

45. Bos, K.I., Schuenemann, V.J., Golding, G.B., Burbano, H.A., Waglechner, N., Coombes, B.K., McPhee, J.B., DeWitte, S.N., Meyer, M., Schmedes, S., et al. (2011). A draft genome of Yersinia pestis from victims of the Black Death. Nature 478, 506–510.

46. Schuenemann, V.J., Singh, P., Mendum, T.A., Krause-Kyora, B., Jäger, G., Bos, K.I., Herbig, A., Economou, C., Benjak, A., Busso, P., et al. (2013). Genome-wide comparison of medieval and modern Mycobacterium leprae. Science 341, 179–183.

47. Bos, K.I., Harkins, K.M., Herbig, A., Coscolla, M., Weber, N., Comas, I., Forrest, S.A., Bryant, J.M., Harris, S.R., Schuenemann, V.J., et al. (2014). Pre-Columbian mycobacterial genomes reveal seals as a source of New World human tuberculosis. Nature 514, 494–497.

48. Fraser, C.M., Norris, S.J., Weinstock, G.M., White, O., Sutton, G.G., Dodson, R., Gwinn, M., Hickey, E.K., Clayton, R., Ketchum, K.A., et al. (1998). Complete genome sequence of Treponema pallidum, the syphilis spirochete. Science 281, 375–388.

49. Bouwman, A.S., and Brown, T.A. (2005). The limits of biomolecular palaeopathology: ancient DNA cannot be used to study venereal syphilis. J. Archaeol. Sci. 32, 703–713.

50. von Hunnius, T.E., Yang, D., Eng, B., Waye, J.S., and Saunders, S.R. (2007). Digging deeper into the limits of ancient DNA research on syphilis. J. Archaeol. Sci. 34, 2091–2100.

51. Montiel, R., Solórzano, E., Díaz, N., Álvarez-Sandoval, B.A., González-Ruiz, M., Cañadas, M.P., Simões, N., Isidro, A., and Malgosa, A. (2012). Neonate human remains: a window of opportunity to the molecular study of ancient syphilis. PLoS ONE 7, e36371.

52. Schuenemann, V.J., Kumar Lankapalli, A., Barquera, R., Nelson, E.A., Iraíz Hernández, D., Acuña Alonzo, V., Bos, K.I., Márquez Morfín, L., Herbig, A., and Krause, J. (2018). Historic Treponema pallidum genomes from colonial Mexico retrieved from archaeological remains. PLoS Negl. Trop. Dis. 12, e0006447.

53. Hofreiter, M., Paijmans, J.L.A., Goodchild, H., Speller, C.F., Barlow, A., Fortes, G.G., Thomas, J.A., Ludwig, A., and Collins, M.J. (2015). The future of ancient DNA: technical advances and conceptual shifts. BioEssays 37, 284–293.

54. Mitchell, P.D., and Brickley, M. (2017). Updated Guidelines to the Standards for Recording Human Remains (Institute of Field Archaeologists).

55. Salo, K. (2007). Osteologinen Analyysi. Porvoo, Porvoon Kirkko 2007 (Archives of the National Board of Antiquities in Finland).

56. Crabtree, J., Agrawal, S., Mahurkar, A., Myers, G.S., Rasko, D.A., and White, O. (2014). Circleator: flexible circular visualization of genome-associated data with BioPerl and SVG. Bioinformatics 30, 3125–3127.

57. Etu-Sihvola, H., Bocherens, H., Drucker, D.G., Junno, A., Mannermaa, K., Oinonen, M., Uusitalo, J., and Arppe, L. (2019). The dIANA database–resource for isotopic paleodietary research in the Baltic Sea area. J. Archaeol. Sci. Rep. 24, 1003–1013.

58. Oinonen, M., Alenius, T., Arppe, L., Bocherens, H., Etu-Sihvola, H., Helama, S., Huhtamaa, H., Lahtinen, M., Mannermaa, K., Onkamo, P., et al. (2020). Buried in water, burdened by nature-Resilience carried the Iron Age people through Fimbulvinter. PLoS ONE 15, e0231787.

59. Hodges, E., Rooks, M., Xuan, Z., Bhattacharjee, A., Benjamin Gordon, D., Brizuela, L., Richard McCombie, W., and Hannon, G.J. (2009). Hybrid selection of discrete genomic intervals on custom-designed microarrays for massively parallel sequencing. Nat. Protoc. 4, 960–974.

60. Briggs, A.W., Stenzel, U., Johnson, P.L.F., Green, R.E., Kelso, J., Prüfer, K., Meyer, M., Krause, J., Ronan, M.T., Lachmann, M., and Pääbo, S. (2007). Patterns of damage in genomic DNA sequences from a Neandertal. Proc. Natl. Acad. Sci. USA 104, 14616–14621.

61. Sawyer, S., Krause, J., Guschanski, K., Savolainen, V., and Pääbo, S. (2012). Temporal patterns of nucleotide misincorporations and DNA fragmentation in ancient DNA. PLoS ONE 7, e34131.

62. Briggs, A.W., Stenzel, U., Meyer, M., Krause, J., Kircher, M., and Pääbo, S. (2010). Removal of deaminated cytosines and detection of in vivo methylation in ancient DNA. Nucleic Acids Res. 38, e87.

63. Maricic, T., Whitten, M., and Pääbo, S. (2010). Multiplexed DNA sequence capture of mitochondrial genomes using PCR products. PLoS ONE 5, e14004.

64. Weissensteiner, H., Pacher, D., Kloss-Brandstätter, A., Forer, L., Specht, G., Bandelt, H.-J., Kronenberg, F., Salas, A., and Schönherr, S. (2016). HaploGrep 2: mitochondrial haplogroup classification in the era of high-throughput sequencing. Nucleic Acids Res. 44 (W1), W58–W63.

65. van Oven, M., and Kayser, M. (2009). Updated comprehensive phylogenetic tree of global human mitochondrial DNA variation. Hum. Mutat. 30, E386–E394.

66. Renaud, G., Slon, V., Duggan, A.T., and Kelso, J. (2015). Schmutzi: estimation of contamination and endogenous mitochondrial consensus calling for ancient DNA. Genome Biol. 16, 224.

67. Mittnik, A., Wang, C.-C., Svoboda, J., and Krause, J. (2016). A molecular approach to the sexing of the triple burial at the upper Paleolithic site of Dolní Věstonice. PLoS ONE 11, e0163019.

68. Skoglund, P., Storå, J., Götherström, A., and Jakobsson, M. (2013). Accurate sex identification of ancient human remains using DNA shotgun sequencing. J. Archaeol. Sci. *40*, 4477–4482.

69. Peltzer, A., Jäger, G., Herbig, A., Seitz, A., Kniep, C., Krause, J., and Nieselt, K. (2016). EAGER: efficient ancient genome reconstruction. Genome Biol. *17*, 60.

70. Giacani, L., Jeffrey, B.M., Molini, B.J., Le, H.T., Lukehart, S.A., Centurion-Lara, A., and Rockey, D.D. (2010). Complete genome sequence and annotation of the Treponema pallidum subsp. pallidum Chicago strain. J. Bacteriol. *192*, 2645–2646.

71. Zobaníková, M., Mikolka, P., Cejková, D., Pospíšilová, P., Chen, L., Strouhal, M., Qin, X., Weinstock, G.M., and Smajs, D. (2012). Complete genome sequence of Treponema pallidum strain DAL-1. Stand. Genomic Sci. *7*, 12–21.

72. Cejková, D., Zobaníková, M., Chen, L., Pospíšilová, P., Strouhal, M., Qin, X., Mikalová, L., Norris, S.J., Muzny, D.M., Gibbs, R.A., et al. (2012). Whole genome sequences of three Treponema pallidum ssp. pertenue strains: yaws and syphilis treponemes differ in less than 0.2% of the genome sequence. PLoS Negl. Trop. Dis. *6*, e1471.

73. Pĕtrošová, H., Zobaníková, M., Čejková, D., Mikalová, L., Pospíšilová, P., Strouhal, M., Chen, L., Qin, X., Muzny, D.M., Weinstock, G.M., and Šmajs, D. (2012). Whole genome sequence of Treponema pallidum ssp. pallidum, strain Mexico A, suggests recombination between yaws and syphilis strains. PLoS Negl. Trop. Dis. *6*, e1832.

74. Zobaníková, M., Strouhal, M., Mikalová, L., Cejková, D., Ambrožová, L., Pospíšilová, P., Fulton, L.L., Chen, L., Sodergren, E., Weinstock, G.M., and Smajs, D. (2013). Whole genome sequence of the Treponema Fribourg-Blanc: unspecified simian isolate is highly similar to the yaws subspecies. PLoS Negl. Trop. Dis. *7*, e2172.

75. Pĕtrošová, H., Pospíšilová, P., Strouhal, M., Čejková, D., Zobaníková, M., Mikalová, L., Sodergren, E., Weinstock, G.M., and Šmajs, D. (2013). Resequencing of Treponema pallidum ssp. pallidum strains Nichols and SS14: correction of sequencing errors resulted in increased separation of syphilis treponeme subclusters. PLoS ONE *8*, e74319.

76. Staudová, B., Strouhal, M., Zobaníková, M., Cejková, D., Fulton, L.L., Chen, L., Giacani, L., Centurion-Lara, A., Bruisten, S.M., Sodergren, E., et al. (2014). Whole genome sequence of the Treponema pallidum subsp. endemicum strain Bosnia A: the genome is related to yaws treponemes but contains few loci similar to syphilis treponemes. PLoS Negl. Trop. Dis. *8*, e3261.

77. Giacani, L., Iverson-Cabral, S.L., King, J.C.K., Molini, B.J., Lukehart, S.A., and Centurion-Lara, A. (2014). Complete Genome Sequence of the Treponema pallidum subsp. pallidum Sea81-4 Strain. Genome Announc. *2*, e00333-14.

78. Sun, J., Meng, Z., Wu, K., Liu, B., Zhang, S., Liu, Y., Wang, Y., Zheng, H., Huang, J., and Zhou, P. (2016). Tracing the origin of *Treponema pallidum* in China using next-generation sequencing. Oncotarget *7*, 42904–42918.

79. Paradis, E., and Schliep, K. (2019). ape 5.0: an environment for modern phylogenetics and evolutionary analyses in R. Bioinformatics *35*, 526–528.

80. Galili, T. (2015). dendextend: an R package for visualizing, adjusting and comparing trees of hierarchical clustering. Bioinformatics *31*, 3718–3720.

81. Duchêne, S., Duchêne, D., Holmes, E.C., and Ho, S.Y.W. (2015). The performance of the date-randomization test in phylogenetic analyses of time-structured virus data. Mol. Biol. Evol. *32*, 1895–1906.

82. Bouckaert, R., Vaughan, T.G., Barido-Sottani, J., Duchêne, S., Fourment, M., Gavryushkina, A., Heled, J., Jones, G., Kühnert, D., De Maio, N., et al. (2019). BEAST 2.5: an advanced software platform for Bayesian evolutionary analysis. PLoS Comput. Biol. *15*, e1006650.

83. Navascués, M., and Emerson, B.C. (2009). Elevated substitution rate estimates from ancient DNA: model violation and bias of Bayesian methods. Mol. Ecol. *18*, 4390–4397.

84. Meyer, A.G., Spielman, S.J., Bedford, T., and Wilke, C.O. (2015). Time dependence of evolutionary metrics during the 2009 pandemic influenza virus outbreak. Virus Evol. *1*, vev006.

85. Ho, S.Y.W., Duchêne, S., Molak, M., and Shapiro, B. (2015). Time-dependent estimates of molecular evolutionary rates: evidence and causes. Mol. Ecol. *24*, 6007–6012.

86. Düx, A., Lequime, S., Patrono, L.V., Vrancken, B., Boral, S., Gogarten, J.F., Hilbig, A., Horst, D., Merkel, K., Prepoint, B., et al. (2020). Measles virus and rinderpest virus divergence dated to the sixth century BCE. Science *368*, 1367–1370.

87. Weinstock, G.M., Hardham, J.M., McLeod, M.P., Sodergren, E.J., and Norris, S.J. (1998). The genome of Treponema pallidum: new light on the agent of syphilis. FEMS Microbiol. Rev. *22*, 323–332.

88. Radolf, J.D., Deka, R.K., Anand, A., Šmajs, D., Norgard, M.V., and Yang, X.F. (2016). Treponema pallidum, the syphilis spirochete: making a living as a stealth pathogen. Nat. Rev. Microbiol. *14*, 744–759.

89. Morton, R.S. (1964). The button scurvy of Ireland: postscript of the MSSVD meeting in Dublin, May 29 and 30, 1964. Br. J. Vener. Dis. *40*, 271–272.

90. Morton, R.S. (1967). The sibbens of Scotland. Med. Hist. *11*, 374–380.

91. Morton, R.S. (1968). Another look at the Morbus Gallicus. Postscript to the meeting of the Medical Society for the Study of Venereal Diseases, Geneva, May 26-28, 1967. Br. J. Vener. Dis. *44*, 174–177.

92. Achtman, M. (2008). Evolution, population structure, and phylogeography of genetically monomorphic bacterial pathogens. Annu. Rev. Microbiol. *62*, 53–70.

93. Hoeppli, R. (1969). Parasitic diseases in Africa and the Western Hemisphere. Early documentation and transmission by the slave trade. Acta Trop. Suppl. *10*, 1–240.

94. Noda, A.A., Grillová, L., Lienhard, R., Blanco, O., Rodríguez, I., and Šmajs, D. (2018). Bejel in Cuba: molecular identification of Treponema pallidum subsp. endemicum in patients diagnosed with venereal syphilis. Clin. Microbiol. Infect. *24*, 1210.e1–1210.e5.

95. Mikalová, L., Strouhal, M., Oppelt, J., Grange, P.A., Janier, M., Benhaddou, N., Dupin, N., and Šmajs, D. (2017). Human Treponema pallidum 11q/j isolate belongs to subsp. endemicum but contains two loci with a sequence in TP0548 and TP0488 similar to subsp. pertenue and subsp. pallidum, respectively. PLoS Negl. Trop. Dis. *11*, e0005434.

96. Ilagan, N.B., Weyhing, B., Liang, K.C., Womack, S.J., and Shankaran, S. (1993). Congenital syphilitic skeletal manifestations in a premature infant revisited. Clin. Pediatr. (Phila.) *32*, 312–313.

97. Antal, G.M., Lukehart, S.A., and Meheus, A.Z. (2002). The endemic treponematoses. Microbes Infect. *4*, 83–94.

98. Meyer, M., and Kircher, M. (2010). Illumina sequencing library preparation for highly multiplexed target capture and sequencing. Cold Spring Harb. Protoc. *2010*, pdb.prot5448.

99. Broad Institute (2019). Picard tools. http://broadinstitute.github.io/picard/.

100. Jónsson, H., Ginolhac, A., Schubert, M., Johnson, P.L.F., and Orlando, L. (2013). mapDamage2.0: fast approximate Bayesian estimates of ancient DNA damage parameters. Bioinformatics *29*, 1682–1684.

101. Van der Auwera, G.A., Carneiro, M.O., Hartl, C, Poplin, R., Del Angel, G., Levy-Moonshine, A., Jordan, T., Shakir, K., Roazen, D., Thibault, J., et al. (2013). From FastQ data to high confidence variant calls: the Genome Analysis Toolkit best practices pipeline. Curr. Protoc. Bioinformatics *43*, 11.10.1–11.10.33.

102. Herbig, A. (2020). MultiVCFAnalyzer. https://github.com/alexherbig/MultiVCFAnalyzer.

103. Quinlan, A.R., and Hall, I.M. (2010). BEDTools: a flexible suite of utilities for comparing genomic features. Bioinformatics *26*, 841–842.

104. Wickham, H. (2009). ggplot2: Elegant Graphics for Data Analysis (Springer).

105. Wickham, H. (2016). ggplot2: Elegant Graphics for Data Analysis (Springer).

106. R Studio Team (2015). RStudio: integrated development for R (RStudio).

107. Kroepelin, A. (2020). SNP_Evaluation (Github). https://github.com/andreasKroepelin/SNP_Evaluation.

108. Keller, M., Spyrou, M.A., Scheib, C.L., Neumann, G.U., Kröpelin, A., Haas-Gebhard, B., Päffgen, B., Haberstroh, J., Ribera i Lacomba, A., Raynaud, C., et al. (2019). Ancient Yersinia pestis genomes from across Western Europe reveal early diversification during the First Pandemic (541–750). Proc. Natl. Acad. Sci. USA 116, 12363–12372.

109. Andrews, S. (2010). FastQC: a quality control tool for high throughput sequence data. https://www.bioinformatics.babraham.ac.uk/projects/fastqc/.

110. Nguyen, L.-T., Schmidt, H.A., von Haeseler, A., and Minh, B.Q. (2015). IQ-TREE: a fast and effective stochastic algorithm for estimating maximum-likelihood phylogenies. Mol. Biol. Evol. 32, 268–274.

111. Stamatakis, A. (2014). RAxML version 8: a tool for phylogenetic analysis and post-analysis of large phylogenies. Bioinformatics 30, 1312–1313.

112. Schubert, M., Lindgreen, S., and Orlando, L. (2016). AdapterRemoval v2: rapid adapter trimming, identification, and read merging. BMC Res. Notes 9, 88.

113. Rambaut, A., Drummond, A.J., Xie, D., Baele, G., and Suchard, M.A. (2018). Posterior summarization in Bayesian phylogenetics using Tracer 1.7. Syst. Biol. 67, 901–904.

114. Yu, G., Smith, D.K., Zhu, H., Guan, Y., and Lam, T.T.-Y. (2017). GGTREE: an R package for visualization and annotation of phylogenetic trees with their covariates and other associated data. Methods Ecol. Evol. 8, 28–36.

115. Larsson, A. (2014). AliView: a fast and lightweight alignment viewer and editor for large datasets. Bioinformatics 30, 3276–3278.

116. Knapas, M.T. (1987). Den medeltida kyrkan i Borgå, forskningsrön och nya alternativ. Finskt Museum, 64–86.

117. Salo, K.H. (2016). Health in Southern Finland: bioarchaeological analysis of 555 skeletons excavated from nine cemeteries (11th-19th century AD). PhD thesis (University of Helsinki).

118. Hiekkanen, M. (2003). Suomen kivikirkot keskiajalla (Otava).

119. Pihlman, S. (1992). Begravningar i Åbo under slutet av 1500-talet och början av 1600-talet, Tolkningsproblem kring Helgeandskyrkans gravar. Finskt Museum, 59–99.

120. Pinhasi, R., Fernandes, D., Sirak, K., Novak, M., Connell, S., Alpaslan-Roodenberg, S., Gerritsen, F., Moiseyev, V., Gromov, A., Raczky, P., et al. (2015). Optimal ancient DNA yields from the inner ear part of the human petrous bone. PLoS ONE 10, e0129102.

121. Översti, S., Majander, K., Salmela, E., Salo, K., Arppe, L., Belskiy, S., Etu-Sihvola, H., Laakso, V., Mikkola, E., Pfrengle, S., et al. (2019). Human mitochondrial DNA lineages in Iron-Age Fennoscandia suggest incipient admixture and eastern introduction of farming-related maternal ancestry. Sci. Rep. 9, 16883.

122. Ascough, P., Cook, G., and Dugmore, A. (2005). Methodological approaches to determining the marine radiocarbon reservoir effect. Prog. Phys. Geogr. 29, 532–547.

123. Longin, R. (1971). New method of collagen extraction for radiocarbon dating. Nature 230, 241–242.

124. Berglund, B.E., Hakansson, S., and Lagerlund, E. (1976). Radiocarbon-dated mammoth (Mammuthus primigenius Blumenbach) finds in South Sweden. Boreas 5, 177–191.

125. van Klinken, G.J. (1999). Bone collagen quality indicators for palaeodietary and radiocarbon measurements. J. Archaeol. Sci. 26, 687–695.

126. Slota, P.J., Jull, A.J.T., Linick, T.W., and Toolin, L.J. (1987). Preparation of small samples for ^{14}C accelerator targets by catalytic reduction of CO. Radiocarbon 29, 303–306.

127. Palonen, V., Pesonen, A., Herranen, T., Tikkanen, P., and Oinonen, M. (2013). HASE–The Helsinki adaptive sample preparation line. Nucl. Instrum. Methods Phys. Res. B 294, 182–184.

128. Tikkanen, P., Palonen, V., Jungner, H., and Keinonen, J. (2004). AMS facility at the University of Helsinki. Nucl. Instrum. Methods Phys. Res. B 223-224, 35–39.

129. Fernandes, R., Millard, A.R., Brabec, M., Nadeau, M.-J., and Grootes, P. (2014). Food reconstruction using isotopic transferred signals (FRUITS): a Bayesian model for diet reconstruction. PLoS ONE 9, e87436.

130. Bronk Ramsey, C., Higham, T.F.G., Brock, F., Baker, D., and Ditchfield, P. (2009). Radiocarbon dates from the Oxford AMS system: archaeometry datelist 33. Archaeometry 51, 323–349.

131. Reimer, P.J., Reimer, R.W., and Blaauw, M. (2013). Radiocarbon dating | Calibration of the ^{14}C record. In Encyclopedia of Quaternary Science, Second Edition (Elsevier), pp. 345–352.

132. Dabney, J., Knapp, M., Glocke, I., Gansauge, M.-T., Weihmann, A., Nickel, B., Valdiosera, C., García, N., Pääbo, S., Arsuaga, J.-L., and Meyer, M. (2013). Complete mitochondrial genome sequence of a Middle Pleistocene cave bear reconstructed from ultrashort DNA fragments. Proc. Natl. Acad. Sci. USA 110, 15758–15763.

133. Kircher, M., Sawyer, S., and Meyer, M. (2012). Double indexing overcomes inaccuracies in multiplex sequencing on the Illumina platform. Nucleic Acids Res. 40, e3.

134. Gansauge, M.-T., and Meyer, M. (2014). Selective enrichment of damaged DNA molecules for ancient genome sequencing. Genome Res. 24, 1543–1549.

135. Gansauge, M.-T., and Meyer, M. (2013). Single-stranded DNA library preparation for the sequencing of ancient or damaged DNA. Nat. Protoc. 8, 737–748.

136. DePristo, M.A., Banks, E., Poplin, R., Garimella, K.V., Maguire, J.R., Hartl, C., Philippakis, A.A., del Angel, G., Rivas, M.A., Hanna, M., et al. (2011). A framework for variation discovery and genotyping using next-generation DNA sequencing data. Nat. Genet. 43, 491–498.

137. Johnson, M., Zaretskaya, I., Raytselis, Y., Merezhuk, Y., McGinnis, S., and Madden, T.L. (2008). NCBI BLAST: a better web interface. Nucleic Acids Res. 36, W5–W9.

138. Strimmer, K., and von Haeseler, A. (1997). Likelihood-mapping: a simple method to visualize phylogenetic content of a sequence alignment. Proc. Natl. Acad. Sci. USA 94, 6815–6819.

139. Strimmer, K., and Rambaut, A. (2002). Inferring confidence sets of possibly misspecified gene trees. Proc. Biol. Sci. 269, 137–142.

140. Kumar, S., Stecher, G., and Tamura, K. (2016). MEGA7: molecular evolutionary genetics analysis version 7.0 for bigger datasets. Mol. Biol. Evol. 33, 1870–1874.

141. Centurion-Lara, A., LaFond, R.E., Hevner, K., Godornes, C., Molini, B.J., Van Voorhis, W.C., and Lukehart, S.A. (2004). Gene conversion: a mechanism for generation of heterogeneity in the tprK gene of Treponema pallidum during infection. Mol. Microbiol. 52, 1579–1596.

142. LaFond, R.E., Centurion-Lara, A., Godornes, C., Van Voorhis, W.C., and Lukehart, S.A. (2006). TprK sequence diversity accumulates during infection of rabbits with Treponema pallidum subsp. pallidum Nichols strain. Infect. Immun. 74, 1896–1906.

143. Centurion-Lara, A., Giacani, L., Godornes, C., Molini, B.J., Brinck Reid, T., and Lukehart, S.A. (2013). Fine analysis of genetic diversity of the tpr gene family among treponemal species, subspecies and strains. PLoS Negl. Trop. Dis. 7, e2222.

144. Strouhal, M., Mikalová, L., Haviernik, J., Knauf, S., Bruisten, S., Noordhoek, G.T., Oppelt, J., Čejková, D., and Šmajs, D. (2018). Complete genome sequences of two strains of Treponema pallidum subsp. pertenue from Indonesia: Modular structure of several treponemal genes. PLoS Negl. Trop. Dis. 12, e0006867.

145. Addetia, A., Tantalo, L.C., Lin, M.J., Xie, H., Huang, M.-L., Marra, C.M., and Greninger, A.L. (2020). Comparative genomics and full-length Tprk profiling of Treponema pallidum subsp. pallidum reinfection. PLoS Negl. Trop. Dis. 14, e0007921.

146. Fieldsteel, A.H., Stout, J.G., and Becker, F.A. (1979). Comparative behavior of virulent strains of Treponema pallidum and Treponema

pertenue in gradient cultures of various mammalian cells. Infect. Immun. *24*, 337–345.

147. Hampp, E.G. (1951). Preservation of viability and pathogenicity of the Nichols' rabbit strain of Treponema pallidum by freeze drying. Public Health Rep. *66*, 501–506.

148. Sandok, P.L., Knight, S.T., and Jenkin, H.M. (1976). Examination of various cell culture techniques for co-incubation of virulent Treponema pallidum (Nichols I strain) under anaerobic conditions. J. Clin. Microbiol. *4*, 360–371.

149. Navascués, M., Depaulis, F., and Emerson, B.C. (2010). Combining contemporary and ancient DNA in population genetic and phylogeographical studies. Mol. Ecol. Resour. *10*, 760–772.

150. Rieux, A., and Balloux, F. (2016). Inferences from tip-calibrated phylogenies: a review and a practical guide. Mol. Ecol. *25*, 1911–1924.

151. Murray, G.G.R., Wang, F., Harrison, E.M., Paterson, G.K., Mather, A.E., Harris, S.R., Holmes, M.A., Rambaut, A., and Welch, J.J. (2016). The effect of genetic structure on molecular dating and tests for temporal signal. Methods Ecol. Evol. *7*, 80–89.

152. Hasegawa, M., Kishino, H., and Yano, T. (1985). Dating of the human-ape splitting by a molecular clock of mitochondrial DNA. J. Mol. Evol. *22*, 160–174.

153. Yang, Z. (1994). Maximum likelihood phylogenetic estimation from DNA sequences with variable rates over sites: approximate methods. J. Mol. Evol. *39*, 306–314.

154. Drummond, A.J., Rambaut, A., Shapiro, B., and Pybus, O.G. (2005). Bayesian coalescent inference of past population dynamics from molecular sequences. Mol. Biol. Evol. *22*, 1185–1192.

155. Drummond, A.J., Ho, S.Y.W., Phillips, M.J., and Rambaut, A. (2006). Relaxed phylogenetics and dating with confidence. PLoS Biol. *4*, e88.

156. Andrades Valtueña, A., Mittnik, A., Key, F.M., Haak, W., Allmäe, R., Belinskij, A., Daubaras, M., Feldman, M., Jankauskas, R., Janković, I., et al. (2017). The Stone Age plague and its persistence in Eurasia. Curr. Biol. *27*, 3683–3691.e8.

157. Radolf, J.D., and Kumar, S. (2018). The Treponema pallidum outer membrane. Curr. Top. Microbiol. Immunol. *415*, 1–38.

158. Bouckaert, R., Heled, J., Kühnert, D., Vaughan, T., Wu, C.-H., Xie, D., Suchard, M.A., Rambaut, A., and Drummond, A.J. (2014). BEAST 2: a software platform for Bayesian evolutionary analysis. PLoS Comput. Biol. *10*, e1003537.

STAR★METHODS

KEY RESOURCES TABLE

REAGENT or RESOURCE	SOURCE	IDENTIFIER
Chemicals, Peptides, and Recombinant Proteins		
EDTA solution, pH 8.0, 0.5 M	AppliChem	Cat#A4892,1000
1x Tris-EDTA pH 8.0	AppliChem	Cat#A8569,0500
Proteinase K, Molecular Biology Grade, 1600 Units	BioConcept AG	Cat#P8107S
Guanidine hydrochloride	Sigma-Aldrich	Cat#G3272-500 g
3M Sodium Acetate pH 5.5	Sigma-Aldrich	Cat#S7899-500ML
Ethanol	Merck	Cat#1009832511
Isopropanol	Merck	Cat#1070222511
BSA Molecular Biology Grade (conc. 20 mg/ml), 12 mg	BioConcept AG	Cat#B9000S
Adenosine 5′-Triphosphate (ATP), 1 ml	BioConcept AG	Cat#P0756S
Bst 2.0 DNA Polymerase, 1600 units	BioConcept AG	Cat#M0275S
dNTPs 25 mM	Thermo Scientific	Cat#R1121
Quick Ligation Kit, 150 reactions	BioConcept AG	Cat#M2200L
T4 DNA Polymerase, 150 units	BioConcept AG	Cat#M0203S
T4 Polynucleotide Kinase, 500 units	BioConcept AG	Cat#M0201S
PfuTurbo Cx Hotstart DNA POL, 1000 U	Agilent Technologies	Cat#600414
Tween 20	Sigma-Aldrich	Cat#P9416-50ML
User Enzyme, 250 units	BioConcept AG	Cat#M5505 L
Water Molecular grade	Sigma-Aldrich	Cat#W4502-1L
Water Chromasolv Plus for HPLC	Sigma-Aldrich	Cat#34877-2.5L
PB-Buffer	QIAGEN	Cat#19066
NEB Buffer 2 (10X)	BioConcept AG	Cat#B7002S
Isothermal Buffer (10x)	BioConcept AG	Cat#B0537S
NaCl solution, 5 M	Sigma-Aldrich	Cat#S5150-1L
SDS solution, 20%	Ambion	Cat#AM9820
SSC buffer, 20X	Ambion	Cat#AM9770
Tris-HCl solution, pH 8, 1M	AppliChem	Cat#A4577,0500
FastAP thermosensitive alkaline phosphatase	ThermoScientific	Cat#EF0651
PEG-4000 solution, 50% (wt/vol)	Sigma-Aldrich	Cat#89782-100ML-F
Dynabeads MyOne streptavidin C1	Life Technologies	Cat#65001
dNTP mix 25mM each	ThermoScientific	Cat#R1121
T4 DNA Polymerase	ThermoScientific	Cat#EP0062
T4 DNA Ligase	ThermoScientific	Cat#EL0012
pUC19	NEB	Cat#N3041S
T4 DNA Ligase, HC (30 U/μL)	ThermoScientific	Cat#EL0013
T4 DNA Ligase (5 U/μL)	ThermoScientific	Cat#EL0012
T4 RNA Ligase Reaction Buffer	BioConcept AG	Cat#B0216L
DNA Polymerase I, Large (Klenow) Fragment (5000U/ml)	BioConcept AG	Cat#M0210L
T4 Polynucleotide Kinase (10U/μl)	ThermoScientific	Cat#EK0032
ATP Solution (100 mM)-0.25 mL	Thermo Fisher / Life Technologies Europe BV	Cat#R0441
Klenow Fragment (10 U/μL)-1,500 units	Thermo Fisher / Life Technologies Europe BV	Cat#EP0052
Agilent Oligo aCGH/Chip-on-Chip Wash Buffer 2, 4L	Agilent	Cat#5188-5222

(Continued on next page)

Continued

REAGENT or RESOURCE	SOURCE	IDENTIFIER
Oligo aCGGH/Chip-onchip Hybridization Kit	Agilent	Cat#5188-5220
Oligo aCGH/ChIP-on-chip Wash Buffer Kit	Agilent	Cat#5188-5226
Agilent Oligo aCGH/Chip-on-Chip Wash Buffer 1, 4L	Agilent	Cat#5188-5221
Amplitaq Gold Kit 1000U mit Puffer + MgCl2	Applied	Cat#4311816
Critical Commercial Assays		
Zymo-Spin V Columns w/ Reservoir	Lucerna Chem AG - Cat.1	Cat#ZYM-C1016-50-50ST
Min Elute PCR Purification Kit	QIAGEN	Cat#28006
SYBR Green PCR Master Mix-2 × 5 mL	Thermo Fisher / Life Technologies Europe BV - Kernsortiment	Cat#4364344
Herculase II Fusion DNA POL, 400 rxn	Agilent Technologies (Schweiz) AG	Cat#600679
D1000 Reagents for 112 samples	Agilent Technologies (Schweiz) AG	Cat#5067-5583
D1000 ScreenTape for 112 samples	Agilent Technologies (Schweiz) AG	Cat#5067-5582
DNA1000 Lab Chip Kit	Agilent	Cat#5067-1504
SureSelect DNA Capture Arrays 1M	Agilent Technologies	Cat#046466
Deposited Data		
T. pallidum aDNA raw data	This study	ENA: PRJEB35855, https://www.ebi.ac.uk/ena/data/view/PRJEB35855
Oligonucleotides		
IS1_adapter.P5 A*C*A*C*TCTTTCCCTACACGACGC TCTTCCG*A*T*C*T	[98]	Sigma Aldrich
IS2_adapter.P7 G*T*G*A*CTGGAGTTCAGACGTGT GCTCTTCCG*A*T*C*T	[98]	Sigma Aldrich
IS3_adapter.P5+P7 A*G*A*T*CGGAA*G*A*G*C	[98]	Sigma Aldrich
IS 7_Short_amp_P5 ACACTCTTTCCCTACACGAC	[98]	Sigma Aldrich
IS 8_short_amp_P7 GTGACTGGAGTTCAGACGTGT	[98]	Sigma Aldrich
IS 5_Reamp_P5 AATGATACGGCGACCACCGA	[98]	Sigma Aldrich
IS 6_Reamp_P7 CAAGCAGAAGACGGCATACGA	[98]	Sigma Aldrich
B04_Blocking Primer GTGACTGGAGTTCAGACGTGTG CTCTTCCGATCT-Phosphat	[98]	Sigma Aldrich
B06_Blocking Primer CAAGCAGAAGACGGCATACGA GAT-Phosphat	[98]	Sigma Aldrich
B08_Blocking Primer GTGTAGATCTCGGTGGTCGCC GTATCATT-Phosphat	[98]	Sigma Aldrich
B10_Blocking Primer GGAAGAGCGTCGTGTAGGGA AAGAATGT-Phosphat	[98]	Sigma Aldrich
B11_Blocking Primer GGAAGAGCGTCGTGTAGGGAA AGAATGT[Phos]	[98]	Sigma Aldrich
Fwd index primer (Extention Primer with Index) CAAG CAGAAGACGGCATACGAGAT-INDEX-GTGACTGGAGTTCAGACGTGT	[98]	Sigma Aldrich
Rvs index Primer (Extention Primer with Index) AATGA TACGGCGACCACCGAGATCTACAC-INDEX-ACACTCTTTCCCTACACGACGCTCTT	[98]	Sigma Aldrich
Software and Algorithms		
EAGER	[69]	https://github.com/apeltzer/EAGER-GUI
MarkDuplicates (Picard) v2.15.0	[99]	http://broadinstitute.github.io/picard/; RRID: SCR_006525

(Continued on next page)

Continued

REAGENT or RESOURCE	SOURCE	IDENTIFIER
MapDamage v.2.0	[100]	https://ginolhac.github.io/mapDamage/; RRID: SCR_001240
GATK UnifiedGenotyper v.3.8.0	[101]	https://software.broadinstitute.org/gatk/; RRID: SCR_001876
MultiVCFAnalyzer	[102]	https://github.com/alexherbig/MultiVCFAnalyzer
BEAST2 v.2.6	[82]	https://www.beast2.org/; RRID: SCR_017307
BEDtools	[103]	http://bedtools.readthedocs.io/en/latest/; RRID: SCR_006646
ggplot2	[104, 105]	http://ggplot2.org/; RRID: SCR_014601
RStudio	[106]	https://rstudio.com/; RRID: SCR_000432
Circleator	[56]	https://github.com/jonathancrabtree/Circleator/; RRID: SCR_002801
SNPEvaluation	[107, 108]	https://github.com/andreasKroepelin/SNP_Evaluation
FastQC	[109]	https://github.com/s-andrews/FastQC/releases; RRID: SCR_014583
IQ-TREE v.1.6.10	[110]	http://www.iqtree.org/
RaxML v. 8.2.12	[111]	https://github.com/stamatak/standard-RAxML
CircularMapper v.1.0	[69]	https://github.com/apeltzer/CircularMapper
AdapterRemoval v.2.2.1	[112]	https://github.com/MikkelSchubert/adapterremoval; RRID: SCR_011834
Tracer v1.7	[113]	http://beast.community/tracer
ggtree	[114]	https://bioconductor.org/packages/release/bioc/html/ggtree.html
AliView 1.21	[115]	https://github.com/AliView
Other		
T. pallidum colonial Mexican aDNA	[52]	ENA: RJEB21276, https://www.ebi.ac.uk/ena/data/view/PRJEB21276
Modern T. pallidum genome set	[41]	SRA: PRJNA313497, https://www.ncbi.nlm.nih.gov/bioproject/?term=PRJNA313497
T. pallidum DAL_1 genome	[71]	GenBank: CP003115.1, https://www.ncbi.nlm.nih.gov/nuccore/CP003115
T. pallidum Nichols genome	[75]	GenBank: NC_021490.2, https://www.ncbi.nlm.nih.gov/nuccore/NC_021490.2
T. pallidum Chicago genome	[70]	GenBank: NC_017268.1, https://www.ncbi.nlm.nih.gov/nuccore/NC_017268.1
T. pallidum SEA81_4 genome	[77]	GenBank: CP003679.1, https://www.ncbi.nlm.nih.gov/nuccore/CP003679.1
T. pallidum P3 genome	[78]	SRA: SRR2996731, https://trace.ncbi.nlm.nih.gov/Traces/sra/?run=SRR2996731
T. pallidum SS14 genome	[75]	GenBank: NC_021508.1, https://www.ncbi.nlm.nih.gov/nuccore/NC_021508.1
T. pallidum Mexico A genome	[73]	GenBank: NC_018722.1, https://www.ncbi.nlm.nih.gov/nuccore/NC_018722.1
T. pallidum Fribourg-Blanc genome	[74]	GenBank: NC_021179.1, https://www.ncbi.nlm.nih.gov/nuccore/NC_021179.1
T. pallidum Gauthier genome	[72]	GenBank: NC_016843.1, https://www.ncbi.nlm.nih.gov/nuccore/NC_016843.1
T. pallidum CDC2 genome	[72]	GenBank: NC_016848.1, https://www.ncbi.nlm.nih.gov/nuccore/NC_016848.1
T. pallidum Samoa D genome	[72]	GenBank: NC_016842.1, https://www.ncbi.nlm.nih.gov/nuccore/NC_016842.1

Continued

REAGENT or RESOURCE	SOURCE	IDENTIFIER
T. pallidum Bosnia A genome	[76]	SRA: SRR3268694, https://www.ncbi.nlm.nih.gov/sra/SRR3268694
T. pallidum PT_SIF1002 genome	Unpublished data	GenBank: NZ_CP016051.1, https://www.ncbi.nlm.nih.gov/nuccore/NZ_CP016051.1

RESOURCE AVAILABILITY

Lead Contact
Additional information and requests for resources and reagents should be directed to and will be fulfilled by the Lead Contact, Verena J. Schuenemann (verena.schuenemann@iem.uzh.ch).

Materials Availability
This study did not generate new unique reagents.

Data and Code Availability
The accession number for the data reported in this paper is ENA: PRJEB35855. The original datasets and code generated during this study are available at DOI: https://doi.org/10.5281/zenodo.3925826. The workflow and scripts for molecular clock dating and date randomisation tests are additionally available at https://github.com/laduplessis/Treponema_pallidum_in_early_modern_Europe.

EXPERIMENTAL MODEL AND SUBJECT DETAILS

Ethical approvals
All ancient human remains used in this study come from archaeological excavations and are over 100 years old. Therefore, they are not subject to the Human Tissue Act (2004) and no ethics approvals are required.

Description of archaeological contexts and sample selection
Porvoo Cathedral burial ground
The stone Dome of Porvoo in Finland gained its status as a Cathedral in 1723 [116], although an earlier, wooden church has been on the site, and the cemetery around it used likely as early as 13th to 14th century on. However, most of the individuals excavated from the site in 2007 were buried in a 17th to 18th century style in coffins, and were relatively wealthy, considering their burial location at the prestigious, southern side of the church. The late timescale is confirmed by the lower bound of the radiocarbon dating of the PD28 individual in 1666 CE, although the upper bound reaches into the modern era (Klaus-Tschira-Archäometrie-Zentrum am Curt-Engelhorn-Zentrum, Mannheim, Germany: MAMS 35328, Figure S1). It is known that the cemetery was formally used until 1789, and the churchyard leveled in 1791, providing a historical limit to date the remains excavated from the site [117,118] .
The Holy Ghost Chapel, Turku
Historical Julin's plot in Turku, Finland, contained the Church of the Holy Ghost and its cemetery. It was also a location of an early hospital for the poor (House of the Holy Ghost). The cemetery was used over at least two hundred years, from the end of the 14th century to the mid-17th century [119]. The remains excavated from the site in 1985 were deposited in the crypt of the Holy Ghost Chapel, located in the Casagrande property later built on the plot. The radiocarbon dating for the individual CHS119 placed the bone material between the years 1443 and 1460 CE (Klaus-Tschira-Archäometrie-Zentrum am Curt-Engelhorn-Zentrum, Mannheim, Germany: MAMS 35325), but the reservoir effect corrections calculated at the Helsinki Natural History Museum Laboratory of Chronology revealed a dual peak pattern of two time windows, one between 1450 and 1525 CE, and another between 1570 and 1630 CE [57, 58] (Figure S1).
St Jacob's cemetery, Tartu
St. Jacob's suburban cemetery in Tartu is archaeologically dated to from the 13th to late 16th centuries. The suburban cemetery was used by lower social strata. Independent radiocarbon dating analyses for the individual SJ219 were produced in two laboratories (Klaus-Tschira-Archäometrie-Zentrum am Curt-Engelhorn-Zentrum, Mannheim, Germany: MAMS 35326 and the AMS laboratory, ETH Zürich: ETH-100446), both of which place the individual in the 15th century (1434-1446 and 1429-1476 CE, respectively, Figure S1). In addition to the bone of individual SJ219, a preserved fragment from her wooden coffin was dated in order to estimate a date that would not be affected by any potential dietary reservoir effect (AMS laboratory, ETH Zürich: ETH-101915). Unfortunately, this dating provided a wider temporal range than that of the human remains from the grave (1463 to 1635 CE). The upper boundary of the wood sample dating was chosen as an upper limit in the BEAST2 analyses to avoid bias from the possible reservoir effect in the bone material.
Gertrude's Infirmary, Kampen
The Kampen sample KM14-7 was radiocarbon dated to 1494-1631 CE (Klaus-Tschira-Archäometrie-Zentrum am Curt-Engelhorn-Zentrum, Mannheim, Germany: MAMS 33918, Figure S1). The sample stems from a collection of disarticulated skeletal material found in a large excavated area within the cemetery of Gertrude's Infirmary in Kampen, the Netherlands. The use of this graveyard

spans from the mid-14th to early 17th century. Reservoir effect corrections are not planned at this time. It is, however, noted from the stable isotope values (δ^{15}N and δ^{13}C) in the bone material, that a marine reservoir effect due to the individual's diet could possibly affect the radiocarbon dates retrieved for the sample.

Altogether nine individuals from Estonian, Finnish and Netherlandic sources were tested for treponemal DNA. (The list of included samples: Porvoo Dome, Porvoo, Finland: grave 28, petrous part of temporal bone; St. Jacob's Cemetery, Tartu, Estonia: individual 219, phalanx and premolar; St. Georges' Cemetery, Tartu, Estonia: individual 34, metacarpal bone and premolar; Holy Ghost Chapel, Turku Finland: individuals 101, molar; 107, molar; 119, premolar; 122, molar; 305, molar; and Gertrude's Infirmary, Kampen, the Netherlands: individual 14, disintegrated tibia fragment N:o 7). Samples confirmed to be positive for the treponemal agent's DNA included the perinatal individual's petrous bone from Porvoo, Finland (PD28), the premolar from Turku, Finland (CHS119), the meta-carpal bone from Tartu, Estonia (SJ219), and the fragment of tibia from Kampen, the Netherlands (KM14-7). The skeletal elements were chosen either due to the visible lesions, or to the individual's perinatal death, indicating a possible congenital case of syphilis. A petrous portion of the skull was used for the perinatal individual from Porvoo, as it is generally the most well-preserved part of the skeleton [120]. Since congenital syphilis is considered to be systemic [96], we expected all of the skeletal elements of this individual to be affected by the potential infection. All the five individuals tested from Turku showed signals of treponemal infection: mulberry molars, bone changes in the skull or lesions in the long bones. The Turku individuals were previously studied for their mitochondrial human DNA and published in a population genetics study [121]. The individuals from the two Tartu sites, St. Jacobs cemetery and St. George's cemetery, were both studied archaeologically and, showing signs of severe infection which affected their skeleton, they were chosen to be tested for treponemal diseases. The Kampen individual is represented by only one fragmented tibia, found dis-articulated from the burial ground at the excavation of Gertrude's Infirmary. The tibia had a periosteal lesion of striated woven bone, also causing a bowing of the bone, which indicates possible treponemal infection in the individual.

METHOD DETAILS

Sample processing

Documentation and UV-irradiation of the bone material for decontamination, as well as laboratory procedures for sampling, DNA extraction, library preparation and library indexing were all conducted in facilities dedicated to ancient DNA work at the University of Tübingen, with necessary precautions taken including protective clothing and minimum contamination-risk working methods.

All post-amplification steps were performed in a laboratory provided by the Department of Toxicology at the University of Tübingen as well as in the post-PCR laboratory of the Paleogenetics Group, Institute of Evolutionary Medicine (IEM), University of Zurich (UZH). DNA sequencing was performed at the sequencing facilities of the Max Planck Institute for the Science of Human History in Jena or at the Functional Genomics Center at the University of Zurich (FGCZ).

Reservoir effect correction of the CHS119 sample

Marine and freshwater reservoir effects can cause an offset in C^{14} ages between contemporaneous remains of humans or animals, depending on whether they relied mainly on terrestrial or aquatic food sources [122]. The protocols for radiocarbon dating and stable isotopic measurements for CHS119 sample at the Laboratory of Chronology, Finnish Natural History Museum, were as follows. The method for collagen extraction was based on the Longin method [123] and followed a previously described protocol by Berglund and colleagues [124]. To check post-mortem alteration, the contents of N and C (wt-%) and the atomic C/N ratio of the collagen were monitored (C-% = 37.4%, N-% = 13.6%, C/N ratio = 3.2) fulfilling the accepted quality criteria for well-preserved collagen i.e., 2.9–3.6 [125].

For radiocarbon analysis, the collagen sample was packed inside a silver cup (Elemental Microanalysis D2001) and the packed sample was combusted with an Elemental Analyzer (Thermo Scientific Flash 2000 NC). The resulting CO_2 was cryogenically trapped and reduced to graphite in the presence of zinc powder and iron catalyst [126] by using the Labview controlled HASE facility [127]. The graphite sample was measured for radiocarbon contents at the Helsinki AMS facility [128]. The result has been normalized for isotopic fractionation by using the δ^{13}C value measured with the AMS facility. Lastly, the radiocarbon date (HeLa-4271) of 383 ± 24 BP was obtained.

Dietary stable isotopic (carbon and nitrogen) ratios were measured from bone collagen parallel to AMS analyses for the sample CHS119 at the Finnish Natural History Museum facility by using EA-IRMS technique. The elemental content and isotopic composition of carbon and nitrogen were measured on a NC2500 elemental analyzer coupled to a Thermo Scientific Delta V Plus isotope ratio mass spectrometer. The raw isotope data were normalized with a two-point calibration using international reference materials with known isotopic compositions (USGS-40, USGS-41). The mean measured raw δ^{13}C and δ^{15}N values for calibration references were −26.7 and −4.7 for USGS-40 and 36.2 and 46.5 for USGS-41, respectively. Replicate analyses of a quality control reference analyzed alongside the unknowns indicate a 1σ internal precision of ≤ 0.1 for both δ^{13}C and δ^{15}N. This process resulted in dietary isotopic values of δ^{13}C = −19.7‰ and δ^{15}N = 12.3‰.

To obtain an estimate for a potential reservoir effect (RE) within the radiocarbon age, dietary modellings with FRUITS software [129] were performed based on an assumption of three food groups (marine, freshwater and terrestrial foods), and adopting the macro-nutrient concentrations, isotopic offsets and the isotopic baseline data [58] from the δIANA database [57] was used for gathering the Northern European isotopic data. The marine isotopic signature and corresponding marine reservoir effect was assumed to come from the vicinity of Finland Proper (Bothnian Sea, Archipelago and its surroundings). It was estimated [58] that this corresponds

to the maximal marine reservoir effect (in marine animals) of 173 ± 41 ^{14}C years. The dietary modeling provided the contribution of bone collagen carbon from such a source and provided means to scale down the potential reservoir age of human bone collagen. Correspondingly, the maximal freshwater reservoir effect (in fish) was estimated as 107 ± 52 ^{14}C years. Eventually, the human bone collagen REs was estimated to be MRE = 28 ± 11 ^{14}C years and FRE = 11 ± 9 ^{14}C years yielding to a RE-corrected radiocarbon age of 345 ± 29 ^{14}C years corresponding to the HeLa-4271 measurement. As the same amount of RE is also assumed for MAMS-35325 measurement (421 ± 18 BP), the same correction was adopted yielding to 383 ± 24 ^{14}C years. Finally, the combined RE-corrected radiocarbon age of 368 ± 19 ^{14}C years was obtained. These ages were calibrated according to Bronk Ramsey et al. [130] and Reimer et al. [131] (Figure S1).

Sampling and DNA extraction

Before extracting DNA from the samples, all surfaces were irradiated with ultraviolet light (UV-irradiated) to minimize potential contamination from modern DNA. DNA extraction was performed according to a well-established extraction protocol for ancient DNA [132]. For DNA extraction, 30-120 mg of bone powder was used per sample. The bone powder was obtained by drilling bone tissue using a dental drill and dental drill bits. For different individuals, variable amounts of extracts were produced. During each extraction, one positive control (ancient cave bear bone powder sample) and one negative control were included for every ten samples. Positive extraction controls were carried along until the indexing of DNA-libraries, and the negative controls were carried through all following experiments and sequenced.

Library preparation

In this study, double-stranded (ds) and single-stranded (ss) DNA-libraries were produced. All DNA library preparation procedures applied in this study are described in the following paragraphs.

Double-stranded DNA library preparation

For the preparation of DNA-libraries 20μl of DNA extract was converted into ds-DNA libraries [133]. For every ten libraries produced, one negative control was used. Negative controls for library preparations were processed in parallel with all following experiments. Sample-specific barcodes (indexes) were added to both ends of the libraries [98]. The indexed libraries were then amplified to reach a minimum DNA concentration of 90ng/μl. The amplification was performed using 1x Herculase II buffer, 0.4 μM IS5 and 0.4 μM IS6 primer [98], Herculase II Fusion DNA Polymerase (Agilent Technologies), 0.25 mM dNTPs (100 mM; 25 mM each dNTP) and 5 μl indexed library as DNA template. Four reactions per library were prepared and the total amplification reaction volume was 100μl. The thermal profile included an initial denaturation for 2 minutes at 95°C and 3-18 cycles, depending on DNA concentration after indexing of the libraries, denaturation for 30 s at 95°C, 30 s annealing at 60°C and a 30 s elongation at 72°C, followed by a final elongation step for 5 minutes at 72°C. All splits of one indexed library were pooled and purified using the QIAGEN MinElute PCR purification kit. The final quantification for all DNA libraries was performed with the Agilent 2100 Bioanalyzer.

Uracil-DNA Glycosylase (UDG) treated double-stranded DNA library preparation

To avoid potential sequencing artifacts caused by the characteristic ancient DNA damage profile [134] additional libraries for genome-wide enrichment were created, namely 30μl of DNA extract was pre-treated with uracil-DNA glycosylase [62]. Controls were also treated accordingly. Sequencing libraries were indexed and amplified as described above.

Single-stranded DNA library preparation

Single-stranded libraries were generated from 20 μL of DNA extract according to established protocols [135]. Two single-stranded libraries were prepared for the four positive individuals. All single-stranded libraries were indexed and amplified with the same experimental procedures as applied and described for the double-stranded DNA libraries. To assess the library concentration, D1000 High Sensitivity ScreenTape was used on an Agilent 2200 Tapestation. All libraries were pooled in equimolar concentration for the genome-wide enrichment step.

Capture techniques
Capture for a first screening for treponemal DNA

For the first screening for *Treponema pallidum* DNA, all double-stranded libraries without UDG treatment for all individuals were pooled. All negative controls were pooled separately. The *T. pallidum* screening was performed using a modified version [41] of the array capture approach originally developed by Hodges and colleagues [59] to enrich the sample libraries for *T. pallidum*-specific DNA. Here, we used arrays designed by Agilent Technology and the blocking oligonucleotides (BO) 4, 6, 8, and 10 [98] in the initial screening and followed the same enrichment procedure as described by Arora and colleagues [41] and Schuenemann and colleagues [52], as follows:

Whole-genome capture

After the analysis of the shotgun screening data from the initial sequencing, UDG-treated double-stranded DNA libraries and single-stranded DNA libraries were produced for samples potentially positive for syphilis and used for whole genome capture. The whole-genome capture was performed as described above using the same array enrichment strategy. In addition to the blocking oligonucleotides for double-stranded libraries, specific blocking oligonucleotides 4, 6, 8, and 11 [98] were used for single-stranded

libraries. The whole-genome enrichment for treponemal DNA was produced in three rounds of array capture and a maximum of two libraries from different individuals were pooled for each array. Enrichment pools were diluted to 10 nMol/L for sequencing.

In-solution capture for KM14-7

An additional in-solution capture procedure was performed for sample KM14-7 to obtain higher coverage. Genome-wide enrichment of single-stranded libraries was performed through custom target enrichment kits (Arbor Bioscience). RNA baits with a length of 60 nucleotides and a 4bp tiling density were designed based on three reference genomes (Nichols, GenBank: CP004010.2, SS14: Gen-Bank CP000805.1, Fribourg Blanc: GenBank CP003902). Five hundred ng library pools were enriched according to the manufacturer's instructions. Captured libraries were amplified in 3 × 100 μL reactions containing 1 unit Herculase II Fusion DNA polymerase (Agilent), 1x Herculase II reaction buffer, 0.25mM dNTPs, 0.4 μM primers IS5 and IS6 [98] and 15 μL library template. The thermal profile was the following: initial denaturation at 95°C for 2 min, 14 cycles of denaturation at 95°C for 30 s, annealing at 60°C for 30 s, and elongation at 72°C for 30 s, followed by a final elongation at 72°C for 5 min. Captured libraries were purified with MinElute spin columns (QIAGEN) and quantified with a D1000 High Sensitivity ScreenTape on an Agilent 2200 TapeStation.

Sequencing

The first two rounds of genome-wide enriched (array enrichment strategy) double-stranded libraries were sequenced at the Max Planck Institute for the Science of Human History in Jena on an Illumina HiSeq 4000 platform with 1*75+8+8 cycles (single-end reads), following the manufacturer's protocols for multiplex sequencing. The third round of genome-wide array capture enrichment for *Treponema pallidum* DNA by double-stranded libraries was sequenced at the Max Planck Institute for the Science of Human History in Jena on an Illumina HiSeq 4000 platform with 2*50+8+8 cycles (paired-end reads), following manufacturer's protocols. In the fourth round of sequencing the single-stranded DNA libraries, enriched by array capture strategy for *Treponema pallidum* DNA, were sequenced. The sequencing was performed on an Illumina NextSeq500 platform 2*75+8+8 cycles (paired-end reads) at the Functional Genomics Center Zurich.

Read processing, mapping and variant calling

The data from the preliminary shotgun-sequencing of the PD28 sample and a screening capture for the samples SJ219, CHS119 and KM14-7 were used to select the four samples in this study as *T. pallidum* positive candidates. The four selected samples then underwent a subsequent enrichment targeted for the genetic sequence of *T. pallidum*. The resulting data was processed as described in the following paragraphs.

The capture data from the sequencing runs were merged sample-wise and data processing was performed using EAGER version 1.92.37 (Efficient Ancient GEnome Reconstruction) [69]. The quality of the sequencing data was assessed using the FastQC [109] and the reads were adaptor trimmed with AdapterRemoval ver. 2.2.1a [112]. Sequencing reads were mapped to a TPA Nichols reference genome (CP004010.2) using CircularMapper version 1.0 [69] with a minimum quality score of 37 and a stringency parameter n = 0.1. Duplicates were removed with MarkDuplicates v2.15.0 [99]. MapDamage version 2.0.6 [100] was used to investigate the damage patterns, which can authenticate the ancient origin of the DNA sequences (Figure S2) and Circleator plots [56] were produced to showcase the different genome coverages among the samples (Figure S3). The Genome Analysis Toolkit (GATK) version 3.8.0 [101, 136] was used to perform SNP calling and generate *vcf.* files for each genome. The same procedure was also employed after mapping reads to the TPE CDC2 genome (CP002375.1), in order to assess potential reference-related biases on the phylogenetic inference.

Genomic dataset and multisequence alignment

We constituted a genomic dataset representative of the extant diversity of *T. pallidum* and including the three previously published ancient genomes from Mexico. Raw sequencing data was gathered for strains that were high-throughput sequenced. The previously exposed procedure was then applied to obtain *vcf.* files for each genome. We used MultiVCFAnalyzer [102] to produce alignments with the following parameters: bases were called if covered by at least two reads with a mapping quality of 30 and a consensus of at least 90% (with the one-read-exception rule implemented in MultiVCFAnalyzer). The resulting alignment was realigned with already assembled genomes (isolates Bosnia A, CDC2, Chicago, Fribourg, Gauthier, Mexico A, PT_SIF1002, SS14, and SEA81_4_1), using AliView version 1.21 [115]. A complete dataset used for the phylogenetic analyses consisted of 26 modern *Treponema pallidum* strains [41, 70–78] including PT_SIF1002 (unpublished, GenBank: NZ_CP016051.1) and all ancient genomes used in this study. For the molecular dating analysis with BEAST2, two highly passaged modern strains (NIC2, Nichols) and the two ancient strains from colonial Mexico [52] (94A and 94B) along with the European ancient genome KM14-7 from this study, were excluded.

SNP quality assessment

Calling SNPs from ancient bacterial DNA data is challenging due to DNA damage, potential environmental contamination and low genome coverage which may lead to the recovery of artifactual genetic variation in reconstructed DNA sequences. This can interfere with all subsequent analyses and, in particular, lead to artificially long branches in phylogenetic trees and impede time-calibrated analyses. Artifactual SNPs resulting from environmental contamination shared between several samples may also lead to biases in inferred phylogenetic tree topologies or generate misleading evidence of genetic recombination.

In order to filter for artifactual SNPs, we used the SNPEvaluation tool [107] as proposed by Keller and colleagues [108]. To generate the required *vcf.* file for genomes generated through Sanger sequencing, we simulated NGS-like reads based on genome assemblies using the tool Genome2Reads (integrated in the EAGER pipeline [69]), which were then mapped to the Nichols and CDC2 reference

genomes according to the previously described procedure. For all newly generated ancient genomes, as well as for all previously published genomes for which the mean sequencing coverage was below 20, we reviewed all unique SNPs (Tables S1 and S2). We also reviewed any SNP shared by less than 6 genomes that had at least one of the following features in a 50-bp window around the SNP: (i) some positions were not covered, (ii) the reference was supported by at least one read or (iii) the coverage changed depending on the mapping stringency (i.e., we compared the initial alignments with "low-stringency" alignments produced with bwa parameter n = 0.01). Any SNP supported by less than four reads was excluded (i.e., N was called at that position) if at least one read supported the reference or if the SNP was "damage-like" (i.e resulting from a C to T or G to A substitution). Furthermore, the specificity of the reads supporting the SNPs was verified by mapping them against the full GenBank database with BLAST [137]. Any SNP supported by reads mapping equally or better to other organisms than *T. pallidum* was excluded. Since many of these false SNPs likely arising from non-specific mapping were located in tRNAs, we excluded all tRNAs from the alignments. The list of excluded positions was written in a gff file (Data S1) and removed from the full alignment (Data S2) generated by MultiVCFAnalyzer using an in-house bash script.

Phylogenetic and recombination analysis

An analysis pipeline described by Pla-Díaz and colleagues (M.P.-D., unpublished data) was used to investigate putative recombining genes, which could potentially interfere with phylogenetic tree topologies between the modern and ancient lineages. Altogether 12 putative recombinant genes were subsequently excluded, resulting in an alternative positioning of the ancient TPA strains close to the Nichols cluster. The pipeline included the following steps: 1) Obtaining an ML tree with the complete multiple alignment, using IQ-TREE v.1.6.10 [110]. 2) Obtaining ML trees for each protein-coding gene. 3) Testing the phylogenetic signal in each gene alignment [138]. 4) Testing the congruence between each gene tree and the complete genome alignment and between each gene alignment and the complete genome tree [139]. 5) Confirming a minimum of three consecutive SNPs congruent with a recombination event for all genes passing the filtering of step 3 and 4 using MEGA7 v. 7.0 [140]. 6) Removing the protein-coding genes with signals of being involved in recombination events.

Prior to the final phylogenetic analyses, genes containing recombining regions identified through the above-mentioned procedure were excluded from the sequence alignment (Data S3). Additionally, 18 genes previously reported as hypervariable, carrying many repetitive regions and inducing recombination-like effects in mapping were considered to potentially bias the phylogenetic signal [38, 141–145] and were also removed. Those included the *arp* gene (TPANIC_0433), *FadL* homolog gene*s* (TPANIC_0548 TPANIC_0856, TPANIC_0858, TPANIC_0859, TPANIC_0865) and all *tpr* genes TPANIC_0009, TPANIC_0011, TPANIC_0117, TPANIC_0131, TPANIC_0313, TPANIC_0316, TPANIC_0317, TPANIC_0610, TPANIC_0620, TPANIC_0621, TPANIC_0897, TPANIC_1031). Finally, positions having > 25% missing data were trimmed, and a SNP alignment was generated, recording the number of constant sites to allow ascertainment bias correction (Data S3). A phylogenetic analysis was performed using RAxML v. 8.2.12 [111] with the rapid bootstrap algorithm. The ASC_GTRGAMMA substitution model was used together with the "stamatakis" ascertainment bias correction to account for the number of constant sites not appearing in the SNP alignment.

The same analysis was conducted on different alignments to assess the effect of data processing on phylogenetic inference (Figures S4 and S5). Using a full genome instead of a SNP alignment (Figure S4B), keeping positions with > 25% missing data (Figure S4C), or using the TPE CDC2 reference genome for read mapping (Figure 2; Data S4) had little effect on the resulting tree topology, which supports the robustness of our results with respect to these aspects of data processing. Conversely, the inclusion of recombining or the abovementioned mapping-obstructing genes in the alignment (Figures S4D and S4E) resulted in topological changes, particularly regarding the position of the PD28, SJ219, 94A and 94B ancient genomes with respect to modern TPA clades. This highlights that genetic recombination may significantly bias phylogenetic reconstruction of *Treponema* if not accounted for.

KM14-7 SNP analysis

In the phylogenetic tree, KM14-7 was placed basal to TPE and TEN clades. Although bootstrap support was very high, we further evaluated the authenticity of this remarkable position because this genome contained a large fraction of missing data. First, we conducted a phylogenetic analysis based on genomic positions that were resolved in KM14-7 only (107 SNPs after exclusion of recombining genes, *FadL* homologs, *tpr* genes and *arp* gene, as well as positions with > 25% missing data). In the resulting tree, KM14-7 was still recovered basal to TPE/TEN with strong support (Figure S4F). We then investigated genomic positions for which the ancestral variant of TPE/TEN and TPA was likely different. Our rationale was that if KM14-7's position on the branch connecting TPE/TEN and TPA was authentic, the genome should contain a significant number of both TPE/TEN and TPA-like variants. Hence, we looked at positions (i) resolved in KM14-7, (ii) for which the majority variant was differing between TPE/TEN and TPA clades, but (iii) shared by more than 90% of the (modern) genomes within each clade. We then looked at the proportion of TPE/TEN and TPA-like variants in KM14-7 and compared that with all other genomes. Because KM14-7 was not included in the recombination analysis, we did not trim the recombining regions for this analysis in order to avoid a bias.

Molecular clock dating

KM14-7 and the Mexican TPA genomes, 94A and 94B, were removed from the molecular clock dating analyses due to their low coverage and the amount of unique SNPs present on these lineages. Furthermore, the Nichols and NIC2 genomes were removed to avoid any bias caused by continuous passaging in rabbit hosts from their isolation in the clinical context in 1912 until at least 1981 [142, 146–148].

The strength of the molecular clock signal in the dataset was investigated by regressing the root-to-tip genetic distance (measured in substitutions/site) of genomes against their sampling dates [149, 150]. Root-to-tip genetic distances were calculated on a midpoint-rooted ML tree estimated in RAxML v. 8.2.11 [111] using the same procedure described above. Sampling dates of ancient sequences were fixed to the middle of the date range defined by radiocarbon dating (Table 3). To assess the significance of the correlation, we permuted the sampling dates across genomes and used the Pearson correlation coefficient as a test statistic [149, 151]. We performed 1000 replicates and calculated the p value as the proportion of replicates with a correlation coefficient greater than or equal to the truth, using the unpermuted sampling dates (Figure S5).

Divergence times and substitution rates were estimated using BEAST2 v. 2.6 [82]. Analyses were performed under an HKY substitution model with Γ-distributed rate heterogeneity [152, 153] and a Bayesian skyline plot demographic model (tree-prior) with 10 groups [154]. To calibrate the clock, an uncorrelated lognormally distributed relaxed clock model [155] was used to allow for rate variation among lineages. An exponentially distributed prior with mean 5×10^{-7} s/s/y was placed on the mean clock rate. To allow for uncertainty in the sampling dates of ancient genomes, uniform priors across the date range defined by radiocarbon dating were placed on their ages (Figures S6I–S6L). Default priors were used for all other model components. To confirm clock-like evolution we performed a Bayesian date randomization test [81, 150, 151] (DRT) by permuting sampling dates across genomes and repeating the analysis. We performed 50 replicates and assessed significance by comparing the molecular clock rate estimates of the replicates to those estimated under the true sampling dates. As in the permutation test for the root-to-tip regression analysis above, we fixed the sampling dates of ancient genomes to the middle of the date range defined by radiocarbon dating.

MCMC chains were run for 50 million steps and parameters and trees sampled every 5000 steps. Convergence was assessed in Tracer v.1.7 [113] after discarding 30% of the chains as burn-in and Treeannotator [82] was used to compute MCC trees of the resulting posterior tree distributions. Results were visualized in Rstudio [106] using ggplots2 [104, 105], ggtree [114] and custom scripts.

Robustness of molecular clock dating

To test the robustness of the molecular clock dating results, we repeated the analyses using different combinations of demographic (constant population size coalescent, exponential growth coalescent, Bayesian skyline plot with 10 groups) and clock (strict and relaxed) models. Default priors were used for all demographic models. The same prior was used for the strict clock rate as for the mean clock rate in analyses with a relaxed clock model (exponential distribution with mean 5×10^{-7}s/s/y). Furthermore, to test the effect of constraining the sampling dates of ancient genomes to the date ranges defined by radiocarbon dating (referred henceforth as narrow uniform priors), we repeated all analyses using wide uniform priors between 1000 CE and 2000 CE.

The demographic model had little effect on the estimated molecular clock rate, divergence times and sampling dates as seen in the graphics (Figure S6). Nonetheless, a constant effective population size leads to slightly older divergence date estimates. The demographic models tested represent very different scenarios (constant effective population size, exponential growth and flexible growth and decline). Since all three models give similar estimates, we are confident that our results are robust to the choice of demographic model.

Estimates under different clock models are largely overlapping. A relaxed clock model leads to wider HPD intervals than a strict clock and thus represents a more conservative choice. Furthermore, the HPD interval of the coefficient of variation (of the clock rate) estimated under a relaxed clock model does not include 0, indicating strong evidence for rate variation among lineages.

Relaxing the constraints on the sampling dates of ancient genomes leads to more recent divergence time estimates more in line with previous analyses [41] and a faster clock rate estimate that is similar to the rate reported by Beale et al. for TPA [8]. Similarly, the sampling date estimates of the ancient TPE genomes are more recent. Nevertheless, posterior distributions of the sampling dates of all ancient genomes except CHS119 place considerable weight on the date range defined by radiocarbon dating, with median estimates either included in the radiocarbon date range (SJ219 and 133) or slightly earlier (PD28) (as seen in Figures S6I–S6L).

Virulence analysis

Virulence factors (details: see below) represented by the four ancient European genomes were assessed through a gene presence/absence analysis as described by Andrades Valtueña et al. [156]. For sanger-sequenced modern genomes used as comparison (Chicago, Mexico A, Sea81-4, SS14), we used artificial, 100nt long reads simulated with the tool Genome2Reads (integrated in the EAGER-pipeline [69]) to facilitate mapping them in a concise manner with all other, NGS-sequenced data. A set of 60 sequences previously associated with putative virulence functions [52, 87, 88, 157] were examined based on the annotated Nichols reference genome (GenBank CP004010.2) [75] with a preliminary quality filtering threshold of 37 and without a quality filtering. The resulting effect of 0-quality filtering is that all reads are allowed to map, despite the presence of duplicated regions (in the *tpr* gene paralogs in particular) whereas quality filtering with a threshold set to larger than 0 omits all reads mapping to identical regions, making the coverage of these regions appear extremely low. The coverage over each gene was calculated using genomeCoverageBed in BEDTools version 2.250 [103] (Table S3). The heatmap visualization of the gene-by-gene coverage of reads was created using ggplot2 package in R [104, 105] (Figure 4).

QUANTIFICATION AND STATISTICAL ANALYSIS

In silico screening

In total, nine samples were screened for the presence of *T. pallidum*. The candidates for further capture methods and genomic analyses were selected according to threshold values as indicated above (see Read processing, mapping and variant calling in METHOD DETAILS).

Phylogenetic analysis

Phylogenetic analyses were performed with the ML algorithm in RAxML v. 8.2.12 [111] (see Read processing, mapping and variant calling in METHOD DETAILS), with the rapid bootstrap algorithm. Positions having > 25% missing data or identified as well as recombining and mapping-obstructing genes (as defined in) were excluded from the nucleotide alignment prior to the analysis.

Molecular clock test

The robustness of the molecular clock dating was conducted by repetitions of different combinations of demographic and clock models in BEAST2 v.2.6 [82]. To confirm clock-like evolution a Bayesian date randomization test (DRT) was used by permuting sampling dates across genomes and repeating the analysis. To test the effect of constraining the sampling dates of ancient genomes to the date ranges defined by radiocarbon dating, we repeated all analyses using wide uniform priors between 1000 CE and 2000 CE. (see Figures S5 and S6 and Molecular clock dating in METHOD DETAILS above).

Dating analysis

Dating analysis was performed with BEAST2 v.2.6 [158] as indicated above (see Molecular clock dating in METHOD DETAILS). MCMC chains were run for 50 million steps, with parameters and trees sampled every 5000 steps.

Supplemental Information

Ancient Bacterial Genomes Reveal

a High Diversity of *Treponema pallidum*

Strains in Early Modern Europe

Kerttu Majander, Saskia Pfrengle, Arthur Kocher, Judith Neukamm, Louis du Plessis, Marta Pla-Díaz, Natasha Arora, Gülfirde Akgül, Kati Salo, Rachel Schats, Sarah Inskip, Markku Oinonen, Heiki Valk, Martin Malve, Aivar Kriiska, Päivi Onkamo, Fernando González-Candelas, Denise Kühnert, Johannes Krause, and Verena J. Schuenemann
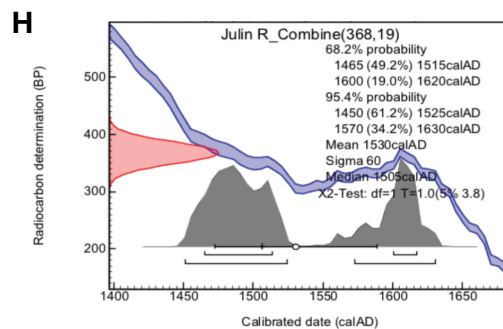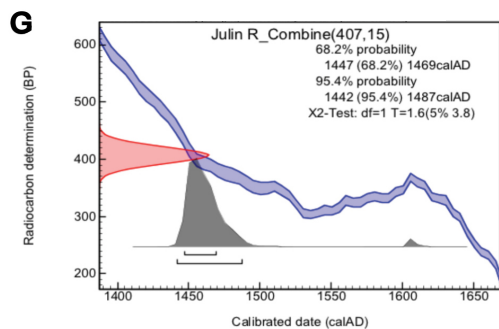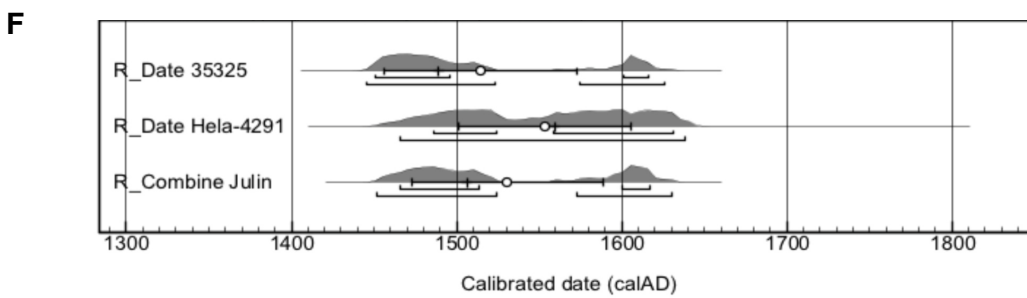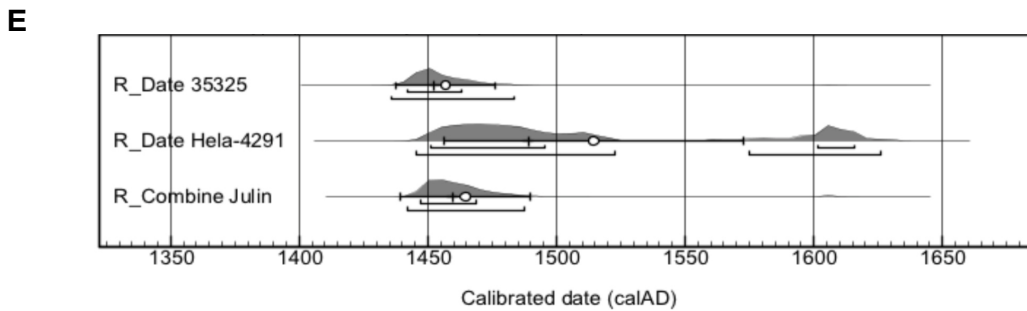
A 35328 (189,18)
68.2% probability
1666 (16.6%) 1680calAD
1763 (24.1%) 1784calAD
1796 (5.4%) 1802calAD
1938calAD (22.1%) ...
95.4% probability
1662 (19.8%) 1684calAD
1735 (52.4%) 1806calAD
1933calAD (23.2%) ...

B 35326 (456,18)
68.2% probability
1434 (68.2%) 1447calAD
95.4% probability
1424 (95.4%) 1453calAD

C 35324 (444,18)
68.2% probability
1436 (68.2%) 1451calAD
95.4% probability
1427 (95.4%) 1461calAD

D 33918 (338,23)
68.2% probability
1494 (21.8%) 1525calAD
1558 (33.2%) 1602calAD
1614 (13.2%) 1632calAD
95.4% probability
1476 (95.4%) 1637calAD

G Julin R_Combine(407,15)
68.2% probability
1447 (68.2%) 1469calAD
95.4% probability
1442 (95.4%) 1487calAD
X2-Test: df=1 T=1.6(5% 3.8)

H Julin R_Combine(368,19)
68.2% probability
1465 (49.2%) 1515calAD
1600 (19.0%) 1620calAD
95.4% probability
1450 (61.2%) 1525calAD
1570 (34.2%) 1630calAD
Mean 1530calAD
Sigma 60
Median 1505calAD
X2-Test: df=1 T=1.0(5% 3.8)

Figure S1. Radiocarbon dating and reservoir effect corrections. Related to STAR Methods.

Radiocarbon curves for the samples positive for *Treponema pallidum* DNA: **A)** PD28, **B)** SJ219, **C)** CHS119 and **D)** KM14-7. Calibrated ^{14}C dating curves are shown for the sample CHS119, prior to the reservoir effect correction in **E)** and **G),** and with the calculated reservoir effect correction in **F)** and **H)**. The results are visualized the OxCal program version 4.3.2 [S1] and produced by Klaus-Tschira-Archäometrie-Zentrum am Curt-Engelhorn-Zentrum, Mannheim, Germany, for all the samples, and independently in the Laboratory of Chronology, Finnish Natural History Museum, Helsinki for the sample CHS119, and the AMS laboratory, ETH Zürich for the sample SJ219.
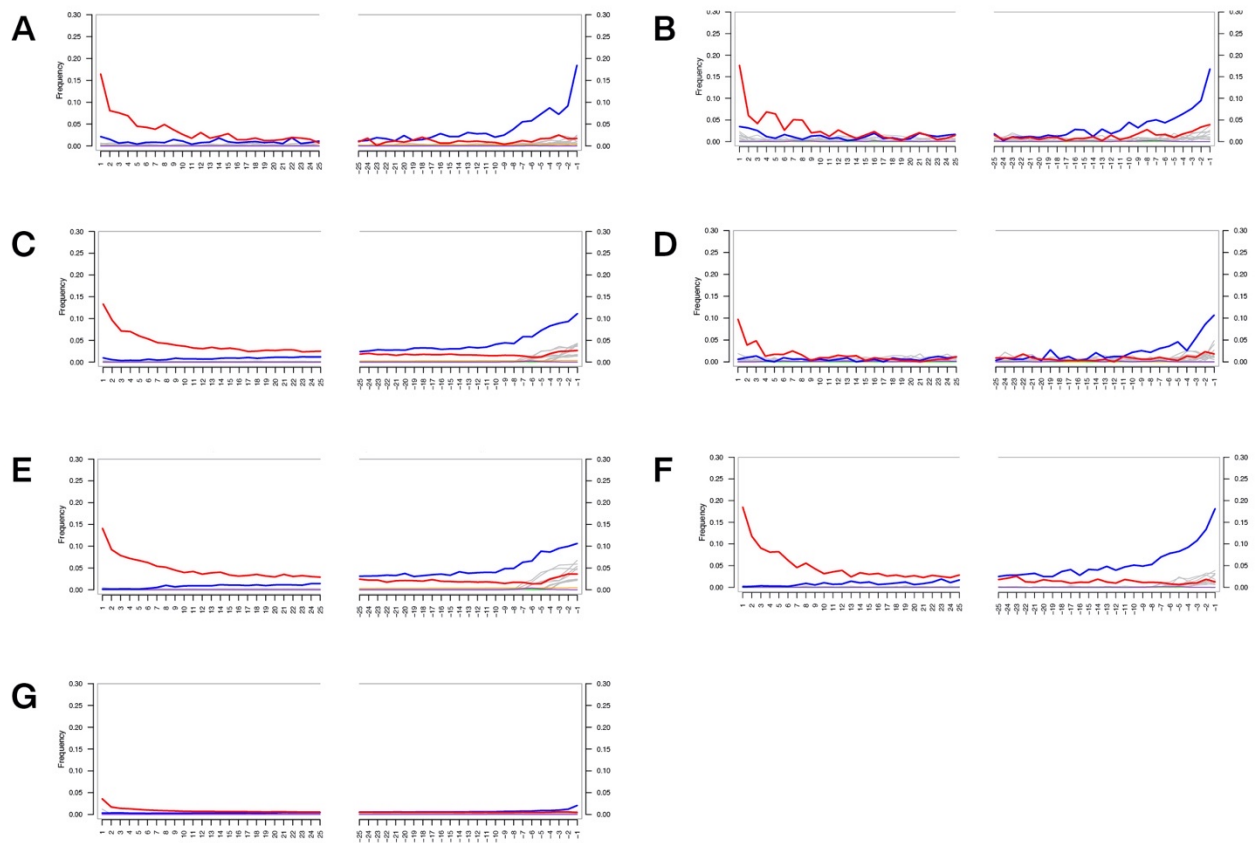
Figure S2. **Damage patterns**. **Related to STAR Methods. Related to Authenticity estimation of ancient DNA and genome reconstruction.** Misincorporation patterns from MapDamage program [S2] showing the damage at the end of sequencing reads of the four *Treponema pallidum* positive samples in this study: **A)** mitochondrial and **B)** *T. pallidum* capture data for KM14-7 sample, **C)** mitochondrial and **D)** *T. pallidum* capture data for CHS119 sample, **E)** mitochondrial and **F)** *T. pallidum* capture data for SJ219 sample and **G)** *T. pallidum* capture data for PD28 sample. A pattern of cytosine-to-thymine base misincorporation accumulated at the end of the reads is indicative of authentic ancient DNA in the sample [S3]. The misincorporation plots show data only from libraries created without UDG treatment which is used for removal of the damaged bases. The sample PD28 shows very little damage, probably due to the relatively recent past from which the individual originates from, and the well-preserved petrosal bone material used.
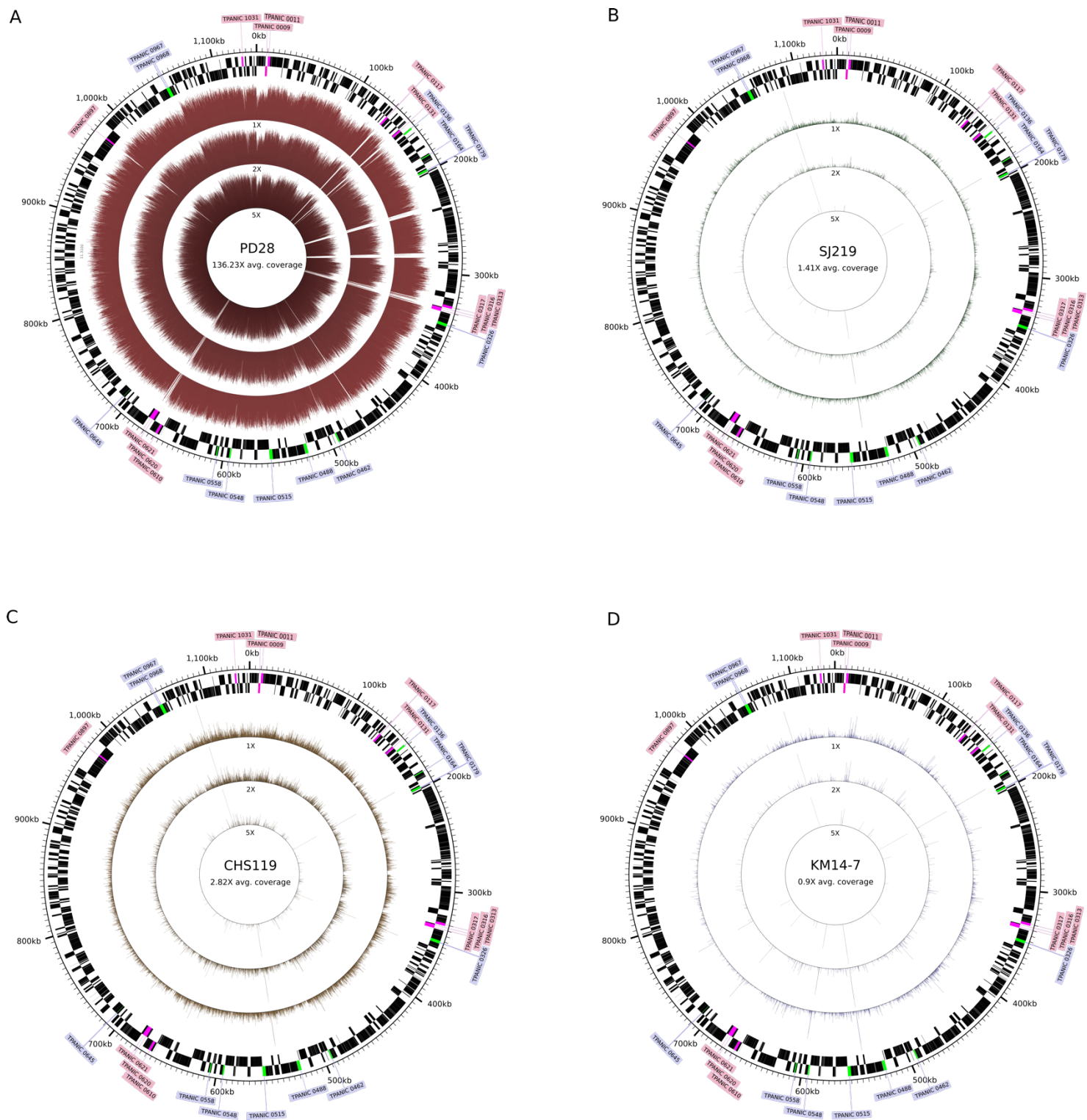
Figure S3. Genome coverage visualization. Related to Figure 1B.

Circleator [S4] plots showing coverage levels 1X, 2X and 5X for the four ancient European genomes in this study, all marked with different colours **A)** PD28 in red, **B)** SJ219 in green, **C)** CHS119 in brown and **D)** KM14-7 in violet. Data presented is after duplicate removal and mapped with a quality threshold 37. Setting the quality threshold above zero allows no reads mapping to identical sequences, causing gaps

in coverage on the identical sequences, such as the paralogous regions of *tpr* genes, which are here highlighted in pink and annotated (*tprA*: TPANIC_0009, *tprB*: TPANIC_0011, *tprC*: TPANIC_0117, *tprD*: TPANIC_0131, *tprE*: TPANIC_0313, *tprF*: TPANIC_0316, *tprG*: TPANIC_0317, *tprH*: TPANIC_0610, *tprI*: TPANIC_0620, *tprJ*: TPANIC_0621, *tprK*: TPANIC_0897 and *tprL*: TPANIC_1031). The genes with recombinant regions are highlighted in green and annotated. The black outer rim around each genome visualizes the protein-coding regions in forward and the black inner rim in the reverse direction, according to the annotation of the Nichols reference genome (CP004010.2).
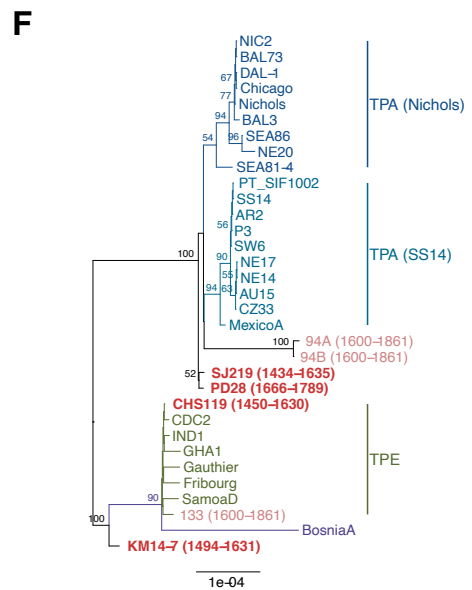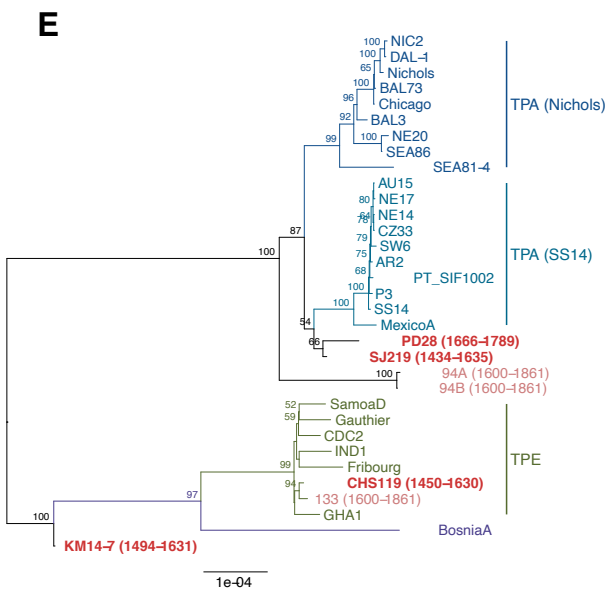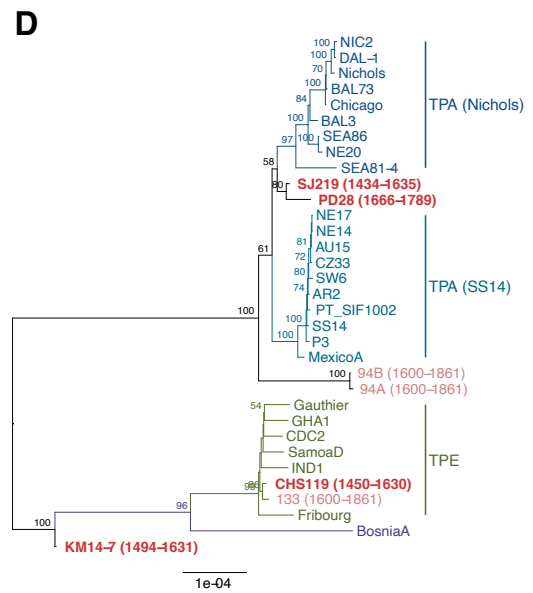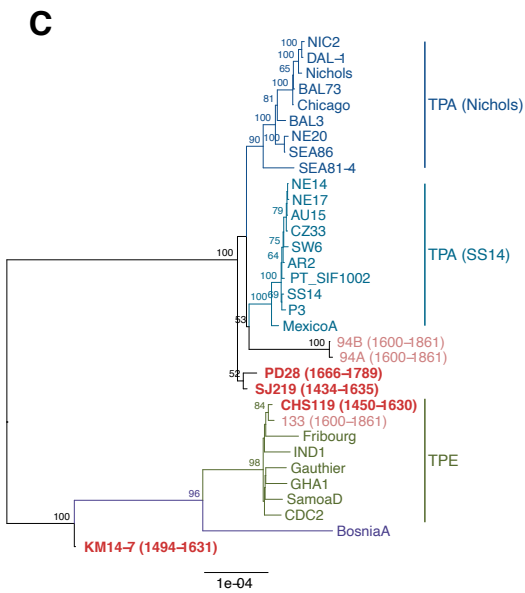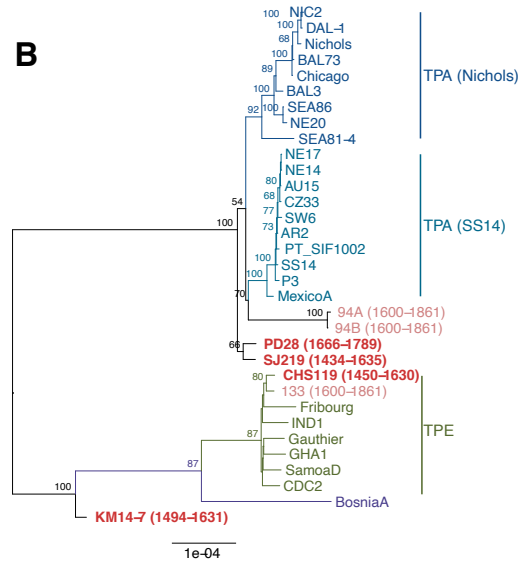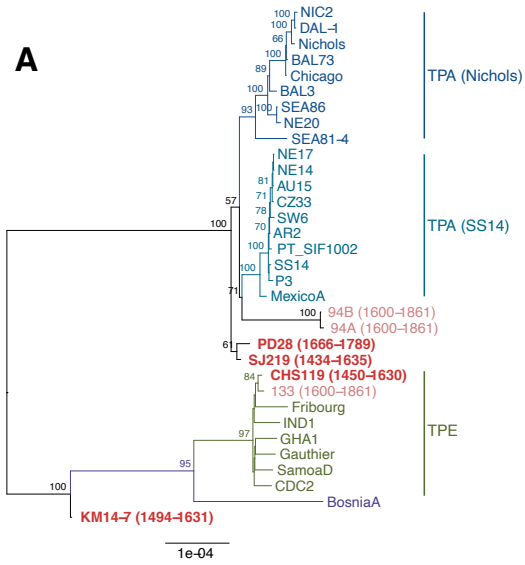
Figure S4. Phylogenetic tree comparisons. Related to Figure 1C. Comparison of *T. pallidum* phylogenetic trees based on different processing of the sequence alignment: **A)** SNP alignment after exclusion of recombining and hypervariable genes, as well as positions with >25% missing data (1631 SNPs). This tree is also presented in main Figure 1.C., and used as a baseline for the following comparisons: **B)** Full genome alignment (1631 SNPs and 1,073,185 invariable positions), **C)** SNP alignment in which no positions were trimmed based on missing data (1696 SNPs), **D)** SNP alignment in which hypervariable genes were not excluded (1841 SNPs), **E)** SNP alignment in which neither hypervariable nor recombining genes were excluded (2205 SNPs), **F)** SNPs that were resolved in KM14-7 only (107 positions). The data derives from a set of 26 modern treponemal genomes [S5–S14], all colonial period Mexican genomes from previously published study [S15] and all four ancient treponemal genomes sequenced for this study, mapped to the Nichols reference genome (CP004010.2). The trees were estimated by maximum likelihood and are midpoint-rooted. Branch lengths represent numbers of substitutions per site. An ascertainment bias correction was used to account for the number of constant sites not appearing in the SNP alignments. Bootstrap support values are written at the nodes when >50. Ancient genomes from this study are marked in red and the published ancient genomes in pink.
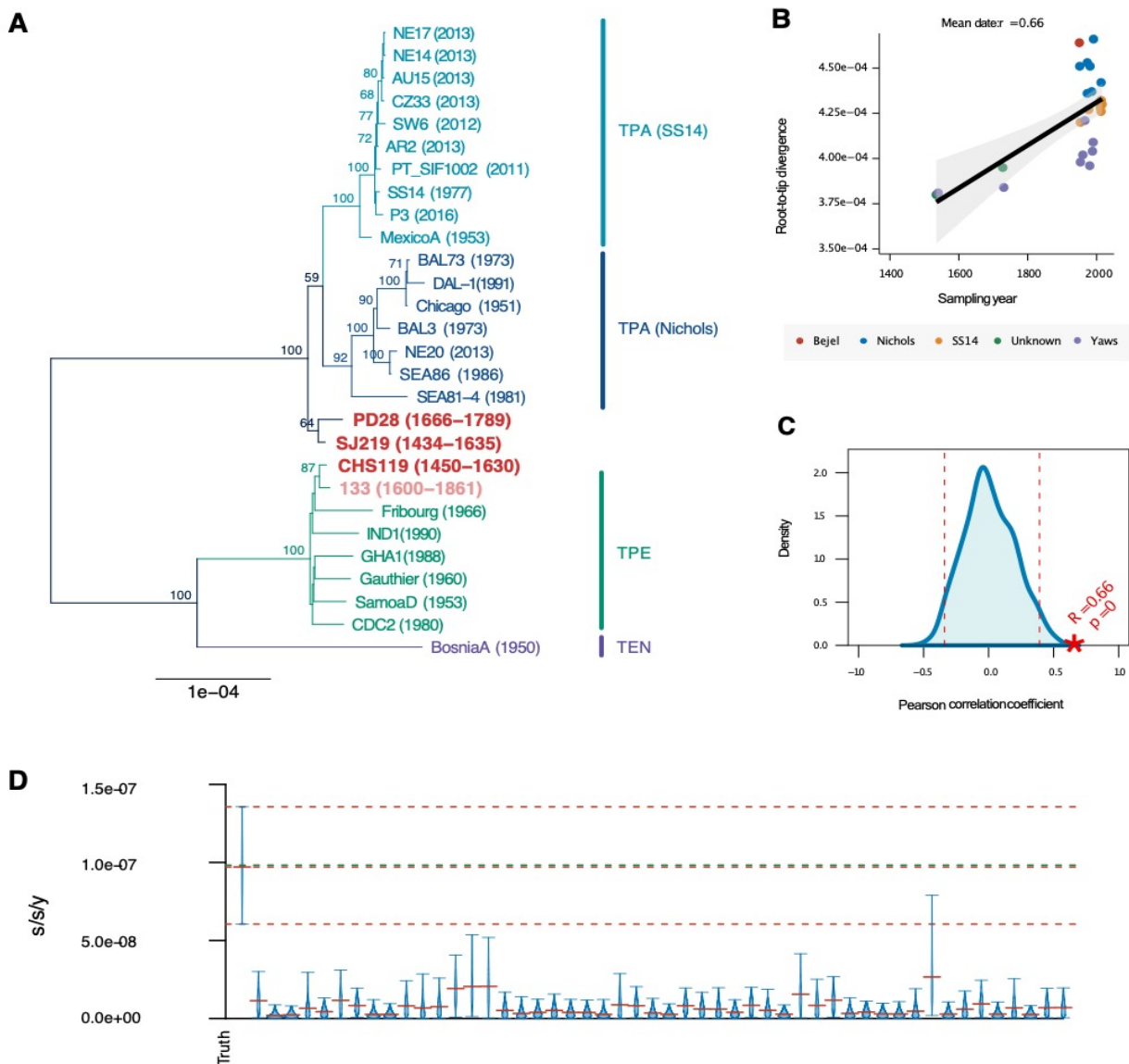
Figure S5. Molecular clock signal. Related to Figure 3. Related to STAR Methods. Related to molecular clock dating.

A) Midpoint-rooted ML tree used to calculate root-to-tip distances in the 28-genome dataset used for molecular clock dating. The tree is based on a SNP alignment in which positions with >25% missing data were excluded. The sampling date range is given in parentheses after the sample name. The ancient samples from this study are highlighted in red and the previously published colonial Mexican genome 133 in pink. **B)** Root-to-tip genetic distance in the ML tree plotted against sampling date, using the mean date of the date range defined by radiocarbon dating. The Pearson correlation coefficient between root-to-tip distance and sampling date is given above the figure ($r = 0.66$). The significance of the correlation was confirmed using a permutation test ($p = 0$). The correlation is higher within the TPA and TPE clades

alone (r = 0.764 and r = 0.785, respectively). Within the TPA cluster the signal is driven by the SS14 clade (r = 0.836), while the Nichols clade does not appear clock-like (r = -0.084). **C)** The null distribution of the Pearson correlation coefficient between root-to-tip distance and sampling date when permuting sampling dates across genomes (1,000 replicates). The dashed lines indicate 2.5 and 97.5 quantiles of the distribution and the star indicates the correlation coefficient using the true (unpermuted) sampling dates. The p-value is the proportion of replicates with the test statistic (Pearson correlation coefficient) greater than or equal to the true value. **D)** The Bayesian date randomization test (DRT) performed with 50 replicates, under a Bayesian skyline plot tree prior with a relaxed clock clock model. The plot shows the posterior distributions for the (mean) clock rates, truncated at the upper and lower limits of the 95% HPD interval. Horizontal red lines indicate the medians of the posterior distributions. The green dashed line indicates the mean estimate and red dashed lines signify the median estimate and the upper and lower limits of the 95% HPD interval of the clock rate inferred under the true sampling dates. **E)** The same as the previous panel, but with a strict clock model.
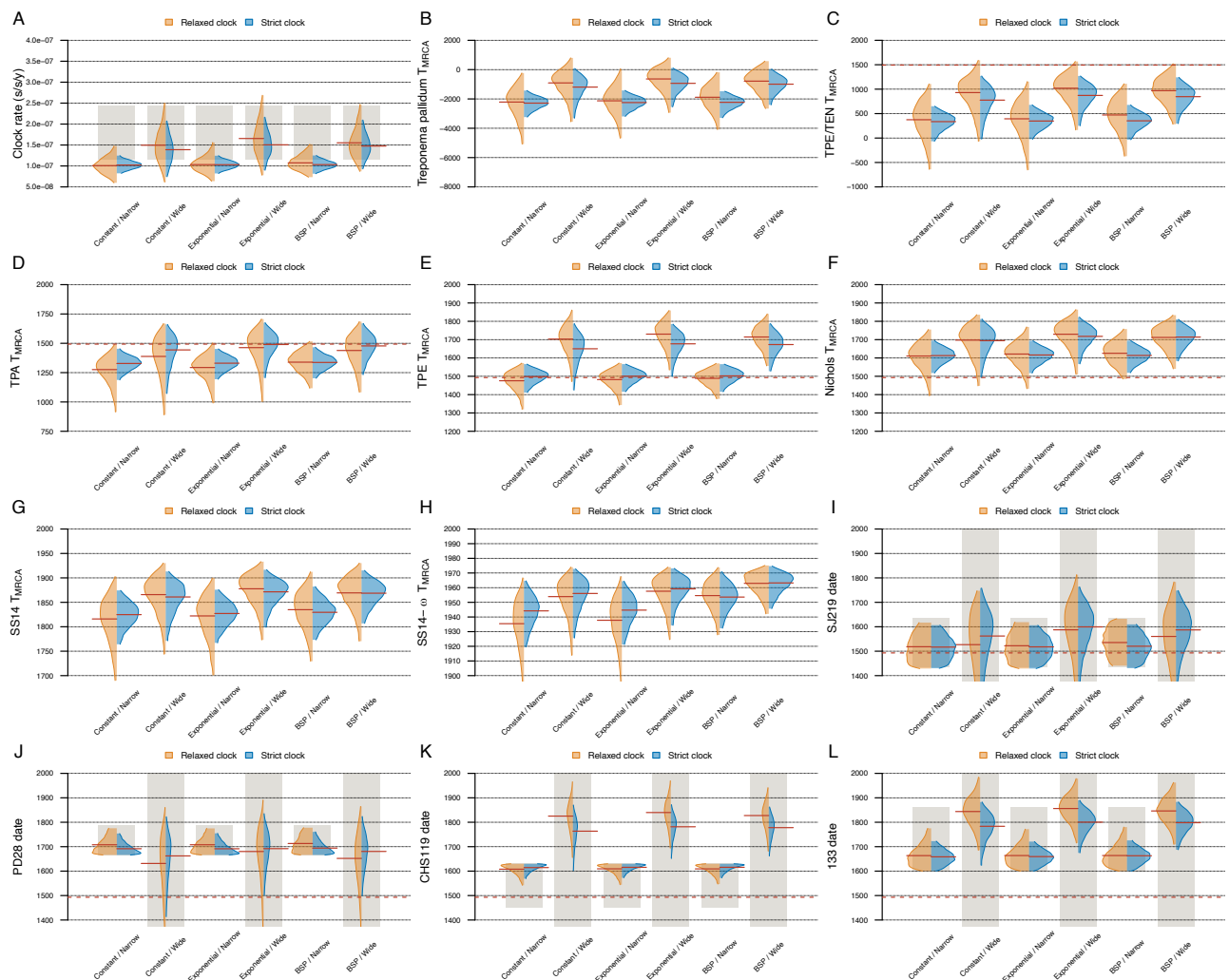
Figure S6. Posterior distributions, divergence dates and sampling date estimates for all tested models. Related to Figure 3. Related to STAR Methods. Related to Molecular clock dating.

Posterior distributions of the mean molecular clock rate **A)**, divergence dates of clades in the tree **B-H)** and sampling dates of the ancient genomes **I-L)**. Posterior distributions are inferred under relaxed (orange) and strict (blue) clock models with different demographic models (constant population size, exponential growth, Bayesian skyline plot) and priors on the sampling dates of ancient genomes (wide/narrow). The distributions are truncated at the upper and lower limits of the 95% HPD intervals and the red lines indicate the median estimates. The shaded boxes in **A)** represent the substitution rate estimates reported in [S16]) for the TPA clade, and in **I-L)** the prior distributions used for the sampling dates. The red horizontal dashed lines indicate the year 1493.

Sample	Number of derived positions recovered	Number of derived positions filtered	% of derived positions filtered
133	607	17	2.8
94A	294	20	6.8
94B	368	3	0.8
KM14-7	54	22	40.7
PD28	244	0	0
SJ219	70	18	25.7
CHS119	377	17	4.5

Table S1. SNP evaluation. Related to Star Methods.

Results of the SNP evaluation procedure for the ancient genomes included in the study. For each genome, the number of initially resolved derived positions (with respect to the Nichols reference genome (CP004010.2); are reported, as well as the number of proportions of these that appeared spurious and were filtered out.

GeneBank ID	Q-0 (PD28)	Q-37 (PD28)	Q-0 (SJ219)	Q-37 (SJ219)	Q-0 (CHS119)	Q-37 (CHS119)	Q-0 (KM14-7)	Q-37 (KM14-7)
TPANIC_0009 (*tprA*)	1	1	0.6907895	0.6830036	0.877193	0.8678058	0.3201754	0.3493705
TPANIC_0011 (*tprB*)	1	1	0.6972755	0.6700252	0.8940464	0.9118388	0.3773966	0.4252729
TPANIC_0040	1	1	0.5969722	0.5969722	0.8805237	0.8805237	0.5707856	0.547054
TPANIC_0092	1	1	0.5286885	0.5286885	0.5840164	0.5840164	0.3627049	0.3627049
TPANIC_0111	1	1	0.7483221	0.7402685	0.904698	0.9026846	0.5939597	0.5939597

TPANIC_0117 (*tprC*)	1	0.2213115	0.8324053	0.1197632	0.9047884	0.1675774	0.7065701	0.0974499
TPANIC_0126	1	1	0.6453055	0.6304024	0.9269747	0.9269747	0.6035768	0.6035768
TPANIC_0131 (*tprD*)	1	0.2222222	0.8273942	0.1416211	0.8864142	0.1215847	0.6497773	0.0473588
TPANIC_0133	1	1	0.5349026	0.5113636	0.6193182	0.5422078	0.4780844	0.3555195
TPANIC_0134	1	1	0.5761062	0.5530974	0.9433628	0.9070796	0.4867257	0.3725664
TPANIC_0136	0.9529253	0.9226631	0.6617351	0.539341	0.5682582	0.3799596	0.4223268	0.3678547
TPANIC_0155	1	1	0.5973094	0.5973094	0.9139013	0.9058296	0.3461883	0.3461883
TPANIC_0163	1	1	0.7840173	0.7840173	0.9006479	0.9006479	0.7041036	0.7041036
TPANIC_0171	1	1	0.7079439	0.7079439	0.9439253	0.9439253	0.6728972	0.6728972
TPANIC_0257	1	1	0.6616822	0.6616822	0.9084112	0.9084112	0.2448598	0.2448598
TPANIC_0292	1	1	0.8699122	0.8699122	0.8651237	0.8651237	0.5618516	0.5618516
TPANIC_0298	1	1	0.6624636	0.6624636	0.9544132	0.9544132	0.5033948	0.5033948
TPANIC_0313 (*tprE*)	1	0.5435268	0.8146853	0.2269345	0.8828672	0.2994792	0.7731643	0.1800595
TPANIC_0316 (*tprF*)	1	0.161857	0.9438861	0	0.9698492	0.0326223	0.8123953	0
TPANIC_0317 (*tprG*)	1	0.3981273	0.8801762	0.1449438	1	0.3183521	0.8515419	0.1853933
TPANIC_0326	0.9976124	0.9964186	0.7524871	0.7445285	0.8933545	0.8834063	0.5972941	0.5865499
TPANIC_0327	1	1	0.5888031	0.5888031	0.6640927	0.6640927	0.6930502	0.6370656
TPANIC_0433 (*Arp*)	1	0.6730981	0.7701213	0.3864388	0.8925028	0.514333	0.6223814	0.2579934
TPANIC_0435	1	1	0.7617021	0.7617021	0.8468085	0.8468085	0.5510638	0.5446808
TPANIC_0453	1	1	0.8180765	0.8169177	0.9513326	0.9513326	0.5388181	0.5388181
TPANIC_0483	1	1	0.8257638	0.8257638	0.8736581	0.8736581	0.5895954	0.5895954
TPANIC_0488	1	1	0.6759953	0.6594403	0.8131651	0.7705952	0.5325187	0.5325187
TPANIC_0493	1	1	0.8348774	0.8027248	0.9416894	0.9046322	0.6572207	0.6152589
TPANIC_0515	1	0.9996639	0.6097479	0.5983194	0.927395	0.9263865	0.5603361	0.537479
TPANIC_0548	0.9723926	0.9662577	0.4677914	0.4677914	0.7377301	0.7208589	0.4348159	0.392638
TPANIC_0571	1	1	0.7969925	0.7969925	0.9203007	0.9203007	0.6045113	0.6045113
TPANIC_0574	1	1	0.7845092	0.7845092	0.9608896	0.9608896	0.6196319	0.6196319
TPANIC_0610 (*tprH*)	1	1	0.6953388	0.6936719	0.861605	0.8508666	0.5564632	0.5320435
TPANIC_0620 (*tprI*)	1	0.3719157	0.8944778	0.1763123	0.9671952	0.2292508	0.781848	0.0529385
TPANIC_0621 (*tprJ*)	1	0.4772048	0.9209139	0.3041854	0.7838313	0.1689088	0.7952548	0.1449925
TPANIC_0639	1	1	0.6215099	0.6163392	0.6623578	0.6587384	0.4172699	0.4172699
TPANIC_0640	1	1	0.5938178	0.5938178	0.8096529	0.8096529	0.3703904	0.3438178
TPANIC_0655	1	1	0.5965583	0.5956023	0.8833652	0.8833652	0.5344169	0.5344169
TPANIC_0700	1	1	0.5765306	0.494898	0.7346939	0.7346939	0.3086735	0.3086735

TPANIC_0733	1	1	0.5341426	0.5341426	0.8224583	0.7481032	0.2989378	0.2230653
TPANIC_0750	1	1	0.3591654	0.3591654	0.8837556	0.8837556	0.5812221	0.5812221
TPANIC_0751	1	1	0.6451613	0.6451613	0.743338	0.743338	0.2636746	0.2636746
TPANIC_0768	1	1	0.6094503	0.6094503	0.7743491	0.7704918	0.3683703	0.3683703
TPANIC_0769	1	1	0.703173	0.5220062	0.8157625	0.6335722	0.3633572	0.3152508
TPANIC_0796	1	1	0.5652574	0.5652574	0.8327206	0.8327206	0.3575368	0.3575368
TPANIC_0819	1	1	0.3131749	0.3131749	0.8812095	0.8812095	0.524838	0.4848812
TPANIC_0856 (*FadL* homol.)	1	1	0.3631757	0.3277027	0.8040541	0.7998311	0.3158784	0.3158784
TPANIC_0858	1	1	0.6435563	0.6435563	0.6109298	0.593801	0.4902121	0.4690049
TPANIC_0859	1	1	0.3921833	0.3915094	0.8160377	0.8160377	0.2068733	0.1718329
TPANIC_0865	1	1	0.7560806	0.7560806	0.9277276	0.9075747	0.3961084	0.3766505
TPANIC_0897 (*tprK*)	0.9315789	0.8697917	0.5322368	0.4473958	0.6434211	0.5619792	0.5111842	0.4401042
TPANIC_0956	1	1	0.4593203	0.4593203	0.8053553	0.8053553	0.2677652	0.2677652
TPANIC_0957	1	1	0.6177043	0.5680934	0.7558365	0.7558365	0.4114786	0.3618677
TPANIC_0966	1	1	0.4902081	0.4902081	0.8029376	0.8029376	0.3635251	0.3635251
TPANIC_0967	1	1	0.4752093	0.4752093	0.7192531	0.7018673	0.3824855	0.3734707
TPANIC_0969	1	1	0.5622618	0.5622618	0.9275731	0.9275731	0.4485388	0.4485388
TPANIC_0971	1	1	0.6009772	0.6009772	0.9934853	0.9381108	0.6872964	0.6872964
TPANIC_1012	1	1	0.7005348	0.7005348	0.9475936	0.9475936	0.6	0.5614973
TPANIC_1031 (*tprL*)	1	1	0.8095855	0.7587448	0.8879533	0.7633745	0.5809585	0.4753087
TPANIC_1038	1	1	0.5497186	0.5497186	0.9737336	0.9549718	0.7598499	0.7598499

Table S3. Putative virulence gene coverage. Related to Figure 4. Related to Star Methods. Related to Virulence analysis.

Comparative values of coverage from the two mapping quality thresholds, 0 and 37, for each virulence factor gene in the ancient European genomes from this study. *Tpr* genes are highlighted in grey.

SUPPLEMENTAL REFERENCES

S1. Ramsey, C.B. (1995). Radiocarbon Calibration and Analysis of Stratigraphy: The OxCal Program. Radiocarbon *37*, 425–430.

S2. Jónsson, H., Ginolhac, A., Schubert, M., Johnson, P.L.F., and Orlando, L. (2013). mapDamage2.0: fast approximate Bayesian estimates of ancient DNA damage parameters. Bioinformatics *29*, 1682–1684.

S3. Sawyer, S., Krause, J., Guschanski, K., Savolainen, V., and Pääbo, S. (2012). Temporal patterns of nucleotide misincorporations and DNA fragmentation in ancient DNA. PLoS One *7*, e34131.

S4. Crabtree, J., Agrawal, S., Mahurkar, A., Myers, G.S., Rasko, D.A., and White, O. (2014). Circleator: flexible circular visualization of genome-associated data with BioPerl and SVG. Bioinformatics *30*, 3125–3127.

S5. Giacani, L., Jeffrey, B.M., Molini, B.J., Le, H.T., Lukehart, S.A., Centurion-Lara, A., and Rockey, D.D. (2010). Complete genome sequence and annotation of the Treponema pallidum subsp. pallidum Chicago strain. J. Bacteriol. *192*, 2645–2646.

S6. Pětrošová, H., Zobaníková, M., Čejková, D., Mikalová, L., Pospíšilová, P., Strouhal, M., Chen, L., Qin, X., Muzny, D.M., Weinstock, G.M., *et al.* (2012). Whole genome sequence of Treponema pallidum ssp. pallidum, strain Mexico A, suggests recombination between yaws and syphilis strains. PLoS Negl. Trop. Dis. *6*, e1832.

S7. Zobaníková, M., Mikolka, P., Cejková, D., Pospíšilová, P., Chen, L., Strouhal, M., Qin, X., Weinstock, G.M., and Smajs, D. (2012). Complete genome sequence of Treponema pallidum strain DAL-1. Stand. Genomic Sci. *7*, 12–21.

S8. Čejková, D., Zobaníková, M., Chen, L., Pospíšilová, P., Strouhal, M., Qin, X., Mikalová, L., Norris, S.J., Muzny, D.M., Gibbs, R.A., *et al.* (2012). Whole Genome Sequences of Three Treponema pallidum ssp. pertenue Strains: Yaws and Syphilis Treponemes Differ in Less than 0.2% of the Genome Sequence. PLoS Neglected Tropical Diseases *6*, e1471.

S9. Pětrošová, H., Pospíšilová, P., Strouhal, M., Čejková, D., Zobaníková, M., Mikalová, L., Sodergren, E., Weinstock, G.M., and Šmajs, D. (2013). Resequencing of Treponema pallidum ssp. pallidum strains Nichols and SS14: correction of sequencing errors resulted in increased separation of syphilis treponeme subclusters. PLoS One *8*, e74319.

S10. Zobanikova, M., Strouhal, M., Mikalova, L., Čejková, D., Ambrožová, L., Pospíšilová, P., Fulton, L.L., Chen, L., Sodergren, E., Weinstock, G.M., *et al.* (2013). Whole genome sequence of the Treponema Fribourg-Blanc: unspecified simian isolate is highly similar to the yaws subspecies. PLoS Negl. Trop. Dis. *7*, e2172.

S11. Giacani, L., Iverson-Cabral, S.L., King, J.C.K., Molini, B.J., Lukehart, S.A., and Centurion-Lara, A. (2014). Complete Genome Sequence of the Treponema pallidum subsp. pallidum Sea81-4 Strain. Genome Announc. *2*.

S12. Štaudová, B., Strouhal, M., Zobaníková, M., Čejková, D., Fulton, L.L., Chen, L., Giacani, L., Centurion-Lara, A., Bruisten, S.M., Sodergren, E., *et al.* (2014). Whole genome sequence of the Treponema pallidum subsp. endemicum strain Bosnia A: the genome is related to yaws treponemes but contains few loci similar to syphilis treponemes. PLoS Negl. Trop. Dis. *8*, e3261.

S13. Arora, N., Schuenemann, V.J., Jäger, G., Peltzer, A., Seitz, A., Herbig, A., Strouhal, M., Grillová, L., Sánchez-Busó, L., Kühnert, D., *et al.* (2016). Origin of modern syphilis and emergence of a pandemic Treponema pallidum cluster. Nat Microbiol *2*, 16245.

S14. Pinto, M., Borges, V., Antelo, M., Pinheiro, M., Nunes, A., Azevedo, J., Borrego, M.J., Mendonça, J., Carpinteiro, D., Vieira, L., *et al.* (2016). Genome-scale analysis of the non-cultivable Treponema pallidum reveals extensive within-patient genetic variation. Nat Microbiol *2*, 16190.

S15. Schuenemann, V.J., Kumar Lankapalli, A., Barquera, R., Nelson, E.A., Iraíz Hernández, D., Acuña Alonzo, V., Bos, K.I., Márquez Morfín, L., Herbig, A., and Krause, J. (2018). Historic Treponema pallidum genomes from Colonial Mexico retrieved from archaeological remains. PLoS Negl. Trop. Dis. *12*, e0006447.

S16. Beale, M.A., Marks, M., Sahi, S.K., Tantalo, L.C., Nori, A.V., French, P., Lukehart, S.A., Marra, C.M., and Thomson, N.R. (2019). Genomic epidemiology of syphilis reveals independent emergence of macrolide resistance across multiple circulating lineages. Nat. Commun. *10*, 3255.